MASSEY UNIVERSITY
TE KUNENGA KI PŪREHUROA
UNIVERSITY OF NEW ZEALAND

Characterisation of plant oil bodies and their application as delivery systems of bioactive compounds

A thesis presented in partial fulfilment of the requirements for the degree of

Master of Food Technology

at Massey University, Manawatū, New Zealand.

Francesca Louise P. Garcia

2021

Riddet Institute
ADVANCING FRONTIERS IN FOOD SCIENCE

Abstract

Oil bodies are small, spherical organelles that store triacylglycerols (TAG) in plants. They are derived as natural oil-in-water emulsions and their unique interface composed of a monolayer of phospholipids embedded with proteins provides great stability against physical and chemical stresses. This study aimed to characterise oil bodies extracted from hemp and mustard seeds and determine their potential as delivery systems to encapsulate β-carotene, a model of hydrophobic bioactive compound.

Hemp and mustard oil body fractions obtained after aqueous extraction were characterised in terms of particle size, surface charge, microstructure, and behaviour at different pH (2-10) conditions and ionic strengths (0-1,000 mM NaCl). β-carotene was then encapsulated into oil body systems at a concentration of 400 μg/g oil using intact and disrupted oil bodies. The colloidal and β-carotene stability of these oil body systems were analysed for 14 days at different storage temperatures (4°C, 22°C, and 50°C) and light conditions (with and without light at ambient temperature) by determining their particle size, surface charge, colour, and β-carotene content.

Mustard oil bodies were entrapped in flocs of extraneous proteins even when extracted at alkaline pH (9), making it difficult to achieve their successful extraction. Hemp oil bodies, however, were isolated with minimal flocculation. They exhibited high electrostatic stability at neutral pH, aggregated at pH values close to the isoelectric point of the oleosins (pH 4 and 5), and had reduced ζ-potential with the addition of salt (NaCl ≥ 62.5 mM).

Hemp oil bodies were used to encapsulate β-carotene in delivery systems. In intact oil bodies, the use of solvents (ethanol, hexane, and diethyl ether) did not enhance the partitioning of β-carotene to the TAG core of oil bodies (low encapsulation efficiency of <40%). In contrast, heating (50°C, 10 min) and mild sonication were able to directly incorporate crystalline β-carotene into the hemp oil body fraction. When oil bodies were homogenised, their membrane material fragments were able to stabilise the interface of newly formed oil droplets, but flocculation was observed. Heat-induced destabilisation of oil bodies (stirred for 1 h at 70°C) led to the extraction of oil body membrane materials (OBMM), which were used as emulsifiers of β-carotene-loaded hemp oil emulsions.

During storage for 14 days, these β-carotene-loaded oil body systems remained stable at 4°C and 22°C, but storage at 50°C caused a significant reduction ($p<0.05$) in their colloidal and chemical stability. However, their stability was unaffected by the presence of light during storage at room temperature. Compared to the WPI-stabilised emulsion, the OBMM-stabilised emulsion exhibited a comparable colloidal stability while the homogenised and non-homogenised oil bodies had a similar retention of β-carotene.

Overall, oil bodies can be utilised as encapsulation systems for bioactive compounds. These systems exhibit comparable stability to protein-stabilised emulsions during storage. However, a balance between their colloidal and chemical stability must be achieved to enhance their functionality for commercial application. Further characterisation of the composition of their membrane materials is recommended to fully elucidate the mechanisms by which they can stabilise emulsions and protect the bioactive compound against degradation.

Acknowledgements

I would like to express my deepest gratitude to all individuals and organisations who in one way or another helped me complete this thesis. To my main supervisor, Dr Alejandra Acevedo-Fani, my sincerest thanks and appreciation for being a great mentor. I am deeply indebted to her for her wisdom, guidance, encouragement, and patience which kept me on track and inspired me to work hard and finish this project to the best of my abilities. I am equally grateful to my co-supervisor, Dr Anant Dave, whose expertise was invaluable for the completion of this project. His support, assistance, and time have helped me in managing this project efficiently and motivated me during my research journey.

I would like to thank Distinguished Professor Harjinder Singh for giving me the opportunity to conduct my research at the Riddet Institute and for providing scientific advice and direction to this project.

My postgraduate study in New Zealand would not have been possible without the scholarship from the Ministry of Foreign Affairs and Trade (MFAT). My sincerest appreciation goes to the New Zealand Scholarships Team of Massey University, especially Mr Jamie Hooper, Ms Saba Azeem, Ms Negin Nematollahi, and Ms Micaela Moll, for taking care of me from pre-departure to NZ until my return to my home country and for ensuring my wellbeing throughout my stay in New Zealand, especially during these unprecedented times.

I would like to express my sincerest appreciation to the lab managers and technicians who have provided me with assistance and guidance on my laboratory experiments: Ms Maggie Zou, Mr Garry Radford, Ms Michelle Tamehana, Mr Steve Glasgow, Mr Warwick Johnson, Ms Ann-Marie Jackson, and Ms Kylie Evans. I am deeply grateful for your help in laboratory matters, inductions and equipment training, and procurement of materials for my experiments.

I am also thankful to Dr Matthew Savoian of the Manawatu Microscopy and Imaging Centre (MMIC) for training me on the use of the confocal laser scanning microscope.

I would like to express my gratitude to the following people who have assisted me with my laboratory work: Mr Sihan Ma for help in oil body-related work, Dr Peter Zhu for assistance on particle size, charge, and colour measurements for my stability tests, Ms

Dan Wu for help in β-carotene analysis, and Ms Renna Alfante for assistance on working at the new lab.

I am thankful to the staff of the School of Food and Advanced Technology and Riddet Institute for the administrative support.

My heartfelt thanks also go to all the staff, researchers, students, and friends I have met while studying at Massey and working at the laboratories, for their incredible support and inspiration.

I would like to express my sincerest appreciation to my family for the love, support, and understanding. I am also extremely thankful to my friends for the encouragement and for making my stay in New Zealand very fun and memorable.

Lastly, my utmost gratitude to the Lord for granting me wisdom, hope, and strength to accomplish this, all glory and honour are Yours.

Table of contents

List of figures

List of tables

Chapter 1 Introduction

1.1 Background

In plant tissues, the oil is contained in small spherical intracellular organelles called oil bodies (Huang, 1992; Tzen & Huang, 1992). They are present in abundant amounts in the seed and are derived as natural oil-in-water emulsions because of their unique structure (Gray et al., 2010; Iwanaga et al., 2007). Oil droplets are protected by an interfacial membrane consisting of a monolayer of phospholipids embedded with unique proteins called oleosins that play a role in their synthesis and stability (Huang, 1994; Tzen & Huang, 1992). The oleosin structure allows them to provide oil bodies with steric hindrance, protecting the phospholipids against attack by phospholipases and preventing the contact of adjacent oil bodies that could result in coalescence or aggregation (Huang, 1994). Moreover, the interaction between the phospholipids and oleosins at the interface gives the oil bodies a negative surface charge that leads to electrostatic repulsion (Huang, 1996). This unique interface allows the oil bodies to maintain their individuality and have remarkable stability in isolated preparations and inside the cell where they are stored for long periods until they are utilised for germination (Huang, 1992; Tzen & Huang, 1992). Because of their unique structure and good stability, there is an increasing interest in exploring the potential functionality of oil bodies as novel ingredients for the food industry.

Hemp seeds are an excellent source of dietary oil, protein, and fibre and the oil extracted from the seeds contains more than 90% of polyunsaturated fatty acids (PUFA) and two essential fatty acids (EFA), which are linoleic acid and α-linolenic acid (Callaway, 2004; Small, 2017). Its high PUFA and EFA contents can improve human health and development when included in the diet as EFAs cannot be synthesised by the human body. Moreover, hempseed oil has an ω-6/ω-3 fatty acid ratio of around 2.5:1 that falls within the optimal balance of 2:1 and 3:1, which is considered essential for the metabolism of these PUFAs (Callaway, 2004). Aside from these, it contains bioactive compounds such as tocopherols, flavonoids, chlorophyll pigments, and phenolic compounds (Teh & Birch, 2013). Because of its high nutritive value, hempseed oil shows great potential as a bioactive food ingredient. The oil is usually extracted by cold-pressing to preserve the bioactive compounds it contains, and solvent extraction usually done with hexane is also used to increase the yield and reduce the cost of extraction (Small, 2017).

However, this makes the oil inedible as it results in oil degradation and includes contamination from residual solvents. To date, the feasibility of extracting oil from hemp seeds in the form of oil bodies has not been reported, as well as the physicochemical nor functional properties of these oil bodies. Therefore, it could be explored to further increase its utilisation in the food industry.

On the other hand, mustard seeds are cultivated primarily as oilseeds and its oil is widely used as a liquid cooking oil in India and other South Asian countries (Edwards et al., 2007; Eskin et al., 2020). The oil contains around 95% of unsaturated fatty acids and high amounts of linoleic, oleic, and erucic acids and contains bioactive compounds such as tocopherol and carotenoids (Richards et al., 2008; Vaidya & Choe, 2011a, 2011b). Oil bodies from mustard seeds have been previously isolated and characterised, having a small droplet diameter of 0.75 μm which is smaller than oil bodies from other plant species (Tzen et al., 1993). Moreover, they are negatively charged at neutral pH with an isoelectric point at around pH 5.7 (Tzen et al., 1993). However, no other studies have investigated their physical and chemical stability and functionality as a novel food ingredient.

Oil bodies have been utilised as delivery systems of lipophilic bioactive compounds because they are extracted as natural oil-in-water emulsions and have noteworthy physical and chemical stability (Acevedo et al., 2014; Boucher et al., 2008; Liu et al., 2020; Murray et al., 2007). With the increasing demand for the use of natural ingredients, the use of synthetic emulsifiers can be avoided since they are naturally emulsified materials (Ishii et al., 2017; Iwanaga et al., 2007). Moreover, such plant materials have additional beneficial substances such as antioxidants that enable the protection of the bioactive compounds they contain (Fisk et al., 2006; Fisk et al., 2008). As such, different methods have been employed to incorporate bioactive compounds in oil bodies in the food, pharmaceutical, and cosmetic industries. Interfacial materials from oil bodies have been isolated and used as emulsifiers in preparing artificial oil body emulsions with improved structural and thermal stability (Chen et al., 2004; Peng et al., 2003), and increased bioaccessibility and high encapsulation efficiency of the bioactive compound (Chang et al., 2013). The oil body membrane has also shown permeability to hydrophobic compounds, allowing their passive partitioning inside the oil body core (Acevedo et al., 2014; Boucher et al., 2008; Murray et al., 2007).

Dietary bioactive compounds are defined as food components that although are not considered essential, provide health benefits as they impart a positive effect on human biological processes (Raikos & Ranawana, 2017). They provide antioxidant, structural, functional, and nutritional functions in the human body. However, lipophilic bioactive compounds are usually difficult to incorporate in food products because of their nonpolar nature that is incompatible with most food matrices, sensitivity to food processing and storage, and poor bioavailability (McClements, 2007; Raikos & Ranawana, 2017). Carotenoids are lipophilic compounds that impart the yellow to red colour of many food products. They serve as vitamin A precursors, possess antioxidant activity, and play a key role in cellular process related to immunity and gap junction communication (Carvalho et al., 2013; Raikos & Ranawana, 2017).

Among the carotenoids, β-carotene is a major carotenoid in the human diet; it is the main source of vitamin A in humans because it has the highest provitamin A activity (Gul et al., 2015). It is responsible for the red and orange-coloured pigment in many fruits and vegetables and is abundant in carrots, sweet potatoes, pumpkin, peppers, greens, and broccoli among others (Boon et al., 2010; Carvalho et al., 2013). It is a highly hydrophobic compound comprised of a long hydrocarbon chain with 11 conjugated double bonds and two β-rings on each end (Gul et al., 2015). Because of its highly unsaturated nature, β-carotene is highly prone to degradation (oxidation and isomerisation) upon exposure to heat, light, oxygen, and other prooxidants in the environment, leading to a loss in its colour and bioavailability (Boon et al., 2010; Mao et al., 2018). Moreover, β-carotene isolates or concentrates have low bioavailability because of crystallinity and lipophilicity that limits their application in food products. Interactions with protein complexes can also hinder its release in the gastrointestinal fluids during digestion (Gul et al., 2015).

Thus, β-carotene is often encapsulated into delivery systems to improve its solubility and chemical stability in the food matrix, protect it against chemical and enzymatic degradation as it passes through the gastrointestinal tract, or control its release at a certain rate or site and/or in response to a specific environmental stimulus (McClements et al., 2007; Raikos & Ranawana, 2017). For example, β-carotene has been successfully incorporated in emulsions, achieving good physical and chemical stability and enhanced bioaccessibility (Jo & Kwon, 2014; Mao et al., 2010; Qian et al., 2012; Salvia-Trujillo et

al., 2013; Verrijssen et al., 2015; Yi et al., 2014). However, β-carotene encapsulation into oil bodies and the impact on the stability of this bioactive compound has not been explored. Additionally, no study has been conducted on the potential of hemp and mustard oil bodies as encapsulation systems for bioactive compounds.

1.2 Aims and objectives

This study aimed to develop a feasible extraction protocol of oil bodies from oleaginous seeds (hemp and mustard seeds), characterise them, and explore their potential application as delivery systems of hydrophobic bioactive compounds, using β-carotene as a model. The specific objectives of the study were to: (1) extract oil bodies from hemp and mustard seeds and determine their physicochemical properties and colloidal stability under external conditions; (2) develop strategies to encapsulate β-carotene in oil bodies through (a) incorporation in intact oil bodies with and without the use of solvents and (b) formation of emulsions using oil bodies membrane materials; and (3) determine the physicochemical stability of β-carotene encapsulated in the oil bodies systems during storage.

Chapter 2 Literature review

2.1 Introduction

With the increasing demand of consumers for natural ingredients and products with health-promoting benefits, bioactive compounds have been incorporated into food products to improve their therapeutic effect. However, their incorporation in foods is a challenge because of their hydrophobic nature, instability during processing and storage, and low bioavailability. Thus, they are often encapsulated into delivery systems to improve their solubility and stability in the food matrix, protect them from degradation during digestion, and control their release in the GIT. For these purposes, the use of nature-assembled colloidal structures, such as oil bodies from plants, are suitable systems for the encapsulation of bioactive compounds because of their structural and functional properties. Being natural systems, the use of synthetic ingredients or chemicals is avoided and their extraction is eco-friendly.

This review aims to present information on the structure and composition of oil bodies, including their physicochemical properties and stability against various environmental factors. The properties of hemp and mustard seeds are also discussed along with the extraction, composition, and applications of their oil. Additionally, the potential applications of oil bodies as carriers of hydrophobic compounds are highlighted, such as the use of intact or disrupted oil bodies and the extraction of oil body membrane materials as emulsifiers to stabilise oil-in-water emulsions. Lastly, the properties of bioactive compounds and their need for encapsulation are presented, with focus on β-carotene and previously developed emulsion-based delivery systems for it.

2.2 Oil bodies

Oil bodies, also known as oleosomes, spherosomes, or lipid bodies, are small spherical intracellular organelles that contain triacylglycerols (TAGs) and are found in many plant tissues, although they are most abundant in seeds and nuts (Huang, 1992; Tzen et al., 1993). Seeds store TAGs into oil bodies as food reserves for germination and post-germinative growth (Huang, 1994). Inside the seed, they are present in abundant amounts, occupy as much intracellular volume as protein bodies, and provide a structure to stabilise the hydrophobic TAGs into oil droplets, preventing their coalescence. These oil bodies provide an increased surface area for lipase action during TAG mobilisation after dormancy or during germination (Huang, 1992).

2.2.1 Structure and composition

An oil body consists of a hydrophobic TAG core surrounded by a complex membrane consisting of a monolayer of phospholipids embedded with proteins, also called oleosins (Tzen & Huang, 1992). Among different species, the relative contents of TAGs, phospholipids, and proteins vary widely and depend on the size of the oil bodies, specifically their surface area (Huang, 1994; Nikiforidis et al., 2014). Generally, the typical composition of oil bodies consists of 94-98% TAG, 0.6-2.0% phospholipids, and 0.6-2.0% protein (Nikiforidis et al., 2014).

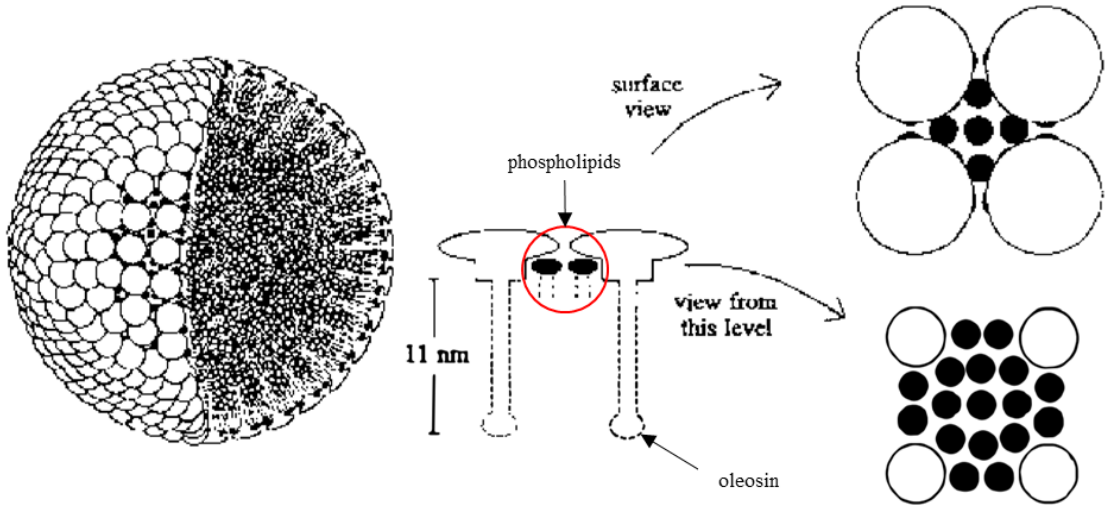

Figure 2.1. Model oil body structure. Adapted with permission from Huang (1992).

The most widely accepted structure of oil body structure is shown in Figure 2.1. The basic structural unit of an oil body membrane has 13 phospholipids and one oleosin molecule. The hydrophobic part which consists of about 40% of the oleosin molecule is embedded into the TAG matrix and the hydrophobic acyl groups of the phospholipid layer, while the remaining 60% covers and protrudes from the surface of the oil body. A schematic representation of the conformation of an oil body membrane is further elucidated in Figure 2.2. As determined by small angle neutron scattering, the interfacial membrane of an oil body has a thickness of 9 nm (Zielbauer et al., 2018). The phospholipids account for 80% of this membrane while the remaining is comprised of the three types of proteins, namely oleosin, caleosin, and steroleosin (Napier et al., 2001).

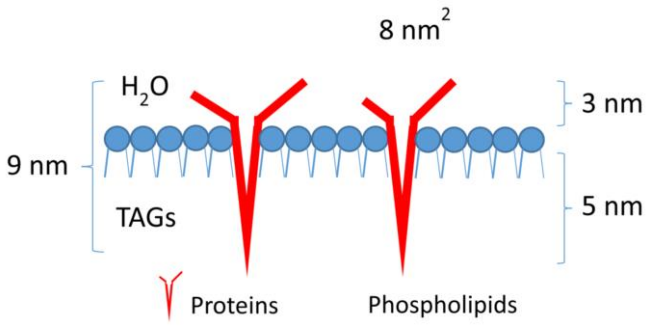

Figure 2.2. Oil body membrane conformation. Reproduced from Nikiforidis (2019).

Within the seed, cells are densely packed with oil bodies (Figure 2.3) (Gray et al., 2010). However, the intracellular distribution of oil bodies is asymmetric (Dave et al., 2019). As shown in the cross-sectional analysis of coconut tissue (Figure 2.4), oil bodies are not uniformly distributed in the tissue as some cells do not contain oil bodies (pointed in grey arrows, image C, see Figure 2.4) (Dave et al., 2019). Structural analysis has also shown that intracellular oil bodies are spherical in shape, although some are irregularly-shaped as a result of being pressed against each other or under compression, indicating that the interfacial membrane is responsive, flexible, and elastic (Dave et al., 2019; Huang, 1992; Nikiforidis et al., 2013).

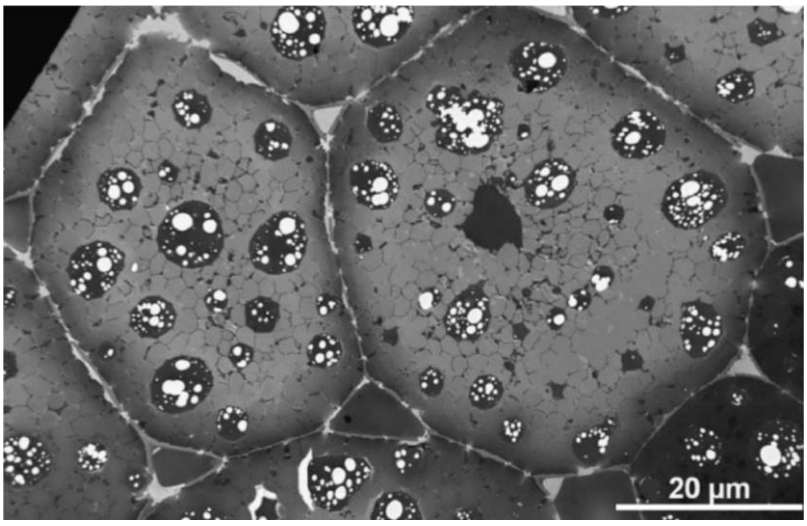

Figure 2.3. Section of *E. plantagineum* seed viewed by transmission electron microscopy. Reproduced with permission from Gray et al. (2010).

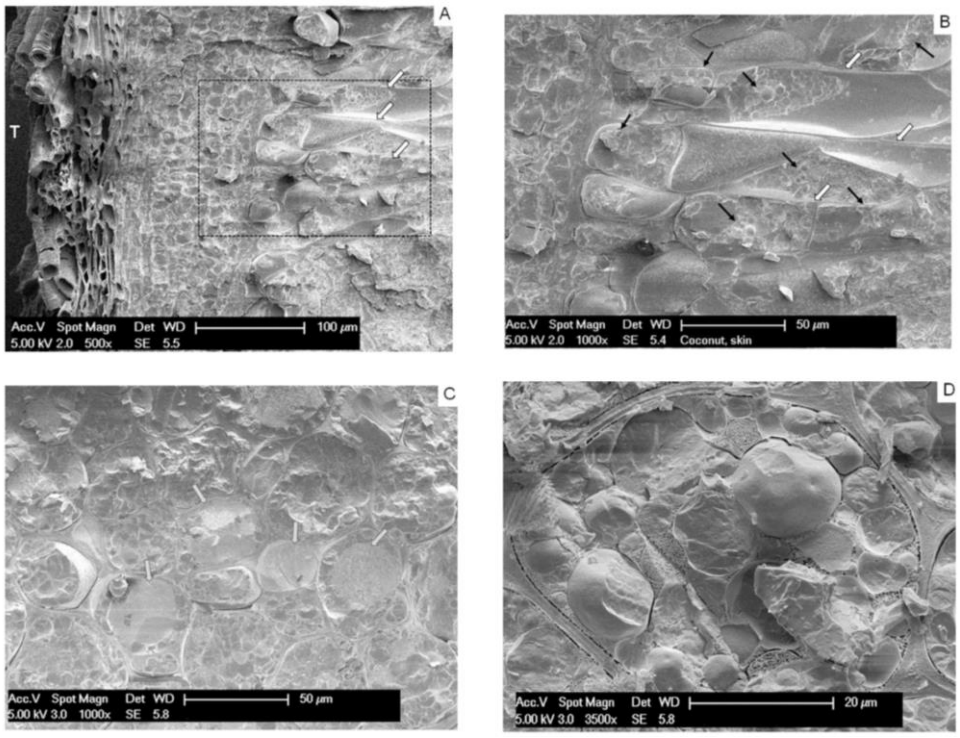

Figure 2.4. Cryo-SEM images of the outer endosperm tissues of coconut adjacent to the testa. Reproduced with permission from Dave et al. (2019).

2.2.1.1 Triacylglycerols (TAG)

The TAG composition in oil bodies, including their acyl composition, is highly species-specific (Huang, 1992). For example, isolated maize oil bodies contain about 95% TAG and 4% diacylglycerols in the hydrophobic core matrix (Tzen & Huang, 1992). Linoleoyl, oleoyl, and palmitoyl acyl moieties were identified as TAGs and acyl lipids present in the matrix. The composition of fatty acids is dependent on the seed source. While coconut oil bodies consist of saturated fatty acids in their TAG, the TAG in the oil bodies from seeds contains unsaturated fatty acids (Dave et al., 2019; Gray et al., 2010).

2.2.1.2 Phospholipids

The phospholipid monolayer surrounds the TAG core and provides stability to TAG against coalescence. The phospholipids are oriented so that the hydrophobic acyl moieties are interacting with the TAG core, while the hydrophilic head groups are facing the cytosol (Huang, 1992; Tzen & Huang, 1992). Analysis of the fatty acid profiles of phospholipids in oil bodies revealed that majority is comprised of saturated fatty acids (~70%), which is opposite to the TAG core that is composed mainly of polyunsaturated fatty acids (Payne et al., 2014). The saturated nature of the fatty acids promotes not only enhanced oxidative stability but also increased physical stability. The lack of double

bonds allows the fatty acids to be fully extended, promoting a firm anchorage of the oleosins and strengthening the oil body interface (Payne et al., 2014).

In oil bodies, phosphatidylcholine is the predominant phospholipid which accounts for around 50% of the total, and minor phospholipids include phosphatidylserine, phosphatidylethanolamine, and phosphatidylinositol (Huang, 1992; Payne et al., 2014). Phosphatidylserine and phosphatidylinositol, which are negatively charged, are deemed unusual phospholipid components in plant tissues. Along with free fatty acids, they are proposed to interact via electrostatic attractive forces with the basic amino acid residues of the oleosins on the oil body membrane, further supporting the interfacial network (Nikiforidis, 2019; Tzen & Huang, 1992).

2.2.1.3 Oleosins

Oil bodies have unique membrane-specific proteins that are distinguished from other proteins because of their extended central hydrophobic domain, which is reported to be the longest hydrophobic sequence found in proteins (Huang, 1996; Nikiforidis et al., 2014). These membrane-specific proteins are categorised into three types: oleosins, caleosins, and steroleosins. Among these, oleosins are the most abundant structural proteins associated with oil bodies and they cover most of the oil body surface (Huang, 1992; Tzen & Huang, 1992). Oleosins are alkaline proteins with a molecular mass of 15-26 kDa and are unique to oil bodies as shown by subcellular fractionation and immunocytochemistry (Huang, 1992).

An oleosin molecule has three (3) structural domains: a central hydrophobic domain with about 70 residues that is flanked by an amphipathic N-terminal region with 50-70 residues and an amphipathic C-terminal domain with variable length (Frandsen et al., 2001; Huang, 1992). The central hydrophobic domain is the longest hydrophobic polypeptide found in diverse organisms and its amino acid sequence is highly conserved among oleosins of various plant species (Huang, 1996). It consists of two anti-parallel β-strands that penetrate the phospholipid monolayer into the TAG matrix of the oil body to form a hairpin-like structure, anchoring the whole protein stably (Huang, 1996; Tzen & Huang, 1992). Its stability is enhanced by the carbonyl and imino groups of the peptide bonds between adjacent strands (Huang, 1992). Meanwhile, the C-terminal domain located on the oil body surface has an α-helical structure, wherein the negatively charged residues are exposed to the surface while the positively charged residues face the negatively

charged lipids (e.g., phosphatidylserine, phosphatidylinositol, and free fatty acids) on the phospholipid layer (Huang, 1992). On the other hand, the N-terminal domain is located in the cytoplasm that faces the cytosol and contains a mixture of structures (Nikiforidis et al., 2014). The N- and C-terminal domains also facilitate the association of the molecule to the polar heads of the phospholipids (Nikiforidis, 2019). Because of these secondary structures, oleosins reside stably on the amphipathic surface of the oil body (Huang, 1996).

Oleosin plays a role in the stability, synthesis, and metabolism of oil bodies. Steric hindrance is provided by the surface proteins that protect the phospholipids against hydrolysis by phospholipases, preventing the contact of the phospholipid surface between adjacent oil bodies that could lead to aggregation or coalescence (Huang, 1994). Moreover, oleosins inhibit the coalescence of oil bodies by providing high surface charge leading to electrostatic repulsion (Huang, 1996). The interaction of the oleosins with the phospholipids at the interface of oil bodies based on charge and polarity distribution confers the oil bodies with a hydrophilic and hydrated surface (Napier et al., 2001). This membrane with an amphipathic surface and steric hindrance also allows the oil bodies to maintain their individuality; they exist as spherical droplets that do not aggregate nor coalesce even when brought against each other in the seed due to seed desiccation or in isolated preparations after flotation centrifugation (Huang, 1992; Tzen & Huang, 1992).

Digestion of oil bodies with enzymes and repeated cycles of freeze-thaw treatments has illustrated the importance of oleosins on oil body stabilisation. Once digested, oil bodies coalesced into large droplets due to the removal of the hydrophilic and charged protein portion on the oil body surface (Maurer et al., 2013). This resulted not only in the alteration of the net surface charge but also in the steric barrier against coalescence. Thus, the removal of oleosins causes the destabilisation of oil bodies as evidenced by increasing polydispersity size of oil bodies, a reduced polydispersity of the droplet interfacial layer, and changing interactions between droplets. Similarly, repeated freeze-thaw cycles have resulted in the destabilisation of oil body emulsions due to aggregation and coalescence; as such, this technique has been used to extract membrane materials from oil bodies (Nikiforidis et al., 2011; Onsaard et al., 2006).

Oleosins also affect the size of oil bodies, as the size is partially controlled by the relative amounts of oil to oleosin (Frandsen et al., 2001). Aside from its structural role, oleosins

provide a specific site for the binding of newly synthesised lipase during germination (Huang, 1994).

2.2.1.4 Minor proteins

Aside from oleosins, other proteins found on the surface of oil bodies are caleosins and steroleosins (Nikiforidis et al., 2014). These proteins are characterised by having shorter hydrophobic sequences and longer hydrophilic sequences that are oriented towards the cytosol on the oil body surface. Caleosins (25-35 kDa) have a similar but smaller hydrophobic domain than oleosins, a fairly hydrophilic N-terminal region with a single Ca^{2+} binding site, and a hydrophilic C-terminal region that contains four (4) potential phosphorylation sites, as in most plant proteins (Frandsen et al., 2001; Nikiforidis, 2019). They comprise about 10% of the total oil body proteins and are identified to impart stability to oil bodies and have the capacity to interact with calcium (Jung et al., 2012). Steroleosins (40-55 kDa), on the other hand, are bigger proteins that have a hydrophobic domain of a similar length as caleosins (Nikiforidis, 2019). They have an extended hydrophilic domain that is structurally similar to sterol-binding dehydrogenases. Their role in the stability of oil bodies seems to be minor as they failed to contribute to the formation of artificial oil bodies, unlike oleosins and caleosins (Chen et al., 2004).

2.2.2 Physicochemical properties and stability of oil bodies

2.2.2.1 Size and shape

Many factors affect the size of oil bodies, which may be physicochemical or biological in nature. Among different species, the size of seed oil bodies varies but falls within a narrow range of 0.5-2.5 μm (Huang, 1992; Tzen et al., 1993). This narrow size range provides a large surface area for the attachment of lipase during germination for the rapid mobilisation of reserve TAG (Tzen & Huang, 1992). Within the same seed, oil bodies may also vary in size depending on the cell types they are present in (Tzen et al., 1993).

The relative oil-to-protein ratio determines the shape and size of the oil bodies in the cell (Huang, 1992; Nikiforidis et al., 2014). Generally, small-sized oil bodies are found in oleaginous seeds that exhibit a low ratio of TAGs to interfacial proteins and larger-sized oil bodies are observed in those that have low interfacial protein content (Nikiforidis et al., 2014). Various parameters affect this ratio of oil to oleosins, such as the genetic background of the species (e.g., relative activities of the enzymes that synthesise the oil

and oleosins and the availability of their substrates) and environmental parameters like the growth temperature and nitrogen availability for oleosin synthesis (Ting et al., 1996).

2.2.2.2 Isoelectric point and ζ-potential

The isoelectric point of oil bodies generally ranges from 5.7 to 6.6 (which is close to the isoelectric point of oleosin), indicating that they have a net negative charge on their outer surface at neutral pH (Maurer et al., 2013; Tzen et al., 1993). This is due to the interaction of the negatively charged phospholipids with the positively charged residues of the surface proteins (Tzen et al., 1993). The variation in the isoelectric point of oil bodies from different species may be attributed to the differences in the extraction process used for oil body isolation since chemicals used for oil body extraction can remove the non-specifically associated proteins on the oil body surface (Chen & Ono, 2010; De Chirico et al., 2018; Sukhotu et al., 2014; Zhao et al., 2016).

The presence of extraneous proteins that remain adsorbed on the oil body surface after extraction has also been shown to cause a decrease in the isoelectric pH of oil bodies. This was attributed to their shielding effect on the oleosins (as they are more acidic) and the possible formation of negatively charged lipids if the adsorbed proteins were enzymes that could promote lipid degradation (Iwanaga et al., 2007; Nikiforidis & Kiosseoglou, 2009). For instance, the isoelectric point for isolated oil bodies was found to be between pH 4.5 and 5 for maize oil bodies, around pH 4 for soybean oil bodies, and around pH 4.8 for peanut oil bodies (Iwanaga et al., 2007; Nikiforidis & Kiosseoglou, 2009; Zhou et al., 2019).

2.2.2.3 Physicochemical stability to detergents and washing agents

Oil bodies have also shown stability against harsh chemical agents used during their extraction. When oil bodies are aqueously extracted, extraneous proteins are loosely bound on their surface and these are removed during subsequent washing steps (Nykiforuk, 2016). Washing the oil body preparation with water removes the loosely adhering proteins on their surface while washing with chaotropic agents (e.g., urea or Tween 20) removes these proteins on the oil body surface by disrupting the proteins' non-covalent interactions (Payne et al., 2014). Oleosins are not removed by washing with urea as they are intrinsically bound to oil bodies during their synthesis through the interaction of the large patches of their hydrophobic sequences with the hydrophobic TAG core (Dave et al., 2019; Fisk et al., 2006; Gray et al., 2010). Since the anchor regions of the

oleosins are conserved, the structure of oil bodies is maintained as evidenced by the staining of their proteins (Dave et al., 2019). Likewise, the distribution of phospholipids on the surface of oil bodies was not affected by washing with Tween 20 and 9 M urea (Dave et al., 2019), indicating the strong integrity of the oil body membrane.

2.2.2.4 Effect of pH and ionic strength

The behaviour of oil bodies at different pH conditions is similar to that of protein-stabilised emulsions because of the oleosins that stabilise the interface. Oil bodies are negatively charged at low pH, have zero net charge at the isoelectric point, and are positively charged at high pH because of the alteration of their net surface charge distribution at different pH values (Maurer et al., 2013; McClements, 2016; Tzen & Huang, 1992). As such, oil bodies repel each other pH values far from their isoelectric point whereas they flocculate at pH values close to their isoelectric point because the electrostatic repulsion is not strong enough to overcome the attractive forces (e.g., hydrophobic and van der Waals interactions) (Maurer et al., 2013).

The pH-dependence of the aggregation behaviour of oil bodies is manifested in particle size and ζ-potential measurements. In soybean oil bodies, the mean particle diameter was found to be small at high pH values and large at intermediate pH values, exhibiting a similar behaviour with protein-stabilised emulsions (Chen et al., 2012). Maize oil bodies have also been found to form aggregates at acidic pH, reaching a maximum mean particle diameter value at pH 4, which decreased with a further increase in pH (Sukhotu et al., 2014). This could be due to the protonation of histidine residues at acidic pH, resulting in the neutralisation of the oil body surface charge and promoting aggregation (Frandsen et al., 2001).

Regarding ionic strength, salt addition has been found to promote the formation of aggregates and reduced the stability of oil body suspensions (Sukhotu et al., 2014). As the concentration of NaCl increased, the mean particle diameter increased while the ζ-potential decreased. The decrease in ζ-potential is due to the electrostatic screening effects and reduced energy of electrostatic interaction brought about by the presence of salt (McClements, 2016). This has been observed in maize, soybean, and safflower oil bodies, wherein an increase in ionic strength has caused a reduction in their ζ-potential and a consequent increase in mean particle diameter (Iwanaga et al., 2007; Lan et al., 2020; Sukhotu et al., 2014).

2.2.2.5 Effect of shear and mechanical force

The structure of oil bodies allows them to remain intact against compression and mechanical force. This is due to the flexibility of their membrane that allows them to be compressed and packed against each other inside the cell (Dave et al., 2019; Nikiforidis, 2019; Nikiforidis et al., 2011). For instance, oil bodies have been shown to withstand compressive strains (ε=0.3) without rupture, indicating that they are soft droplets (Yang et al., 2020). The mechanical strength of the membrane was also correlated with the size of the oil bodies, wherein smaller oil bodies that have a higher protein to oil ratio have a stronger resistance to deformation. However, when subjected to a strong mechanical force (i.e., high shear homogenisation), the oil body membrane ruptures: the interfacial proteins and phospholipids go to the new oil/water interface and the TAG core merges with the added dispersed phase (Ishii et al., 2017).

2.2.2.6 Effect of heating

Oil bodies have been shown to exhibit temperature stability. After thermal treatment of up to 90°C, there was no significant structural change observed in soybean oil bodies except for a slight increase in size caused by thermal expansion (Zielbauer et al., 2018). Similarly, heating of up to 90°C for soybean oil bodies and 100°C for maize oil bodies did not affect their particle size nor cause coalescence which was attributed to the stability of the oleosins and phospholipids at the interface that resisted the increase in surface hydrophobicity caused by heating (Chen & Ono, 2010; Nikiforidis et al., 2011; Sukhotu et al., 2014). Thermal treatment has also been shown to improve both the physical and oxidative stability of oil bodies due to the thermal deactivation of microorganisms and lipolytic enzymes (Chen et al., 2012; De Chirico et al., 2020).

In contrast, other studies have shown that heating causes the destabilisation of oil bodies. At temperatures above 50°C, a reduction in ζ-potential was observed in peanut oil bodies due to enhanced thermal motion that caused increased collisions and a consequent increase in particle diameter (Zhou et al., 2019). Heating at 70°C also caused the release of a few of 24 kDa oleosin from the oil body membrane into the aqueous phase of an oil body suspension, and its release was weakly enhanced by thermal treatment (Yan et al., 2016). Moreover, heating at temperatures above 70°C resulted in the detachment of extrinsic proteins, particularly the hydrophilic proteins, on the surface of oil bodies due to protein denaturation (Ding et al., 2020; Peng et al., 2016; Yan et al., 2016). An increase

in the temperature determines the extent of the unfolding of co-extracted extrinsic proteins as the denaturation temperature of different protein subunits is achieved. This has been explained in the formation of protein particles in soymilk, wherein intermediate temperatures (65-75°C) caused the release of 7S and 11S subunits in the soluble fraction, and high temperatures (75-95°C) resulted in their denaturation and dissociation (Peng et al., 2016). Protein particles were then formed from the aggregation of β and B subunits, while the *α*, *α'*, and A subunits were retained in the soluble fraction. These extraneous proteins that were co-extracted with oil bodies have been shown to have a high tendency to denature and interact in the continuous phase of emulsions, forming aggregates and causing the oil bodies to precipitate.

2.2.2.7 Oxidative stability

Oil bodies have been shown to exhibit oxidative stability as the oil inside the oil bodies can be protected from oxidation for several years (Gray et al., 2010). They are known to contain significant levels of natural antioxidants (e.g., tocopherol) that are proposed to protect the polyunsaturated fatty acids in oil bodies from oxidation (Fisk et al., 2006; Gray et al., 2010). The oil body emulsions have been found to have higher oxidative stability compared to emulsions stabilised by synthetic emulsifiers (Fisk et al., 2008). This oxidative stability is attributed not only to their natural antioxidant content but also to the strongly stabilised interface. The oil body interface, with the tight association of the oleosins and phospholipids, acts like a protein layer surrounding the oil body surface and offers a protective effect against oxidation by serving as a barrier to oxygen and reactive hydroperoxides, minimising the risk of oxidation reactions (Fisk et al., 2008; Gray et al., 2010). Furthermore, the sacrificial protection offered by the surface or carry-over proteins enhance oxidative stability since proteins can act as antioxidants by chelating metal ions or through sacrificial oxidation (Gray et al., 2010).

2.3 Hemp seeds and hempseed oil

Hemp (*Cannabis sativa* L.) has been used for thousands of years as a source of fibre, food, and medicine (Callaway, 2004). The hemp plant bears fruit botanically termed as 'achenes' which is usually referred to as 'seeds' (Small, 2017). Their size ranges from 2.5 to 4 mm in diameter and 3 to 6 mm in length depending on the cultivar. A 'hull' or 'shell' protects the inner part of the seed within the fruit wall or pericarp (Figure 2.5), and the embryo which is rich in oil, proteins, and carbohydrates utilised during germination

fills most of the seed (Small, 2017). The proximate composition and nutritional content of the hemp seeds are shown in Tables 2.1 and 2.2, respectively.

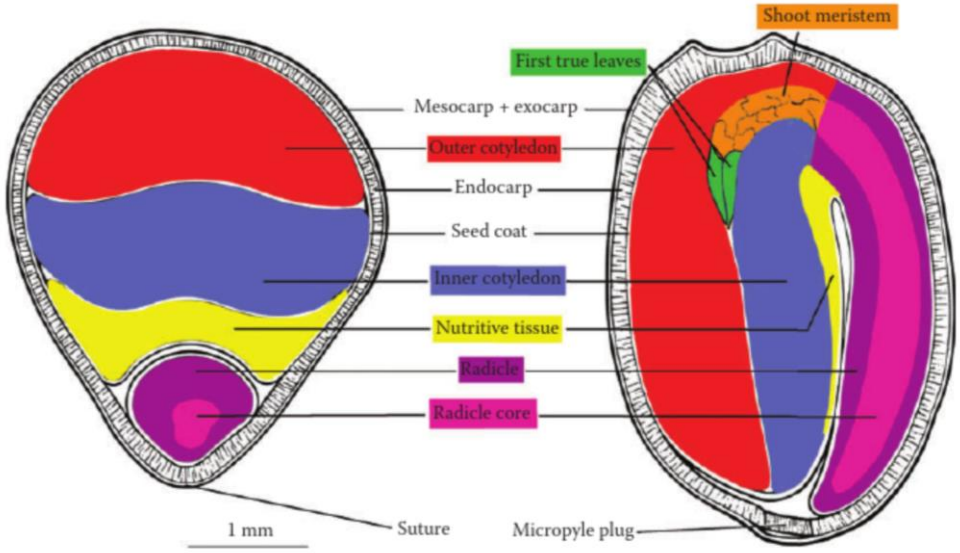

Figure 2.5. Sectioned hemp seeds: cross-section (left) and longitudinal section through widest dimension (right). Reproduced with permission from Small (2017).

Table 2.1. Typical nutritional content (%) of hempseed (Finola variety). Reproduced with permission from Callaway (2004).

	Whole seed	**Seed meal**
Oil (%)	35.5	11.1
Protein	24.8	33.5
Carbohydrates	27.6	42.6
Moisture	6.5	5.6
Ash	5.6	7.2
Energy (kJ/100 g)	2200	1700
Total dietary fiber (%)	27.6	42.6
Digestable fiber	5.4	16.4
Non-digestable fiber	22.2	26.2

Table 2.2. Typical nutritional values (mg/100 g) for vitamins and minerals in hempseed (Finola variety). Reproduced with permission from Callaway (2004).

Vitamin E	90.0
Thiamine (B1)	0.4
Riboflavin (B2)	0.1
Phosphorous (P)	1160
Potassium (K)	859
Magnesium (Mg)	483
Calcium (Ca)	145
Iron (Fe)	14
Sodium (Na)	12
Manganese (Mn)	7
Zinc (Zn)	7
Copper (Cu)	2

2.3.1 Hempseed oil extraction

Hemp seeds contain 28-35% oil that varies depending on the variety, year of cultivation, climatic conditions, and growing location (Matthaus & Bruhl, 2008). Its oil can be extracted through various methods that may either be pressure or solvent-based (Small, 2017). Oil extraction using screw presses is economical and can extract 60-80% of the oil (Matthaus & Bruhl, 2008). Hempseed oil is usually used as an edible oil and is mostly cold-pressed, which allows for the preservation of the bioactive compounds it contains (Small, 2017). It is characterised as having a dark green colour with a pleasantly nutty taste and sometimes a slightly bitter aftertaste (Matthaus & Bruhl, 2008; WHO Expert Committee on Drug Dependence, 2018).

Furthermore, cold-pressed hemp seed oil has good quality characteristics because it is low in moisture, unsaponifiable matter, and free fatty acids; and the level of compounds used for oxidative stability tests is lower than the maximum allowed (Teh & Birch, 2013). On the other hand, solvent extraction, mostly using hexane, may also be used to extract the oil because it is cheaper, faster, and has a higher yield. However, it is deemed unsuitable for edible hempseed oil because it causes oil degradation and the residual solvents contaminate the final product (Small, 2017).

2.3.2 Hempseed oil composition

Hempseed oil has a high nutritional value because it has a high polyunsaturated fatty acids (PUFAs) content. It typically contains more than 90% of unsaturated fatty acids and the oil from non-drug varieties of the seed is an excellent source of two essential fatty acids (EFA): linoleic acid (18:2 ω-6) and α-linolenic acid (18:3 ω-3) (Callaway, 2004; Small, 2017). The major fatty acid in the oil is linoleic acid which comprises 56.9% of its fatty acid composition (Teh & Birch, 2013). Since essential fatty acids cannot be synthesised by humans, supplementation of the diet with oil containing high amounts of EFAs and other PUFAs can improve human health and development. Moreover, hempseed oil contains the biological metabolites of these two EFAs, which are γ-linolenic acid (18:3 ω-6) and stearidonic acid (18:4 ω-3) (Matthaus & Bruhl, 2008). These fatty acids serve as precursors for the synthesis of eicosanoids and long-chain PUFAs. Hempseed oil also has an ω-6/ω-3 ratio of around 2.5:1 which is within the optimal balance of 2:1 and 3:1 (Callaway, 2004). Having an optimal ω-6/ω-3 balance is considered essential for the metabolism of these PUFAs. Because of the high levels of EFAs and other PUFAs, hemp seed oil has been associated to contribute to immune response (Callaway, 2004).

Aside from its PUFA content, hempseed oil contains bioactive compounds like tocopherol, chlorophyll pigments, flavonoids, and phenolic compounds (Table 2.3) (Callaway, 2004; Teh & Birch, 2013). It has high amounts of tocopherol, with γ-tocopherol as the predominant tocopherol representing around 85% of the total tocopherols (Oomah et al., 2002; Teh & Birch, 2013). Tocopherols protect the oil against oxidative reactions and act as vitamin E in human nutrition, serving a role in minimising the risk of cardiovascular disease, cancer, and macular degeneration (Matthaus & Bruhl, 2008). Hempseed oil also contains phytosterols, such as β-sitosterol, campesterol, Δ5-avenasterol, and stigmasterol, that lower the LDL-cholesterol levels in the blood (Matthaus & Bruhl, 2008). The high content of chlorophyll pigments that is extracted along with the oil imparts the oil with its intensive green colour (Matthaus & Bruhl, 2008; Teh & Birch, 2013). Furthermore, it has the highest amounts of flavonoids and total phenolic acids compared to flaxseed and canola oil (Teh & Birch, 2013).

Table 2.3. Bioactive and antioxidant compounds in hempseed oil.

Compound	Concentration (mg/100 g)	Reference
α-tocopherol	2.78 ± 0.01	Teh and Birch (2013)
	5	Callaway (2004)
	3.4	Oomah et al. (2002)
γ-tocopherol	56.41 ± 0.02	Teh and Birch (2013)
	85	Callaway (2004)
	73.3	Oomah et al. (2002)
Chlorophyll	75.21 ± 0.04	Teh and Birch (2013)
Total phenolic acids, as gallic acid equivalents	188.23 ± 2.51	Teh and Birch (2013)
Total flavonoids, as luteolin equivalents	19.50 ± 0.28	Teh and Birch (2013)

Since hempseed oil contains high amounts of PUFAs, it is prone to oxidation during storage. Moreover, chlorophyll is a photosensitiser that increases its susceptibility to oxidative deterioration; thus, the oil is usually stored in dark bottles to protect it from light (Matthaus & Bruhl, 2008). In contrast, the seeds are more stable against oxidation during storage since the hull protects the oil inside over long periods (Matthaus & Bruhl, 2008).

Hemp seeds contain minimal amounts of cannabinoids (no more than 1% Δ-9-tetrahydrocannabidol (THC)), and the maximum allowed level of total THC in hemp seed oil is no more than 10 mg/kg (Ministry for Primary Industries, 2020). Food products made from hemp seed only contain trace amounts of THC and other cannabinoids, and low levels of THC have no significant effect on intoxication nor any negative impact on human health and drug testing (Callaway, 2004). If the oil has measurable THC content, it is an indication of the seed hull being in contact with the resins in bracts and leaves containing cannabinoid since THC has been found to be located outside of the hulls (Matthaus & Bruhl, 2008). With thorough cleaning of the hemp seed, using low THC cultivars, and complete removal of the hull during processing, THC levels in the oil can be reduced (Callaway, 2004; Matthaus & Bruhl, 2008; WHO Expert Committee on Drug Dependence, 2018).

2.3.3 Use of hempseed oil in the food industry

Hempseed oil has great potential as a bioactive food ingredient because of its nutritional value and physicochemical properties. It has been used as the dispersed phase in oil-in-water emulsions because of its potential use in food fortification; encapsulation in emulsions can enhance the bioavailability of the essential fatty acids it contains and could serve as a source of natural antioxidants for health promotion and disease prevention (Mikulcová et al., 2017; Yin et al., 2017; Yu et al., 2005). Moreover, hempseed oil has been used as a carrier of baicalein, a flavonoid with pharmacological activity, in nanoemulsions to increase its oral bioavailability (Yin et al., 2017). It showed the highest solubilisation towards baicalein among the tested oils due to its high PUFA content. In contrast, hempseed oil was found to be susceptible to heat- and light-induced oxidation when used as the dispersed phase in oil-in-water emulsions; thus, incorporating a natural antioxidant can improve its utilisation in food products that need processing (Raikos et al., 2015).

The extraction and characterisation of oil bodies from hemp seeds have not yet been investigated. With the growing hemp industry in New Zealand and the potential of the oil as a bioactive food ingredient, the determination of the physicochemical properties and functionality of hemp oil bodies presents an interesting area of work to enhance its utilisation and possible commercial application in the future.

2.4 Mustard seeds and mustard seed oil

Mustard (*Brassica juncea* L.), also known as oriental, Indian, or brown mustard, is used worldwide as an oilseed, condiment, and vegetable (Edwards et al., 2007; Thomas et al., 2012). It is an annual crop that grows across different continents and is closely related botanically to canola (*B. napus*) and turnip rape (*B. rapa*) (Edwards et al., 2007). Its seeds are small and contain 35% of oil (Thomas et al., 2012). The nutritional composition of mustard seeds is shown in Table 2.4.

In India, where most of the world's mustard seeds are grown, mustard is cultivated primarily as an oilseed. The oil extracted is mostly used for edible purposes as a liquid cooking oil in India and other South Asian countries (Edwards et al., 2007; Eskin et al., 2020). The quality characteristics of the mustard seed used for oil extraction differ depending on the region. Traditionally, mustard cultivars containing high amounts of erucic acid and glucosinolates are used for oil production in India, China, and eastern

Europe (Edwards et al., 2007; Eskin et al., 2020). However, due to the negative impacts of high amounts of erucic acid and glucosinolates – with erucic acid contributing to issues on the cardiac muscle tissue of laboratory animals and glucosinolates causing palatability and nutritional problems when the meal was fed to ruminants – India, China, and eastern Europe are switching to canola-quality cultivars which are low in erucic acid and glucosinolates (Edwards et al., 2007). Meanwhile, canola-quality cultivars similar to *B. napus* and *B. rapa* are commonly used for commercial oilseed production in western countries. Roasting the mustard seed before oil extraction is usually done to impart the characteristic flavour of mustard seed oil and to improve its storage stability (Vaidya & Choe, 2011a).

Table 2.4. Nutritional composition of mustard seed per 100 g. Adapted with permission from Thomas et al. (2012).

Composition	Amount
Water (g)	3.0
Protein (g)	32
Fat (g)	42.6
Carbohydrates (g)	18.5
Ash (g)	4.0
Calcium (g)	0.3
Phosphorus (mg)	790
Potassium (mg)	700
Sodium (mg)	10
Iron (mg)	8.3
Thiamine (mg)	0.65
Riboflavin (mg)	0.45
Niacin (mg)	8.5
Ascorbic acid (mg)	22
Vitamin A activity (RF)	6

2.4.1 Mustard seed oil composition

Mustard seed oil contains around 95% of unsaturated fatty acids, with around 60% of monounsaturated and 35% of polyunsaturated fatty acids (Vaidya & Choe, 2011b). Whether roasted or unroasted, it has high amounts of linoleic, oleic, and erucic acids;

moderate amounts of eicosenoic and linolenic acids; and low amounts of palmitic, stearic, arachidic, and eicosadienoic acids (Vaidya & Choe, 2011a, 2011b). It also contains bioactive compounds such as tocopherols and carotenoids. γ-tocopherol is the predominant tocopherol while lutein is the major carotenoid, with the oil containing trace amounts of β-carotene (Richards et al., 2008; Vaidya & Choe, 2011a, 2011b). Tables 2.5 and 2.6 show the fatty acid composition and composition of bioactive and antioxidant compounds in mustard seed oil, respectively.

Roasting the seed before oil extraction has been shown to improve oxidative stability and enhance the retention of bioactive compounds in mustard oil during storage. Maillard reaction products that are known to act as antioxidants in the oil are produced during seed roasting, thereby enhancing the heat stability of tocopherols (Shrestha et al., 2012). Roasting of the mustard seed produces canolol (2,6-dimethoxy-4-vinylphenol), a potent radical scavenger, and results in phospholipid browning, whose reaction products possess antioxidant activity through various mechanisms such as chelating agent, hydrogen transfer, reducing agent, free radical scavenger, and peroxide breakdown (Shrestha et al., 2013; Shrestha et al., 2012).

Table 2.5. Fatty acid composition of unroasted mustard seed oil. Adapted with permission from Vaidya and Choe (2011b).

Fatty acid	Relative percentage
16:0	2.5 ± 0.1
18:0	1.3 ± 0.0
18:1	18.9 ± 0.3
18:2	20.8 ± 0.4
18:3	13.3 ± 0.2
20:0	0.7 ± 0.0
20:1	13.4 ± 0.1
20:2	1.0 ± 0.0
22:1	28.2 ± 0.8

Table 2.6. Bioactive and antioxidant compounds in unroasted mustard seed oil.

Compound	Concentration (μg/g)	Reference
α-tocopherol	200	Richards et al. (2008)
	75.51	Vaidya and Choe (2011b)
	145.25 ± 2.64	Vaidya and Choe (2011a)
γ-tocopherol	379	Richards et al. (2008)
	318.30	Vaidya and Choe (2011b)
	431.95 ± 3.46	Vaidya and Choe (2011a)
δ-tocopherol	16.01	Vaidya and Choe (2011b)
	24.89 ± 1.22	Vaidya and Choe (2011a)
Lutein	96.87 ± 4.66	Vaidya and Choe (2011b)
	78.15 ± 4.3	Vaidya and Choe (2011a)

2.4.2 Mustard seed oil bodies

Oil bodies from mustard seeds have been isolated by Tzen et al. (1993). The average diameter is 0.75 μm and the composition of the other constituents is listed in Table 2.7. Mustard oil bodies have a similar size to those from rapeseed but are smaller than other oil bodies such as those isolated from peanut and maize (Tzen et al., 1993). Seed oil bodies generally have a smaller size compared to fruit mesocarp which contains large oil droplets that are not mobilised by the plant (Tzen et al., 1993). Mustard oil bodies also contain little amounts of free fatty acids and phosphatidylcholine is the predominant phospholipid component. They were also isoelectrofocused at pH 5.7, indicating that they are negatively charged at pH 7 (Tzen et al., 1993).

Table 2.7. Chemical constituents of oil bodies isolated from mustard seeds. Adapted with permission from Tzen et al. (1993).

Major constituents	**Percentage (%, w/w)**
Neutral lipids	94.64
Proteins	3.25
PL	1.60
FFA	0.17
PL composition	
PC	53.1
PE	15.5
PI	13.1
PS	18.3

2.5 Potential applications of oil bodies

Oil bodies have potential applications in various industries, such as food, pharmaceuticals and cosmetics, because they are derived as natural oil-in-water emulsions and have noteworthy physical and chemical stability (Murray et al., 2007; Nikiforidis, 2019). In emulsion-based applications, synthetic oil droplets are being replaced by oil bodies because their membrane confers them high stability against various environmental stresses and allows them to interact with biopolymers in the continuous phase, resulting in the improvement of the rheological properties of emulsions.

In food formulations, oil bodies have been used to produce plant-based beverages and other plant-based dairy analogues with similar or improved characteristics as their dairy counterparts. Plant-based milk has been formulated from oil bodies from pistachio and coconut (Seow & Gwee, 1997; Shakerardekani et al., 2013), yoghurt-like formulations from maize germ and soybean oil bodies (Mantzouridou et al., 2019; Mishra & Mishra, 2013), and other beverages with probiotic properties from walnut oil bodies (Cui et al., 2013). Oil-in-water emulsion-type food products like mayonnaise and model salad dressing emulsions have also been investigated using rapeseed and maize germ oil bodies, respectively (Nikiforidis et al., 2012; Romero-Guzmán, Köllmann, et al., 2020). Oil bodies from maize germ have been incorporated in edible films which had improved flexibility and surface hydrophobicity (Matsakidou et al., 2013; Matsakidou et al., 2019).

Owing to their high interfacial activity, oil bodies and their membrane materials have been used as substitutes to synthetic emulsifiers in preparing emulsions. Intact oil bodies have been shown to act as interfacial stabilisers by adsorbing on droplet interfaces following a Pickering mechanism (Karefyllakis, van der Goot, et al., 2019a). Moreover, membrane materials from oil bodies have been isolated through the removal of the core TAG from oil bodies or by recombinant protein production (Bonsegna et al., 2011; Chen et al., 2004; Karefyllakis, Octaviana, et al., 2019; Tzen & Huang, 1992; Zhou et al., 2019). For example, oil bodies have been used in the pharmaceutical industry as nanocarriers for drugs, foreign proteins, and therapeutic peptides due to their simple extraction process from plant materials and the possibility of creating artificial or reconstituted oil bodies from recombinant oil body membrane proteins (Bonsegna et al., 2011; Chiang et al., 2011). Moreover, the membrane confers a protective ability to the oil body contents, like sensitive fatty acids or incorporated molecules for cosmetic use, against oxidation (Kawa et al., 2009; Nikiforidis et al., 2014). Lastly, researchers have explored the use of oil bodies in environmental protection, specifically the decontamination of aqueous environments from toxic organic molecules (Boucher et al., 2008). Organic pesticides have been successfully absorbed in the hydrophobic core of oil bodies, which displayed good mass transfer properties compared to other synthetic techniques.

One of the significant applications of oil bodies is the encapsulation of hydrophobic molecules. The permeability of the oil body membrane to lipophilic compounds, such as volatiles, bioactive molecules, therapeutics, and other sensitive compounds, has allowed these molecules to be entrapped and protected in the inner TAG core of oil bodies. The resulting delivery system has proved to be stable even during digestion wherein a slower digestion rate was observed compared to surfactant- or protein-stabilised artificial oil droplets (Nikiforidis, 2019).

2.5.1 Advantages and challenges

The use of oil bodies in the development of delivery systems for hydrophobic compounds presents many advantages because of their inherent physical and chemical stability properties. First, they can be derived using simple steps from their plant sources without the need for intensive bulk oil extraction (Nikiforidis, 2019). Oil bodies are also extracted in their native form, which allows their utilisation as natural or pre-emulsified oil-in-water emulsions (Iwanaga et al., 2007; Nikiforidis & Kiosseoglou, 2009). This avoids the

need for the energy-intensive homogenisation step and additional emulsifiers. The presence of antioxidants like tocopherols have also been intrinsically associated with oil bodies and they are found to have inherent oxidative stability which enables the protection of the sensitive compounds they contain (Fisk et al., 2006; Fisk et al., 2008). Aside from the safety of incorporation of oil bodies in food formulations, they also have a great impact on the clean label trend given the increasing attention of the food industry for the use of more sustainable processes and utilisation of green and natural food ingredients (Abdullah et al., 2020; Acevedo-Fani et al., 2020).

Despite this high potential of oil bodies for niche and advanced applications in the food industry, there are also challenges to their incorporation in food systems. In emulsion applications, there is a possibility of incompatibility between the oil body membrane materials and other food ingredients (Nikiforidis et al., 2014). This could lead to a product having inferior quality and sensory properties or a different structure compared to its counterpart prepared using the usual procedure. Over time, the incompatibility may also result in the instability of the system in the form of oil separation during storage. As opposed to ingredients from animal sources, the extraction of plant-based materials poses challenges due to the difficulty of breaking down the cell structure caused by sturdy cell walls and the presence of various compounds (Karefyllakis, van der Goot, et al., 2019b). Thus, the isolation of oil bodies from the plant matrix could result in complexation with other compounds, such as proteins, phenols, and polysaccharides, which could affect their stability once used as a food ingredient. As such, further investigation on the optimisation of the extraction process, identification of factors that can affect their physicochemical properties, and determination of their interactions with various food ingredients at different conditions is necessary to enhance the utilisation of oil bodies and improve their stability once included in food formulations.

2.5.2 Use of intact oil bodies

Intact oil bodies have been used in the encapsulation of hydrophobic compounds through a diffusion mechanism. When placed in contact with oil bodies, hydrophobic compounds partition inside the oil body membrane and become encapsulated in the TAG core. Through this mechanism, the integrity of oil bodies and their membrane is maintained, allowing them to maintain their physical and chemical stability.

The permeability of the oil body membrane has allowed for the entrapment of hydrophobic compounds in the oil body core; various mechanisms have been employed for the encapsulation of such compounds into intact oil bodies. Compared to biological membrane bilayers, oil bodies only have a half unit membrane comprised of a phospholipid monolayer with embedded oleosins. Thus, the partitioning of hydrophobic compounds is easier due to the decreased hindrance posed by the surface density of the phospholipid layer (Boucher et al., 2008). Moreover, once the compound partitions in the membrane, the concentration gradient and solubility of the hydrophobic compound in the lipid phase favour its diffusion inside the oil core, as observed in curcumin partitioning into intact milk fat globules (Alshehab & Nitin, 2019).

The partitioning of hydrophobic compounds can be enhanced using solvents since they can improve their dispersibility in the aqueous environment, thereby facilitating their interaction with oil bodies. For example, a system using two solvents has been developed: the bioactive compound is dissolved in a first solvent, mixed with a second solvent, and this mixture is brought into contact with oil bodies (Murray et al., 2007). Preferably, the first solvent is an organic solvent that can be readily removed by evaporation or reduced in concentration upon mixing with the second solvent, which can be water, oils, aqueous buffers, fatty acids, or lipids. Partitioning is then facilitated by incubating the solvent/bioactive compound mixture with oil bodies at a temperature above 0°C overnight or longer. These indicate that the high surface charge and the steric effects of the oleosins do not hinder the partitioning of hydrophobic bioactive compounds from the solvents or aqueous phase into the oil body core.

In cell membranes, the successful partitioning of lipophilic compounds depends on the partition coefficient of the compound (K_{ow}), steric effects, and density of the phospholipid layer, which presents a hindrance to transfer due to the orientational ordering of the phospholipid chains (Boucher et al., 2008; De Young & Dill, 1988; Dimitrov et al., 2002). For instance, in the partitioning of lipophilic compounds in milk fat globules, the high hydrophobicity of bioactive compounds such as curcumin and vitamin D3, as evidenced in their high octanol/water partitioning coefficient, facilitated their partitioning in the milk fat globule membrane (MFGM) trilayer (Alshehab & Nitin, 2019; Alshehab et al., 2019). Increasing the concentration of the compound in the aqueous phase also enhances their loading capacity inside milk fat globules (Alshehab & Nitin, 2019). Moreover, the

composition of the membrane and TAG core influence the diffusion of compounds, wherein a higher degree of unsaturation of the oil core increases the solubility of hydrophobic compounds (Alshehab et al., 2019). Similarly, a high degree of unsaturation enhances the fluidity of the membrane, enhancing the partitioning of the hydrophobic compounds. Some solvents (e.g., ethanol) also increase the permeability of cellular membranes, resulting in a consequent increase in the partitioning of molecules across a membrane (Ingram, 1989; Komatsu & Okada, 1997). Lastly, the molecular mass of the compound can affect its diffusion across a membrane, as small molecules are not greatly influenced by the steric effects within the membrane, thereby enhancing their encapsulation (Acevedo et al., 2014).

Hydrophobic compounds have been successfully incorporated into intact oil bodies through a diffusion mechanism. Hydrophobic organic pesticides have successfully partitioned into rapeseed oil bodies through the process of mixing a solution of pesticide in water with an oil body suspension followed by agitation (Boucher et al., 2008). All pesticides analysed have effectively diffused into the oil body core without interfering with the membrane, indicating that the oil body membrane does not participate in the sorption of compounds nor pose resistance to mass transfer. Compared to pure oil, there was faster partitioning of pesticides in oil bodies as opposed to pure oil even at a lower agitation rate due to the higher surface area of oil bodies. Similarly, astaxanthin was effectively microencapsulated in rapeseed oil bodies through the optimisation of encapsulation conditions such as the contact time, stirring rate, and astaxanthin/oil body ratio (Acevedo et al., 2014). A high microencapsulation efficiency of >99.7% was attributed to the high affinity of astaxanthin for TAG because of its high hydrophobicity and small molecular mass, which enhanced its mobility towards the TAG core. Higher oxidative stability and antioxidant power were observed in encapsulated astaxanthin compared to free astaxanthin, indicating the protective ability of oil bodies against astaxanthin degradation.

Another encapsulation method involves the modification of the external conditions to load bioactive compounds inside oil bodies. Zheng et al. (2019) used a pH-shift method to encapsulate curcumin in soy oil bodies. The principle was based on the pH-dependence of curcumin's water solubility: at high pH values, curcumin has high water solubility and reducing the pH decreases its water solubility, which drives it towards the lipophilic

interior of the oil bodies. After solubilising curcumin in a strongly alkaline solution (pH 12.5), it was mixed with commercial soymilk by stirring, followed by a pH adjustment to 6.8, and further stirring for 10 minutes in the dark. However, curcumin must be kept at the highly alkaline pH only for a short time because of its poor chemical stability at high pH (Zheng & McClements, 2020). An encapsulation efficiency of 94% was obtained and the resulting creamy yellow-orange dispersion with good stability against gravitational separation during storage manifested the successful incorporation of curcumin.

2.5.3 Use of oil bodies as emulsifiers

Oil bodies can also be incorporated into emulsions to serve as natural emulsifiers because of the interfacial activity of their membrane components. One approach is the incorporation of the bioactive compound in the lipid phase and then homogenising it with an aqueous oil body suspension. This has been investigated for curcumin containing emulsions that were prepared from rapeseed and soybean oil bodies (He et al., 2020; Liu et al., 2020). Both systems were able to control the rate of release of curcumin during gastrointestinal digestion although emulsions stabilised by soybean oil bodies exhibited better heat stability compared to those stabilised by rapeseed oil bodies. Through this approach, the bioactive compound can be handled easier (easier incorporation into the oil phase) while still utilising the emulsifying properties of the oil bodies.

Moreover, intact oil bodies have been shown to act as Pickering stabilisers in the oil/water interface. The behaviour of sunflower oil bodies at the interface has been investigated and their mechanism of stabilising the interface was found to depend on the size of oil bodies (Karefyllakis, van der Goot, et al., 2019a). When homogenisation was used to create an emulsion from isolated oil bodies, the smaller oil bodies (size < 5 μm) remained intact and absorbed on the oil/water interface whereas the larger oil bodies (size > 5 μm) ruptured, and their membrane material fragments acted on the interface by merging with newly formed oil droplets. The interfacial activity of sunflower oil bodies was also compared with sunflower protein isolate and oil bodies were able to diffuse faster and absorb readily at the interface immediately after droplet formation.

2.5.4 Fabrication of emulsions using oil body membrane materials

Oil body membrane materials can act as emulsifiers due to their high interfacial activity. Proteins (oleosin, caleosin, and steroleosin) and phospholipids comprise the oil body membrane, and these materials have been extracted from oil bodies by solvent extraction

and recombinant protein production (Chen et al., 2004; Tzen et al., 1997). From these interfacial-active materials, the creation of artificial or reconstituted oil bodies or oil body membrane-stabilised emulsions for novel applications has been made possible.

2.5.4.1 Extraction methods for oil body membrane materials

Membrane materials from oil bodies have been extracted through various techniques and used as emulsifiers in creating artificial oil body emulsions. Compared to the use of intact oil bodies, the use of their membrane materials presents advantages, such as the direct incorporation of the bioactive compound in the dispersed phase, customisation of the TAG composition of the lipid phase, use of conventional processing equipment for preparing emulsions, and preparation of an emulsion of the desired droplet size by controlling the emulsifier-to-oil ratio (Acevedo-Fani et al., 2020; Boon et al., 2010).

Membrane materials from oil bodies are extracted through the removal of TAG and then using the aqueous extracts as emulsifiers. This could be achieved through the disruption of the oil body membrane through methods such as repeated cycles of freeze-thaw treatments and the use of solvents for oil extraction (Beisson et al., 2001; Karefyllakis, van der Goot, et al., 2019a; Onsaard et al., 2006; Tzen & Huang, 1992; Zhou et al., 2019). Upon their rupture, the oil body membrane materials remain as membrane fragments that can adsorb at the oil/water interface to stabilise emulsion droplets (Ishii et al., 2017; Waschatko et al., 2012). The strong association of its components results in the formation of membrane fragments instead of phospholipid or oleosin micelles upon rupture (Karefyllakis, van der Goot, et al., 2019a).

Moreover, individual oil body proteins have been isolated, purified, and produced through recombinant DNA technology and used as emulsifiers separately or in combination with one another (Chen et al., 2004; Chen et al., 2005). Reconstituted oil bodies had similar structures to native oil bodies and increasing the ratio of TAG to oil body proteins resulted in smaller size distributions and improved thermostability (Peng et al., 2003). Moreover, oleosin and caleosin were found to be effective in producing artificial oil bodies while steroleosin was not because it only had two as opposed to three structural domains that are present in oleosin and caleosin (Chen et al., 2004).

2.5.4.2 Encapsulation of hydrophobic compounds using oil body membrane materials

The reconstitution of oil bodies using their constituents has resulted in emulsions having improved structural and thermostability and this method has been applied further in the encapsulation of lipophilic compounds. For example, extracting the membrane materials and TAG of almond and hazelnut oil bodies and reconstituting them with lipophilic fluorescent dyes through sonication resulted in reconstituted oil bodies with similar size to native ones (Bonsegna et al., 2011). The incorporation of dyes in the oil bodies further showed the potential of using oil bodies as delivery systems for natural bioactive drugs as demonstrated by the results of their uptake by breast cancer cells. In a similar application, cyclosporine A, a hydrophobic drug, was encapsulated in artificial oil bodies using recombinant caleosin (Chen et al., 2005). The successful encapsulation of the drug was evident in the form of milky particles and further analysis by light microscopy indicated that the artificial oil bodies stabilised by caleosin formed spherical particles with a diameter of 50-200 nm which remained stable after a week's storage. Without caleosin, artificial oil bodies were unstable and coalesced immediately after emulsification. Cyclosporine A-loaded oil bodies also had a higher relative and oral bioavailability than the commercial reference drug, demonstrating the protective effect that the artificial oil body structure has on protecting cyclosporine A against gastrointestinal degradation.

In food applications, curcumin was encapsulated into artificial oil bodies stabilised by recombinant sesame caleosin for increased bioavailability (Chang et al., 2013). Since curcumin was insoluble in seed oils, it was dissolved in a mixed dissolvent and mixed with other oil body constituents followed by sonication. This resulted in a yellow emulsified solution with an encapsulation efficiency of ~95%. Compared with native sesame oil bodies, artificial oil bodies with or without curcumin were 10 times smaller, showing that caleosin determined the size of artificial oil bodies regardless of the encapsulated material and lipid matrix used. Additionally, the artificial oil bodies were stable due to steric effects and a highly negative pH and the bioavailability of curcumin was significantly elevated by 47.7 times after encapsulation.

Acevedo-Fani et al. (2020) summarised examples of bioactive compounds that have been encapsulated using oil body membrane materials. The artificial oil bodies improved the

stability of the encapsulated compound, indicating the similarity of their structural features with native oil bodies.

Table 2.8. Bioactive compounds encapsulated in artificial oil bodies. Adapted from Acevedo-Fani et al. (2020).

Bioactive compound	Outcome/EE
Fish oil	Enhanced stability of fish oils to oxidation as compared to small molecule surfactant- or protein-stabilised emulsions
Curcuminoids	Enhanced stability of curcuminoids against degradation
Curcumin	Enhanced stability, high bioavailability of curcumin (rat model)
Curcumin	Inhibition of growth in HER2/neu-positive tumour cells (*in vitro*)
Cyclosporine A	Enhanced bioavailability of the drug (rat model)
Model hydrophobic molecules	Targeted delivery of hydrophobic molecules
Anti-cancer drug Camptothecin	High stability of the drug, oral administration of the drug encapsulated in oleosomes led to regression of tumour in a rat model

2.6 Bioactive compounds

Dietary bioactive compounds are food components that are not essential but are beneficial to health as they provide a positive effect on human biological processes (Raikos & Ranawana, 2017). Most of these bioactive compounds are highly hydrophobic, such as polyunsaturated lipids, fat-soluble vitamins, phytosterols, curcuminoids, carotenoids, and flavonoids. These lipophilic bioactive compounds exert biological effects in humans and fulfil important antioxidant, functional, nutritional, and structural functions in the body (Raikos & Ranawana, 2017). However, because of their lipophilic nature, they are incompatible with many food matrices, which limits their application into commercial food products. Moreover, they are highly sensitive to food processing and storage conditions and may have poor bioavailability (Raikos & Ranawana, 2017). Thus, a widely explored approach to overcome some of these hurdles is the incorporation of hydrophobic bioactive substances into delivery systems to improve their compatibility with aqueous

food matrices, especially with the increased interest in the development of nutraceutical and functional foods in the industry.

Generally, bioactive delivery systems should have the following characteristics: (1) food-grade; (2) can be economically manufactured from low-cost ingredients such that the benefits gained from encapsulating the bioactive outweigh the costs associated with encapsulation; (3) a high loading capacity that is retained until it needs to be delivered; (4) withstand changes during manufacturing and maintain its physical and chemical stability for a long period of time; (5) food matrix compatibility (should not adversely affect the appearance, flavour, texture, or stability of the final product); (6) should enhance or not adversely affect the bioactivity of bioavailability of the encapsulated compound; and (7) protect the bioactive from chemical and enzymatic degradation as it passes through the gastrointestinal tract so it can be released and absorbed in its active form at a particular site of action, at a controlled rate, or in response to a specific environmental stimulus (McClements et al., 2007; Raikos & Ranawana, 2017).

2.6.1 Carotenoids

Carotenoids are a family of natural pigments that are abundant in plants and other organisms like algae, bacteria, fungi, and animals (Carvalho et al., 2013; Gul et al., 2015; Raikos & Ranawana, 2017). They are responsible for the red, orange, and yellow pigments of many foods and structurally are tetraterpenes that contain 3 to 13 conjugated double bonds and, in some cases, 6 carbon ring structures at one or both ends of the molecule (Boon et al., 2010; McClements, 2007). Carotenoids are highly hydrophobic and are usually located in the core of membranes or other hydrophobic locations where they function as antioxidants and play special roles in the protection of tissues from light and oxygen damage (Boon et al., 2010). From vegetable and animal sources, more than 600 carotenoids with varying levels of provitamin A activity have been isolated (Carvalho et al., 2013). However, six specific types of carotenoids predominate in human tissue, namely α-carotene, β-carotene, β-cryptoxanthin, lutein, lycopene, and zeaxanthin (Raikos & Ranawana, 2017). Carotenoids from fruits and vegetables provide around 68% of vitamin A in the human diet (Carvalho et al., 2013).

2.6.1.1 Structure

Carotenoids have 40 carbon chains and are divided into two groups based on structure: the oxicarotenoids (xanthophylls) that contain at least one oxygen atom (e.g., α-carotene,

β-carotene, and lycopene) and those that only contain carbon and hydrogen (e.g., lutein, zeaxanthin) (Carvalho et al., 2013; Gul et al., 2015). Each molecule can have multiple *cis*/*trans* configurations based on the number of double bonds and these structural changes are brought about by chemical reactions. Endogenous carotenoids in foods are generally stable, with the *trans* isomer being the natural configuration of most carotenoids in plants (Carvalho et al., 2013; McClements, 2007). However, they are relatively unstable in food systems as additives because they are susceptible to light, oxygen, and autooxidation. Carotenoid degradation reactions result in the scission of the molecule or the loss of double bonds (McClements, 2007). Moreover, their highly unsaturated nature makes them prone to isomerisation during processing and storage. Exposure to heat, light, and acidity promotes their isomerisation to the *cis* configuration, resulting in the reduction in their colour and provitamin A activity (Carvalho et al., 2013; McClements, 2007). For this chapter and the work done in this thesis, the discussion is restricted to β-carotene only (see Section 2.6.2).

2.6.1.2 Functions

Carotenoids play a major role in human biological functions related to immunity and gap junction communication and function as beneficial xenobiotics in the body (Raikos & Ranawana, 2017). The main carotenoids in human health are β-carotene, α-carotene, lycopene, lutein, β-cryptoxanthin, and zeaxanthin (Carvalho et al., 2013). All these compounds except for zeaxanthin can be easily obtained from food, with β-carotene being the most abundant in the human diet and having the highest provitamin A activity. Aside from serving as vitamin A precursors and their role as macular pigments of the eye, carotenoids have been suggested to prevent some types of cancers, protect the gastric mucosa against ulcers, prevent photosensitisation in skin diseases, enhance the immune response against infection, and provide anti-aging properties (Carvalho et al., 2013; McClements, 2007; Raikos & Ranawana, 2017). They also possess antioxidant activity and play a role in cellular process such as modulating the inflammatory response and preventing cardiovascular diseases and cataract.

Various factors influence the absorption and utilisation of carotenoids in the human body, such as the properties of the food matrix, food processing conditions, co-ingestion with fibre and fat, gastrointestinal diseases, and malnutrition status. Their absorption and transport are similar to that of lipids: they are incorporated into mixed micelles comprised

of fatty acids, bile acids, monoglycerides, and phospholipids upon ingestion. They are then converted into retinol and transported to the liver where 90% of vitamin A in the body are stored. For the provitamin A carotenoids, the *trans* isomer is more easily converted into vitamin A compared to the *cis* isomer (Carvalho et al., 2013).

2.6.1.3 Limitations for incorporation in foods

Although carotenoids are abundant in foods, they are poorly bioavailable. Processing conditions cause structural changes and affect their bioavailability. Moreover, it is difficult to maintain their integrity in food systems as they are susceptible to both autooxidation and oxidation by heat, light, and oxygen. They also have a high melting point, making them crystalline at body temperatures and at ambient conditions, which is a challenge in their utilisation in functional foods (McClements, 2007; Raikos & Ranawana, 2017). Crystalline materials are difficult to incorporate in liquid food products due to their tendency to aggregate and sediment, posing problems concerning consistent dosing as some of the bioactive component may not be ingested (McClements, 2012). The appearance, texture, or mouthfeel of the product may also be adversely affected, making consumers unwilling to consume them. The crystallinity of carotenoids also affects their absorption in the GIT as it reduces their solubility and permeability (McClements, 2012).

2.6.2 β-carotene

β-carotene is a major carotenoid present in the human diet and is responsible for the red and orange-coloured pigment in many fruits and vegetables. Good sources of β-carotene include mangoes, carrots, sweet potatoes, cantaloupe, melons, pumpkin, peppers, greens (collard, spinach, lettuce, kale), asparagus, and broccoli among others (Boon et al., 2010; Carvalho et al., 2013; Gul et al., 2015). It is the main source of vitamin A in humans as it has the highest provitamin A activity among the carotenoids: it can yield two retinol molecules in the presence of oxygen upon the action of β-carotene-15,15'-monooxygenase (Gul et al., 2015). As an additive, it occurs as red to brownish red to violet crystals or crystalline powder.

2.6.2.1 Structure

β-carotene ($C_{40}H_{56}$) is characterised by a polyene structure having 11 conjugated double bonds and two β-rings (Figure 2.6). The *trans* isomer is a linear and rigid molecule while the *cis* isomers are bent structures. Naturally occurring β-carotene is predominantly in the

form of *trans* isomers, although some amounts of *cis* are also present. The *trans* configuration is highly unstable and can easily undergo isomerisation to the *cis* form upon exposure to heat, light, and oxygen during processing and storage as a result of thermal and chemical oxidation and photosensitisation (Gul et al., 2015).

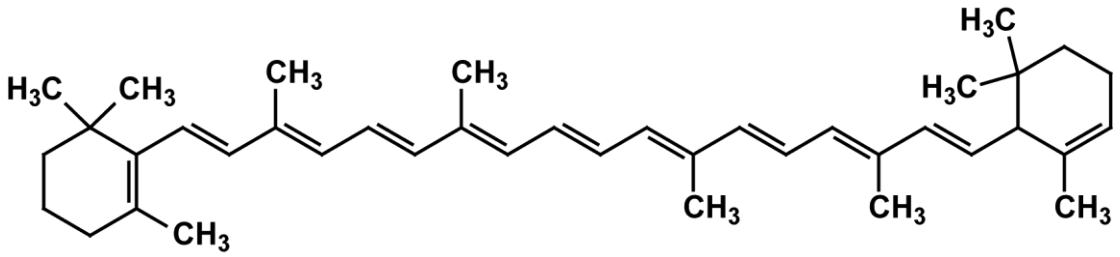

Figure 2.6. Structure of β-carotene (*trans* isomer).

Because of its characteristic conjugated polyene chain, β-carotene is highly susceptible to degradation to several agents. Its degradation is mainly caused by oxidation and the mechanisms of oxidation are highly influenced by the agent involved in the initiation of degradation. The main mechanisms of carotenoid oxidation are the following: autoxidation, thermal degradation, photodegradation, electron transfer, hydrogen abstraction, adduction formation, and reaction with singlet oxygen, acid, iron and iodine, and free radicals (Boon et al., 2010).

Carotenoid oxidation follows a first-order kinetics and occurs as follows: part of the *trans* molecule is isomerised into *cis* forms, then both *trans* and *cis* isomers are oxidised. Epoxidation and hydroxylation then occurs and results in carotenoid fragmentation, which generates low molecular weight compounds like aldehydes, ketones, and aromatic compounds that are responsible for either desirable or off-flavours in processed foods (Mao et al., 2018). Once oxidation is initiated by one or a number of the oxidising agents, carotenoids further react with themselves or other chemical species within the environment to form various degradation products that could result in loss of bioactivity or adversely affect the product quality (e.g., colour loss, rancidity) (Boon et al., 2010; Mao et al., 2018). Carotenoids also undergo isomerisation due to electron transfer reactions from neutral carotenoids to radicals or compounds like iron and acids that can easily transfer charge (Boon et al., 2010).

2.6.2.2 Health benefits

β-carotene is of major interest in the food industry because of its provitamin A activity. Vitamin A is not synthesised by the body so it must be obtained in the diet as it is essential for maintaining good eye health and preventing night blindness and xeropthalmia (Gul et al., 2015). Other health benefits of β-carotene once converted into vitamin A include the maintenance of healthy skin and mucus membrane, embryonic development, and enhancement of immune response (Boon et al., 2010; Carvalho et al., 2013; Mao et al., 2018). Moreover, it has a high antioxidant capacity, allowing it to protect animal and plant tissues by quenching singlet oxygen and reducing lipid oxidation by acting as free radical scavengers (Boon et al., 2010). Because of its antioxidant activity, β-carotene has been proposed to (1) play a role in the prevention of cardiovascular disease by protecting LDL cholesterol from oxidation or reducing platelet aggregation and (2) reduce the risk of certain cancers by participating in gap junctional communication, which allows cell-to-cell communication and could help prevent the growth of altered cells (Boon et al., 2010).

2.6.2.3 Bioavailability

Bioavailability is defined as the proportion of a nutrient that is digested, absorbed, and metabolised through normal pathways (Gul et al., 2015). It is partially determined by its bioaccessibility, which refers to the fraction of the ingested nutrient that is incorporated into mixed micelles and become available for absorption in the body (Mao et al., 2018). The absorption of β-carotene goes as follows (Mao et al., 2018): upon its release from the food matrix, β-carotene has to be incorporated into oil droplets formed during lipid digestion or present from the original food (e.g., emulsions). Then, lipid digestion is initiated by the attachment of lipases from the gastric juices at the oil droplet surface. Mixed micelles containing bile salts, phospholipids, and the digested lipid products are then formed, and these act as carriers to solubilise β-carotene and facilitate its transport to the epithelium cells before absorption. As such, factors that affect lipid digestion influence how β-carotene is absorbed in the body.

Many factors affect the bioavailability of β-carotene, such as the food composition and structure, methods of processing, co-ingested food, and physiological differences among individuals (e.g., eating behaviour, compositions of digestive juices, health status) (Gul et al., 2015; Mao et al., 2018). The type of food matrix is the main factor that affects β-

carotene bioavailability; naturally occurring β-carotene has low bioavailability because they exist as crystals or are involved in protein complexes that are not fully released during digestion within the GIT (Gul et al., 2015). Moreover, the intestinal absorption of β-carotene in humans varies depending on the amount of β-carotene consumed in a meal and its conversion into vitamin A, rate of absorption, transport, chemical nature, nutrient status of the host, genetic factors, host-related factors, and the complexity of release in the GIT during digestion (Gul et al., 2015).

2.6.3 Emulsions as delivery systems

Emulsions are suitable delivery systems for β-carotene because they are relatively easy and inexpensive to prepare compared to other types of delivery systems, and they can be easily added into food products as the production of many food products involves emulsification (Mao et al., 2018; McClements, 2010).

An emulsion is composed of two immiscible liquids, usually oil and water, in which one of the liquids is dispersed as small spherical droplets in the other (McClements, 2016). There are two major classifications of emulsions: an oil-in-water (O/W) emulsion wherein oil droplets are dispersed in a watery phase, and a water-in-oil (W/O) emulsion wherein water droplets are dispersed in an oily phase. The liquid that makes up the droplets is termed the dispersed phase whereas the surrounding liquid is the continuous phase. Emulsions are also classified depending based on the droplet size of the dispersed phase: (1) a conventional emulsion or macroemulsion that has droplet diameters between 100 nm and 100 μm, (2) a nanoemulsion with droplets that range from 20 to 100 nm in diameter, and (3) a microemulsion with droplet diameters of 5 to 50 nm (McClements, 2010). Except for microemulsions, emulsions (conventional emulsion and nanoemulsion) are generally thermodynamically unstable because of the large interfacial area between the two immiscible liquids. Hence, they tend to break down over time due to gravitational separation, flocculation, coalescence and/or Ostwald ripening (McClements, 2016). Nonetheless, kinetic stability can be achieved through the incorporation of stabilisers in the system, such as emulsifiers, texture modifiers, weighting agents, and ripening retarders.

Oil-in-water emulsions are usually prepared by homogenising an oil phase and an aqueous phase together with a water-soluble emulsifier. In emulsion-based delivery systems, the hydrophobic bioactive compounds are usually incorporated in the oil phase

before homogenisation with the water phase. If the bioactive compound is crystalline, it is important to ensure that crystallisation is avoided or that the emulsion remains stable even if crystallisation occurs because it can promote the destabilisation of the delivery system throughout its lifetime (McClements, 2012). Hence, crystalline bioactives should be added at a level below its saturation concentration in the carrier oil or to heat the oil phase to dissolve the crystalline compounds before homogenisation (McClements, 2010).

Moreover, homogenisation conditions must be carefully controlled if the bioactive compound is susceptible to chemical degradation to reduce their exposure to factors that will enhance their degradation, such as high temperatures, oxygen, light, or transition metals. Lastly, the emulsion should be designed such that the encapsulated bioactive compound will be released within the GIT and absorbed by the body; otherwise, its bioactivity will be reduced (McClements, 2012).

2.6.3.1 Advantages and limitations of emulsion-based delivery systems

The delivery of bioactive compounds in edible form is done in the food and pharmaceutical industries since a diet-based approach is usually used for the prevention of chronic diseases. Despite its wide range of health benefits, the application of β-carotene is limited by its hydrophobicity, crystallinity at ambient temperature, and chemical instability. Naturally occurring β-carotene is also usually complexed with proteins, which hinders its absorption in the human body (Mao et al., 2018). As such, most food systems use emulsion-based delivery systems because these are easy and inexpensive ways to encapsulate the bioactive compound and improve their bioactivity since they can be incorporated into a food or beverage that can easily be consumed by eating or drinking.

Emulsions can be ideal systems for the delivery of β-carotene and its incorporation in foods since the bioavailability of β-carotene can be enhanced by co-ingestion with lipids, as digested products of lipids form mixed micelles that can solubilise and transport β-carotene to epithelium cells (Mao et al., 2018). Also, they are efficient, affordable, and convenient methods to enhance the dispersibility, stability, and bioactivity of bioactives in food products (Boon et al., 2010). All three components of the emulsion (i.e., dispersed phase, continuous phase, and emulsifier) can be engineered to enhance the stability of the system: (1) the emulsifier can provide a physical or electrostatic barrier on the interface to prevent contact with prooxidants in the aqueous phase; (2) the oil where β-carotene is dispersed can be selected or added with antioxidants to improve stability; and (3) the pH

may be controlled to ensure the physical stability of the emulsion. Moreover, the homogenisation pressure can be controlled to produce a smaller droplet size with better physical stability and which is more readily adsorbed (Mao et al., 2018).

However, emulsions are prone to flocculation, coalescence, or creaming upon exposure to environmental stresses commonly encountered during food processing (e.g., changes in temperature and pH) (Boon et al., 2010; Mao et al., 2018). Furthermore, the large surface area of emulsified lipids, especially in nanoemulsions, increases the contact and interactions of the bioactive compounds in the oil droplets with prooxidants present in the aqueous phase (Boon et al., 2010; Mao et al., 2018).

2.6.3.2 Emulsions as delivery systems for β-carotene

Examples of emulsion-based delivery systems β-carotene stabilised by proteins, phospholipids, and surfactants are summarised in Table 2.9. The design of the delivery system is vital to ensure its stability and ability to protect the bioactive compound from degradation. First, the physical state of the lipid carrier affects the stability of the bioactive compound. The stability of β-carotene during storage at room temperature was higher when it was encapsulated in a solid lipid matrix, increasing its bioavailability and protecting it from damage due to reactive species (Cornacchia & Roos, 2011). The decreased degradation was attributed to the solid state of the lipid which made it unavailable to act as a medium for reactions to occur due to reduced molecular movement, resulting in limited transport and exchange of reactive species and products.

Another factor that affects the stability of delivery systems is the type of emulsifier used. Although small molecule surfactants are more effective at producing smaller emulsion droplets with better physical stability, emulsions stabilised by globular proteins have been shown to be more effective at reducing β-carotene degradation (Jo & Kwon, 2014; Mao et al., 2010; Qian et al., 2012). In β-carotene nanoemulsions, the least degradation was observed when whey protein isolate (WPI) was used as an emulsifier, wherein 66% of β-carotene was retained after 12 days at 55°C (Mao et al., 2018). This was attributed to the cysteyl residues, disulphide bonds, and thiol functional groups in WPI which can prevent lipid oxidation by free radicals. Moreover, the rate of β-carotene degradation in β-lactoglobulin nanoemulsions was significantly slower compared to emulsions stabilised by Tween 20 (Qian et al., 2012). The mechanisms for the protective effect of proteins were attributed to the (1) antioxidant activity of proteins either through the chelation of

transition metals or by acting as free radical scavengers; (2) formation of molecular complexes with carotenoids through hydrophobic interactions; (3) steric hindrance due to the adsorbed proteins at the interface that prevented the contact of the bioactive in the oil droplets with any prooxidants in the aqueous phase; or (4) smaller interfacial area compared to Tween-stabilised emulsions (Jo & Kwon, 2014; Qian et al., 2012).

Lastly, homogenisation pressure greatly influences the physical stability of emulsion-based delivery systems. With an increase in mechanical energy, which can be achieved through the increase in homogenisation pressures or homogenisation cycles, smaller droplet sizes can be produced which are more stable to gravitational factors during storage (Jo & Kwon, 2014; Mao et al., 2010). However, a drawback to having a small droplet diameter is the increase in the surface area of the droplets, which enhances the contact of the bioactive with prooxidants in the aqueous phase, and the possible formation of free radicals due to cavitation during microfluidizer processing (Jo & Kwon, 2014).

Table 2.9. Emulsion-based delivery systems for β-carotene.

Delivery system	β-carotene concentration	Oil type and content	Emulsifier type and content	Processing method	Reference
Emulsion	0.05% (w/w)	Sunflower oil (10%), hydrogenated palm kernel oil (10%)	WPI (0.8%) Sodium caseinate (0.8%)	Homogenisation	Cornacchia and Roos (2011)
Nanoemulsion	1% (w/w)	MCT oil	DML (10%) Tween 20 (10%) WPI (10%) OSA (10%)	Microfluidisation	Mao et al. (2010)
Nanoemulsion	0.25% (w/w)	Orange oil (10%)	β-lactoglobulin (2%)	Microfluidisation	Qian et al. (2012)
Nanoemulsion	0.03% (w/w)	MCT oil (3%)	Tween 20 Tween 80 WPI Sodium caseinate Soy protein isolate	Microfluidisation	Jo and Kwon (2014)
Emulsion	0.03 % (w/w)	Soybean oil (1.8%)	Lecithin (1.0% w/w) + WPI (2.0% w/w)	Homogenisation	Guan et al. (2016)

Table 2.9. Emulsion-based delivery systems for β-carotene (continued).

Delivery system	β-carotene concentration	Oil type and content	Emulsifier type and content	Processing method	Reference
Emulsion	0.1% (w/w)	Soybean oil (10%)	MFGM (0.25-4% w/w)	Homogenisation	He and Ye (2019)
Emulsion		Olive oil (5%)	L-α-phosphatidylcholine (1, 2, 3, 4%)	Homogenisation	Verrijssen et al. (2015)
Emulsion	0.075 % (w/w)	MCT oil (5%)	WPI (0.5%)	Microfluidisation	Xu et al. (2013)
Emulsion	0.15% (w/w)	MCT oil (10%)	Soybean soluble polysaccharides WPI Decaglycerolmonolaurate (ML750)	Homogenisation	Hou et al. (2014)
Emulsion	0.3% (w/w)	Sunflower oil (10%)	Tween 20 (2% w/w) BSA (1% w/w) WPC (1% w/w) BSA (1% or 2% w/w) + Tween 20 (2% w/w) WPC (1% or 2% w/w) + Tween 20 (2% w/w)	Premix membrane emulsification	Trentin et al. (2011)
Emulsion	0.1% (w/w)	Corn oil (5 or 10%)	Sodium caseinate (2%)	Microfluidisation	Yi et al. (2014)

Due to the increasing demand for green products, novel encapsulation systems that could better protect bioactive compounds without the need for synthetic emulsifiers are still being developed. These include multilayer emulsions, solid lipid particles, microemulsions, Pickering emulsions, multiple emulsions, gelled emulsions (filled hydrogel), and protein-polysaccharide coacervates. However, these are sometimes more costly, difficult to prepare, and more unstable than conventional delivery systems. Thus, further research is needed to explore more systems that can effectively encapsulate bioactive compounds and potentially enhance their functionality while still being economical to produce.

2.7 Research gap

Oil bodies are promising materials that can be used as delivery systems of hydrophobic compounds because of their complex interfacial structure that impart their stability inside the cell or in isolated preparations. Hence, there is an increasing interest in the food industry to utilise oil bodies as novel ingredients. Studies have also shown that emulsion-based delivery systems fabricated from oil bodies exhibited not only physical stability but also chemical stability of the entrapped functional compound. However, the properties of oil bodies after extraction vary depending on the source; thus, the characterisation of new potential materials is necessary before their application. Challenges have also been associated with the extraction of oil body membrane materials. Hence, the development of suitable methods to isolate oil body membrane materials will help to advance its applications. Moreover, studies on the encapsulation of bioactive compounds in oil bodies for food applications are limited, and most were done on a laboratory scale. Therefore, the exploration of other techniques to encapsulate such compounds presents novel findings on how the structure of oil bodies allow the incorporation of other compounds and how the interfacial materials stabilise delivery systems. Further investigation is also needed on the behaviour of the encapsulation systems during storage to determine if they are comparable or better than conventional emulsion-based delivery systems for bioactive compounds.

This study aimed to utilise oil bodies from hemp and mustard seeds as encapsulation systems for β-carotene. Different strategies to prepare delivery systems from oil bodies and their membrane materials were used, and their ability to successfully encapsulate β-carotene were compared.

Chapter 3 Materials and methods

3.1 Materials

Unless stated otherwise, all chemicals were purchased from Sigma Aldrich Ltd. (St. Louis, MO, USA) and the reagents were made up in Milli-Q water (Milli-Q apparatus; Millipore Corp., Bedford, MA, USA). Hemp seeds, hempseed oil, and mustard seeds were bought from a local supermarket.

3.2 Methods

3.2.1 Microstructure of oil bodies in seeds

The oil bodies in cells of seeds (hemp or mustard) were examined by cryo-SEM imaging.

3.2.1.1 Sample preparation

Mustard seeds or dehulled hemp seeds were placed in the sample holder and flash-frozen by dipping in liquid nitrogen. After 10 min of contact with liquid nitrogen, the frozen sample was transferred to the cryo-unit sectioning chamber and placed under vacuum. The temperature of the sample was lowered to -120°C followed by fracturing using a cold knife.

3.2.1.2 Sample imaging

The temperature of the sample was gradually raised to -100°C for 20 min for sublimation. The fractured surface of the seeds was then coated with a thin platinum coating (10 mA for 240 s) and the samples were transferred to the imaging chamber. SEM images of fractured sections were recorded at 6 to 20 kV on a Joel JSM 6500F Field Emission Scanning Microscope. A total of five (5) different sections were examined and images were captured at different resolutions.

3.2.2 Extraction of oil bodies from hemp and mustard seeds

Hemp seeds were soaked overnight in Milli-Q water at a seed-to-water ratio of 1:4 (w/w). Then, the mixture was ground using a colloid mill at a frequency of 30 Hz. To remove the solids, the resulting mixture was passed through a clarifier and the hemp milk was collected for cream extraction. Hemp oil bodies were extracted from the milk by centrifugation at 10,000 *g* for 20 min at 20°C. The cream layer called ‘oil body fraction’ was then carefully removed from the aqueous layer for experimental studies and added with sodium azide (0.02% w/w) to inhibit the growth of microorganisms.

To extract oil bodies from mustard seeds, the seeds were soaked overnight in Milli-Q water at a seed-to-water ratio of 1:4 (w/w). The mixture was then ground for 5 min using a hand blender and filtered using a 200 μm nylon mesh fabric to obtain the mustard milk. Oil bodies were obtained by centrifugation, as specified above, and the cream layer (also called 'oil body fraction') was separated. Sodium azide was added as an antimicrobial before storage.

3.2.3 Characterisation of oil body fractions

3.2.3.1 Particle size

The particle size of the oil body fractions was measured by static light scattering using a Mastersizer 2000 (Hydro MU, Malvern, Worcestershire, UK). Samples were dispersed in Milli-Q water or a sodium dodecyl sulphate (SDS) solution (1.2% w/v). The data was reported in Sauter-average diameter ($d_{3,2}$), volume-mean diameter ($d_{4,3}$), and particle size distributions. The refractive index of hempseed oil, mustard oil, and water used in the protocols for measurement was 1.475, 1.45, and 1.33, respectively. The mean particle size was calculated as the average of triplicate measurements.

3.2.3.2 ζ-potential

The ζ-potential of the oil body fractions was determined using a Zetasizer Nano ZS (Malvern Instruments Ltd., Malvern, UK) equipped with a 4 mW He/Ne laser at a wavelength output of 633 nm. Samples were diluted to a final particle concentration of 0.01% (v/v) in Milli-Q water and put in an electrophoresis cell (Model DTS1070, Malvern Instruments Ltd.) at 25°C. The ζ-potential was read at least 10 times for each sample and the ζ-potential values were calculated by Smoluchowski approximation. Mean values were calculated from triplicate measurements.

3.2.3.3 Microstructure

The microstructure of the oil body fractions was investigated using a confocal laser scanning microscope (Model Leica SP5, DM6000B, supplied by Leica Microsystems, Heidelberg, Germany) with a 63-mm oil immersion objective lens. Nile Red (1 mg/mL in acetone) and Fast Green FCF (1 mg/mL in Milli-Q water) were used to selectively stain neutral lipids and proteins, respectively, based on the staining protocols described by Gallier et al. (2012). Briefly, 200 μL of the diluted oil body fraction (0.1% v/v fat) was mixed with 12 μL of Nile Red and 6 μL of Fast Green FCF. The stained sample was placed on a concave microscope slide, covered with a cover slip (0.17 mm thick), and

immediately examined using the confocal laser scanning microscope. On the other hand, the dye Lissamine™ rhodamine B (Rd-DHPE, 1 mg/mL in chloroform) was used to stain the samples to determine the distribution of phospholipids on the interface of the oil droplets. Briefly, 100 µL of the diluted oil body fraction (0.1% v/v fat) was added with 5 µL of Lissamine™ rhodamine B (Rd-DHPE). The stained sample was placed on a concave microscope slide, covered with a cover slip (0.17 mm thick), and examined using the confocal laser scanning microscope.

The morphology of the hemp oil body fraction was also examined by cryo-SEM. The sample preparation for cryo-SEM imaging was followed as per the protocol described by Efthymiou et al. (2017). Briefly, a drop of oil body suspension was placed between two small copper grids and the excess sample was gently soaked dry by a filter paper. The sample sandwiched between the grids was then placed in a jet freezer assembly (Baltec JFD 030) and frozen rapidly to -186°C using a continuous propane stream for 30 min. Upon freezing, the copper grid from one of the sides was removed and the sample was placed on the sample holder maintained at -180°C of the cryo-SEM apparatus and was transferred to the cryo-unit sectioning chamber and placed under vacuum. The sample imaging was done as described in Section 3.2.1.2 with modifications. Instead of a platinum coating, the surface of the sample was coated with a thin palladium coating and SEM images of the fractured sections were recorded at 5 kV at -120°C on a Joel JSM 6500F Field Emission Scanning Microscope equipped with an energy-dispersive detector and a Gatan Alto2500 cryo-unit.

3.2.4 Colloidal stability of oil body fractions

The stability of oil bodies in the food matrix must be ensured once they are incorporated in the food matrix in commercial applications. Their stability may be affected by changes in their environment such as variations in pH, ionic strength, and temperature. For instance, aggregation of oil bodies may be promoted at pH values close to the isoelectric point of the interfacial proteins and in the presence of salt due to the alterations in their net surface charge. Thus, to predict their potential interactions within the food matrix, the colloidal stability of the hemp and mustard oil body fractions were determined by changing their pH and ionic strength in solution. To determine the influence of pH on the colloidal stability of the oil body fractions, hemp and mustard cream (also called the 'oil body fraction') were suspended in Milli-Q water at an oil body fraction-to-water ratio of

1:3 (w/w). The suspensions were then adjusted to pH 2-10 using 0.1 M HCl or 0.1 M NaOH. For the effect of ionic strength, the hemp oil body fraction was suspended at different concentrations of NaCl (0, 62.5, 125, 250, 500, and 1,000 mM). The particle size and ζ-potential of the samples were determined as described in Section 3.2.3.1 and Section 3.2.3.2, respectively.

3.2.5 Composition of hemp oil body fraction

The analysis of the composition, such as moisture content, fat content, crude protein content, ash content, and fatty acid profile, of the hemp oil body fraction was performed at the Nutrition Laboratory of Massey University, Palmerston North, New Zealand. The following methods were used for analysis: vacuum oven drying (AOAC 990.19, 990.20) for moisture, Mojonnier method (flour, baked, extruded products, AOAC 922.06) for fat, Dumas method (AOAC 968.06) for crude protein, and furnace drying at 550°C (AOAC 942.05 for feed, meat) for ash content. Moreover, the fatty acid composition of the hemp oil body fraction was determined using gas chromatography based on the protocol of Sukhija and Palmquist (1988).

3.2.6 Fat content of hemp oil body fraction

The fat content of the samples was analysed using the protocol of Bligh and Dyer (1959). Briefly, 2 g of sample was placed into centrifuge tubes and added with 2 mL of chloroform and 4 mL of methanol. This was blended for 2 min using a vortex mixer. Then, 2 mL of chloroform was added and blended for 30 s, followed by 2 mL of Milli-Q water, and blending for a further 30 s. The tubes were then centrifuged at 3,000 *g* for 10 min. After centrifugation, the mixture was separated into the methanol layer and a heavier chloroform layer containing the extracted neutral lipids. The methanol layer was carefully removed by aspiration using a transfer pipette and the bottom chloroform layer was collected into a pre-weighed beaker and left in the fume hood overnight to evaporate the chloroform. The amount of extracted fat left in the beaker was weighed and expressed as a percentage (w/w) of the sample.

3.2.7 Protein content of hemp oil body fraction

The protein content was determined by measuring the total organic nitrogen content using the Kjeldahl method (AOAC Official Method 991.20), which involved three steps: digestion, distillation, and titration. For digestion, approximately 10 g of oil body fraction was placed into each digestion tube and added with two Kjeltabs (each containing 3.5 g

K_2SO_4 and 0.0035 g Se) and 15 mL concentrated H_2SO_4. At the same time, a blank digestion tube was prepared and it contained all the other reagents except the sample. The digestion tubes were then placed in a block digestor unit (Kjeltec 2100, Sweden) and the samples were digested at 420°C until they became clear. After digestion, the tubes were removed from the digestion block, cooled for 10 min, and added with approximately 70 mL of reverse osmosis (RO) water while shaking gently to mix.

For distillation, conical flasks were added with 25 mL of 4% boric acid solution (w/v, with 0.1% bromocresol green and 0.1% methyl red as indicators) and each was placed on the platform of the distillation apparatus (Kjeltec 2100, Sweden) per trial. Each digestion tube was then connected to the distillation apparatus that was set on 'automatic' and automatically added with 40 mL of 40% NaOH. The safety door of the unit was closed to begin the distillation process. After distillation, the digestion tube was removed from the apparatus and the receiver conical flask containing the distillate was titrated with standardised 0.1 M HCl to a grey-mauve endpoint. The volume of HCl used was recorded and used to calculate the protein content using the following equations:

$$\% \text{ Nitrogen} = \frac{\text{volume of HCl used (mL)} \times \text{molarity of HCl} \times 14 \times 100}{1{,}000 \times \text{weight of sample (g)}} \quad (1)$$

$$\% \text{ Protein} = \% \text{ Nitrogen} \times 6.25 \quad (2)$$

3.2.8 Encapsulation methods of β-carotene using the hemp oil body fraction

3.2.8.1 Solubility of β-carotene in hempseed oil

To determine the amount of β-carotene that can be incorporated into oil bodies, the solubility of β-carotene in hempseed oil was first analysed. β-carotene was added to hempseed oil at different concentrations (125, 250, and 500 μg/g) and the mixture was heated to 50°C with stirring for 10 min and sonicated for 5 min to dissolve any remaining crystals. The mixture was then centrifuged at 6,000 rpm or min to remove any undissolved crystals. Two (2) extraction procedures were used to determine the method to be used for β-carotene quantification in hempseed oil: one was using a mixture of hexane and dichloromethane based on the method described by Lin et al. (2018) and the other was using hexane based on the method of Yuan et al. (2008) with modifications. For comparison, the method was also tested on soybean oil based on the known solubility of β-carotene which is 203.7 μg/mL (Peng et al., 2018).

3.2.8.2 Encapsulation of β-carotene using intact oil bodies

This approach aimed to promote the diffusion of β-carotene inside the oil bodies without causing significant changes in their structure. This was tested using two methods: (1) incorporation with organic solvents and (2) without solvents.

3.2.8.2.1 With solvents

In the first method, ethanol, hexane, and diethyl ether were used to dissolve β-carotene, which was in crystalline form, at a concentration of 500 μg/mL of solvent. This was then injected from a syringe to a hemp oil body suspension (10% w/w), at a concentration of 400 μg/g of oil. The β-carotene-loaded oil body suspensions were then either left unstirred or stirred for 4 h at room temperature (~22°C). The solvents were removed by centrifugation and evaporation using a vacuum concentrator (Savant SC250EXP SpeedVac Concentrator, Thermo Scientific, US) set at 25°C at the maximum vacuum pressure (20.0) for 20 min. The β-carotene content of the cream layer and serum layer was quantified by the method described in Section 3.2.9.2.

3.2.8.2.2 Without solvents

In the second method, β-carotene was added into the hemp oil body fraction without dilution and the mixture was heated in a water bath at 50°C and stirred for 10 min. After heating, the mixture was sonicated for 5 min to ensure the full dissolution of β-carotene crystals. The resulting β-carotene-loaded hemp oil body fraction contained ~400 μg/g of β-carotene by oil weight. A 10% (w/w) oil body suspension was then prepared by mixing the β-carotene-loaded oil body fraction with Milli-Q water and stirring the mixture for 5 min at room temperature (~22°C).

3.2.8.3 Encapsulation of β-carotene using disrupted oil bodies

This approach explored the disruption of the membrane of hemp oil bodies to entrap β-carotene. This was tested by using two methods: (1) re-emulsification of intact oil bodies and (2) emulsification using oil body membrane materials (OBMM).

3.2.8.3.1 Re-emulsification of intact oil bodies

The hemp oil body fraction was treated by homogenisation to induce membrane disruption and re-emulsification of the oil bodies. The effect of different homogenisation pressures was first examined to determine the level of membrane disruption. The hemp oil body fraction was dispersed in Milli-Q water to create a 10% (w/w) oil body

suspension and a coarse emulsion was prepared using a high-speed blender (LabServ D-500 Homogenizer, Biolab Limited, New Zealand) at 10,000 rpm for 2 min. After blending, the primary emulsion was homogenised as follows: (1) passing twice through a two-stage valve homogeniser (also called 'low-pressure homogeniser') (FBF Homolab Laboratory Homogeniser, FBF Italia, Italy) at a pressure of 250/50 bar; or (2) passing thrice through a microfluidizer (M110P Microfluidizer, Microfluidics, USA) at a pressure of 500, 750, or 1,000 bar. The resulting samples were named 'homogenised oil bodies'.

Based on the results from the previous study, a homogenisation treatment using the low-pressure homogeniser was selected to prepare homogenised oil bodies containing β-carotene. First, the β-carotene-loaded hemp oil body fraction, obtained from the method described in Section 3.2.8.2.2, was added with Milli-Q water to make a 10% oil body emulsion (w/w). A coarse emulsion was first prepared by blending using a high-speed blender (LabServ D-500 Homogenizer, Biolab Limited, New Zealand) at 10,000 rpm for 2 min. After blending, the primary emulsion was passed twice through a two-stage valve homogeniser (FBF Homolab Laboratory Homogeniser, FBF Italia, Italy) at a pressure of 250/50 bar.

3.2.8.3.2 Emulsification using oil body membrane materials (OBMM)

The OBMM was also extracted from the hemp oil body fraction and used as an emulsifier to produce oil body emulsions. First, the hemp oil body fraction was mixed with Milli-Q water to a 1:1 ratio (w/w). The mixture was then heated at different temperatures (50°C, 70°C, and 100°C) with continuous stirring for 1 h. The samples were cooled to room temperature and centrifuged at 3,000 *g* for 10 min to separate the different fractions. The top free oil and remaining cream layer were removed by suction under vacuum and the serum and sediment layers were collected and stirred together for 5 min. The combined serum and sediment fractions were deemed as the 'oil body membrane material (OBMM) fraction'. These fractions were analysed by optical microscopy using a light microscope (Nikon, Japan). The total solids, fat, and crude protein content of the OBMM were determined as described in Sections 3.2.5, 3.2.6, and 3.2.7, respectively.

Oil-in-water emulsions containing 2.5% β-carotene-loaded hempseed oil were prepared by mixing different proportions of extracted oil body membrane material at the following protein-to-oil ratios: 0.14:1, 0.28:1, 0.42:1, and 0.55:1. Then, a coarse emulsion was prepared by blending using a high-speed blender (LabServ D-500 Homogenizer, Biolab

Limited, New Zealand) at 10,000 rpm for 3 min. After blending, the primary emulsion was passed once through a two-stage valve homogeniser (FBF Homolab Laboratory Homogeniser, FBF Italia, Italy) at a pressure of 100/50 bar.

3.2.9 Characterisation of β-carotene-loaded hemp oil body systems

3.2.9.1 Physical and structural properties

The particle size and ζ-potential of the β-carotene-loaded oil body systems were analysed according to Sections 3.2.3.1 and 3.2.3.2. The structural properties of these systems were determined by confocal laser scanning microscopy according to Section 3.2.3.3.

3.2.9.2 Determination of β-carotene concentration and encapsulation efficiency

After the incorporation of β-carotene, the β-carotene-loaded emulsions were centrifuged at 10,000 *g* for 20 min for phase separation. The orange-coloured cream and the serum layer were collected and analysed separately for β-carotene concentration spectrophotometrically following the method of Yuan et al. (2008). Briefly, 1 g of either cream or serum sample was weighed into a centrifuge tube and was first extracted with a mixture of 2 mL ethanol and 3 mL of hexane. The mixture was then shaken and the hexane phase was removed and transferred into another tube. The extraction was repeated twice more and the hexane phases were combined. After appropriate dilutions with hexane, the absorbance of the samples was measured at 450 nm using a UV-Vis spectrophotometer (Genesys 10-S, Thermo Fisher Scientific Inc., USA). The concentration of β-carotene was determined by referring to a standard curve of β-carotene in hexane prepared at the following concentrations: 1, 2, 2.5, 3, 3.5, 4, 4.5, 5, 5.5, 6, 6.5, 7, and 8 μg/mL. The standard curve showing the absorbance of different β-carotene concentrations in hexane is shown in Figure 3.1.

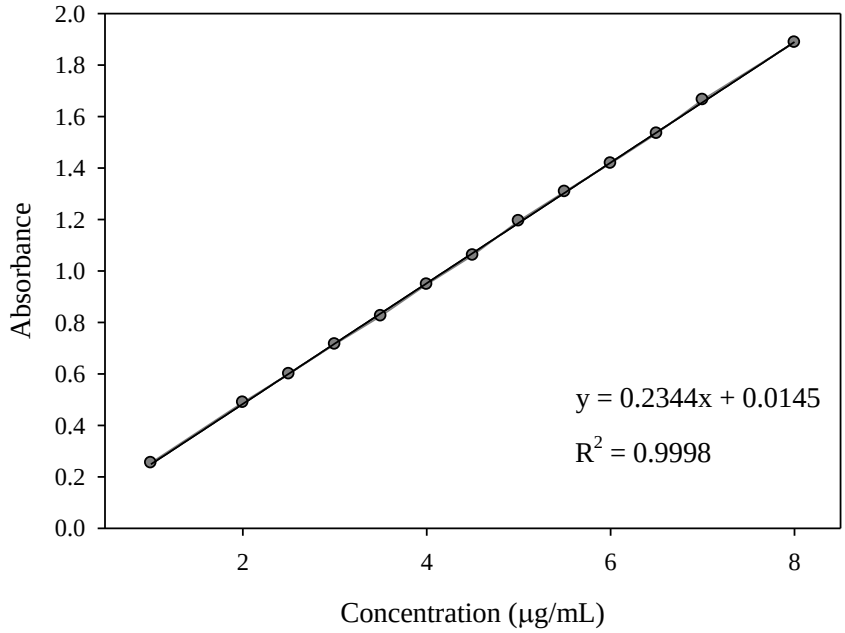

Figure 3.1. Standard curve for the determination of β-carotene concentration.

The encapsulation efficiency of β-carotene in the hemp oil body systems was determined using the equation below:

$$\text{Encapsulation efficiency (\%)} = \frac{\text{amount of encapsulated β-carotene}}{\text{amount of β-carotene initially added}} \times 100 \quad (3)$$

3.2.9.3 Colour

The chemical degradation of β-carotene during storage was monitored by colourimetry. The tristimulus colour coordinates (L^*, a^*, and b^*) of the oil body systems were measured using a handheld colourimeter (Chroma Meter, Konica Minolta, Tokyo, Japan). L^* values indicate lightness, a^* values indicate redness/greenness, and b^* values indicate yellowness/blueness. Oil body systems (6 mL) were placed into a transparent petri dish and placed over the measuring device of the colourimeter. The colour was recorded and mean L^*, a^*, and b^* values were calculated from triplicate measurements.

The total colour difference (ΔE^*) was calculated using the tristimulus colour values using the following equation:

$$\Delta E^* = \sqrt{(L^* - L_0^*)^2 + (a^* - a_0^*)^2 + (b^* - b_0^*)^2} \quad (4)$$

wherein L^*, a^*, and b^* are the measured colour coordinates of the oil body system at storage time t, and L_0^*, a_0^*, and b_0^* are the initial colour coordinates of the sample.

3.2.10 Physicochemical stability of β-carotene-loaded oil body systems during storage

Based on the methods that were able to successfully encapsulate β-carotene, β-carotene-loaded oil body systems were selected and explored for their performance over a 14-day storage period. These systems include the (1) homogenised and (2) non-homogenised oil bodies that encapsulated β-carotene by heating and sonication, and the (3) OBMM-stabilised hemp oil emulsions. The physicochemical properties of these systems were compared against a WPI-stabilised (0.5% w/w) emulsion containing β-carotene at a concentration of 400 μg/g during storage at different temperatures and light conditions. The systems were analysed for their particle size, ζ-potential, colour, and β-carotene concentration according to Sections 3.2.3.1, 3.2.3.2, 3.2.9.3, and 3.2.9.2, respectively.

3.2.10.1 Effect of temperature

The effect of different temperatures (4°C, 22°C, and 50°C) on the stability of β-carotene encapsulated in various oil body systems was investigated in this study. Oil body systems (10 mL) were placed in 15 mL amber UVSafe^{TM} centrifuge tubes, flushed with nitrogen gas, and covered with Parafilm before storage inside a cool room (4°C), at room temperature (22°C), and inside an incubator (50°C) for 14 days. Samples were analysed every two days for particle size, particle charge, colour, and β-carotene content (as described in Sections 3.2.3.1, 3.2.3.2, 3.2.9.3, and 3.2.9.2, respectively). The degradation of β-carotene was expressed as mass ratios of C_t/C_0, where C_t is the β-carotene content after a certain treatment time (t) and C_0 is the initial β-carotene content of the samples.

3.2.10.2 Effect of light

Oil body systems (10 mL) were placed in transparent glass tubes, flushed with nitrogen gas, and covered with Parafilm before placing at a distance of 115 cm under an LED lamp (Philips CoreRange Batten BN188C LED40 NW ACF L1200 BR) of 38.5 W, with a colour temperature of 4000 K and luminous flux of 4000 lm, at room temperature (~22°C) for 14 days. The effect of light on the degradation of β-carotene in the samples was determined by comparing the light-exposed samples to those stored at dark conditions (contained in 15 mL amber UVSafe^{TM} centrifuge tubes) at room temperature (~22°C). β-carotene degradation was also expressed as mass ratios of C_t/C_0, where C_t is the β-carotene content after a certain treatment time (t) and C_0 is the initial β-carotene content of the samples.

3.3 Statistical analysis

The following experiments were repeated for a minimum of two times: microstructure of oil bodies in seeds (Section 3.2.1) and physicochemical stability of β-carotene-loaded oil body systems during storage (Section 3.2.10). Meanwhile, the following were repeated for at least three times: extraction of oil bodies from hemp and mustard seeds (Section 3.2.2), characterisation of oil body fractions (Section 3.2.3), colloidal stability of oil body fractions (Section 3.2.4), encapsulation methods of β-carotene using the hemp oil body fraction (Section 3.2.8), and characterisation of β-carotene-loaded hemp oil body systems (Section 3.2.9). Analyses were performed at least two times unless otherwise specified. The data were analysed by one-way analysis of variance (ANOVA) using Minitab 19 software. Significant differences of means were determined by Tukey's post hoc test at α=0.05.

Chapter 4 Extraction and characterisation of oil bodies (hemp and mustard seeds)

4.1 Introduction

The utilisation of oil bodies as novel food ingredients is promising due to their unique structure and stability. Oil bodies can be isolated from oilseeds aqueously through liquid-liquid phase separation, which involves the process of (1) grinding of the seeds with the extraction buffer; (2) removal of the solids from the mixture; and (3) separation of the oil body phase from the aqueous phase. An additional washing step of the oil body phase may be added to increase their purity (Nykiforuk, 2016).

In this chapter, the physicochemical properties of a crude (unwashed) oil body fraction from two types of oleaginous seeds (hemp and mustard seeds) are presented and discussed. Based on previous studies, oil bodies from these seeds possess different oil droplet sizes; thus, it is expected that they would behave differently in various food applications. Extracted oil bodies were characterised for their physicochemical properties, microstructure, and behaviour in solutions with different pH and ionic strengths.

4.2 Results

4.2.1 Characterisation of mustard oil bodies

The characterisation of mustard oil bodies was less exhaustive compared to hemp oil bodies because they were entrapped in protein flocs and difficulties were encountered in obtaining a ‘purified’ oil body fraction. As such, the proximate composition including the fatty acid profile of the mustard oil body fraction was not determined.

4.2.1.1 Microstructure of mustard seeds

The microstructure of mustard seeds was investigated by subjecting the cross-section of the seed to cryo-SEM imaging. As seen in Figure 4.1, the distribution and shape of oil bodies inside the cell were not clearly shown even at high magnification (Figure 4.1 B). This indicates that their size might be too small (less than 1 μm) for the magnification used but zooming in further would cause the melting of the area under observation. Only the cell walls (indicated in green arrows) could be identified and no other structural elements could be recognized from the images. Cavities that were roughly spherical in

shape that were similar to oil bodies in size of less than 1 μm could also be seen (black arrows) and could be part of the cytoplasmic material.

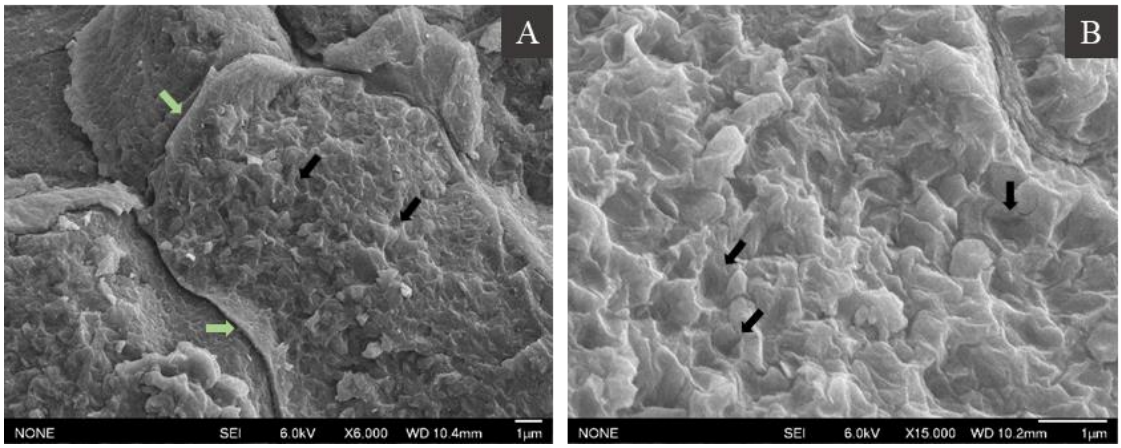

Figure 4.1. Cryo-SEM images of the cross-section of mustard seeds. See the text for the description of the arrows.

4.2.1.2 Particle size and particle charge

The particle size distributions of the mustard oil body fraction suspended in water and 1.2% SDS are shown in Figure 4.2. These results were obtained from samples treated at different pH of grinding (6.4 or 9.0), but the samples were all measured at around pH 5.3. Mustard oil bodies had a monomodal size distribution both in water and SDS, but there was a significant decrease in the particle size of oil bodies in the presence of SDS (Table 4.1). The $d_{4,3}$ and $d_{3,2}$ of the oil bodies were found to be 12.4 ± 1.4 μm and 8.6 ± 1.0 μm, respectively, which was significantly larger compared to the size in SDS (0.62 ± 0.004 μm for $d_{4,3}$ and 0.46 ± 0.012 μm for $d_{3,2}$).

Because of the large size of isolated mustard oil bodies in suspension compared to the value reported in literature (Tzen et al., 1993), the oil bodies were extracted under alkaline conditions to obtain a more purified oil body fraction (refer to Section 4.3.1.1), wherein the extraneous proteins that were not intrinsically bound to the oil body surface would have been removed. After soaking the mustard seeds in Milli-Q water overnight, the water was drained and the seeds were soaked for 30 min in the grinding medium with a pH of 9.0 (adjusted using 0.1 M NaOH). As seen in Figure 4.2, the oil bodies extracted at pH 9.0 had a similar monomodal particle size distribution with the oil bodies obtained at pH 6.4 and a smaller size distribution was also observed in the presence of SDS, indicating flocculation of oil bodies in suspension.

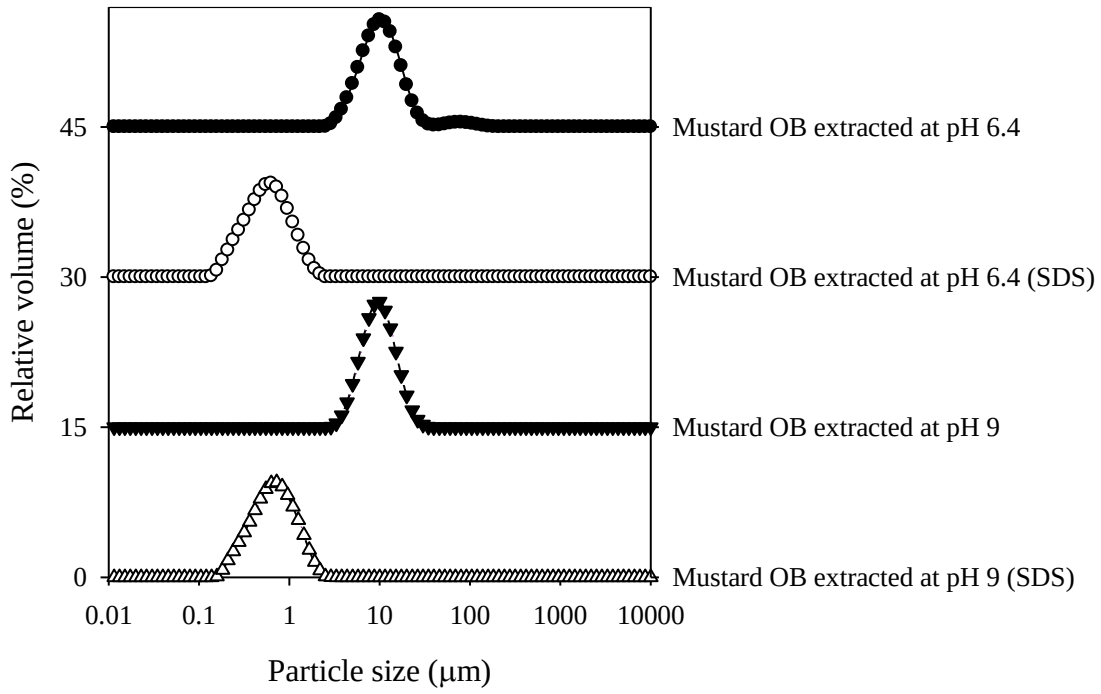

Figure 4.2. Particle size distributions of mustard oil bodies (OB) aqueously extracted at neutral (6.4) and alkaline (9.0) pH.

Table 4.1. Particle size ($d_{4,3}$ and $d_{3,2}$) and ζ-potential of mustard oil bodies extracted at neutral pH (6.4) and alkaline pH (9.0).

Parameter	Mustard OB extracted at pH 6.4	Mustard OB extracted at pH 9.0
$d_{4,3}$ (μm)	12.45 ± 1.36[a]	9.82 ± 0.70[b]
$d_{4,3}$ (SDS) (μm)	0.62 ± 0.004[b]	0.70 ± 0.003[a]
$d_{3,2}$ (μm)	8.64 ± 1.030[a]	8.26 ± 0.44[a]
$d_{3,2}$ (SDS) (μm)	0.46 ± 0.012[b]	0.53 ± 0.002[a]
ζ-potential (mV)	-21.10 ± 2.586[a]	-17.86 ± 2.30[b]

**Means that do not share a letter within the same row are statistically significant at α=0.05.*

Compared to the mustard oil body fraction extracted at neutral pH (6.4), oil bodies extracted at alkaline pH (9.0) had a significantly lower $d_{4,3}$ value of 9.8 ± 0.7 μm (Table 4.1). However, the $d_{4,3}$ in the presence of SDS (0.70 ± 0.003 μm) of oil bodies extracted at pH 9.0 was significantly larger compared to those extracted at neutral pH. No significant difference was observed in the $d_{3,2}$ values at both extraction conditions, while there was a small but significant difference in $d_{3,2}$ values when dispersed in SDS.

The ζ-potential of mustard oil bodies at neutral (6.4) and alkaline (9.0) pH were found to be -21.1 ± 2.6 mV and -17.9 ± 2.3 mV, respectively (Table 4.1). These ζ-potential values were taken at around pH 5.3 for the samples treated at different pH of grinding (6.4 or 9.0). Oil bodies extracted under alkaline conditions had a significantly lower magnitude of ζ-potential compared to those extracted at neutral pH.

4.2.1.3 Microstructure of mustard oil body fraction

Confocal laser scanning microscopy (CLSM) was used to examine the structural characteristics of oil bodies. The dyes Nile Red and Fast Green FCF (FG-FCF) were used in staining the neutral lipids and the proteins on the surface of oil bodies, respectively. Mustard oil bodies had very small sizes and existed as flocs in solution, as seen on their red core region indicative of the presence of TAGs-rich oil droplets (Figure 4.3 A). The size of the flocs ranged from less than 5 to around 12 μm, which confirms the particle size data from the light scattering measurements. In Figure 4.3 A, the small red dots in the flocs indicate individual oil bodies, whose size were below 1 μm in the presence of SDS based on the light scattering data. On the other hand, FG-FCF staining showed the distribution of proteins on the surface of the oil bodies (Figure 4.3 B). The image shows the presence of protein clumps that were covering the lipid fraction of the oil bodies. On the aqueous phase, a small proportion of protein flocs that were not adhered to the oil droplets was also observed.

Oil bodies extracted at alkaline pH showed similar staining with Nile Red and FG-FCF (Figure 4.3 D and E). However, there was also the presence of large oil droplets with a diameter ranging from 1 to 8 μm, which could be indicative of the coalescence of oil droplets as a result of the removal of proteins from the oil body surface. Nevertheless, the large clumps made up of smaller oil bodies as observed in extracts at pH 6.4 (Figure 2 A) were still observed. FG-FCF staining for alkali-extracted oil bodies had a less intense fluorescence, indicating that alkaline extraction was able to remove some extraneous proteins bound on the surface of oil bodies.

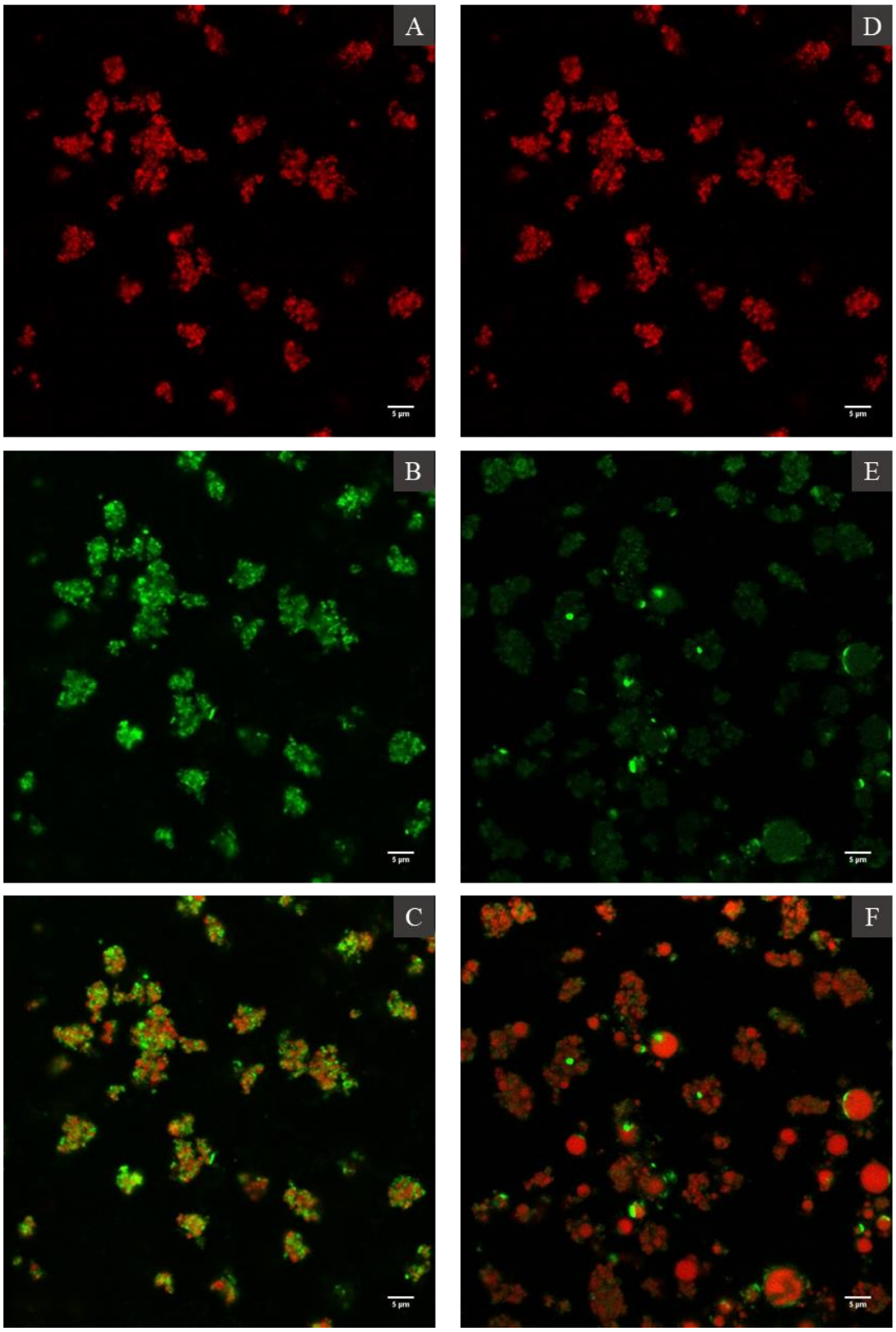

Figure 4.3. Confocal laser scanning microscopy images of mustard oil bodies extracted aqueously at neutral pH (6.4) (A, B, and C) and alkaline pH (9.0) (D, E, and F). Neutral lipids are stained by Nile Red (A and D) while proteins are stained by FG-FCF (B and D), and the merged channels showing both lipids and proteins are shown in C and F.

4.2.1.4 Effect of pH on particle size and particle charge

The effect of pH on the particle size ($d_{4,3}$) of the two types of isolated mustard oil bodies is shown in Figure 4.4. The particle size distributions of oil bodies isolated at neutral and alkaline pH are shown in Figure 4.5 and Figure 4.6, respectively. The average size ($d_{4,3}$) of mustard oil bodies extracted at neutral pH showed a significant increase until pH 3, then it decreased and became stable at pH 4-7, and then further decreased at pH 8-10. The highest size of 16.9 ± 2.3 μm was observed at pH 3, 8.8 ± 0.4 μm at pH 6, and the lowest was 5.6 ± 2.3 μm at pH 10.

The particle size distribution plot (Figure 4.5) showed a polydisperse size distribution at pH 8-10 due to the presence of a small population of smaller-sized oil bodies at those pH values. On the other hand, mustard oil bodies extracted at pH 9 did not show any significant change in $d_{4,3}$ at all the pH values, except at pH 8-9 which had a slightly higher particle size. This was also evident in the particle size distributions shown in Figure 4.6, wherein monomodal and similar size distributions were observed across all the pH values. The lowest particle size of 7.8 ± 0.04 μm was recorded at pH 2 and the highest was 10.9 ± 2.3 μm at pH 9.

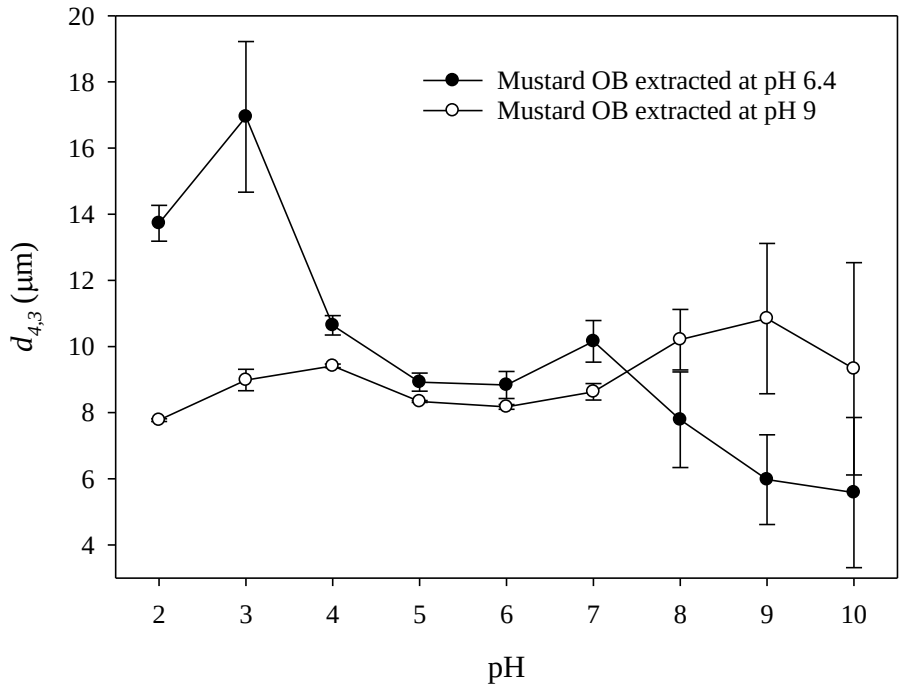

Figure 4.4. Effect of pH on the particle size ($d_{4,3}$) of mustard oil bodies (OB) aqueously extracted at neutral (6.4) and alkaline (9.0) pH.

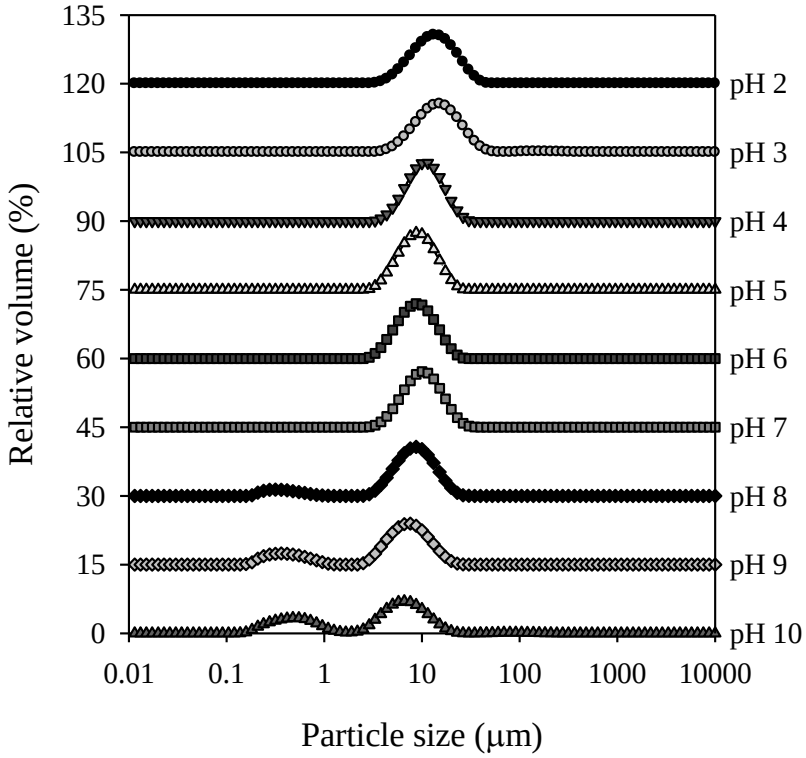

Figure 4.5. Effect of pH on the particle size distribution of mustard oil bodies extracted at neutral pH (6.4).

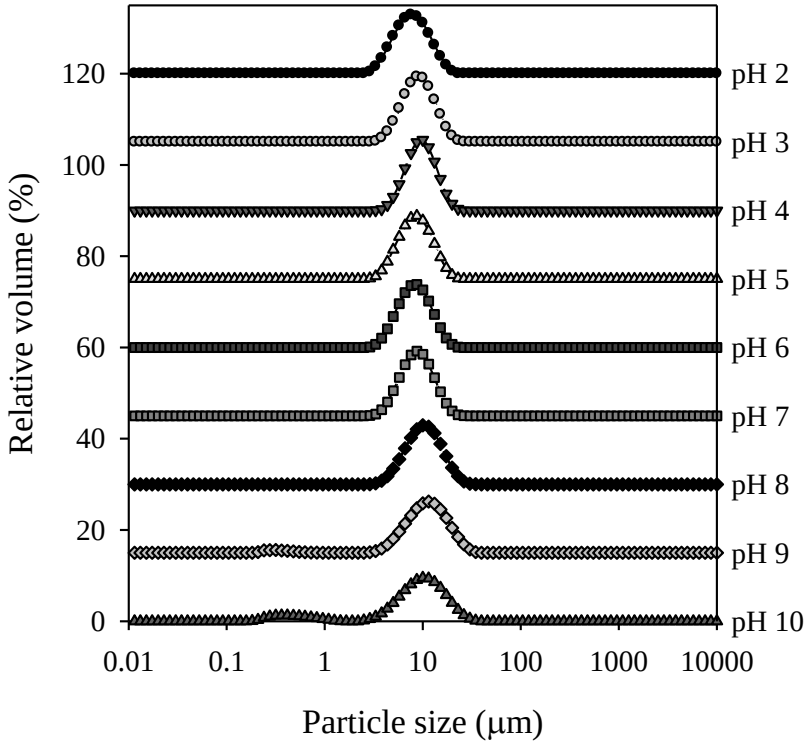

Figure 4.6. Effect of pH on the particle size distribution of mustard oil bodies aqueously extracted at alkaline pH (9.0).

The effect of pH on the ζ-potential of mustard oil bodies is shown in Figure 4.7. Changing the pH of the oil body fractions from 2 to 10 led to a linear decrease in ζ-potential regardless of the extraction method used (pH of grinding media: 6.4 or 9.0). As the pH increased, the surface charge changed from positive to negative. For oil bodies extracted at neutral pH, the point of zero charge or the isoelectric point was observed between pH 3-4 and the oil bodies possessed a negative charge at neutral pH. With the increase in pH, the magnitude of the ζ-potential also increased and the highest ζ-potential value of -48.4 ± 1.1 mV was observed at pH 10. On the other hand, for oil bodies extracted at pH 9.0, the point of zero charge was observed between pH 4-4.5 and the highest magnitude of ζ-potential of -39.4 ± 0.8 was obtained at pH 10.

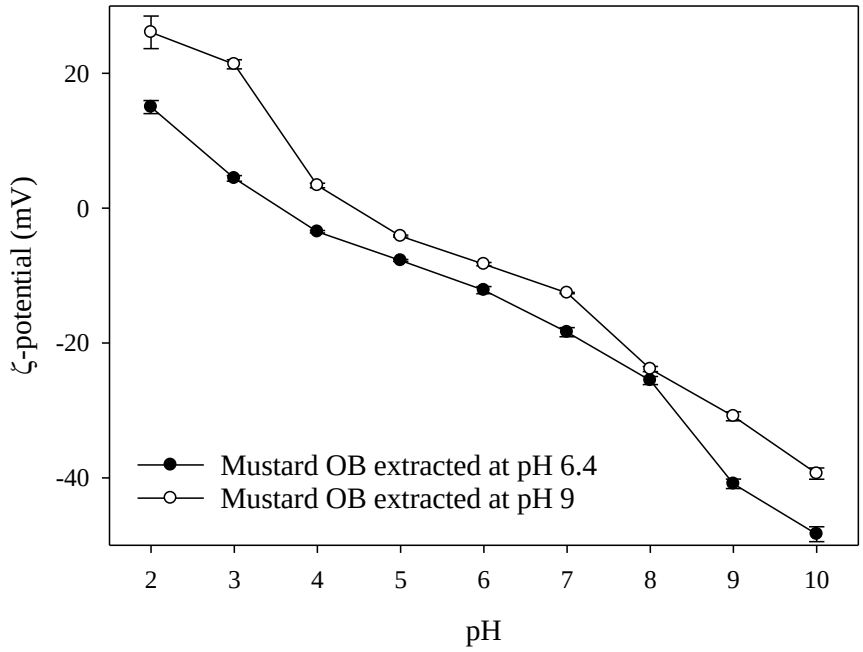

Figure 4.7. Effect of pH on the ζ-potential of mustard oil bodies (OB) aqueously extracted at neutral (6.4) and alkaline (9.0) pH.

Further characterisation of mustard oil bodies was not conducted in this study due to the difficulties encountered in obtaining an oil body fraction with minimal amounts of extrinsic proteins bound at the interface, as these could affect their stability and functionality.

4.2.2 Characterisation of hemp oil bodies

4.2.2.1 Microstructure of hemp seeds

The microstructure of hemp seeds was investigated by subjecting the cross-section of the seed to cryo-SEM imaging. Figure 4.8 shows that hemp seeds are filled with oil bodies (shown in white arrows) that are sporadically distributed inside the cell (cell wall indicated in green arrows). Such oil bodies appeared to have a spherical shape with a diameter ranging from 3 to 5 μm, and minor irregularities in the shape could be due to the oil bodies being pressed together against each other and with other components inside the cell. Aside from the cell walls and the oil bodies, no other structural elements could be identified from the images. In Figure 4.8 B, oil bodies appeared to have an outer covering that may or may not be part of the oil body membrane or the seed membrane. Moreover, some cells seemed to be devoid of any oil bodies in the plane of imaging as seen in Figure 4.8 A (black arrows). Cavities in the same shape as the oil bodies were also seen (black arrows, Figure 4.8 B) which could be part of the cytoplasmic material.

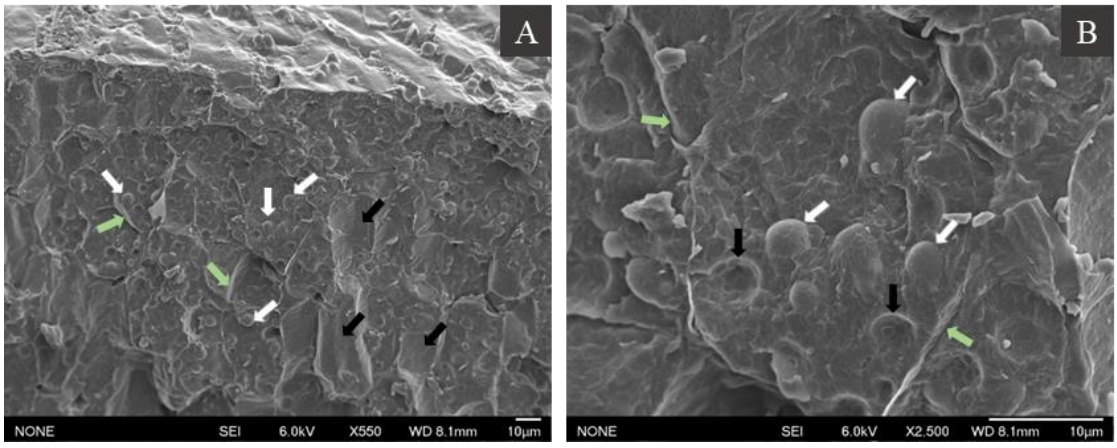

Figure 4.8. Cryo-SEM images of the cross-section of hemp seeds. See the text for the description of the arrows.

4.2.2.2 Composition of hemp oil body fraction

The proximate composition of the hemp oil body fraction obtained after aqueous extraction is shown in Table 4.2. Under the conditions of extraction, the hemp oil body fraction had a high recovery of fat and protein, amounting to 79.3 ± 2.8% and 1.5 ± 0.2%, respectively.

Table 4.2. Proximate composition of hemp oil bodies.

Parameter	Composition (%, wb)
Moisture	22.80 ± 2.09
Fat	79.30 ± 2.78
Crude protein	1.50 ± 0.22
Ash	0.20 ± 0.01

Table 4.3. Fatty acid composition of hemp oil bodies.

Total fatty acid	Total fat %	Standard deviation
C6:0 Caproic	0.019	0.003
C12:0 Lauric	0.006	0.001
C14:0 Myristic	0.025	0.001
C16:0 Palmitic	3.905	0.146
C16:1n7c-cis-9-Palmitoleic	0.065	0.011
C17:0 Margaric	0.055	0.008
C18:0 Stearic	1.80	0.100
C18:1n9c Oleic	8.732	0.485
C18:1n7c Vaccenic	0.474	0.018
C18:2n6c Linoleic	41.456	1.479
C18:3n6-cis-6,9,12-Gamma linolenic	2.518	0.082
C20:0 Arachidic	0.555	0.004
C20:1n9-cis-11-Eicosenoic	0.281	0.012
C18:3n3-cis-9,12,15-Alpha linolenic	12.334	0.320
C21:0 Heneicosanoic	0.007	0.001
C20:2n6-cis-11,14-Eicosadienoic	0.051	0.001
C22:0 Behenic	0.215	0.007
C22:1n9-cis-13-Erucic	0.015	0.001
C20:3n3-cis-11,14,17-Eicosatrienoic	<0.01	-
C23:0 Tricosanoic	0.022	0.006
C22:2n6-cis-13,16-Docosadienoic	<0.01	-
C24:0 Lignoceric	0.093	0.006
C24:1n9-cis-15-Nervonic	0.016	0.004

Table 4.3 shows the fatty acid composition of the hemp oil body fraction. The values indicate that hemp oil bodies predominantly contain polyunsaturated fatty acids, with linoleic acid comprising 41.5% of the total fatty acids. Other major fatty acids of hemp oil bodies are α-linolenic acid (12.1%), oleic acid (8.4%), palmitic acid (3.8%), γ-linolenic acid (2.6%), and stearic acid (1.8%).

4.2.2.3 Particle size and charge

The particle size and charge of the hemp oil body fraction were also characterised from dispersions in water or 1.2% SDS. Table 4.4 shows the $d_{4,3}$ and $d_{3,2}$ values of the hemp oil body fraction dispersed in water and SDS. The $d_{4,3}$ was found to be 4.9 ± 0.7 μm whereas the $d_{3,2}$ was 3.1 ± 0.1 μm for the oil body fraction dispersed in water. On the other hand, the $d_{4,3}$ and $d_{3,2}$ of the oil body fraction suspended in SDS were 5.1 ± 0.8 μm and 2.9 ± 0.2 μm, respectively. There was no significant difference in the particle size of the oil bodies dispersed in water and SDS, and the particle size distributions were both monomodal and fairly similar for the two systems (Figure 4.9). On the other hand, the ζ-potential of hemp oil bodies at pH 7 was found to be -32.8 ± 5.1 mV, indicating that the oil bodies are negatively charged at neutral pH. The ζ-potential was reported at pH 7 because of the wide variation in the pH of hemp oil body fractions upon extraction, which also resulted in variations in the ζ-potential (results not shown).

Table 4.4. Particle size ($d_{4,3}$ and $d_{3,2}$) of hemp oil bodies.

Parameter	Value	Value (SDS)
$d_{4,3}$ (μm)	4.87 ± 0.72	5.12 ± 0.83
$d_{3,2}$ (μm)	3.09 ± 0.12	2.94 ± 0.19

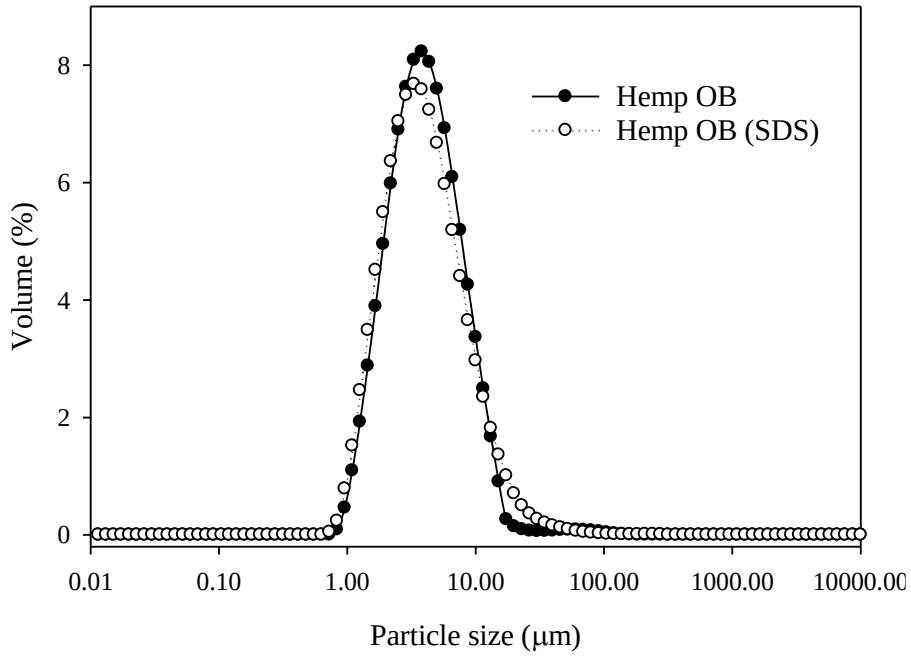

Figure 4.9. Particle size distributions of hemp oil bodies (OB) suspended in water and SDS.

4.2.2.4 Microstructure of hemp oil body fraction

CLSM was used to examine the structural characteristics of the hemp oil body fraction. The following dyes were used to examine different structural components of the oil bodies: Nile Red for neutral lipids, FG-FCF for proteins, and Lissamine^{TM} rhodamine B (Rd-DHPE) for phospholipids. Based on the obtained images, oil bodies exist as spherical droplets in solution. The diameter ranged from 3 to 7 μm, and this narrow range agrees with the monomodal size distribution based on light scattering data. Oil bodies consisted of a large intense red fluorescent core region which represents the neutral lipids or TAGs (Figure 4.10 A). No flocculation was observed, which agrees with the size of the oil bodies in SDS. Meanwhile, staining with FG-FCF showed that the surface of the oil bodies appeared to be uniformly covered by proteins regardless of the oil body size (Figure 4.10 B). No protein aggregates were observed in the continuous phase of the suspension. Lastly, staining with Rd-DHPE showed uniform intense red fluorescence on the surface of the oil droplets and the size which was around 5 μm also corresponded to the particle diameter obtained from light scattering measurements (Figure 4.11).

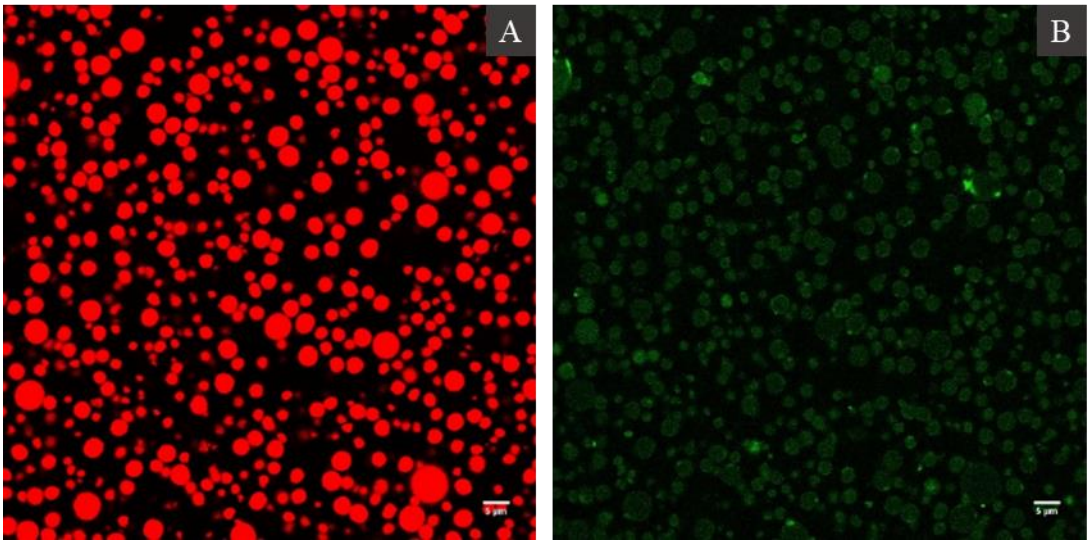

Figure 4.10. CLSM images of hemp oil bodies showing neutral lipids stained by Nile Red (A) and proteins stained by FG-FCF (B).

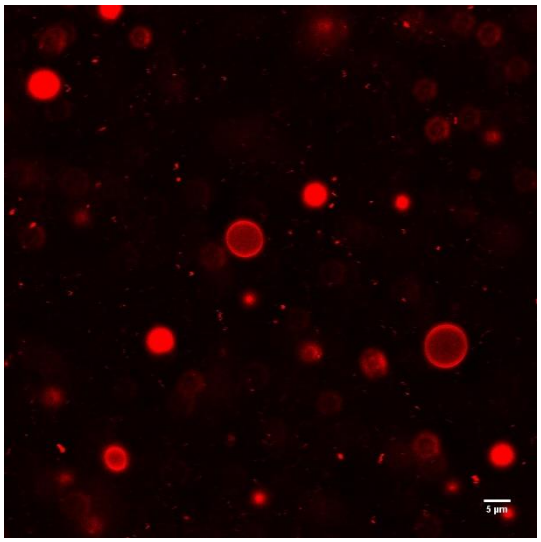

Figure 4.11. CLSM image of hemp oil bodies stained by Rd-DHPE showing the interfacial distribution of phospholipids.

Cryo-SEM imaging was also conducted to further examine the structural properties of extracted oil bodies in suspension. Oil bodies appeared to be spherical in shape (white arrows, Figure 4.12 A), with the diameter ranging from 2 to 5 μm. These observations on the shape and size of oil bodies in solution agree with the CLSM images and particle size distribution data. Moreover, the size of the oil bodies in suspension was in agreement with the size of oil bodies in the seed (Figure 4.8). At high magnification (Figure 4.12 B), the oil bodies appeared to have an irregular spherical shape, rough surface, and seemed flocculated. Furthermore, thread-like structures or connections between oil droplets were

observed (white arrows, Figure 4.12 A), but these could be artefacts of the sublimation of water that occurred during imaging.

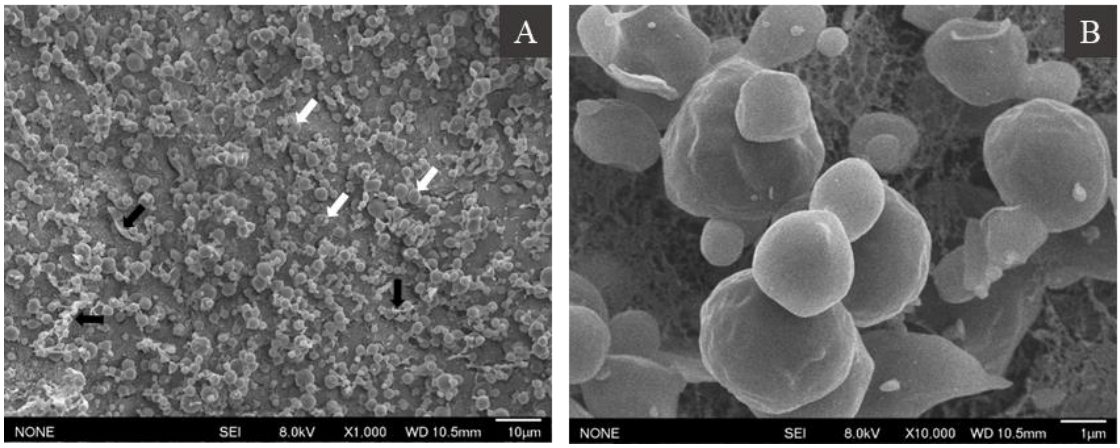

Figure 4.12. Cryo-SEM images of hemp oil body fraction at low (A) and high (B) magnification.

4.2.2.5 Effect of pH and ionic strength on particle size and particle charge

The influence of pH and ionic strength on the colloidal stability of oil body fractions extracted from hemp seeds was determined. It involved the measurement of the following properties: mean particle diameter, particle size distribution, and electrical charge. These parameters provide an insight into the composition and properties of the interfacial components of the oil bodies and their behaviour and possible utilisation in various food matrices.

The effect of pH on the particle size and charge of hemp oil bodies was investigated by adjusting the pH of the oil body fractions from 2 to 10 using 0.1 M HCl or 0.1 M NaOH. Results showed that extreme pH values (highly acidic and highly alkaline) did not affect the mean particle diameter ($d_{4,3}$) of oil bodies (Figure 4.13 A). The particle size increased between pH 4 to 5, reaching a maximum value of 14.4 ± 2.9 µm at pH 5. However, as the pH further increased to alkaline values, the oil bodies maintained their particle size that ranged from 3.3 ± 1.2 µm to 5.1 ± 0.7 µm, with no significant difference observed. Similarly, the particle size distributions showed a similar monomodal size distribution at all the pH values (Figure 4.14), except at pH 4 and 5 wherein a shift to the right was observed, indicating the presence of larger sized droplets.

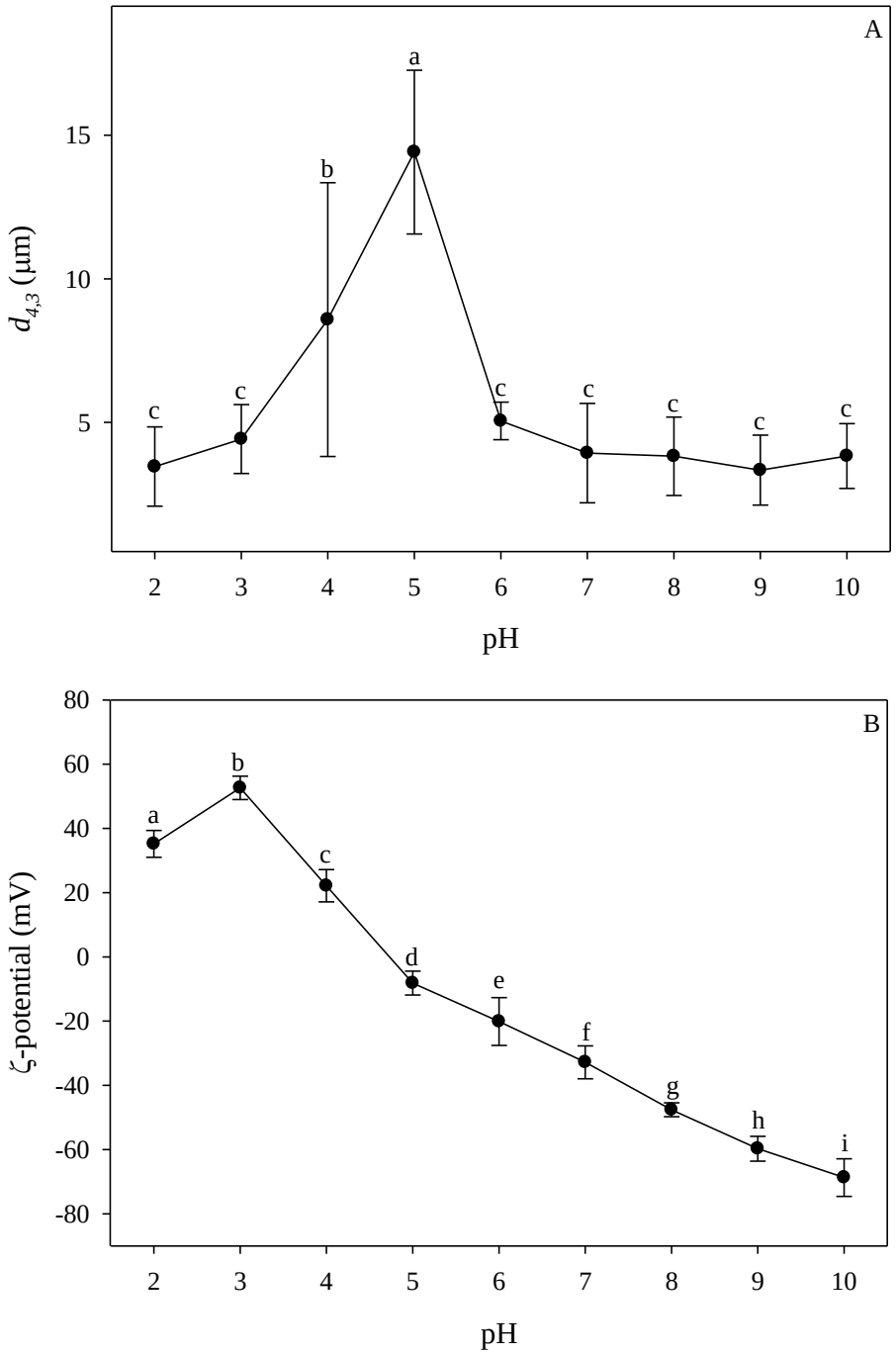

Figure 4.13. Effect of pH on the particle size (A) and ζ-potential (B) of hemp oil bodies. Means that do not share a letter in the same graph are statistically significant at α=0.05. Error bars indicate standard deviations.

Meanwhile, the effect of pH on the ζ-potential of hemp oil bodies is illustrated in Figure 4.13 B. As the pH increased, the surface charge moved from positive to negative, and hemp oil bodies were found to be negatively charged at neutral pH. The point of zero charge was observed between pH 4 and 4.5; at pH values below this, oil bodies were positively charged and at pH values above this, they were negatively charged. The highest ζ-potential value of -68.7 ± 5.9 mV was observed at pH 10.

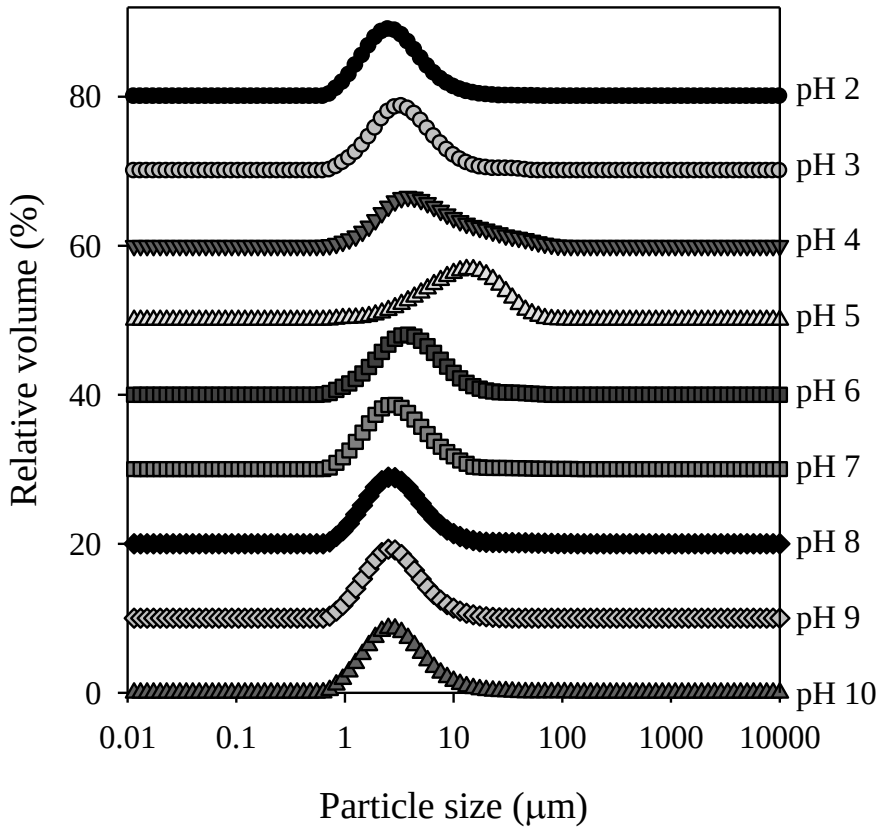

Figure 4.14. Effect of pH on the particle size distribution of hemp oil bodies.

The effect of ionic strength on the particle size and charge of hemp oil bodies was investigated by adjusting the oil body fractions to different NaCl concentrations (0 to 1000 mM). The change in the particle size ($d_{4,3}$) and ζ-potential of the oil bodies at different ionic strengths is shown in Figure 4.15. Different NaCl concentrations did not have a significant effect on the $d_{4,3}$ of hemp oil bodies. This was evident in the particle size distribution of the oil bodies, wherein a monomodal and similar distribution were observed at all the ionic strengths examined (Figure 4.16).

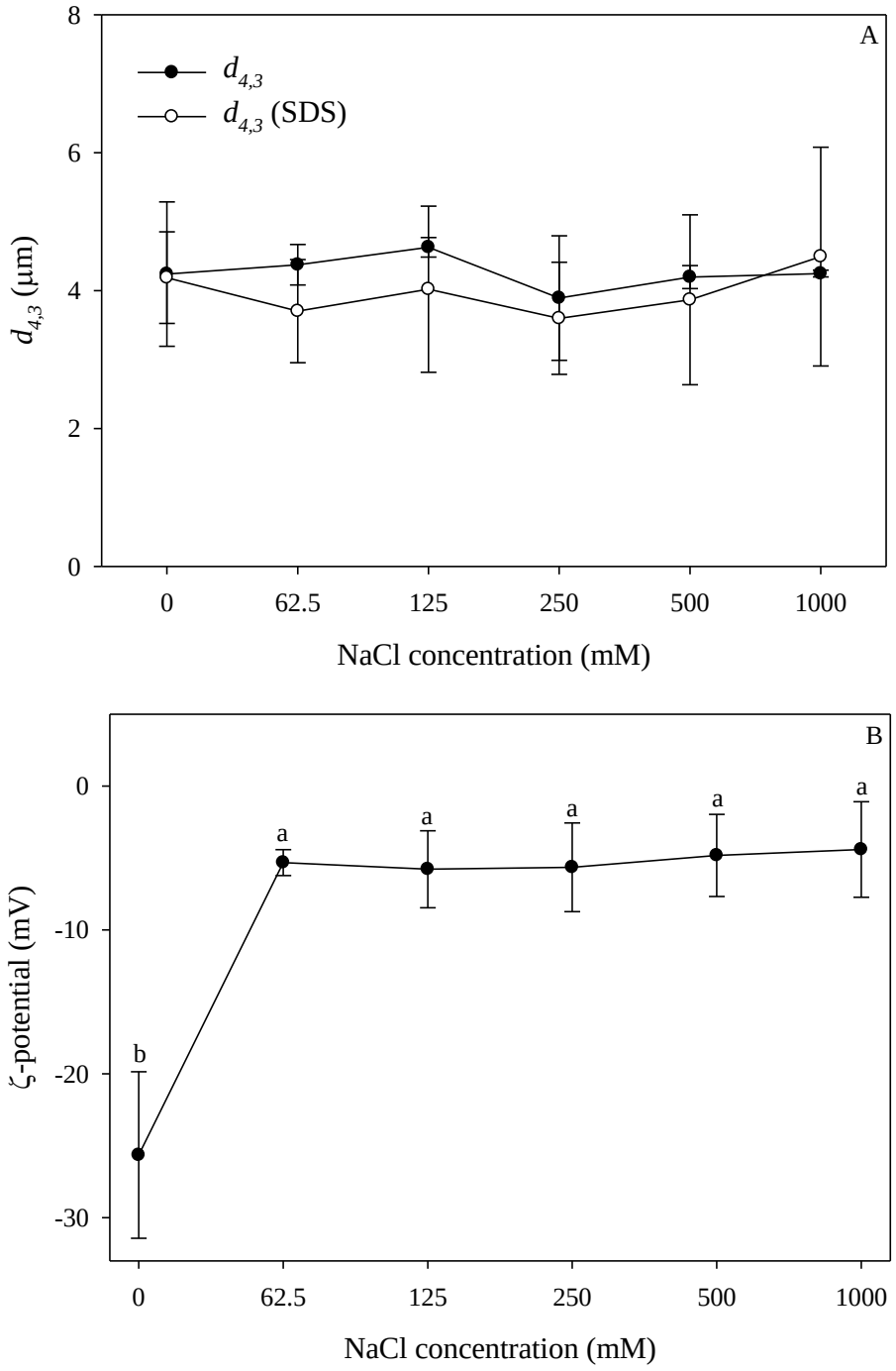

Figure 4.15. Effect of ionic strength on the $d_{4,3}$ (A) and ζ-potential (B) of hemp oil bodies. Means that do not share a letter are statistically significant at α=0.05. Error bars indicate standard deviations.

Meanwhile, the increase in NaCl concentration resulted in a significant decrease in the ζ-potential of the oil bodies. After the addition of NaCl, the magnitude of the ζ-potential decreased from -25.8 ± 5.8 to around -5 mV at 62.5 to 1000 mM NaCl concentration. No significant difference was observed for the ζ-potential at all the NaCl concentrations studied.

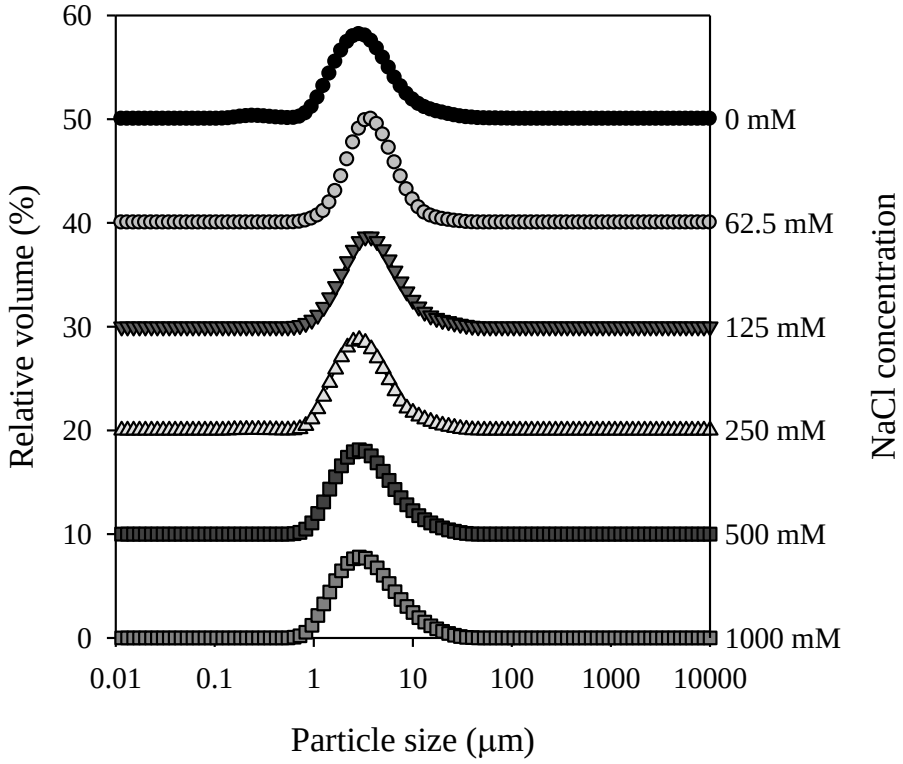

Figure 4.16. Effect of ionic strength on the particle size distributions of hemp oil bodies.

4.3 Discussion

4.3.1 Mustard seeds

4.3.1.1 Physical and structural properties

Within the mustard seed matrix, the microstructure of oil bodies was investigated by cryo-SEM microscopy. Even at high magnification, the structure and distribution of oil bodies within the seed were not clearly elucidated. This could be attributed to their small size, which was possibly below the detection limit of the method used. Hence, the use of other techniques to characterise mustard oil bodies in the seed matrix is recommended. The microstructure of oil bodies in mustard seeds has not been reported in literature, but other studies have determined the structural properties of other oil-bearing seeds and tissues and are discussed in Section 4.3.2.1.

Particle size measurements for mustard oil body fractions showed a high particle size when dispersed in water. This could be attributed to the presence of large structures of extrinsic proteins that contained oil bodies embedded in them. These structures were not removed/dissociated due to the absence of a washing procedure to obtain purified oil bodies. These flocs were held together strongly and were unaffected at various pH (see discussion in Section 4.3.1.2). Because of difficulties encountered in obtaining a 'purified' fraction of mustard oil bodies, the characterisation of the proximate composition including the fatty acid profile of mustard oil bodies was not conducted in this study.

The co-extraction of extrinsic proteins, including globulins, albumin, and enzymes, has also been observed in the extraction of oil bodies from other types of seeds such as jicama, sunflower, castor bean, rapeseed, and sesame (Zhao et al., 2016). Moreover, extraneous proteins that are tightly adsorbed to the droplet surface are sometimes not removed despite the washing steps applied to the cream to isolate oil bodies (Nikiforidis & Kiosseoglou, 2009). For instance, a minor amount of extraneous proteins aside from the interfacial oil bodies was observed for sunflower oil bodies despite doing a washing procedure after oil body isolation (Karefyllakis, van der Goot, et al., 2019a). These storage proteins were co-extracted with the oil bodies and interacted with the interfacial proteins through hydrophobic interactions, acting as bridges between neighbouring oil bodies (Nikiforidis et al., 2013).

Another possible reason for the broad size distribution is the high solid load of the grinding medium which could destabilise the interface and cause coalescence of oil bodies during extraction. In the extraction of rapeseed oil bodies, a more diluted grinding media of 1:7 seed-to-water ratio was able to reduce the particle size of oil bodies due to the lower density of seed solids in the grinding medium which could damage the oil body surface (De Chirico et al., 2018). Further experiments are necessary to ascertain this hypothesis.

The size of individual mustard seed oil bodies has been reported to be 0.73 μm (Tzen et al., 1993). The true size of individual oil body droplets from the mustard seeds was determined by adding SDS. The presence of SDS in the aqueous medium disrupted the protein flocs, indicating that these flocs were held together by hydrophobic interactions among protein polypeptides. Thus, when the hydrophobic interactions between the

oleosins on the oil body surface and the extrinsic proteins are disrupted, flocs disintegrated and the mean particle diameter represented the real size of individual oil bodies (Sukhotu et al., 2014). The size of mustard oil bodies determined in SDS is in agreement with that reported in literature. Oil bodies that are small in size usually exhibit a low TAG to interfacial protein ratio, while those that are bigger sized have lower interfacial protein content (Huang, 1992; Nikiforidis et al., 2014).

The surface charges of the mustard oil bodies extracted at both neutral and alkaline pH were below 30 mV in magnitude, indicating low electrostatic stability. A ζ-potential magnitude of 30 mV is an indication of good electrostatic stability of emulsions (McClements, 2016). It must be noted that the ζ-potential values reported here were for the oil body-containing protein flocs and not the isolated oil bodies themselves.

When the mustard oil bodies were extracted at alkaline pH, a decrease in particle size was observed, which could be attributed to the partial disruption of flocs of storage proteins and release of oil bodies therein. The use of alkaline solutions with a pH above 8 as extraction media for oil body isolation has been shown to be effective in removing exogenous proteins and other seed material (Chen & Ono, 2010; De Chirico et al., 2018; Zhao et al., 2016). Moreover, holding the pH of the grinding media above 8.5 has been shown to prevent aggregation and limit the coalescence of droplets during comminution due to the increase in the electrostatic repulsion at the interface (De Chirico et al., 2018). In contrast, the confocal images of the oil body fraction at pH 9 showed a population of larger sized oil droplets despite the alkaline extraction of mustard oil bodies. This could be attributed to the partial coalescence of oil bodies upon extraction (Karefyllakis, van der Goot, et al., 2019a). Moreover, flocs of proteins consisting of oil bodies were still evident in CLSM images although the pH of the grinding medium was increased. This is in agreement with the results for rapeseed oil bodies (which is in the similar *Brassica* species as mustard), wherein extraction even at pH 11 still contained many proteins, especially enzymes such as myrosinase-associated protein, β-glucosidase, and myrosinase-binding protein (Zhao et al., 2016). Hence, optimisation of the extraction conditions may be needed for these types of oilseeds and further elucidation of the protein profile of mustard oil bodies is needed to give better insights into their interfacial properties.

4.3.1.2 Effect of external conditions on colloidal stability

The effect of pH on the surface charge of mustard oil body fraction is consistent with other types of oil bodies, wherein the ζ-potential changes from positive to negative with the increase in pH (Iwanaga et al., 2007; Nikiforidis & Kiosseoglou, 2009). This behaviour of oil body fraction at different pH conditions is similar to that of protein-stabilised emulsions, wherein the charge of the droplets goes from positive at low pH, to zero at the isoelectric point, to negative at high pH (McClements, 2016). Since the oil bodies in the extracts were embedded in flocs of proteins, the bulk properties are representative of the flocs and not the individual oil bodies. The ζ-potential of more purified oil bodies presents an interesting area for future work.

For the mustard oil body fraction, the point of zero charge for the oil bodies extracted at neutral and alkaline pH was lower compared to what was previously reported which was 5.7 (Tzen et al., 1993). The isoelectric pH was 1 to 2 units lower than those initially described for oil bodies from other plant species that ranged from 5 to 6, which is close to the isoelectric point of oleosin (Maurer et al., 2013; Tzen et al., 1993). This difference in the isoelectric pH may be attributed to the extraneous proteins (which were not characterised in this study) that were co-extracted with the oil bodies and present as flocs. The lower isoelectric point could be attributed to the presence of proteins that were more acidic than oleosin which shield the oleosins at the interface, thereby reducing the isoelectric pH value (Nikiforidis & Kiosseoglou, 2009). Another possible reason proposed for an isoelectric pH to be on the acidic side is the formation of negatively charged surface-active lipids which could occur if the co-extracted proteins were enzymes that could cause lipid degradation (Iwanaga et al., 2007). This would result in the migration of negatively charged free fatty acids on the oil body interface, causing a decrease in the isoelectric pH. However, this can be ruled out based on the confocal images which showed flocs. Further experiments to test the presence of free fatty acids may elucidate more details to test this theory.

Particle size data on mustard oil bodies indicate the presence of aggregation at pH values close to the point of zero charge. Similarly, other authors observed that the particle size of most droplets in oil body fractions was relatively small at pH values far from the isoelectric point (Iwanaga et al., 2007). Aggregation of oil bodies at different pH values is dependent on electrostatic interactions: a strong electrostatic repulsion prevents the oil

bodies from aggregating at pH values far away from their isoelectric point (Sukhotu et al., 2014). On the other hand, at pH values close to the isoelectric point, there is weak electrostatic repulsion that cannot overcome the attractive forces, thereby causing oil bodies to flocculate (Demetriades et al., 1997; Maurer et al., 2013; Nikiforidis & Kiosseoglou, 2009). In the case of mustard oil bodies extracted at pH 9, there was no significant difference in the mean particle diameter from pH 2 to 10. Similarly, Maurer et al. (2013) reported a narrower range where soybean oil bodies are unstable at different pH, which was attributed to the removal of residual storage proteins after the centrifugation of the oil bodies at pH 11. In this study, the difference in the aggregation behaviour of the two types of oil body fractions can be attributed to the presence of extraneous proteins that entrapped them. The use of alkaline grinding medium was not able to result in the isolation of mustard oil bodies from the protein flocs. Thus, the bulk properties are representative of the flocs and not the individual oil bodies. Future studies examining the effect of pH on the mustard seed purified oil bodies free from protein flocs are necessary.

A ‘purified’ oil body fraction without any aggregation or protein flocs caused by extraneous proteins could be used to gain better insights into the oil body functionality since the presence of non-intrinsic proteins on the oil body interface affects their physical and chemical stability. Thus, further investigation of the characteristics of mustard oil bodies was not examined due to the challenges in removing extrinsic proteins during their isolation.

4.3.2 Hemp seeds

4.3.2.1 Physical and structural properties

The microstructure of oil bodies within the matrix of the hemp seed was investigated in this study. Oil bodies were found to be sporadically distributed within the hemp seed, with most cells being densely packed with oil bodies while other cells were devoid of any. Although there have been no reports in literature on the microstructure of oil bodies in the hemp seed, other studies examined the structural characteristics of other oleaginous seeds and tissues. For instance, oil bodies with an apparent diameter of 1 to 3 μm were found to be densely packed in *E. plantagineum* seeds (Gray et al., 2010). The dense cell environment causes the compression of oil bodies, hence they are fully compressed and packed (Capuano et al., 2018). This also makes them appear not totally spherical as their

shape inside the cell is determined by the amount of available space they can occupy. The same was observed for oil bodies in maize germ (Nikiforidis et al., 2013). On the contrary, oil bodies in sunflower seeds appear to have more spherical shapes even if they are present in high amounts because they have more space available due to the less dry environment (Nikiforidis et al., 2013). Meanwhile, an asymmetric intracellular distribution of oil bodies was found in coconut tissue, with most cells being rich in oil bodies while some are devoid of any oil bodies (Dave et al., 2019). These regions in the cell without any oil bodies could be occupied by other intracellular organelles. As such, the appearance of oil bodies prior to isolation depend on the type of matrix they are located and the availability of space for them to occupy.

Once extracted, the hemp oil body fraction had a high percentage of fat and proteins based on proximate analysis. The protein content determined fell within the range of 0.59 to 3.46 % (w/w) that was determined from seeds of various species (Tzen et al., 1993). This could represent the interfacial proteins on the oil body surface and possibly extrinsic proteins that were extracted along with the oil bodies. Typically, oil is extracted from hemp seeds because of their high nutritional value. It has been reported that oil bodies predominantly contain unsaturated fatty acids whose composition is similar to those extracted from the seed source (Gray et al., 2010). Similar to hempseed oil, the fatty acid profile of hemp oil bodies was composed mainly of polyunsaturated fatty acids, with linoleic acid as the fatty acid with the highest percentage. This is in accordance with reports in literature wherein linoleic acid comprised around 56% of the fatty acid composition of hempseed oil (Teh & Birch, 2013). Aside from linoleic acid, the oil bodies also contained high amounts of α-linolenic acid which is another essential fatty acid. Their ratio (ω-6/ω-3) of around 2.5:1 also agrees with the optimal balance of essential fatty acids (2:1 to 3:1), which is vital for the metabolism of the PUFAs (Callaway, 2004).

Hemp oil bodies had a monomodal and similar size distribution when dispersed in water and SDS. Since particle size measurements in SDS give the size of individual droplets, results indicate that there was minimal flocculation of oil bodies upon extraction even without an extensive washing procedure. This was confirmed by the CLSM images of the oil body fraction, wherein no aggregation was observed in the oil droplets stained by Nile Red. No protein aggregates (stained by FG-FCF) were observed in the aqueous phase, indicating that the protocol was able to isolate intact oil bodies with minimal amounts of

extraneous proteins. Further structural characterisation of the hemp oil body interface suggested a uniform distribution of phospholipids on the oil body interface as indicated by the intense red fluorescence on the oil body surface upon staining with Rd-DHPE. Moreover, the size of oil bodies dispersed in water (based on cryo-SEM imaging) agrees with the light scattering data, indicating that the integrity and structure of hemp oil bodies in the seed is maintained upon extraction and that they exist as spherical droplets in solution. Although the size of hemp oil bodies is higher than the range reported for other plant species which ranged from 0.5 to 2.5 μm, the size of oil bodies is generally influenced by physicochemical or biological factors (Huang, 1992; Tzen et al., 1993). Along with the particle size results, the surface charge of oil bodies demonstrates their stability in suspension upon extraction. At neutral pH, the oil bodies also exhibited a high magnitude of ζ-potential (absolute value above 30 mV) which indicates the good electrostatic stability of the oil bodies dispersed in water.

4.3.2.2 Effect of external conditions on colloidal stability

Similar to mustard oil bodies, hemp oil bodies exhibited a similar behaviour to protein-stabilised emulsions at different pH conditions. The ζ-potential changed from positive to negative with increase in pH and had a zero value at the isoelectric point. Hence, it can be inferred that the oleosins at the oil body interface remained after the extraction procedure applied and were responsible for electrostatic interactions of the oil bodies at various pH conditions (Demetriades et al., 1997; Iwanaga et al., 2007). The isoelectric pH determined for hemp oil bodies was comparable to those reported for maize and soybean oil bodies which fell between pH 4 to 5 (Iwanaga et al., 2007; Nikiforidis & Kiosseoglou, 2009; Sukhotu et al., 2014). These results are also in accordance with the particle size distribution data that showed a monomodal and similar particle size distribution of oil bodies at the pH values investigated, except at pH 4 and 5 wherein a population of larger sized oil bodies was observed. Flocculation of oil bodies at pH values close to the isoelectric point could be attributed to the weak electrostatic repulsion due to the zero net charge of the oleosins at the interface (Maurer et al., 2013; Nikiforidis et al., 2013).

The effect of salt on the stability of oil body suspensions was investigated to determine the type of food matrices that are suitable for utilising the functionality of oil bodies. Generally, increasing the ionic strength of the solution causes a decrease in the ζ-potential

of colloidal suspensions due to electrostatic screening effects (McClements, 2016). The charges are screened until a point where flocculation cannot be prevented, thereby causing the formation of aggregates. In the case of hemp oil bodies, a reduction in ζ-potential was observed with the addition of NaCl at the lowest concentration; it remained similar as the salt concentration increased. This indicates that the particle charge of oil bodies is sensitive to the addition of relatively low amounts of salt such that electrostatic interactions were reduced. Similarly, other types of oil bodies such as maize, soybean, and safflower exhibited a reduction in ζ-potential with the addition of salt (Iwanaga et al., 2007; Lan et al., 2020; Sukhotu et al., 2014). However, contrary to the decrease in electric potential, no significant change in the mean particle diameter was observed despite the increase in the ionic strength of the solution. The resistance of oil bodies to flocculation can be attributed to the oleosins at the interface which not only provide electrostatic repulsion but also steric hindrance that enhances their stability (Maurer et al., 2013). Emulsions that are sterically stabilised are more resistant to variations in pH and ionic strength compared to electrostatically-stabilised emulsions (McClements, 2016). Thus, the reduction in electrical potential was not enough to cause the flocculation of oil bodies due to steric effects provided by the oleosins at the oil body surface.

4.4 Conclusion

In summary, oil bodies can be obtained from oilseeds in the form of a natural oil-in-water emulsion through aqueous extraction techniques. Mustard and hemp oil bodies were isolated via aqueous extraction and their physicochemical characteristics were analysed. The extraction conditions applied were effective in isolating intact oil bodies, although it was not efficient in removing extraneous proteins that entrap the oil bodies inside protein flocs. In contrast, hemp oil bodies did not flocculate in suspension, indicating better stability compared to mustard oil bodies. Microscopy techniques such as CLSM and cryo-SEM were also used to elucidate the microstructure of oil bodies in the seed and isolated preparations. The composition and properties of the interfacial layer also determine the behaviour of oil bodies at different environmental conditions (pH and ionic strength) and provide guidelines on how they can be utilised in food matrices. Due to the ease of their extractability compared to mustard oil bodies, hemp oil bodies were used for further investigation of oil body functionality as a delivery system for bioactive compounds.

Chapter 5 Approaches for the encapsulation of β-carotene into hemp oil bodies

5.1 Introduction

Lipophilic bioactive compounds are utilised in the food industry because of their beneficial effects on the human body. However, their poor solubility into water-based food matrices, instability to environmental stresses during processing and storage, and poor bioavailability provide a challenge for their incorporation into food products. Hence, these bioactive substances are encapsulated into delivery systems to protect them from degradation against chemical and enzymatic factors and/or improve their digestibility in the gastrointestinal tract.

In this study, the potential of hemp oil bodies as an encapsulation system of β-carotene was investigated through various approaches. This involved the use of both non-destructive (partitioning into intact oil bodies) and destructive methods (homogenisation) to create oil body systems containing β-carotene. Moreover, it examined heat treatments to obtain the membrane material fractions from oil bodies for their use as emulsifiers in oil-in-water emulsions. Lastly, the physicochemical properties of the emulsions were characterised, and the β-carotene concentration and encapsulation efficiency of the different systems were determined.

In this chapter, the following terms are used and defined as follows: (1) 'native oil bodies' refer to the isolated form of oil bodies after aqueous extraction, also known as 'oil body fraction'; (2) 'oil body suspension' refers to an oil body fraction that was dispersed in water (10% by oil weight); (3) 'homogenised oil bodies' refer to an oil body suspension that was homogenised using three different equipment (high-speed blender, low-pressure homogeniser, and microfluidizer); and (4) 'oil body emulsion' refers to an oil-in-water emulsion prepared with OBMM as emulsifier.

5.2 Encapsulation of β-carotene using intact oil bodies

5.2.1 With solvents

The potential of intact oil bodies as delivery systems for β-carotene was first examined using organic solvents, wherein β-carotene was dissolved in ethanol, hexane, and diethyl ether and the solution was allowed to remain in contact with the hemp oil body suspension for four (4) hours with or without stirring. After centrifugation of the samples, the β-

carotene concentration in the cream phase of the oil body suspensions was quantified to determine the partitioning of β-carotene in the oil bodies. The encapsulation efficiency was also calculated (Figure 5.1). For the unstirred sample with ethanol, the β-carotene content of the cream layer was found to be 143.5 ± 2.2 μg/g fat, with an encapsulation efficiency of 32.6%. To confirm that β-carotene was not in the aqueous phase, its concentration in the serum layer was quantified and expectedly, the value was -0.01 ± 0.08 μg/g fat. For samples containing hexane, the β-carotene content in the oil body fat extracts was below detection limits for both unstirred and stirred samples. On the other hand, stirred samples with diethyl ether had a slightly higher β-carotene content of 5 μg/g fat than unstirred samples which had 2 μg/g fat. These results show that not all β-carotene added to the solution partitioned into the oil body fraction of the suspension, especially when hexane and diethyl ether were used as solvents.

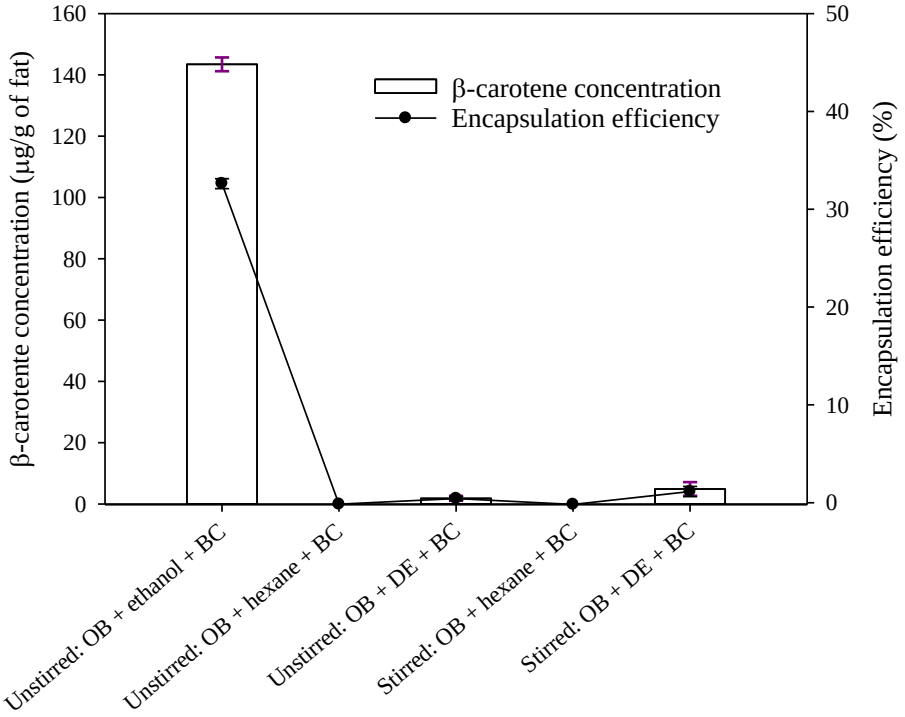

Figure 5.1. β-carotene (BC) concentration of the cream fraction and encapsulation efficiency of the oil body (OB) suspensions after four (4) hours of contact (unstirred or stirred) with β-carotene-loaded ethanol, hexane, and diethyl ether (DE).

In terms of appearance, no phase separation within the oil body suspension phase was observed in unstirred samples after four (4) hours of contact with the β-carotene-loaded solvent (Figure 5.2). The sample with ethanol had a uniform appearance with a slight

tinge of orange colour (Figure 5.2 B). In contrast, hexane and diethyl ether (Figure 5.2 C and D) floated at the top of the oil body suspension, which remained white and barely had any tinge of orange colouration.

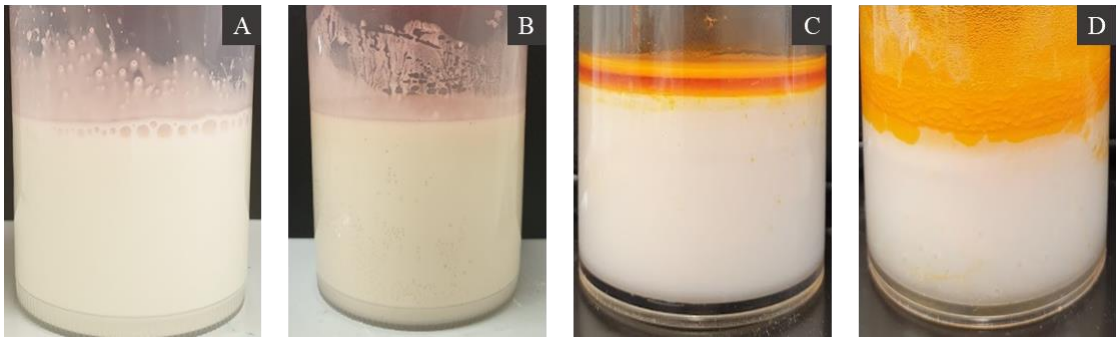

Figure 5.2. Appearance of unstirred oil body suspensions without β-carotene (A) and containing β-carotene-loaded ethanol (B), hexane (C), and diethyl ether (D) after four (4) hours.

Samples containing hexane and diethyl ether were stirred to improve the contact with the oil bodies in suspension given their poor miscibility with water. The sample containing hexane (Figure 5.3 A) did not show apparent phase separation of the oil bodies in suspension. However, mixing of the β-carotene-loaded solvent with the oil body suspension led to a change in its appearance from a white cream to yellow colour, although it was not uniform as the contents on the bottom of the container remained white. Similarly, the sample with diethyl ether did not exhibit phase separation of the oil body suspension (Figure 5.3 B). However, the sample had a bright orange colouration at the top, while most of the bottom part remained white with a tinge of orange.

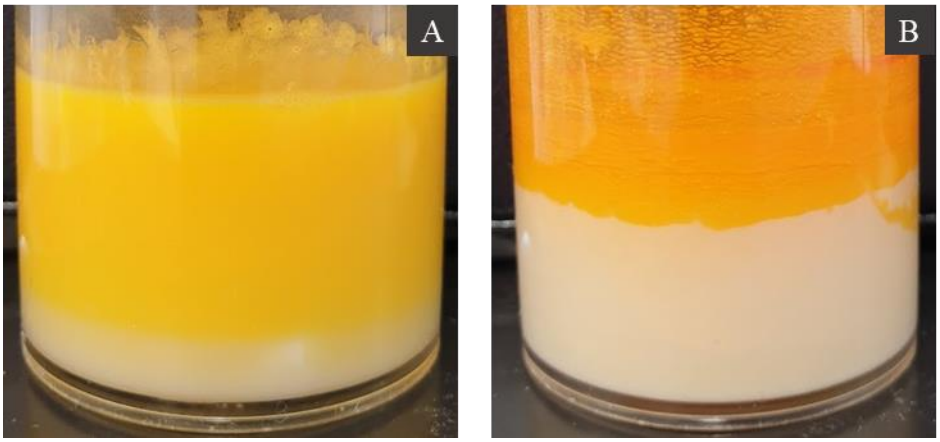

Figure 5.3. Appearance of oil body suspensions mixed with β-carotene-loaded hexane (A) and diethyl ether (B) after stirring for four (4) hours.

Centrifugation was used to separate the solvent from the oil body suspension. The samples, both unstirred and stirred, were centrifuged to separate the cream and serum layer to determine if β-carotene migrated to the oil body phase. For unstirred samples, undissolved β-carotene crystals were observed at the bottom of the container in the sample with ethanol (Figure 5.4 A). As expected, ethanol did not separate from the suspension because of its miscibility in water. Likewise, the sample with hexane had specks of crystalline β-carotene but they were found at the top of the cream phase of the sample (Figure 5.4 B). Centrifugation at 10,000 *g* for 20 min was able to separate hexane from the suspension, as seen on the orange colouration observed at the top of the centrifuge tube, with the cream phase remaining mostly white in colour. Lastly, the unstirred sample with diethyl ether did not show any undissolved β-carotene crystals (Figure 5.4 C). However, centrifugation was not able to separate the solvent from the suspension as it resulted in a concentrated orange solvent layer at the top, with the rest of the cream layer having a faint orange gradient colouration.

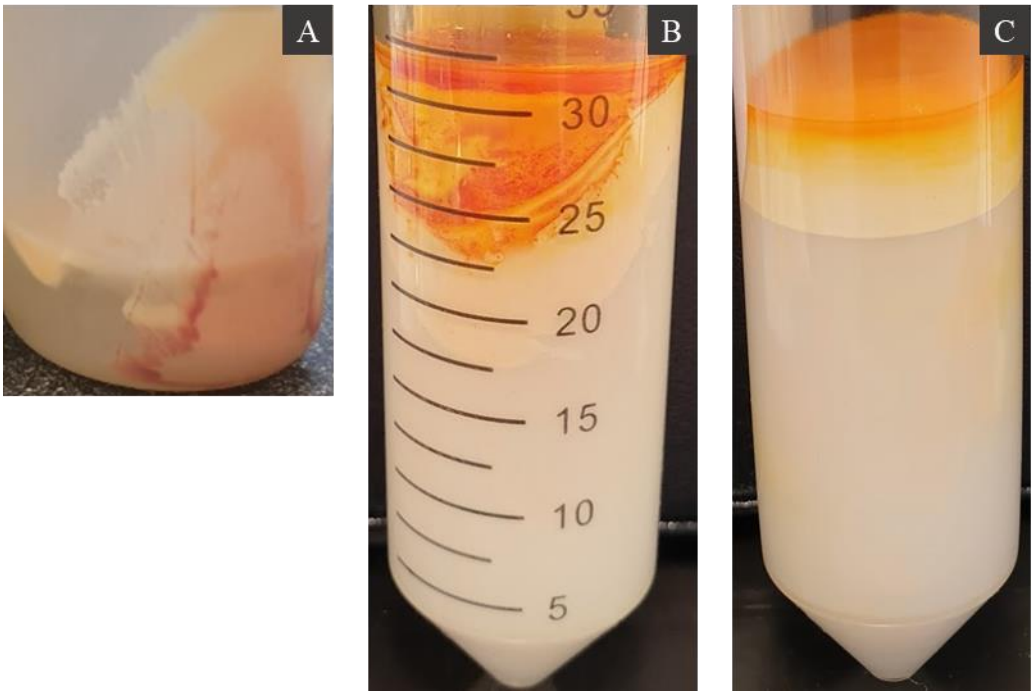

Figure 5.4. Appearance of unstirred oil body suspensions incorporated with β-carotene-loaded ethanol (A), hexane (B), and diethyl ether (C) after centrifugation at 10,000 *g* for 20 min.

In the case of stirred samples, centrifugation was not effective in removing hexane from the oil body suspension since an orange jelly-like layer containing β-carotene and hexane

was formed (Figure 5.5 A). Centrifugation at higher speeds (1,000 and 10,000 *g*) was ineffective in the clear separation of solvents from the cream as most of them remained in the cream layer. The use of a vacuum concentrator improved the extraction of hexane from the system, but it resulted in an orange gradient in the cream layer, making it hard to obtain representative samples for β-carotene quantification. Similarly, it was difficult to separate diethyl ether from the oil bodies by centrifugation, as it resulted in a concentrated orange layer at the top, with the rest of the cream layer having a faint orange gradient colouration (Figure 5.5 B). Even at the highest centrifugation speed used (10,000 *g*), no solvent was separated from the oil body suspension.

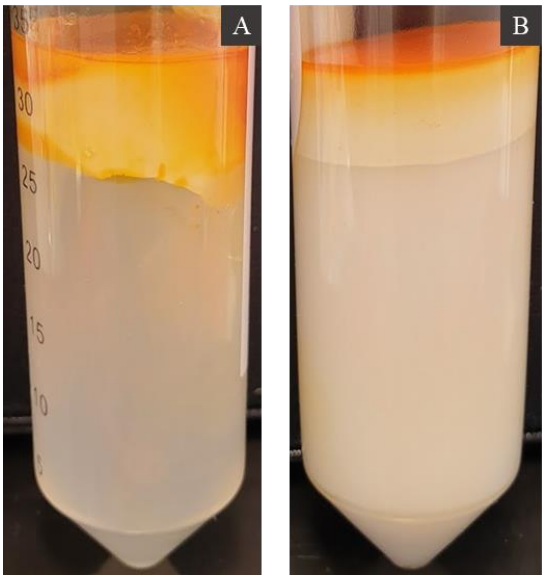

Figure 5.5. Appearance of stirred oil body suspensions incorporated with β-carotene-loaded hexane (A) and diethyl ether (B) after centrifugation at 10,000 *g* for 20 min.

Compared to the unstirred samples, the stirred samples with hexane did not show any trace of undissolved β-carotene crystals. Most of the cream layer was also tinged with an orange colouration in the stirred sample, whereas the orange colour remained in the solvent phase in the unstirred sample. On the other hand, the behaviour of stirred and unstirred samples with diethyl ether was similar, wherein an orange gradient was observed in the cream phase of the suspension. Nevertheless, the stirred sample had a more intense orange colour at the top. This indicates that stirring somehow improved the contact of β-carotene in the solvents with the oil bodies suspended in water.

5.2.2 Without solvents

The solubility of β-carotene in hempseed oil (with soybean oil as reference) was quantified using two extraction techniques to determine the amount to be directly incorporated in hemp oil bodies. Figure 5.6 shows the solubility of β-carotene in soybean oil. Using hexane for extraction of fat, the β-carotene quantified was 177.4 ± 7.1 μg/g fat, with a recovery (percentage of the amount of β-carotene extracted over the amount added) of 88.7%. When hexane:dichloromethane was used, a higher amount of β-carotene was quantified (228.4 ± 17.9 μg/g fat) but there was an overestimation of the β-carotene content as the recovery calculated was 114.2%.

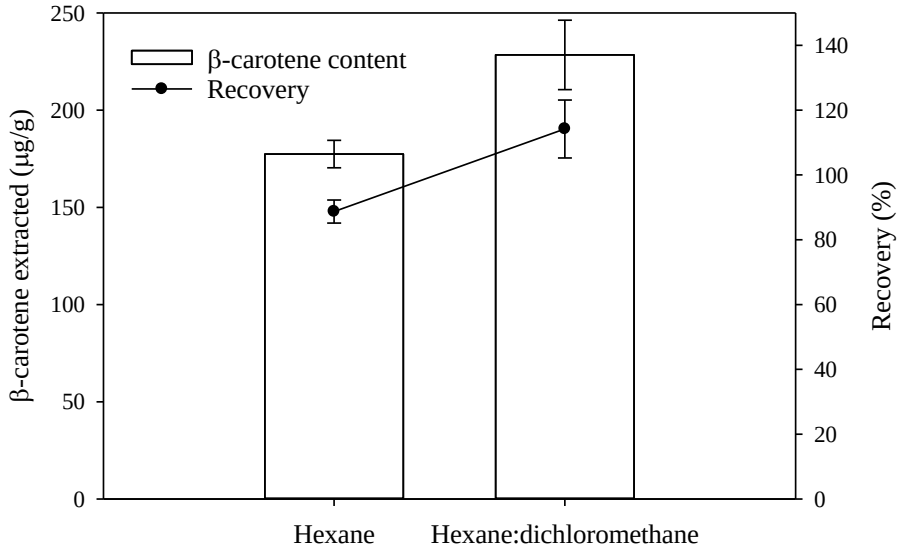

Figure 5.6. Solubility of β-carotene in soybean oil extracted with hexane and hexane:dichloromethane (1:4), presented in terms of β-carotene content and recovery (percentage of the amount of β-carotene extracted over the amount added).

In hempseed oil, the solubility of β-carotene analysed using the two extraction techniques is shown in Figure 5.7. The amount of β-carotene quantified using hexane as the extraction solvent was 108.2 ± 2.5 μg/g fat for the low concentration of β-carotene added (125 μg/g fat), 212.5 ± 9.4 μg/g fat for the medium concentration (250 μg/g), and 343.7 ± 5.2 μg/g fat for the high concentration (500 μg/g). The recovery of β-carotene for 125, 250 and 500 μg/g added to oil was 86.6%, 85.0%, and 68.7%, respectively. When hexane:dichloromethane was used for extraction, the concentration of β-carotene determined from the lowest to the highest amount added (125, 250, and 500 μg/g fat) was

162.6 ± 15.1 μg/g fat, 276.2 ± 35.6 μg/g fat, and 482.7 ± 47.1 μg/g fat, with a recovery of 130.1%, 110.5%, and 96.5%, respectively.

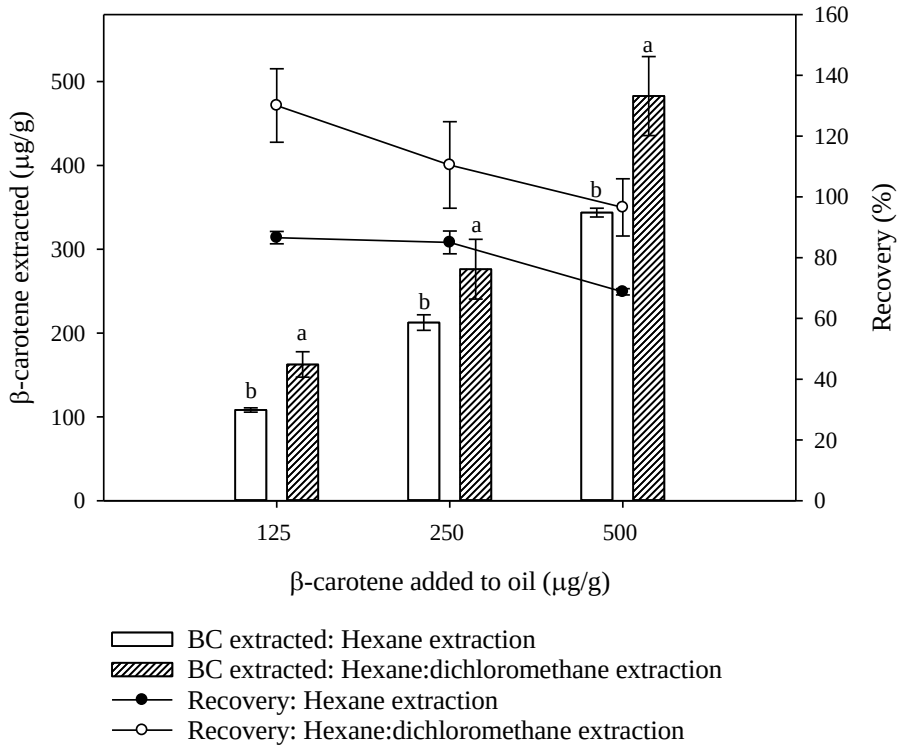

Figure 5.7. Solubility of β-carotene (BC) in hempseed oil using hexane extraction or hexane:dichloromethane (1:4) extraction. Recovery (%) refers to the percentage of the amount of β-carotene extracted over the amount added to the oil. Means that do not share a letter within the same group are significantly different at α=0.05. Error bars indicate standard deviations.

Based on the results, the use of hexane for extraction resulted in a significantly lower concentration of β-carotene quantified in hempseed oil, compared to hexane:dichloromethane. However, there was an overestimation and higher variability of β-carotene content when hexane:dichloromethane was used for extraction. Thus, hexane extraction was used for the quantification of β-carotene in the oil body systems prepared in this study. A β-carotene concentration of 400 μg/g (by oil weight) was used for its encapsulation into hemp oil bodies based on the maximum solubility of β-carotene in hempseed oil measured by hexane extraction.

Direct incorporation of β-carotene crystals into hemp oil bodies was done through heating and sonication as detailed in Section 3.2.8.2.2. The incorporation of β-carotene inside the oil bodies was evident from the appearance of cream as β-carotene encapsulation resulted

in an orange-coloured hemp cream (data not shown). Moreover, there was barely any undissolved β-carotene crystals after sonication. Quantification of the β-carotene content of the cream indicated a concentration of 552.5 ± 36.3 μg/g (by oil weight) and an encapsulation efficiency of 138.2 ± 8.5 %. This overestimation of β-carotene content was consistent across the analysis of multiple samples prepared at different time points; the reason for this is not known. A correction factor of 0.7235 was henceforth applied to the β-carotene contents to estimate the encapsulation efficiency determined using this method.

5.3 Encapsulation of β-carotene using disrupted oil bodies

5.3.1 Re-emulsification of intact oil bodies

5.3.1.1 Effect of homogenisation of the properties of oil bodies

In this study, the effect of increasing the homogenisation pressure (250, 500, 750, and 1000 bar) on the particle size of oil body systems was investigated to understand the level of disruption of the membrane of oil bodies. The particle size ($d_{4,3}$) of native and homogenised hemp oil bodies is shown in Figure 5.8. There was no significant difference in the $d_{4,3}$ of oil bodies before (native oil bodies) and after re-emulsification with a high-speed blender (10,000 rpm, 2 min), and a slight increase was observed with the low-pressure homogeniser (250 bar). The homogenised oil bodies prepared by microfluidization showed a different trend: the $d_{4,3}$ increased as the homogenisation pressure increased from 500 bar to 1000 bar. Although this increase was not linear, the droplet size of the homogenised oil bodies was largely similar at pressures greater than 500 bar. However, $d_{4,3}$ values measured in the presence of 1.2% SDS resulted in particle sizes between 4 and 6 μm. Furthermore, the particle sizes in the homogenised oil bodies were not significantly different from that of native oil bodies (except for the homogenised oil bodies obtained at 250 bar).

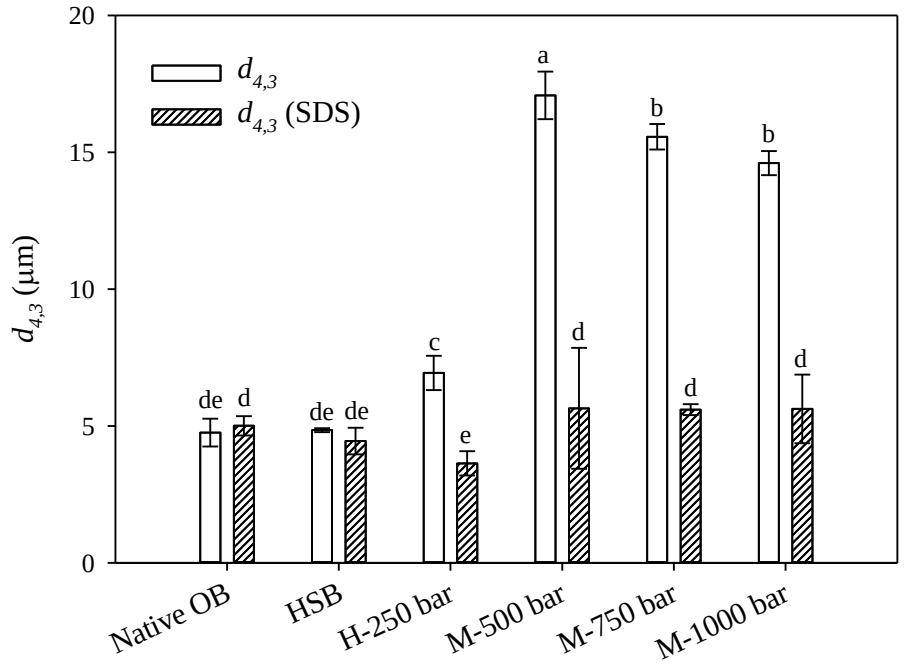

Figure 5.8. Effect of homogenisation on the particle size ($d_{4,3}$) of hemp oil bodies: native oil bodies (OB) and homogenised oil bodies prepared using a high-speed blender at 10,000 rpm for 2 min (HSB), low-pressure homogeniser at 250 bar (H-250), and microfluidizer at 500, 750, and 1000 bar (M-500, M-750, and M-1000). Means that do not share a letter are significantly different at α=0.05. Error bars indicate standard deviations.

The particle size distributions of homogenised oil bodies are shown in Figure 5.9 A. Native and homogenised oil bodies prepared with a high-speed blender had a similar span and monomodal size distribution, with a peak at around 5 μm. When a low-pressure homogeniser was used at 250 bar, the size distribution remained monomodal but shifted to the right, with a peak at around 8 μm. Microfluidization at higher pressures (500 to 1000 bar) resulted in bimodal size distributions that had a wider span: there was a population of smaller droplet sizes below 1 μm and peaks above 10 μm. The size distributions were largely similar at homogenisation pressures above 500 bar.

The droplet size distributions of the native and homogenised oil bodies dispersed in SDS is shown in Figure 5.9 B. Regardless of the homogenisation conditions, native and homogenised oil bodies exhibited fairly similar monomodal size distributions. However, there was a narrower span for native oil bodies and homogenised oil bodies prepared with the high-speed blender. The narrowest size distribution was observed for the oil bodies

homogenised at 250 bar with a low-pressure homogeniser. At higher pressures (500 to 1000 bar), homogenised oil bodies showed wider size distributions, with peaks at around 10 μm.

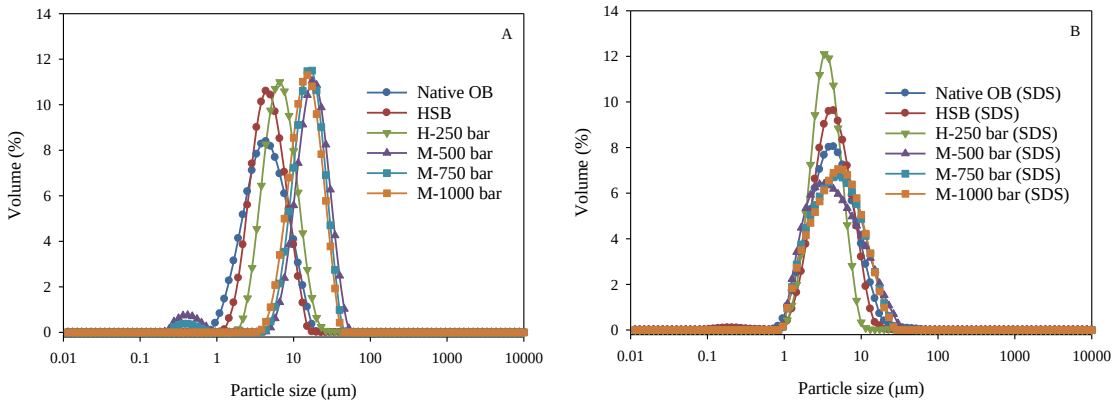

Figure 5.9. Effect of homogenisation treatment on the particle size distributions of native and homogenised hemp oil bodies (OB) dispersed in Milli-Q water (A) and SDS (B). Homogenised oil bodies were prepared using a high-speed blender at 10,000 rpm for 2 min (HSB), low-pressure homogeniser at 250 bar (H-250), and microfluidizer at 500, 750, and 1000 bar (M-500, M-750, and M-1000).

Compared to the size distributions of the oil bodies dispersed in SDS, the original size distributions of the homogenised oil bodies were wider, indicating flocculation of oil droplets. This behaviour was more evident at homogenisation pressures above 500 bar, as the size distributions of native oil bodies and homogenised oil bodies obtained with the high-speed blender and low-pressure homogeniser did not show much difference when dispersed in SDS. Hence, a homogenisation pressure of 250 bar was used for preparing homogenised oil bodies for further investigation in this study.

The ζ-potential of native and homogenised oil bodies, including their pH, is shown in Figure 5.10. At the pH of extraction (~6.8, taken after suspending the native or homogenised oil bodies in Milli-Q water for ζ-potential measurements), the ζ-potential of native oil bodies was -20.4 ± 6.6 mV while the magnitude was significantly higher for homogenised oil bodies (-23.2 ± 2.0mV). The pH of the medium also varied for each extraction for native oil bodies which ranged from 5.9 to 8.2, whereas minimal deviation was observed for homogenised oil bodies.

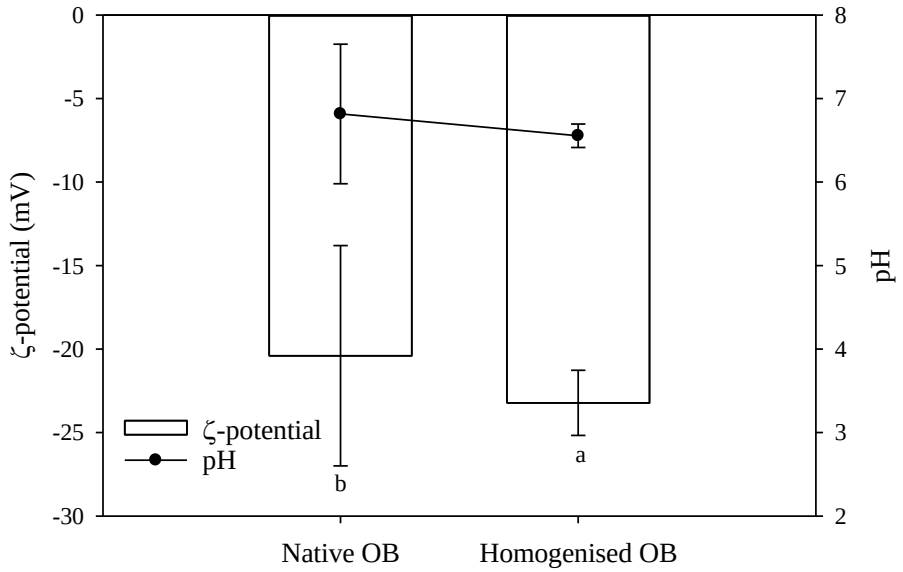

Figure 5.10. ζ-potential of native and homogenised (using a low-pressure homogeniser at 250 bar) oil bodies (OB) at the pH of extraction. Means that do not share a letter are significantly different at α=0.05. Error bars indicate standard deviations.

The microstructure of homogenised hemp oil bodies was further characterised by CLSM (Figures 5.11 and 5.12). The structural components examined as stained by different dyes are as follows: neutral lipids by Nile Red, proteins by FG-FCF, and phospholipids by Rd-DHPE. Based on the images, the droplet size of both native and homogenised oil bodies ranged from 3 to 6 μm, which agrees with the particle size data previously discussed. However, homogenised oil bodies also showed coalescence (white arrows, Figure 5.11 C). While the surface of native oil bodies was uniformly covered by proteins (Figure 5.11 B), homogenised oil bodies showed a more intense intermittent fluorescence along their circumference indicating that some regions had more proteins or their aggregates (Figure 5.11 D).

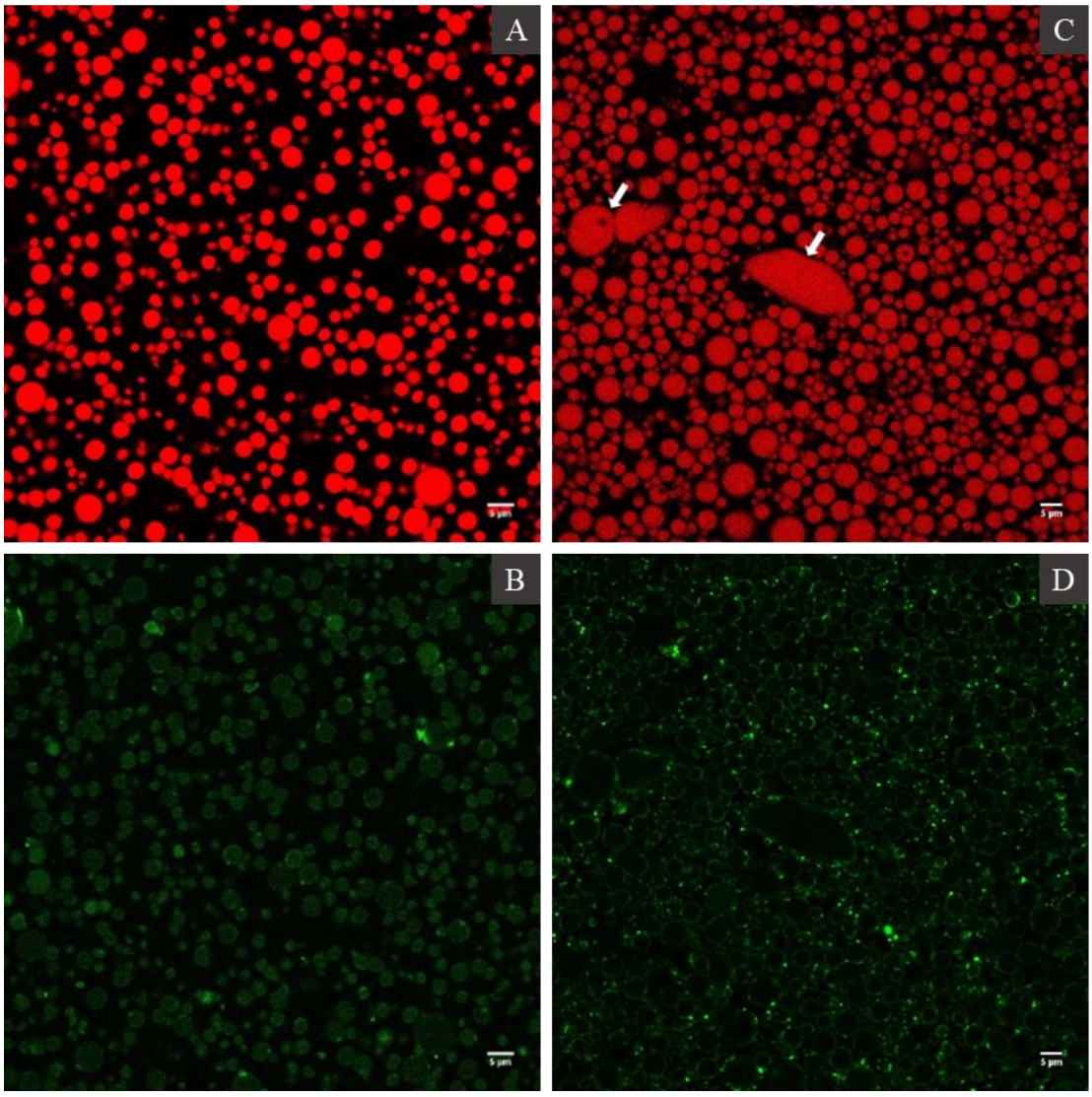

Figure 5.11. CLSM images of native (A and B) and homogenised (using a low-pressure homogeniser at 250 bar) (C and D) oil bodies (OB) showing the neutral lipids stained by Nile Red (A and C) and proteins stained by FG-FCF (B and D).

The staining with Rd-DHPE indicates that even after being subjected to shear, phospholipids still covered the oil droplet surface, although not as uniformly compared with native oil bodies as protrusions and small flocs of red particles were observed on the surface of the oil droplets (Figure 5.12). These results suggest that when the structure of oil bodies is disrupted due to homogenisation, the membrane materials can restabilise oil droplets in a similar size range as native oil bodies, although there is some flocculation and coalescence observed.

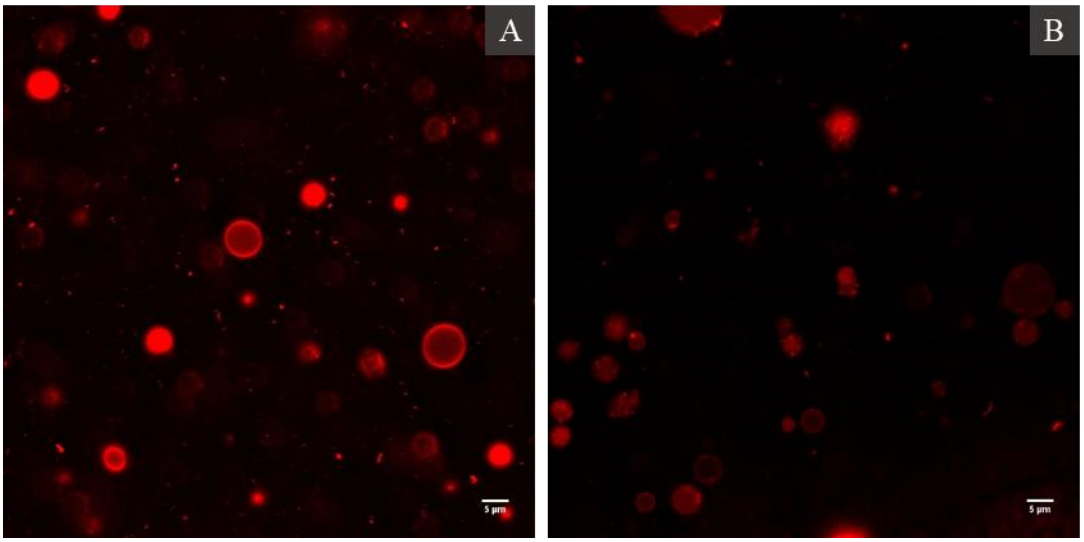

Figure 5.12. CLSM images of native (A) and homogenised (B) oil bodies showing the phospholipids stained by Rd-DHPE.

5.3.1.2 Effect of addition of β-carotene on the properties of homogenised oil bodies

Homogenised oil bodies containing β-carotene were obtained by homogenising the β-carotene-loaded oil bodies (herein referred to as non-homogenised oil bodies with β-carotene) from the method of 'encapsulation without solvents' described in Section 3.2.8.2.2. The particle size and size distributions of β-carotene-loaded homogenised oil bodies are shown in Figure 5.13. As seen in Figure 5.13 A, the incorporation of β-carotene in native oil bodies showed a significant increase in $d_{4,3}$ (8.7 ± 0.8 μm) even in the presence of SDS (8.4 ± 1.3 μm), indicating flocculation and/or coalescence. Upon homogenisation, the $d_{4,3}$ was not significantly changed (7.5 ± 0.7 μm), although it was significantly reduced with a value of 3.4 ± 0.1 μm in the presence of SDS. Particle size distribution data (Figure 5.13 B) shows a monomodal distribution of all systems, with the homogenised oil bodies having the narrowest distribution. In the presence of SDS, the size distributions for non-homogenised oil bodies with β-carotene did not show much difference. However, the distribution for the homogenised oil bodies had a pronounced shift to lower particle sizes (Figure 5.13 C). These results indicate that homogenisation was able to reduce the size of individual droplets of homogenised oil bodies containing β-carotene; however, flocculation and/or coalescence still occurred.

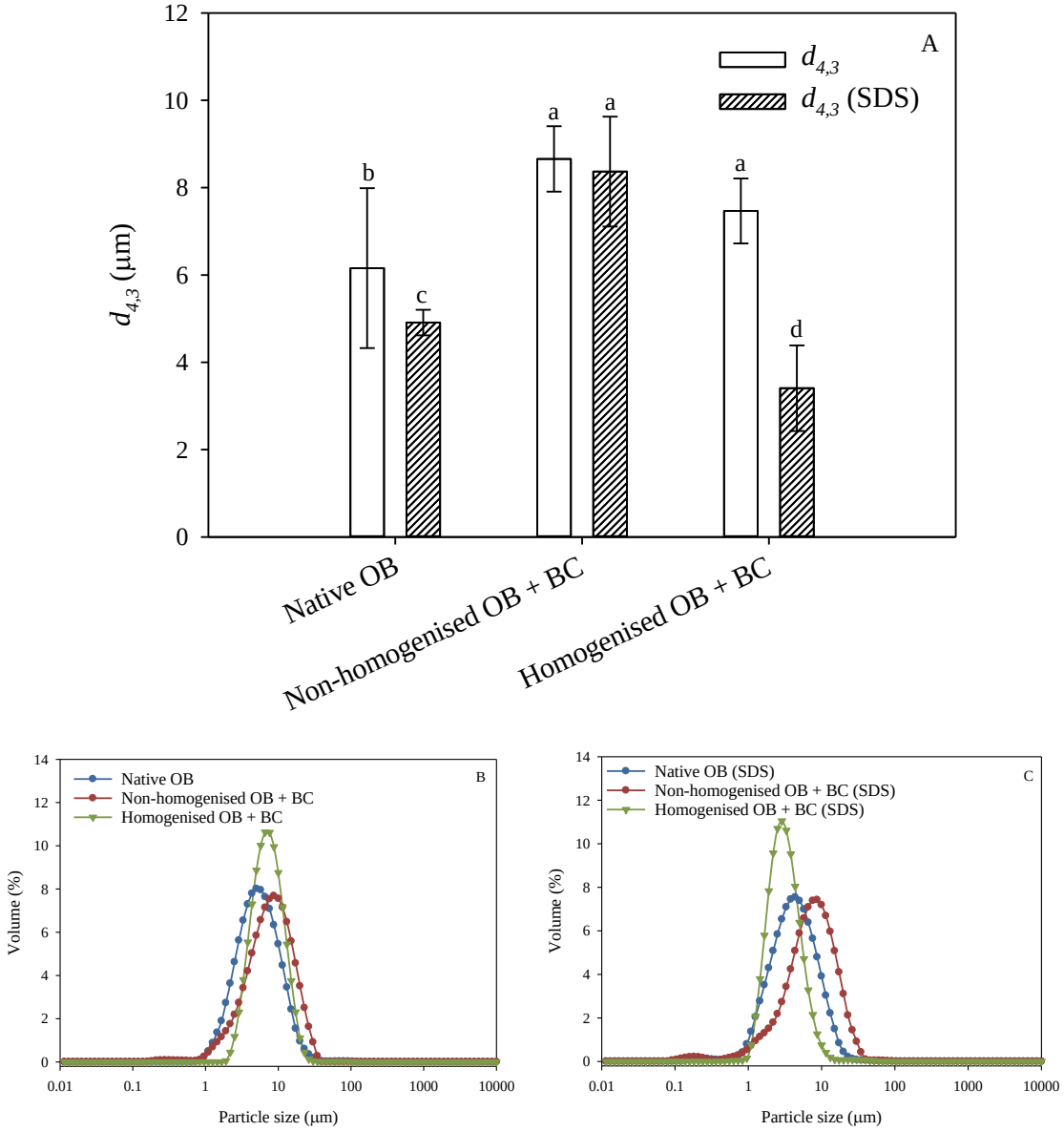

Figure 5.13. Particle size (A) and size distributions (B and C) of native oil bodies (OB), non-homogenised oil bodies containing β-carotene (non-homogenised OB + BC), and homogenised oil bodies (using low-pressure homogeniser at 250 bar) containing β-carotene (homogenised OB + BC) dispersed in Milli-Q water (B) and SDS (C). Means that do not share a letter are significantly different at α=0.05. Error bars indicate standard deviations.

The β-carotene concentration of the oil body systems, including the cream and serum phase obtained after centrifugation, was determined by solvent extraction and UV-Vis spectrophotometry. As seen in Figure 5.14, the β-carotene concentration of the homogenised oil bodies was 307.8 ± 26.0 µg/g fat with an encapsulation efficiency of 77.0 ± 6.4%. A separate analysis of the β-carotene concentration of the cream phase

indicated the absence of a significant difference while β-carotene was not quantified in the serum phase of the emulsion. These results confirm that β-carotene successfully migrated into the oil bodies based on the method indicated in Section 5.2.2. Furthermore, β-carotene was not detected in the serum phase, indicating that there were no undissolved β-carotene crystals after incorporation in the cream and after mixing with Milli-Q water to create the emulsions.

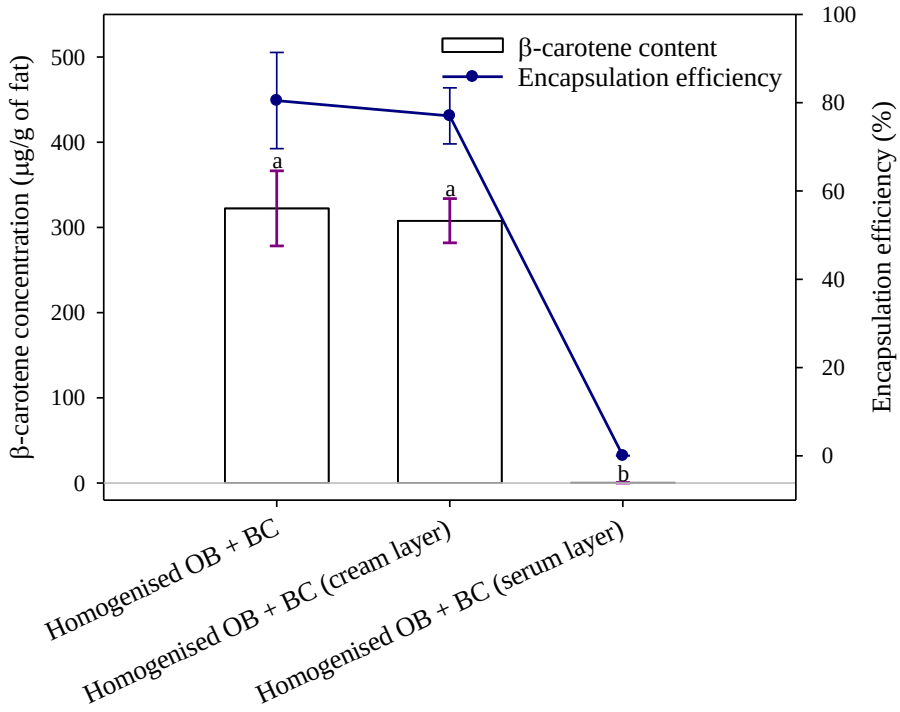

Figure 5.14. β-carotene concentration and encapsulation efficiency of the homogenised oil bodies (OB) containing β-carotene (BC), including the β-carotene concentration in the cream and serum phase. The emulsion was centrifuged at 10,000 *g* for 20 min, resulting in an oil body-rich cream phase and an oil body-depleted serum phase. Means that do not share a letter are significantly different at α=0.05. Error bars indicate standard deviations.

5.3.2 Emulsification using oil body membrane materials (OBMM)

5.3.2.1 Extraction and characterisation of oil body membrane material extracts

To determine the optimal temperature for extracting the membrane materials, heating was done at 50°C, 70°C, and 100°C. After centrifugation of the heated oil bodies, four layers were observed: (1) free oil, (2) cream phase, (3) serum, and (4) sediment fraction (Figure 5.15). Aside from the sediment layer, the serum fraction was thought to contain the

proteins that were dislodged from the oil body interface after heating. Optical microscopy images of the serum and sediment fraction of the heated oil body system (Figure 5.16) showed that at 50°C and 70°C, oil droplets which could be free oil or intact oil bodies were present at the serum layer while the sediment fraction contained protein aggregates as well as oil droplets. Compared to 50°C, more extensive protein aggregation was observed at 70°C. Heat treatment at 100°C resulted in the highest extent of protein aggregation due to denaturation, which was observed both at the serum and sediment fractions (Figure 5.16 E and F). Thus, the proteins from the oil body interface or possibly some extraneous proteins were found to be present in the serum and sediment fractions.

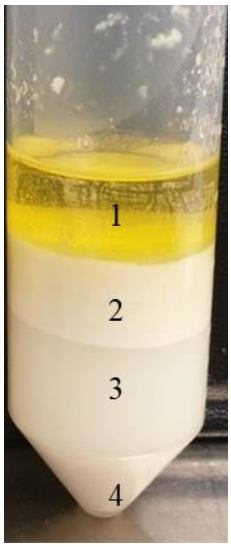

Figure 5.15. Oil body fractions after heating and centrifugation: free oil (1), cream (2), serum (3), and sediment (4) layer.

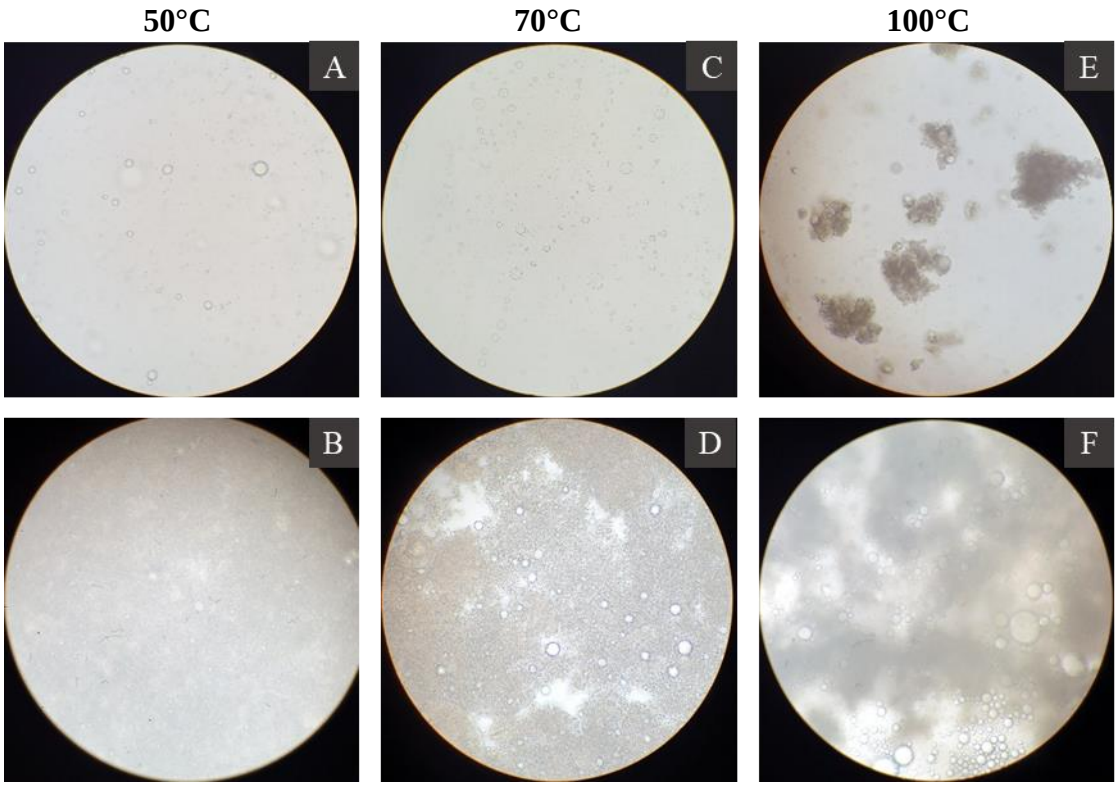

Figure 5.16. Optical microscopy images of the serum (A, C, and E) and sediment (B, D, and F) fractions of membrane material extracted from hemp oil bodies by heat treatment at 50°C (A and B), 70°C (C and D), and 100°C (E and F).

The potential of the combined serum and sediment/aggregate fractions (termed as the 'membrane material') to act as emulsifiers was initially tested by creating coarse emulsions which were characterised structurally by optical microscopy (Figure 5.17). Using the membrane material fraction heated at 50°C resulted in an emulsion with very large oil droplets and un-emulsified oil. In contrast, the 70°C emulsion was able to produce a coarse emulsion with fairly uniform droplet size and without the presence of free oil. Lastly, the 100°C emulsion showed the presence of protein aggregates, un-emulsified oil, and emulsified oil droplets that varied in size. Since the membrane material fraction obtained at 100°C was not effective in creating a stable emulsion, presumably because of the extensive protein denaturation, only the 50°C and 70°C membrane material fractions were further investigated for their emulsification properties.

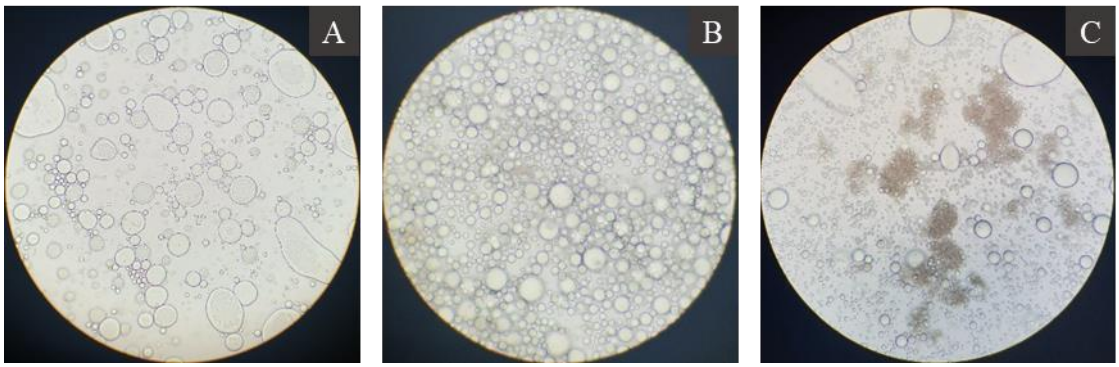

Figure 5.17. Optical microscopy images of coarse emulsions prepared from extracting membrane materials from hemp oil bodies at 50°C (A), 70°C (B), and 100°C (C).

The proximate composition of the membrane material fractions extracted at 50°C and 70°C was determined by analysing their total solids, crude protein, and fat content. A control which was unheated hemp oil bodies dispersed in Milli-Q water but was stirred and centrifuged for the same duration and speed was also analysed for comparison. Based on Table 5.1, there was no significant difference in the total solids, crude protein, and fat content of the membrane material fractions extracted at 50°C and 70°C. Nevertheless, these samples had a significantly higher crude protein content (% dry basis) compared to the unheated sample, indicating that heating resulted in destabilisation of oil bodies and the interfacial proteins were concentrated in the serum and sediment phase of the system. The fat content (% wet basis) of the 50°C and 70°C samples was also significantly lower compared to the control since the oil was liberated from the oil body structure and removed after heating. Despite the centrifugation and removal of the free oil and cream fraction, some oil droplets were still contained in the isolated membrane material fraction.

Table 5.1. Composition of oil body membrane material extracted by heat treatment.

Sample	Total solids (%)	Crude protein content		Fat content	
		% wet basis	% dry basis	% wet basis	% dry basis
Unheated	8.75 ± 1.07^{a}	1.68 ± 0.11^{a}	19.23 ± 1.26^{b}	6.36 ± 1.38^{a}	72.73 ± 15.76^{a}
50°C	2.69 ± 0.16^{b}	1.55 ± 0.14^{a}	57.63 ± 5.15^{a}	1.88 ± 0.15^{b}	69.75 ± 5.76^{a}
70°C	2.29 ± 1.20^{b}	1.41 ± 0.40^{a}	61.37 ± 17.58^{a}	1.64 ± 0.26^{b}	71.59 ± 11.26^{a}

**Means that do not share a letter within the same column are statistically significant at α=0.05.*

The microstructure of the membrane material fractions containing both the serum and sediment layer was examined using CLSM. As discussed in Section 5.4.4, the membrane material fraction could contain intact oil bodies or oil droplets stabilised by a mixed membrane comprised of storage proteins or oil body proteins. As seen in Figure 5.18 A, the unheated sample contained intact oil bodies whose size ranged from 3 to 6 μm and protein clumps were found to have adhered at the interface. Such protein clumps could have been extraneous proteins or oil body interfacial proteins that were concentrated in the membrane material fraction after intensive stirring of the oil body suspension. The 50°C membrane material fraction contained oil droplets, which could be intact oil bodies or free oil, of size ranging from around 3 to 10 μm that were more intensely covered by protein fractions. Similarly, the 70°C membrane material fraction had oil droplets in the size of around 3 to 8 μm, whose surface was more uniformly covered by protein aggregates compared to the 50°C sample. The 70°C sample had a smaller oil droplet size, which could be due to the higher protein content of the sample that was sufficient to cover the smaller surface area of the oil droplets. The structures formed also may act as Pickering stabilisers and these membrane material structures were further tested for their ability to stabilise hempseed oil emulsions.

5.3.2.2 Properties of emulsions made from OBMM

The membrane material structures discussed above were used as emulsifiers to create a 2.5% (w/w) hempseed oil emulsion. Analysis of the particle size ($d_{4,3}$) and size distributions of the emulsions (Figure 5.19) shows that emulsions made with 50°C and 70°C membrane material fractions dispersed in water had a significantly lower particle size compared to the unheated membrane material fraction (unheated oil bodies that were stirred and centrifuged as the heated samples). However, a significant decrease in the mean particle diameter was observed in the presence of SDS, indicating extensive flocculation of the emulsions at the high homogenisation pressure used. This is seen in the size distributions that shifted to lower particle sizes in the presence of SDS, especially for the samples made from the 50°C and 70°C membrane material fractions. Moreover, there was no significant difference in the ζ-potential of the emulsions (results not shown).

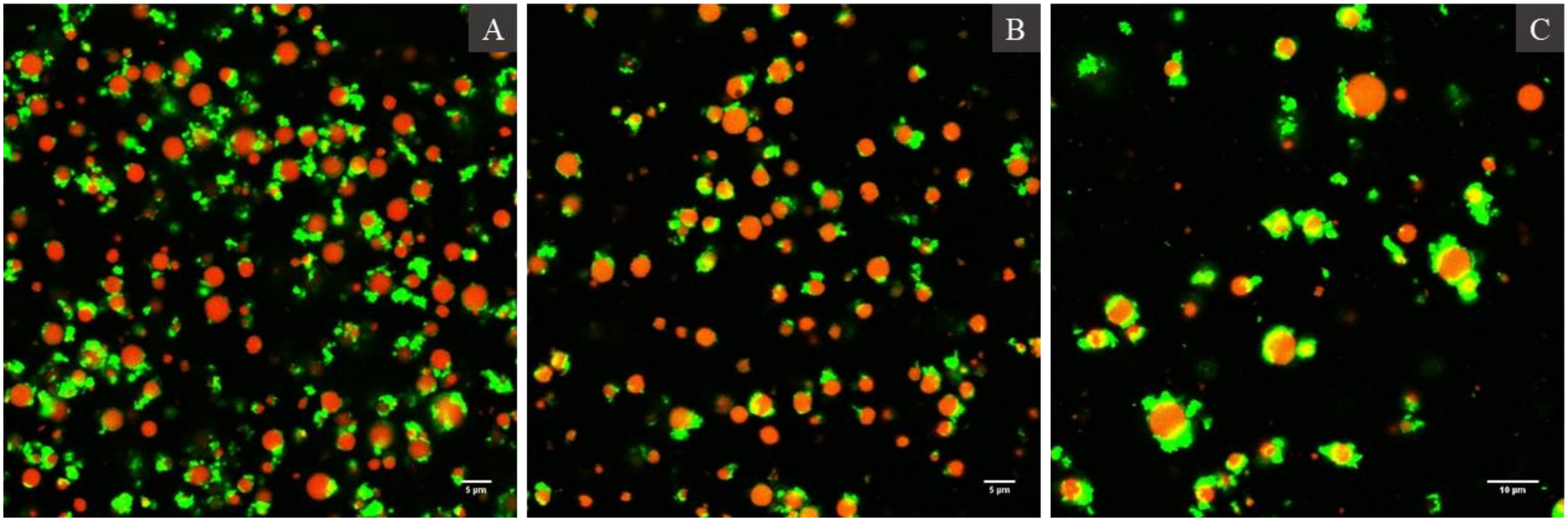

Figure 5.18. CLSM images of hemp oil body membrane materials extracted by heating at 50°C (B) and 70°C (C), including the control sample (A) which was unheated but treated at the same conditions. Neutral lipids are shown in red (stained by Nile Red) while proteins are shown in green (stained by FG-FCF).

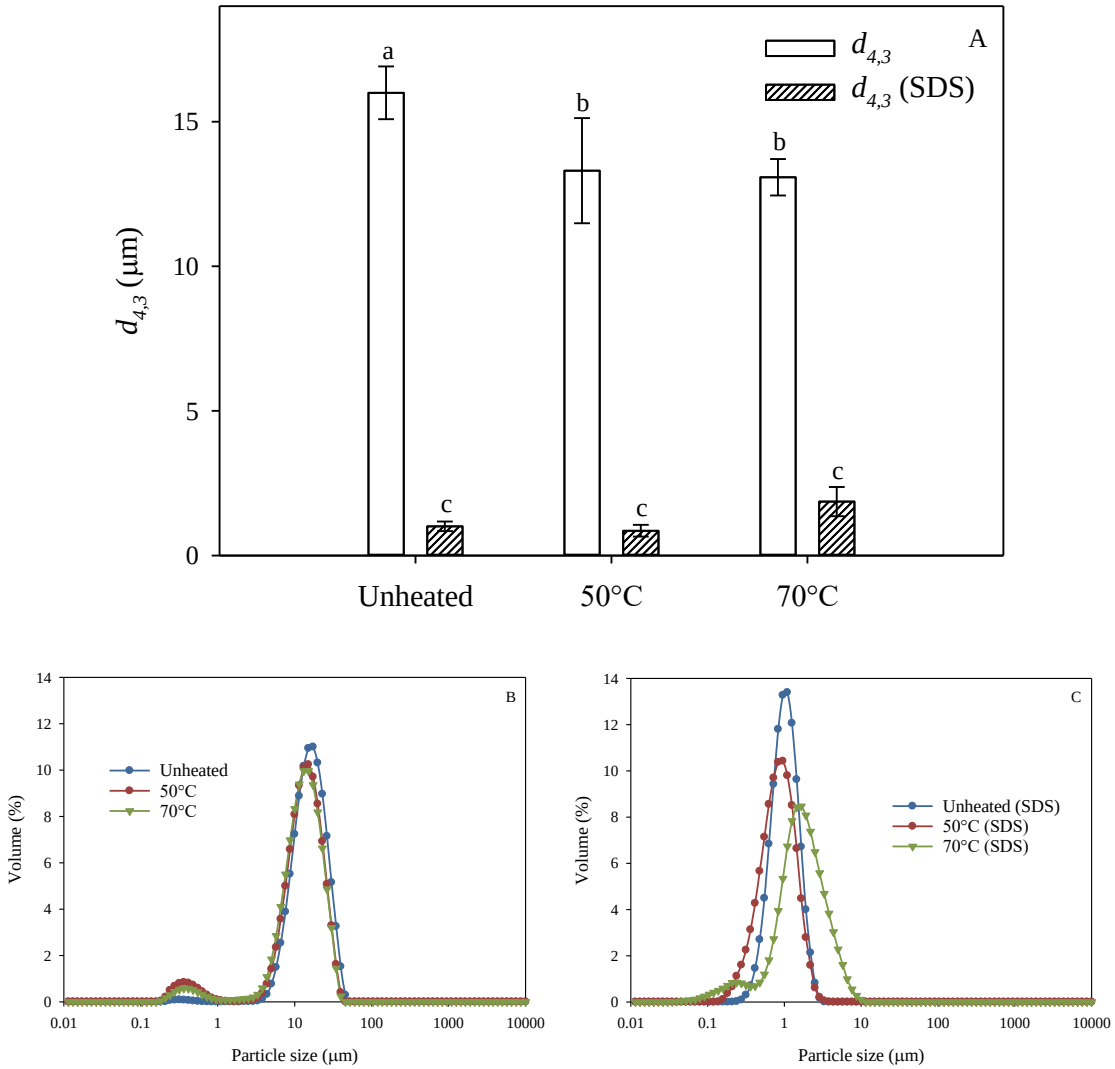

Figure 5.19. Particle size (A) and size distributions (B and C) dispersed in Milli-Q water (B) and SDS (C) of emulsions made from membrane material fractions extracted from oil bodies by heat treatment at 50°C and 70°C, including the unheated sample.

Based on the characterisation of the membrane material from Section 5.3.2.1, the membrane material fraction extracted at 70°C was chosen for encapsulating β-carotene. This is because of its ability to create a more uniform droplet size in the emulsions and the structures formed (based on confocal images) could be more effective in stabilising the oil droplet interface.

Emulsions were prepared by mixing β-carotene-loaded hempseed oil with varying proportions of the membrane material fraction (refer to Section 5.4.4 for composition) based on the protein-to-oil ratio. Particle size ($d_{4,3}$) and size distribution data indicate that the decrease in the protein-to-oil ratio caused a significant decrease in the $d_{4,3}$ of emulsions (Figure 5.20). However, the mean particle diameter in the presence of SDS did not show any significant difference across all samples. The samples with the lowest protein-to-oil ratio of 0.28:1 and 0.14:1 had extensive flocculation since a significant decrease in mean particle diameter was observed in SDS. This is indicative that the amount of emulsifier present was insufficient to stabilise the oil droplets in the emulsion. Particle size distribution data of the emulsions further confirmed this as a wider size distribution was observed at the lowest protein-to-oil ratio used.

Further characterisation of the emulsions by CLSM validated that decreasing the protein-to-oil ratio caused an increase in the droplet size (Figure 5.21). The emulsion with the highest protein-to-oil ratio of 0.55:1 (Figure 5.21 A) had the smallest oil droplet size which ranged from around 1 to 5 μm in diameter and proteins in clumps appeared to be bound to the droplet interface. As the concentration of membrane material increased, the size of oil droplets increased and flocculation was observed. This was apparent in the sample having the lowest protein-to-oil ratio (Figure 5.21 D), wherein aggregation and large droplets greater than 5 μm in size were observed.

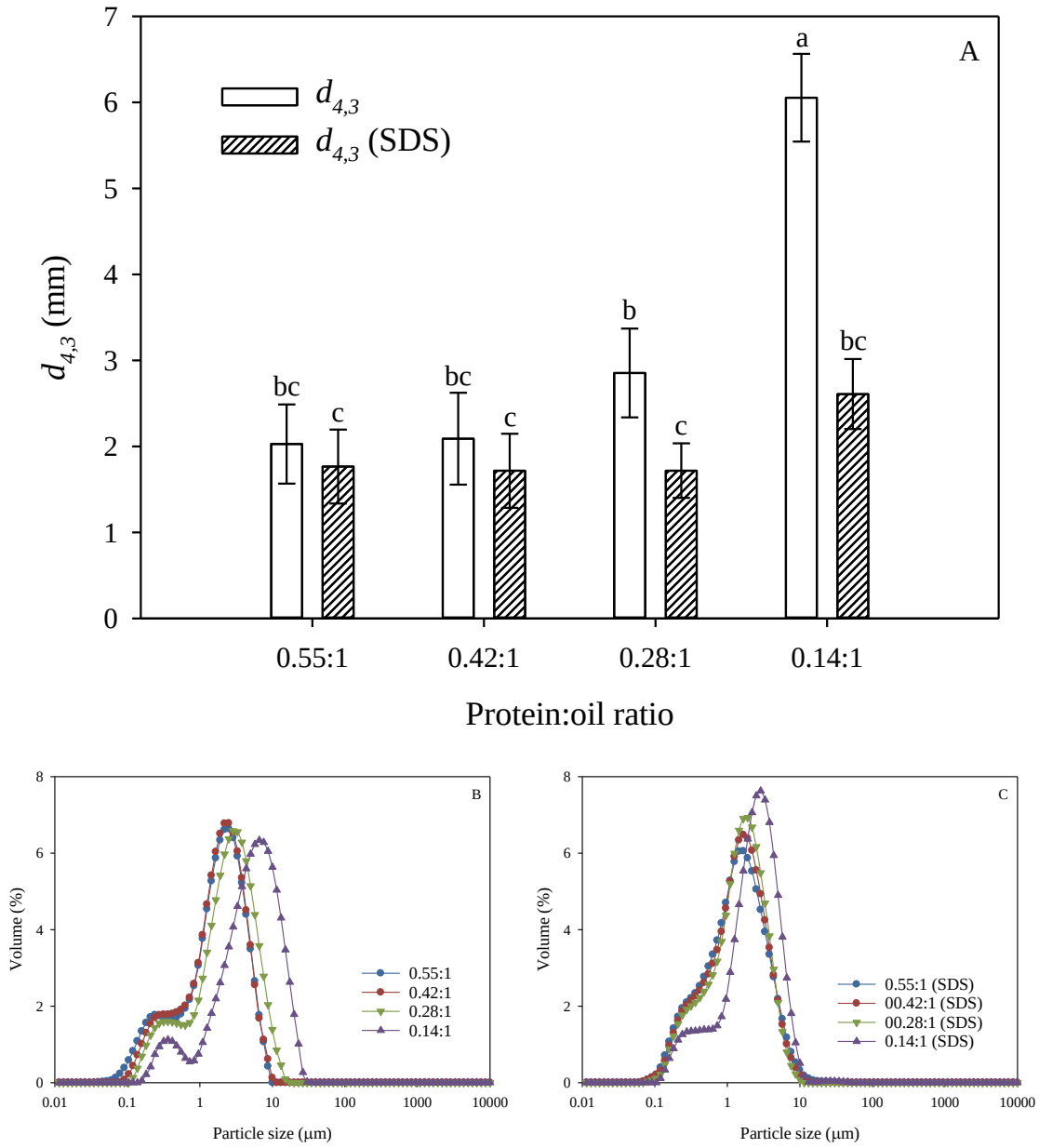

Figure 5.20. Particle size (A) and size distributions (B and C) dispersed in Milli-Q water (B) and SDS (C) of oil body membrane material (OBMM)-stabilised emulsions containing β-carotene at different protein-to-oil ratios. Means that do not share a letter are significantly different at α=0.05. Error bars indicate standard deviations.

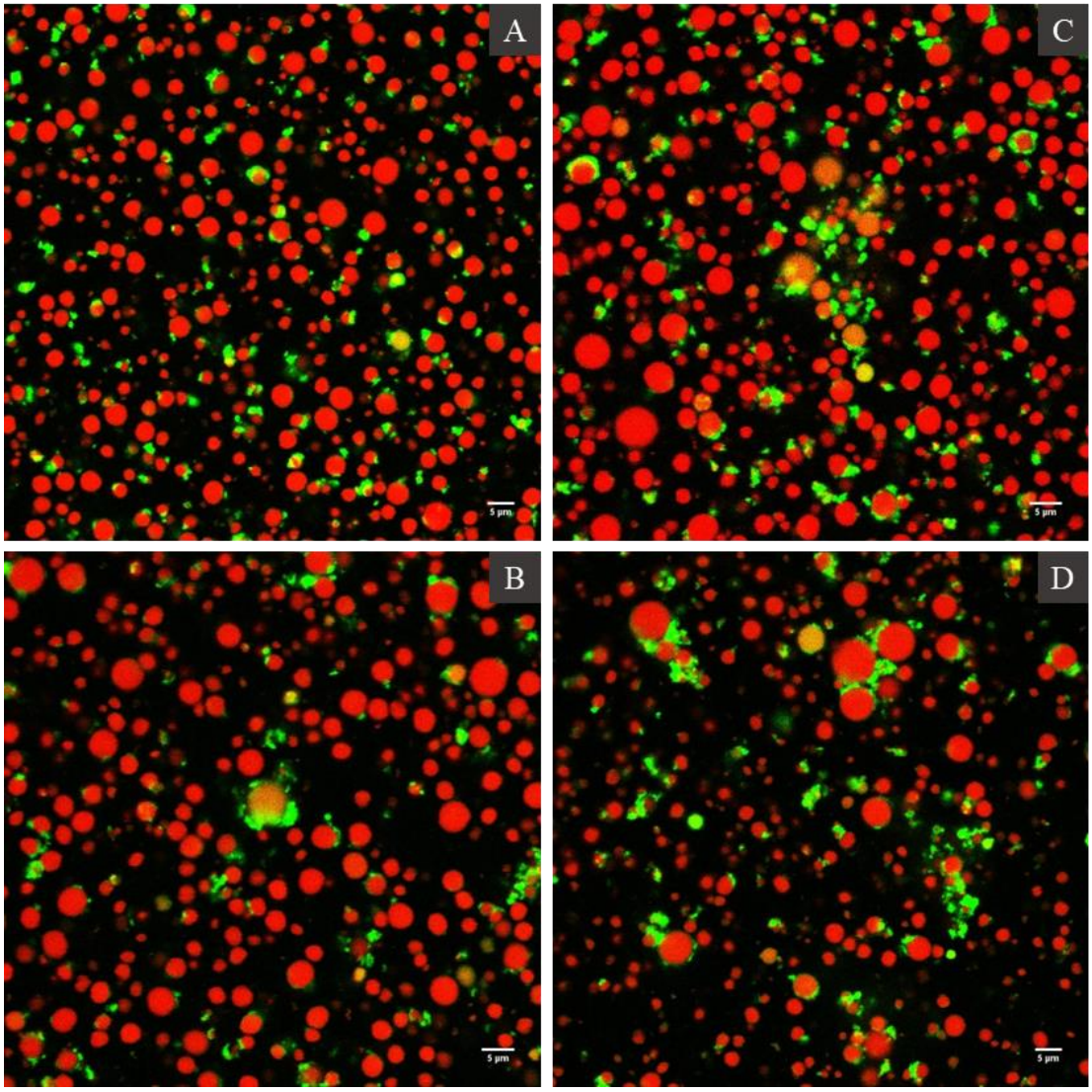

Figure 5.21. CLSM images of emulsions made from heat-extracted membrane material from oil bodies at varying protein-to-oil ratios: 0.55:1 (A), 0.42:1 (B), 0.28:1 (C), and 0.14:1 (D).

Quantification of the β-carotene content of the emulsions shown in Figure 5.22 revealed that there was no significant difference in the β-carotene content of the samples at all the protein-to-oil ratios examined. The highest β-carotene concentration was determined for the sample 0.42:1 with a value of 389.4 ± 10.1 μg/g of oil with an encapsulation efficiency of 97.4 ± 2.5%.

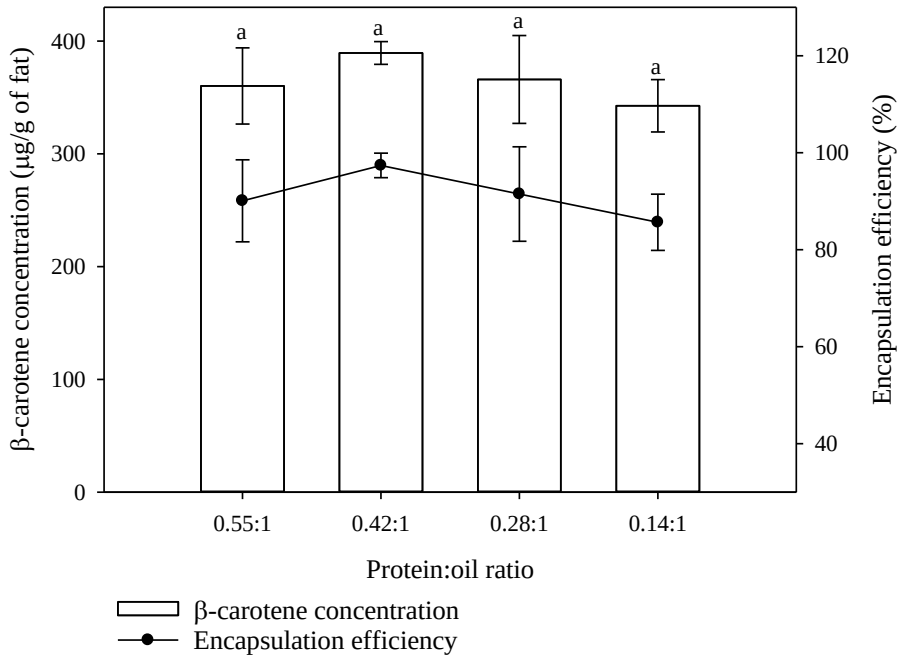

Figure 5.22. β-carotene concentration of emulsions made from heat-extracted membrane material from hemp oil bodies at varying protein-to-oil ratios: 0.55:1, 0.42:1, 0.28:1, and 0.14:1. Means that do not share a letter are significantly different at α=0.05. Error bars indicate standard deviations.

5.4 Discussion

Intact oil bodies have been investigated for their use as delivery systems for lipophilic compounds because of their inherent physical and chemical stability. The use of crude oil body extracts in delivery systems is more efficient as it avoids the need for non-food-grade chemicals for extraction and equipment for further purification of oil bodies (Acevedo-Fani et al., 2020). Moreover, the extraneous proteins that are co-extracted with oil bodies have been found to contribute to their stability; as such, higher stability is expected from oil body delivery systems that are formulated using crude extracts.

5.4.1 Incorporation of β-carotene using solvents

The interfacial membrane of oil bodies has been shown to have a high permeability to hydrophobic compounds (Boucher et al., 2008). However, to be able to successfully incorporate the bioactive molecule inside the oil bodies, the molecule has to remain soluble in the phase surrounding the oil bodies. Solvents can be used as encapsulation aids in the partitioning of bioactive compounds into oil bodies by solubilizing them. The solvent should be easily removed from the system by evaporation or diluted upon mixing

with a second solvent (Murray et al., 2007). In this study, ethanol, hexane, and diethyl ether were chosen as the organic solvents to dissolve β-carotene.

Among these solvents, the highest encapsulation efficiency was obtained from ethanol, followed by diethyl ether and then hexane. However, the encapsulation efficiencies for these samples were very low (below 40%), especially for hexane and diethyl ether. This is likely due to a higher affinity of β-carotene for these solvents than hempseed oil. The poor partitioning of β-carotene in the oil bodies can be attributed to the differences in solubility of β-carotene in these solvents. In the case of ethanol, β-carotene has relatively low solubility in it (30 mg/L) (Craft & Soares, 1992) and this could have posed as a hindrance in its diffusion into oil bodies as seen in the presence of undissolved crystals after centrifugation. However, it still exhibited a higher efficiency compared to the other solvents, which could be attributed to its ability to increase the permeability of biological membranes and enhance the partitioning of compounds through the membrane (Fukushima, 1969; Ingram, 1989; Komatsu & Okada, 1997). For example, ethanol has been previously used to partition curcumin and vitamin D3 across the milk fat globule membrane (MFGM) by causing a partial opening of the membrane (Alshehab & Nitin, 2019; Alshehab et al., 2019). Moreover, it was able to maintain the integrity of the MFGM and was not expected to diffuse through the membrane as it favours the aqueous phase.

In unstirred samples, β-carotene mostly remained in the solvent phase of the emulsion in the case of hexane and diethyl ether. Stirring was able to increase the contact of β-carotene with the oil bodies in the suspension; however, it did not result in an appreciable increase in encapsulation efficiency. β-carotene exhibits high solubility in the solvents, with a solubility of 600 mg/L in hexane and 1,000 mg/L in diethyl ether (Craft & Soares, 1992). However, this high solubility also posed a hindrance to the partitioning of β-carotene into the oil bodies because of the higher affinity of β-carotene in the solvents rather than in the TAG core of the oil bodies. Moreover, solvents that are immiscible with water have been found to be unable to penetrate the hydrophobic core of soy protein isolates with a hydrophilic and hydrated outer layer (Fukushima, 1969); thus, the hydrophilic and hydrated interface of the oil body membrane could also have posed a hindrance to the partitioning of β-carotene from the solvent phase. The partitioning of carotenoids like β-carotene could be improved by using a combination of other solvents or the application

of other treatments such as heat, as has been used in the extraction of β-carotene in other plant materials (Amorim-Carrilho et al., 2014; Fikselova et al., 2008).

Challenges were also encountered in the removal of hexane and diethyl ether from the oil body suspensions, which was not expected given the known immiscibility of hexane and diethyl ether with water. As such, interactions between the solvents and oil bodies could have occurred, especially in the stirred samples, which hindered the separation of the solvents from the oil body system. For instance, changes in the structure and integrity of cell membranes take place as a result of the partitioning of hydrophobic compounds, and these depend on the structure of the compound and how they partition into the bilayer (Sikkema et al., 1995). As an example, hexane has been shown to enter the hydrocarbon region of the lipid bilayer by interacting with the acyl chains of the phospholipids, as seen in the presence of approximately one hexane molecule per phospholipid in the bilayer (MacCallum & Tieleman, 2006; Sikkema et al., 1995; White et al., 1981). This indicates that hexane aligns with the fatty acid chains of the phospholipids, causing the reduction of the ordering of the lipid bilayer (Sikkema et al., 1995). Also, once trapped in the bilayer, it takes a relatively long time to reorient or move to another position (MacCallum & Tieleman, 2006). On the other hand, diethyl ether has been shown to partition into the membrane bilayer because of its hydrophobicity; it has also caused membrane fluidisation or disordering in phospholipid bilayers (Cobb et al., 1990). Diethyl ether has also been used to extract phospholipids and protein in the form of lipid-protein complexes in aqueous dispersions (Parenti-Castelli et al., 1974). Hence, stirring could have enhanced the interaction between the solvents and membrane components of the oil bodies and formed a matrix that hindered their separation from the oil body systems. Further characterisation of the oil body-solvent system is needed to ascertain this hypothesis.

The partitioning of lipophilic bioactive substances has been demonstrated by other researchers (Acevedo et al., 2014; Boucher et al., 2008; Murray et al., 2007). Astaxanthin, another carotenoid, was successfully microencapsulated in rapeseed oil bodies by optimising the contact time, stirring rate, and astaxanthin/oil body ratio (Acevedo et al., 2014). A high microencapsulation efficiency (>99.7%) was attributed to the small molecular mass of astaxanthin, which enhanced its migration to the TAG core of oil bodies and its natural affinity for TAG due to its high hydrophobicity. Similarly, hydrophobic organic pesticides have been successfully partitioned into rapeseed oil

bodies by mixing the pesticide solution with the oil body suspension followed by agitation (Boucher et al., 2008). The effective diffusion of the pesticides into the TAG core of the oil bodies was attributed to the high surface area of oil bodies and their half unit membrane, which did not participate in the sorption of compounds (Boucher et al., 2008).

5.4.2 Incorporation of β-carotene without solvents

β-carotene, because of its crystalline nature, is sparingly soluble in oil at room temperature (Gul et al., 2015). Thus, mild heating at 50°C has been used to increase the dissolution of β-carotene crystals in the oil phase of emulsions (Chen et al., 2017; Qian et al., 2012; Salvia-Trujillo et al., 2013; Yi et al., 2014). Moreover, sonication has shown to improve the dissolution of β-carotene in oil, with 1 min of cold-sonication-assisted treatment resulting in a high carotenoid load and minimal β-carotene degradation (Chen et al., 2017).

In this study, crystalline β-carotene was successfully incorporated into hemp oil bodies using mild heating and sonication. Heating at temperatures of 50°C and below was found to result in the partial unfolding of storage proteins loosely bound on the interface, causing a reduction in the amount of adsorbed extraneous proteins (Fu et al., 2020). The stability of oil bodies is also maintained, as they exhibit similar particle size and ζ-potential with unheated oil bodies (Iwanaga et al., 2007; Zhou et al., 2019). As such, the incorporation of β-carotene in native oil bodies could be attributed to enhanced molecular movement brought about by heating and release of some extrinsic proteins from the interface (Chen et al., 2014; Ding et al., 2020; Yan et al., 2016).

Sonication may also have facilitated the further dissolution of β-carotene crystals in hemp oil bodies after heating, as seen in the absence of solid β-carotene after the treatment. This could be attributed to the ability of ultrasound to improve the diffusion of solutes due to the cavitation phenomena: the implosion of the cavitation bubbles on the surface of particles results in the peeling, erosion, or breakdown of the particle that provides exposure of new surfaces, thereby enhancing mass transfer (Vilkhu et al., 2008; Vinatoru, 2001). Cavitation during ultrasound treatment has also been shown to cause increased permeability in cell membranes (Chemat et al., 2011; Miller et al., 2002). It is possible that ultrasound dislodged loosely adhered serum proteins on the oil body surface by a similar mechanism (Loman et al., 2018; Zderic et al., 2016). However, further experiments are necessary to test this hypothesis.

Based on these results, the incorporation of β-carotene inside oil bodies can be attributed to the transient permeabilization of the oil body membrane caused by heating and sonication. A short treatment time could have been sufficient for this to occur as the oil body only has a monolayer membrane compared to the cell membrane bilayer or MFGM trilayer. The fatty acid composition inside the oil also remains unchanged, as seen in the extraction of oil from hemp seeds, wherein the optimal ω6:ω3 fatty acid ratio was maintained even with the ultrasound pretreatment of hemp seeds (Da Porto et al., 2015).

5.4.3 Effect of homogenisation on the properties of oil bodies

The effect of homogenisation as a treatment to disrupt the membrane of oil bodies and promote the incorporation of β-carotene was investigated. Different homogenisation conditions were examined to determine the optimal condition to achieve the disruption of the oil body membrane without causing extensive droplet flocculation. Generally, an increase in homogenisation pressure causes a reduction in the particle size of emulsions (Keogh & O'Kennedy, 1999; McClements, 2016). This results in the increase in the interfacial surface area between the aqueous phase and the lipids, which must be coated with additional emulsifier to prevent coalescence and phase separation (Everett, 2007). Typically, a homogenisation pressure of 200 bar causes a thousand-fold increase in the number of fat droplets, a ten-fold increase in total surface area, and a ten-fold reduction in the average diameter (Everett, 2007).

Smaller emulsion droplet size can be attained using a microfluidizer than a low-pressure homogeniser because of the higher level of mechanical energy supplied at very high pressures (Mao et al., 2010; McClements, 2016). Thus, their effect on the level of membrane disruption in oil bodies was examined. In the case of hemp oil bodies, the increase in homogenisation pressure using the microfluidizer (500 to 1000 bar) did not cause a significant decrease in the particle size of homogenised oil bodies, but it was significantly higher compared to native oil bodies and homogenised oil bodies prepared using a high-speed blender and low-pressure homogeniser. Moreover, microfluidization caused the flocculation of oil droplets, since the particle size in SDS reflected that the small size of individual oil droplets (similar to the size of native oil bodies) was maintained despite the increase in homogenisation pressure. This can be attributed to the use of higher shear rates that increased the rate of collision of oil droplets and resulted in their aggregation (Everett, 2007). Moreover, the disruption of the oil body membrane at

a higher extent than low-pressure homogenisation could have resulted in an insufficient amount of membrane material to restabilise the higher interfacial area of the oil droplets. Thus, the amount of emulsifier, which in this case is the oil body membrane material, in the system greatly influenced the size and aggregation behaviour of homogenised oil bodies, especially at high pressures. As such, low-pressure homogenisation (250 bar) was chosen in preparing homogenised oil bodies since it resulted in a milder disruption of the membrane and a size similar to native oil bodies.

The oil body systems might behave similarly to protein-stabilised emulsions because a large proportion of their membrane is composed of oleosins. Upon homogenisation, oil bodies rapidly rupture due to the high shear applied and the surface-active membrane fragments adsorb at the oil/water interface to stabilise newly formed droplets (Ishii et al., 2017; Waschatko et al., 2012). Because of the strength of the oil body membrane, the strong association of its components results in the formation of membrane fragments instead of phospholipid or oleosin micelles upon rupture (Karefyllakis, van der Goot, et al., 2019a). These membrane fragments then spread to the interface of the newly created droplets and the TAG core merges with the added oil in the dispersed phase for emulsification. A similar disruption in oil bodies and re-emulsification of oil droplets was observed for hemp oil bodies, as evidenced in the aggregation of homogenised oil bodies compared to the more stable native oil bodies. Moreover, the staining of proteins on the oil droplets after homogenisation differed from native oil bodies, indicating the possible rearrangement of membrane fragments at the interface. A more thorough analysis of the membrane composition of homogenised oil bodies is however needed to elucidate the interfacial structure of re-emulsified oil droplets.

In this study, the homogenisation of oil bodies resulted in their extensive flocculation. This may be in part due to the presence of extraneous proteins in the oil bodies since a crude extract was used. In homogenised soybean oil bodies, the surface protein composition was found to reflect that of the original oil body fraction; aside from the membrane oleosins, other storage proteins adsorbed onto the droplet interface (Ishii et al., 2017). Hence, the tendency of the droplets to flocculate is enhanced due to the bridging action of the extraneous proteins at the newly formed interface (Ishii et al., 2017; Karefyllakis, van der Goot, et al., 2019a). Another cause for bridging flocculation is the insufficient amount of interfacial materials to cover the interface of the new oil droplets.

After homogenisation, the particle size of the emulsion became significantly smaller (based on measurements in SDS); thus, the increase in surface area of the oil resulted in the oil droplets sharing the interfacial materials initially present in the system, causing flocculation (McClements, 2016). The same trend was observed for homogenised rapeseed oil body emulsions, wherein the increase in the oil body concentration resulted in the decrease in particle size of the emulsions (He et al., 2020). This was attributed to the higher amount of proteins and phospholipids that adsorbed onto the oil droplet surface and prevented flocculation during homogenisation. Therefore, flocculation can be avoided and a reduction in particle size can be achieved in homogenised oil body emulsions as long as the amount of interfacial materials is enough to stabilise the newly formed oil droplets.

The ζ-potential of homogenised oil bodies had a higher magnitude compared to the non-homogenised oil bodies. This indicates better electrostatic stability of the homogenised oil bodies, which agrees with the size results wherein a smaller size (in SDS) was observed compared to native oil bodies. However, since flocculation still occurred despite the high magnitude of ζ-potential, the electrostatic repulsion cannot overcome the attractive forces and resulted in flocculation (Maurer et al., 2013; Nikiforidis & Kiosseoglou, 2009). The variability in the ζ-potential of native oil bodies could be attributed to the differences in pH for each extraction (Figure 5.10). Since the ζ-potential of oil bodies is influenced by the pH of the medium (as discussed in the previous chapter), the pH of the oil body systems was adjusted to 7 (using 0.1 M NaOH or 0.1 M HCl) when measuring the ζ-potential for a uniform comparison of the electrical potential across different systems.

The encapsulation efficiency of β-carotene was lower in homogenised compared to non-homogenised samples. A possible reason for this is the degradation of β-carotene due to the increase in the sample temperature after homogenisation; however, the temperature of the homogenised oil bodies was not measured after processing. Another study has shown that the increase in homogenisation pressure caused an elevation in the temperature of the samples after processing, which could cause the isomerisation and oxidation of β-carotene because of its heat instability (Chen & Zhong, 2015; Mao et al., 2010). In contrast, Borba et al. (2019) reported a minimal variation in the β-carotene content (2%) of nanoemulsions before and after homogenisation, despite using higher

pressures than what was used in this study. Thus, further investigation on the cause of this decrease in β-carotene concentration after homogenisation is necessary.

5.4.4 OBMM as emulsifiers

The oil body membrane materials (OBMM) have also been extracted and used as emulsifiers to stabilise emulsions and encapsulate bioactive compounds because of their high surface activity. Compared to intact oil bodies, the use of membrane materials as emulsifiers shows the following advantages: direct incorporation of the bioactive in the dispersed lipid phase, customisation of the TAG composition of the lipid phase, easier handling of the bioactive compound, and use of conventional processing/emulsification equipment (Acevedo-Fani et al., 2020). The dispersed phase may contain or be added with antioxidants that can enhance the oxidative stability of the system, and emulsions of a desired oil droplet size can be easily achieved by controlling the emulsion formulation as opposed to using intact oil bodies (Acevedo-Fani et al., 2020; Boon et al., 2010). Oil body emulsions reconstituted from membrane materials have also been shown to exhibit similar structural features and a similar or higher stability compared to native oil bodies (Chang et al., 2013; Chen et al., 2004; Peng et al., 2003).

The methods to extract membrane materials from oil bodies involve the removal of TAG from the oil bodies and using the aqueous extracts for emulsification. Examples of such methods include freeze-thaw treatments and the use of solvents (Beisson et al., 2001; Karefyllakis, van der Goot, et al., 2019a; Onsaard et al., 2006; Tzen & Huang, 1992; Zhou et al., 2019). However, to avoid the laborious process of freeze-thaw and the use of harsh organic solvents, heating the oil bodies with the application of shear was investigated as a method for extracting OBMM.

The heat-induced destabilisation of oil bodies has been reported by several researchers (Ding et al., 2020; Peng et al., 2016; Yan et al., 2016; Zhou et al., 2019). At temperatures above 50°C, a reduction in ζ-potential was observed in peanut oil bodies due to enhanced thermal motion that caused increased collisions and a consequent increase in particle diameter (Zhou et al., 2019). At temperatures above 70°C, the detachment of extrinsic proteins, particularly the hydrophilic proteins, on the surface of oil bodies has been observed as a result of protein denaturation (Ding et al., 2020; Peng et al., 2016; Yan et al., 2016). As discussed in Chapter 2, heating results in the alteration of the interfacial composition of the oil body membrane and the release of extrinsic proteins from its

surface. Extraneous proteins that are co-extracted with oil bodies have also shown to have a high tendency to denature and interact in the continuous phase of emulsions, forming aggregates and causing the oil bodies to precipitate (Peng et al., 2016). Thus, the heat-induced unfolded proteins interact with the extraneous proteins in the aqueous phase via hydrophobic interactions, which can result in the formation of a dense surface covering on the oil bodies (Nikiforidis et al., 2016). This could explain the presence of oil droplets in the precipitated fraction in Figure 5.16, as the large protein particles could have "glued" together neighbouring oil bodies that caused their aggregation (Nikiforidis et al., 2011).

Heating at temperatures of 50°C and above for one hour resulted in rupture of oil bodies and release of free oil. The free oil is associated with the TAG released from the oil body core due to the application of shear and heat treatment that denatured and displaced the membrane components. Upon centrifugation of the heated oil bodies, their components are separated into different fractions: free oil, cream layer, supernatant, and sediment fraction. The sediment layer is likely to consist of precipitated proteins that were formed from the aggregation of dissociated subunits upon heating, while the serum or supernatant fraction contains the soluble proteins (Nikiforidis et al., 2016; Nikiforidis et al., 2011; Peng et al., 2016). A cream layer upon centrifugation indicates that some oil bodies may have remained intact after heating. Heat treatment results in protein unfolding and release from oil bodies and increases the collision among oil bodies and between oil bodies and free proteins. This results in the coalescence of oil bodies and since the hydrophobic sites are exposed due to protein denaturation, the unfolded proteins could have gotten embedded into the oil bodies. As the amount of extrinsic proteins reach a critical value, further coalescence is prevented as the membrane of the oil bodies and coalesced oil bodies become fully embedded with oleosins, phospholipids, and extrinsic proteins (Yan et al., 2016). Hence, the remaining cream layer after centrifugation could be a combination of intact oil bodies or oil droplets with the mentioned membrane composition.

Since protein was contained in the serum and sediment layers, these fractions were combined and examined for their emulsifying capacity. The oil present in the combined fraction could be intact oil bodies. Previous research studies have shown that intact oil bodies were present in protein isolates, which were co-extracted (Karefyllakis, Octaviana, et al., 2019; Ntone et al., 2020). The presence of oil bodies in these protein mixtures have

little effect on the functional properties when compared to pure protein isolates (Karefyllakis, Octaviana, et al., 2019). Another possibility is that the particles are not intact oil bodies but are re-emulsified lipids. The proteins in the aqueous medium could stabilise the residual oil or intact oil bodies into emulsified droplets (Karefyllakis, Octaviana, et al., 2019). Such droplets could have a mixed membrane comprised of storage proteins or oil body proteins and a larger size than native oil bodies as they were not homogenised. This was observed in Figure 5.18 wherein oil droplets present in the extracted membrane material fractions were bigger than native hemp oil bodies and whose interface was covered by protein aggregates instead of a uniform oleosin coating.

The possible mechanism for emulsification of the membrane material fraction extracted at 70°C could be the adsorption of the aggregates on the newly created droplet interface. As observed from the confocal images (Figure 5.21), protein aggregates were present on the surface of the oil droplets. When the membrane material fraction (in the form of particles or aggregates that are comprised of proteins and intact oil bodies or lipid droplets with a mixed membrane composition) was homogenised, its components could have stabilised the oil droplet interface after being disrupted by homogenisation. Once they reach the interface, quick rearrangements occur, thereby allowing the proteins to reduce the interfacial tension (Karefyllakis, Octaviana, et al., 2019). Moreover, some extrinsic proteins could have only been partially denatured at 70°C: unfolded proteins could have been embedded into the lipid droplets and undenatured ones could interact with the oil body proteins by noncovalent interactions (Yan et al., 2016). Although phospholipids were not characterised from the membrane material, they could have participated in the stabilisation of droplets along with the oil body proteins since phospholipids have been shown to be bound to intact oleosins even after trypsin digestion (Maurer et al., 2013). Furthermore, because of the strong association of the components of the oil body membrane, its rupture would be in the form of membrane fragments rather than pure oleosin or phospholipid micelles (Karefyllakis, van der Goot, et al., 2019a). Thus, it is possible that phospholipids were also present (although not quantified in this study) in the extracted membrane material. As such, the emulsified lipids produced could have a mixed membrane composed of oleosins, extrinsic proteins, and phospholipids that provide steric hindrance and prevent the interaction between neighbouring droplets.

Another possible mechanism for the emulsification of the droplets is Pickering stabilisation. Because low homogenisation pressure (250 bar) was used, it was hypothesised that the membrane materials could have remained intact and adsorbed at the droplet interface upon homogenisation. However, this is ruled out in this study as the droplets formed after homogenisation were smaller compared to the OBMM structures obtained after heating based on confocal images. In contrast, Pickering stabilisation has been observed in other oil body-stabilised systems. For example, sunflower oil bodies that were less than 5 μm in diameter were found to stabilise emulsions via a Pickering mechanism, as observed in the presence of small, spherical, non-protein material on the droplet interface upon CLSM-imaging (Karefyllakis, van der Goot, et al., 2019a). Moreover, multicomponent protein extracts from sunflowers that contained oil bodies and polysaccharides showed a delayed diffusion of protein molecules at the interface due to the large size of the aggregates (Karefyllakis, Octaviana, et al., 2019).

The increase in the concentration of the membrane material fraction also showed a smaller droplet size of the emulsion. At a higher concentration, the membrane material particles can cover the droplet interface at a faster rate, thereby providing better protection against recoalescence within the homogeniser (Ma et al., 2017). This was observed in Figure 5.21 wherein a larger droplet size and aggregation was observed at the lowest protein-to-oil ratio. The presence of aggregates can be attributed to the bridging effect of the proteins because the amount of proteins was not sufficient to form smaller droplets (Karefyllakis, Octaviana, et al., 2019). β-carotene was also successfully incorporated in the form of an emulsion because of the emulsifying activity exhibited by the extracted membrane material. Higher encapsulation efficiency was observed for OBMM-stabilised emulsions compared to the homogenised and non-homogenised oil bodies, in which β-carotene was encapsulated in intact oil bodies by heating and sonication. This can be attributed to the ease of incorporating β-carotene directly into hempseed oil without the hindrance presented by the membrane components in the case of intact oil bodies.

5.5 Conclusion

The utilisation of oil bodies as encapsulation systems can be achieved through various techniques. However, an understanding of the interfacial composition and their functional behaviour is necessary for the successful incorporation of the bioactive compound and to create a stable emulsion for use in food systems. For instance, further investigation is

needed for the passive partitioning of hydrophobic bioactive substances into intact oil bodies without the use of harsh organic solvents. On the other hand, a combination of heating and sonication was able to incorporate crystalline β-carotene directly into hemp oil bodies. When oil bodies are homogenised, their membrane fragments adsorbed at the interface of the merged lipid phase and stabilised the newly formed droplets. However, it could result in bridging flocculation if the concentration of the membrane materials is not enough to cover the surface area of the droplets. Lastly, membrane materials were isolated through the application of heat and shear and were able to stabilise β-carotene-loaded emulsions through the embedment of the oleosins, phospholipids, and extrinsic proteins on the lipid phase. For these systems, the stability of the emulsions was largely affected by the presence of co-extracted extrinsic proteins. Further characterisation of the emulsions, specifically their membrane composition, could give better insights on the mechanism for emulsification of the oil body emulsions.

Chapter 6 Physicochemical stability of β-carotene-loaded oil body systems during storage

6.1 Introduction

In the previous chapter, β-carotene was successfully encapsulated into hemp oil body systems through the following methods: (1) encapsulation into intact oil bodies by mild heating and sonication and (2) use of oil body membrane materials (OBMM) as emulsifiers of hemp oil body emulsions. Using these techniques, three oil body systems were prepared and compared against a protein-stabilised emulsion for colloidal and chemical stability. Heating and sonication were used to incorporate β-carotene in (1) homogenised and (2) non-homogenised oil body system, and (3) a β-carotene-loaded oil body emulsion was prepared using OBMM as emulsifier. These oil body systems are herein referred to as H-OB (homogenised oil bodies), NH-OB (non-homogenised oil bodies), and OBMM-E (OBMM-stabilised oil-in-water emulsion), while a β-carotene-loaded WPI-stabilised emulsion (WPI-E) was used as control. Their colloidal and chemical stability were investigated for 14 days, with particle size and charge measurements as indicators for colloidal stability, and colour and β-carotene content as indirect and direct indicators, respectively, of β-carotene storage stability.

6.2 Results

6.2.1 Effect of storage conditions on the colloidal stability of oil body systems

6.2.1.1 Particle size

Table 6.1 shows the initial particle size of the oil body systems before the storage trial. The samples had significantly different particle sizes, with NH-OB having the largest $d_{4,3}$ of around 10 μm, followed by H-OB with around 8 μm, and OBMM-E and WPI-E not having a significant difference in size at around 3-4 μm. Upon dispersion in SDS, no significant difference was observed in the size of the samples except for H-OB which showed a significant reduction in size. This was also observed in their size distributions (Figure 6.1), wherein H-OB exhibited a shift to smaller particle sizes in SDS but no noticeable change was observed from the other systems.

Table 6.1. Particle size ($d_{4,3}$) of β-carotene-loaded oil body systems on Day 0.

Sample	$d_{4,3}$ (μm)	$d_{4,3}$ (μm) (SDS)
H-OB	7.5 ± 1.3^{b}	4.9 ± 1.6^{c}
NH-OB	10.1 ± 0.7^{a}	10.5 ± 1.0^{a}
OBMM-E	3.3 ± 0.2^{d}	4.1 ± 0.2^{cd}
WPI-E (control)	4.4 ± 0.3^{c}	4.3 ± 0.4^{c}

** Means that do not share a letter are significantly different at α=0.05.*

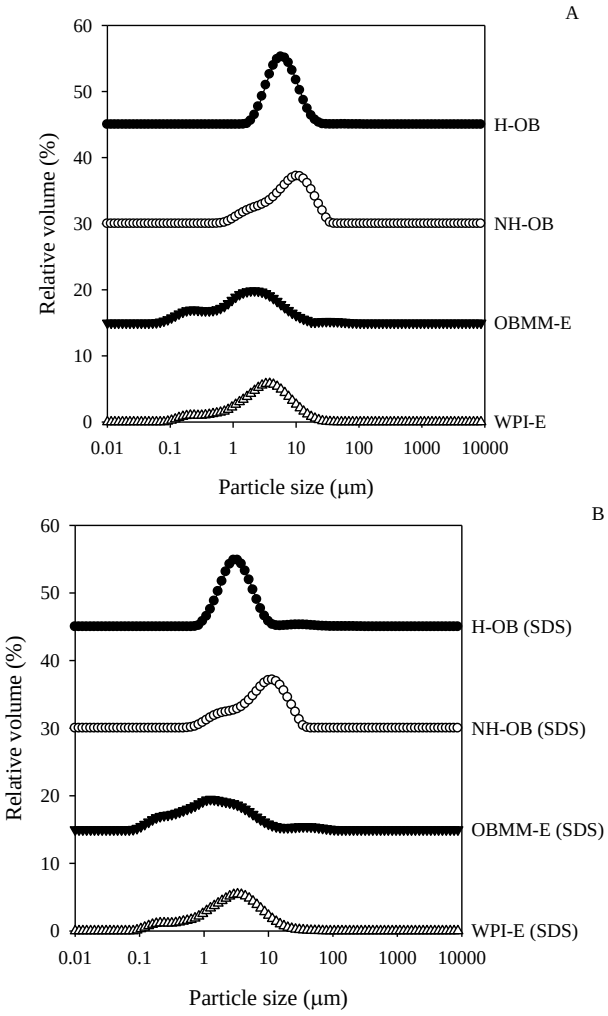

Figure 6.1. Particle size distributions of β-carotene-loaded oil body systems dispersed in water (A) and SDS (B). The oil body systems were as follows: homogenised oil bodies (H-OB), non-homogenised oil bodies (NH-OB), and oil body membrane materials-stabilised emulsion (OBMM-E), with a WPI-stabilised emulsion (WPI-E) as control.

The effect of temperature on the particle size ($d_{4,3}$) of the oil body systems during the 14-day storage period is shown in Figure 6.2. Storage at 4°C and 22°C did not cause a significant effect on the particle size of all samples. However, a significant increase in the particle size of the oil body systems compared to WPI-E was observed at 50°C. H-OB exhibited the highest increase in size, followed by NH-OB and OBMM-E. Meanwhile, no significant change was observed for WPI-E. The particle size distributions of the samples (Figures 6.3, 6.4, 6.5, and 6.6) confirmed that there was not much difference at 4°C and 22°C as they showed a similar span and location of peaks. However, storage at 50°C caused a shift of the peaks to the right, indicating a bigger particle size. This effect of temperature was consistent with particle size measurements in SDS, wherein a significant increase in size and shift of the peaks of the size distributions to higher particle size was only observed at 50°C. For H-OB, the increase in size was also observed in dispersions in SDS, indicating that the destabilisation may be attributed to a combination of flocculation and coalescence.

Among the oil body systems, the average particle size of OBMM-E did not significantly differ from WPI-E during storage, as confirmed in their size distributions. The particle size distribution of WPI-E did not show a difference throughout the storage period (Figure 6.6). Meanwhile, OBMM-E showed a minimal shift of the size distribution to higher particle sizes during storage (Figure 6.5). In contrast, H-OB and NH-OB had a significantly higher increase in size, with H-OB having the largest increase in size during the storage period. This shows that storage at 50°C had a greater effect on the size of H-OB and NH-OB compared to OBMM-E and WPI-E. As seen on their size distributions at 50°C (Figures 6.3 C and 6.4 C), H-OB and NH-OB exhibited a greater shift of the peak of the size distributions to higher particle size during the storage, with the peak at around 90 μm after 14 days.

Particle size measurements also showed that dispersion in SDS did not have a significant effect on the size of WPI-E, OBMM-E, and NH-OB. On the other hand, there was a significant reduction in the size of H-OB when dispersed in SDS, indicating extensive flocculation of droplets and coalescence. This is seen in the size distributions of H-OB in SDS (Figure 6.3 D, E, and F), wherein the peaks are located at lower particle sizes compared to the size distributions of the oil body dispersion in water.

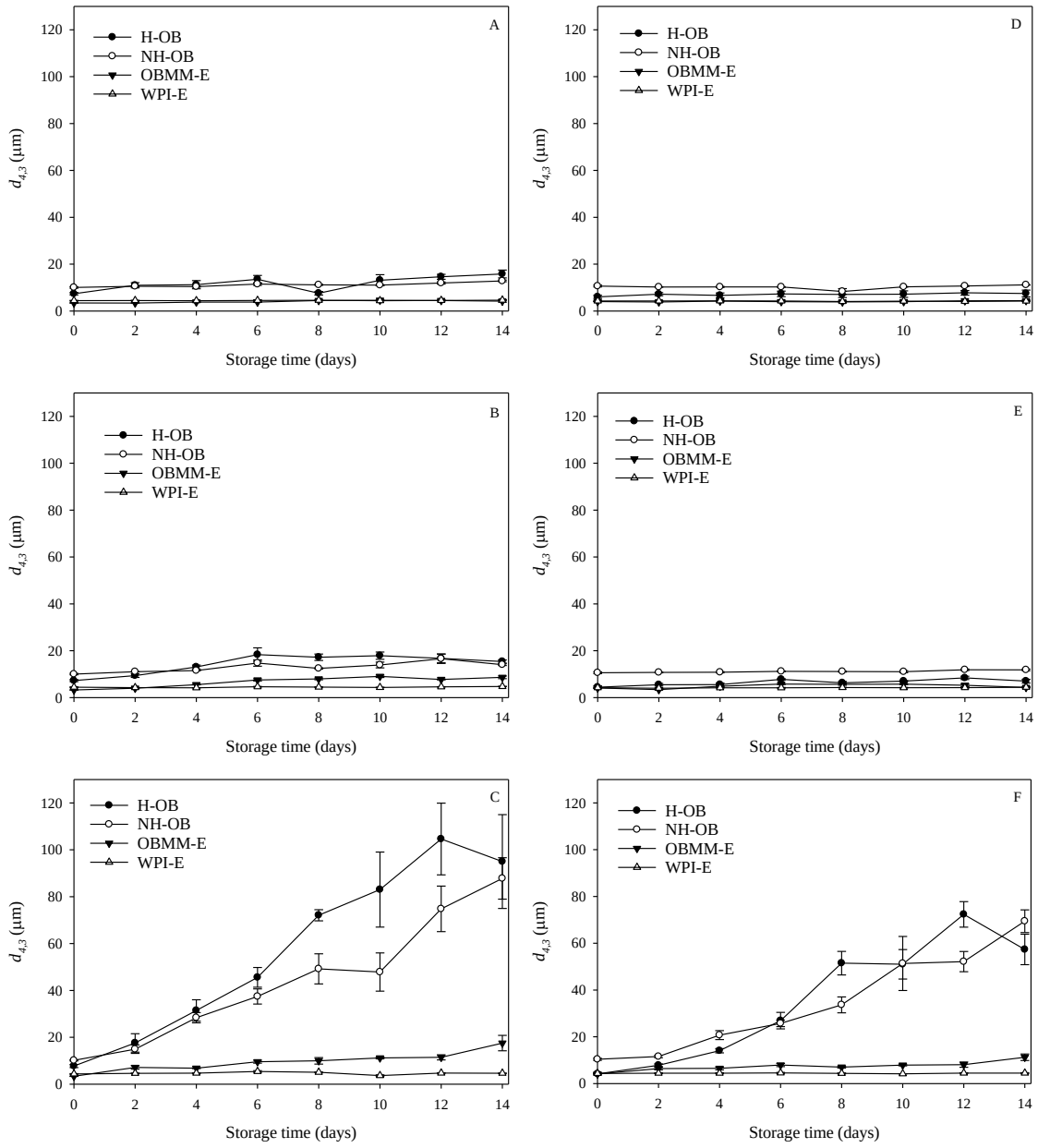

Figure 6.2. Particle size ($d_{4,3}$) of β-carotene-loaded oil body systems dispersed in water (A, B, and C) and SDS (D, E, and F) at 4°C (A and D), 22°C (B and E), and 50°C (C and F) for 14 days. The oil body systems were as follows: homogenised oil bodies (H-OB), non-homogenised oil bodies (NH-OB), and oil body membrane materials-stabilised emulsion (OBMM-E), with a WPI-stabilised emulsion (WPI-E) as control. Error bars indicate standard error of mean.

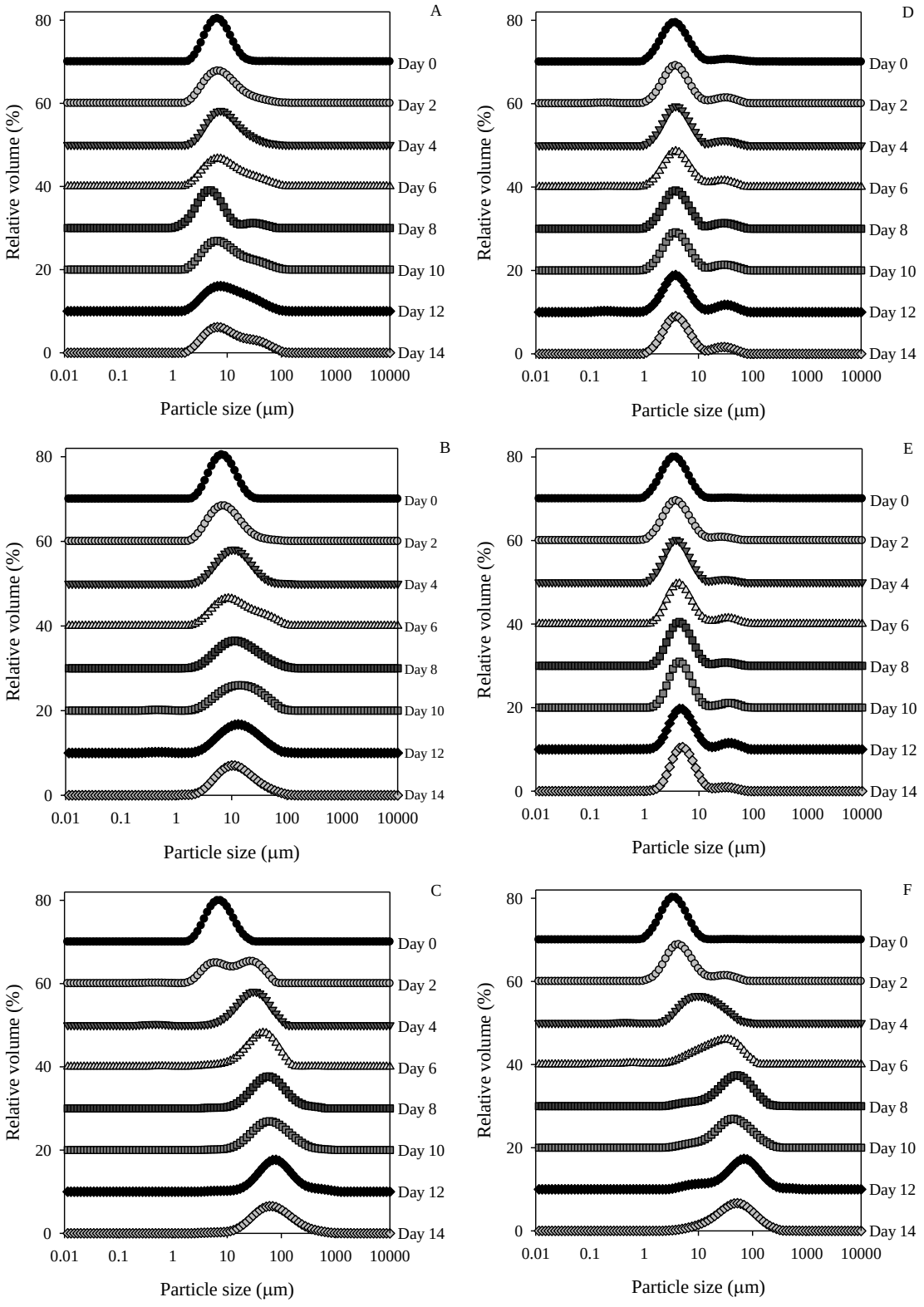

Figure 6.3. Particle size distributions of β-carotene-loaded homogenised oil bodies (H-OB) dispersed in water (A, B, and C) and SDS (D, E, and F) stored at 4°C (A and D), 22°C (B and E), and 50°C (C and F) for 14 days.

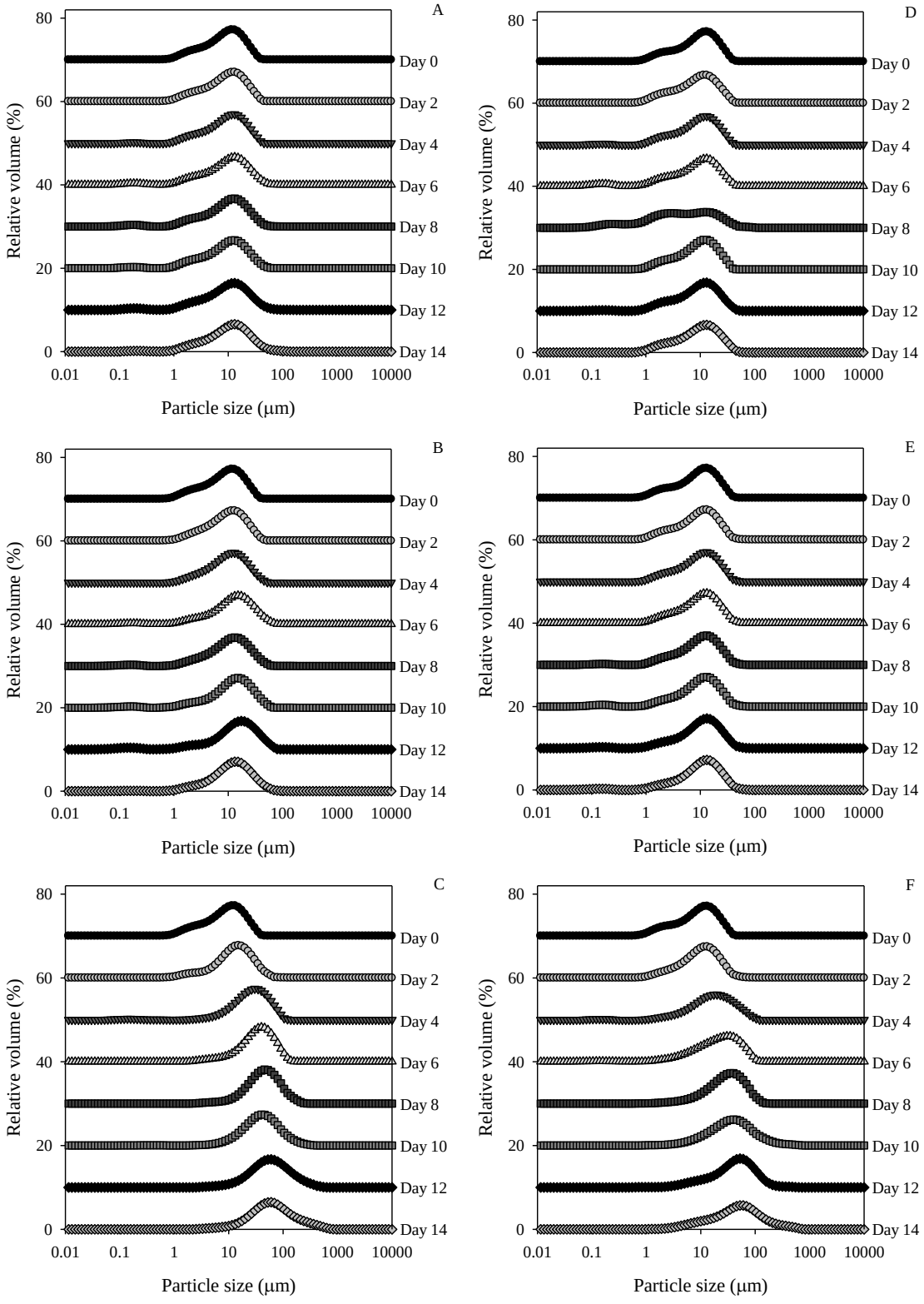

Figure 6.4. Particle size distributions of β-carotene-loaded non-homogenised oil bodies (NH-OB) dispersed in water (A, B, and C) and SDS (D, E, and F) stored at 4°C (A and D), 22°C (B and E), and 50°C (C and F) for 14 days.

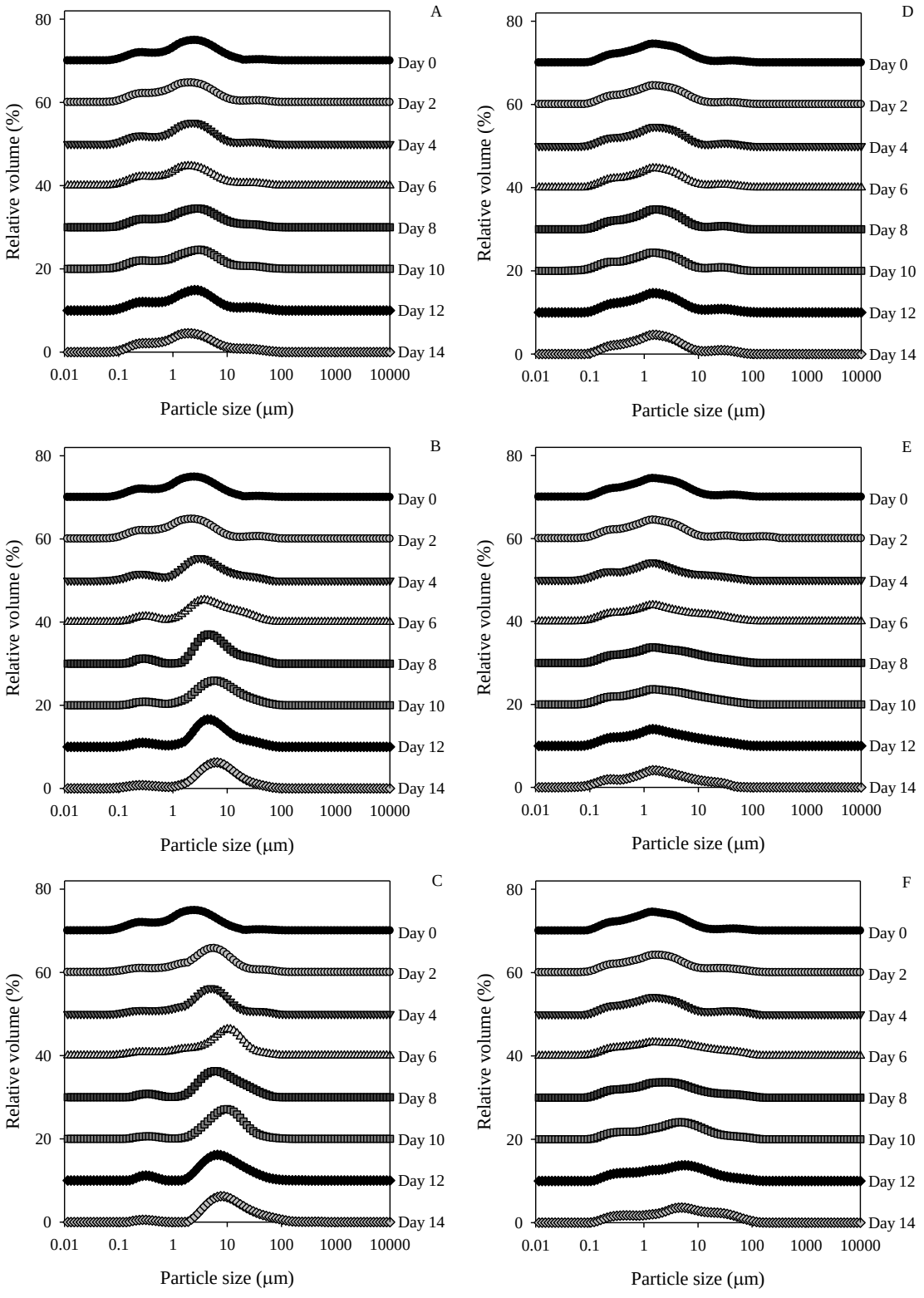

Figure 6.5. Particle size distributions of β-carotene-loaded oil body membrane materials-stabilised emulsion (OBMM-E) dispersed in water (A, B, and C) and SDS (D, E, and F) stored at 4°C (A and D), 22°C (B and E), and 50°C (C and F) for 14 days.

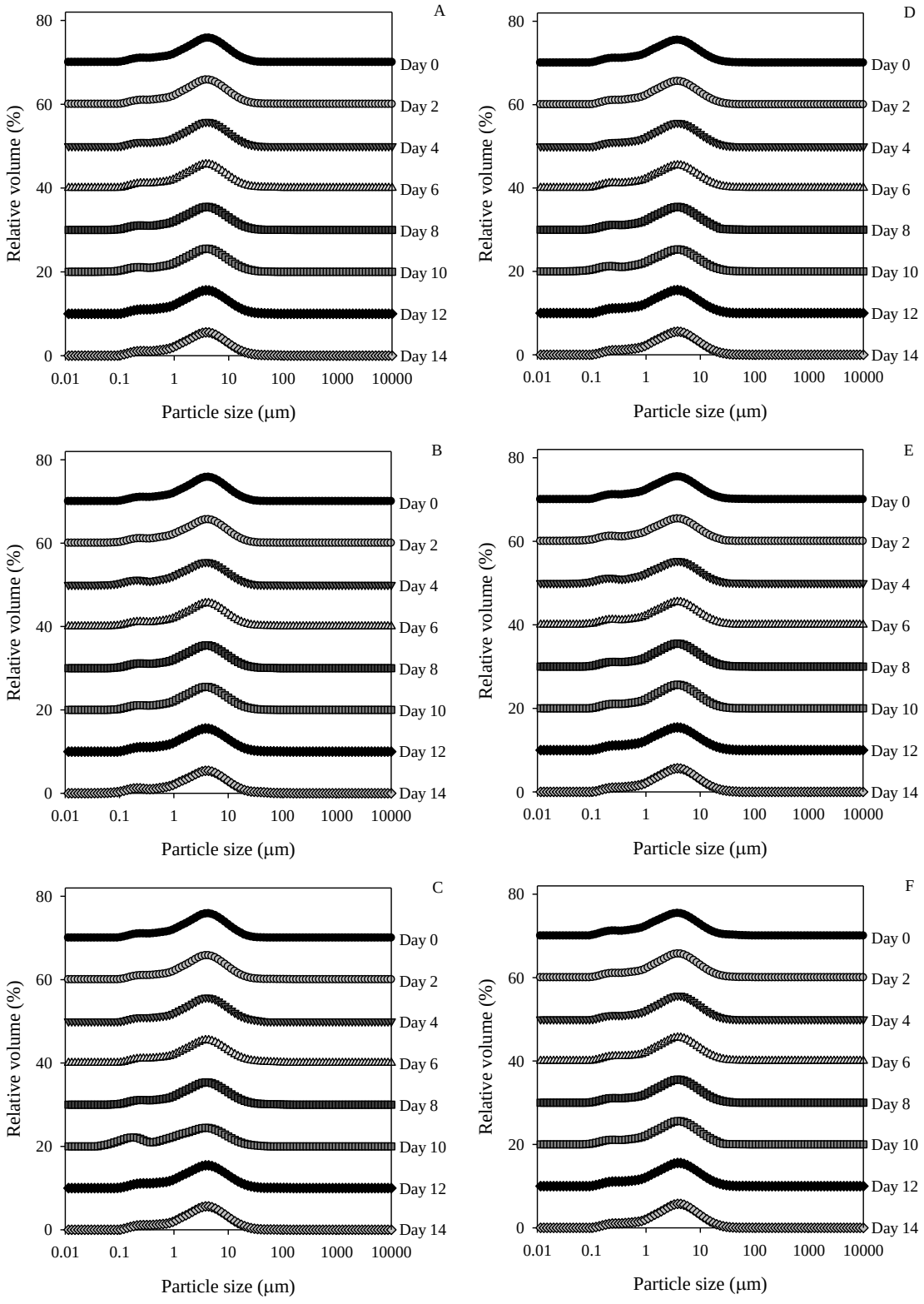

Figure 6.6. Particle size distributions of β-carotene-loaded WPI-stabilised emulsion (WPI-E) dispersed in water (A, B, and C) and SDS (D, E, and F) stored at 4°C (A and D), 22°C (B and E), and 50°C (C and F) for 14 days.

The effect of the presence of light on the particle size ($d_{4,3}$) of the oil body systems during 14 days of storage at room temperature (~22°C) is shown in Figure 6.7. Storage at light and dark conditions did not have a significant effect on the particle size of all the samples. This was also observed in their size distributions which did not exhibit any difference at light and dark storage conditions (Figures 6.8, 6.9, 6.10, and 6.11).

On the other hand, the oil body systems behaved differently during the storage period. WPI-E exhibited the least increase in particle size, followed by OBMM-E, NH-OB, and H-OB with the highest increase in size during storage. This increase was evident in the size distributions of H-OB (Figure 6.8) wherein the span widened and the peak shifted to higher particle size with the increase in storage time. The other samples, however, did not exhibit much difference in size distributions over time. Particle size measurements also did not show a significant difference in the size of WPI-E when dispersed in water and SDS. However, a significant difference was observed for H-OB, NH-OB, and OBMM-E, indicating flocculation of droplets during storage. This was observed in the size distributions particularly for H-OB, wherein bimodal distributions were obtained in SDS with a peak below 10 μm and the presence of a population of larger-sized droplets above 10 μm (Figure 6.8 C and D).

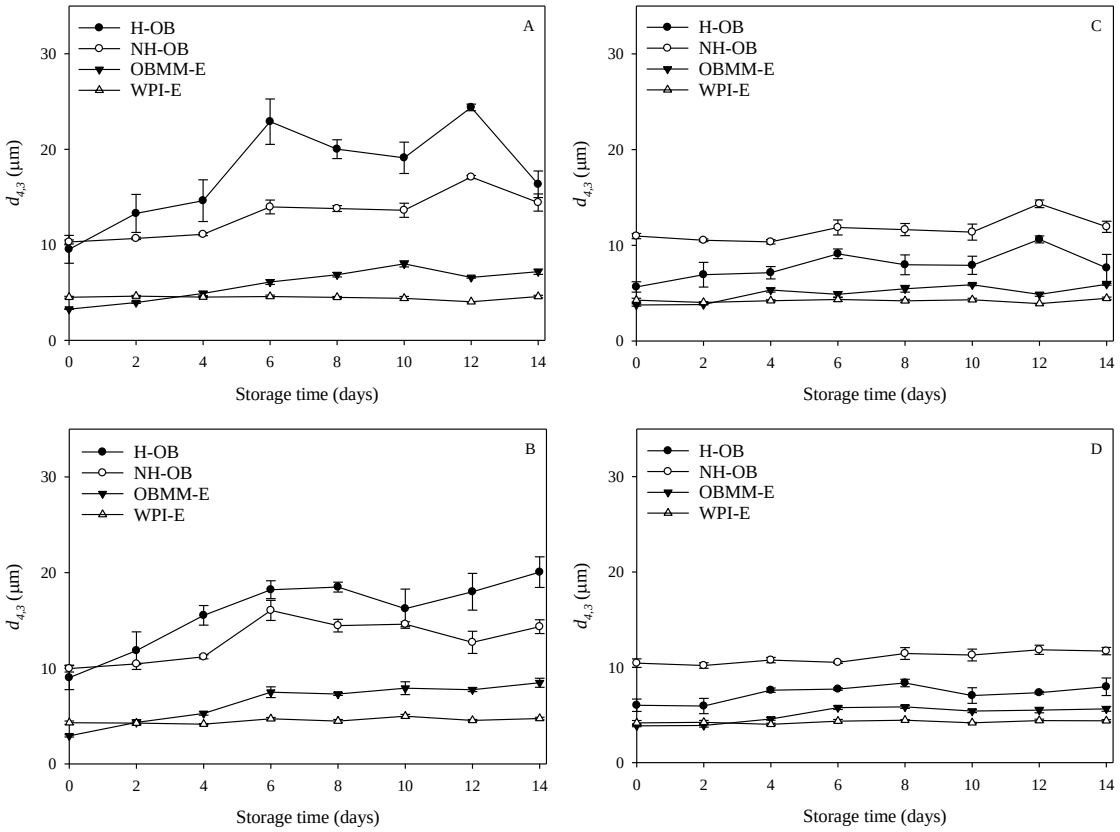

Figure 6.7. Particle size ($d_{4,3}$) of β-carotene-loaded oil body systems dispersed in water (A and B) and SDS (C and D) stored under light (A and C) and dark (B and D) conditions at room temperature (~22°C). The oil body systems were as follows: homogenised oil bodies (H-OB), non-homogenised oil bodies (NH-OB), and oil body membrane materials-stabilised emulsion (OBMM-E), with a WPI-stabilised emulsion (WPI-E) as control. Error bars indicate standard error of mean.

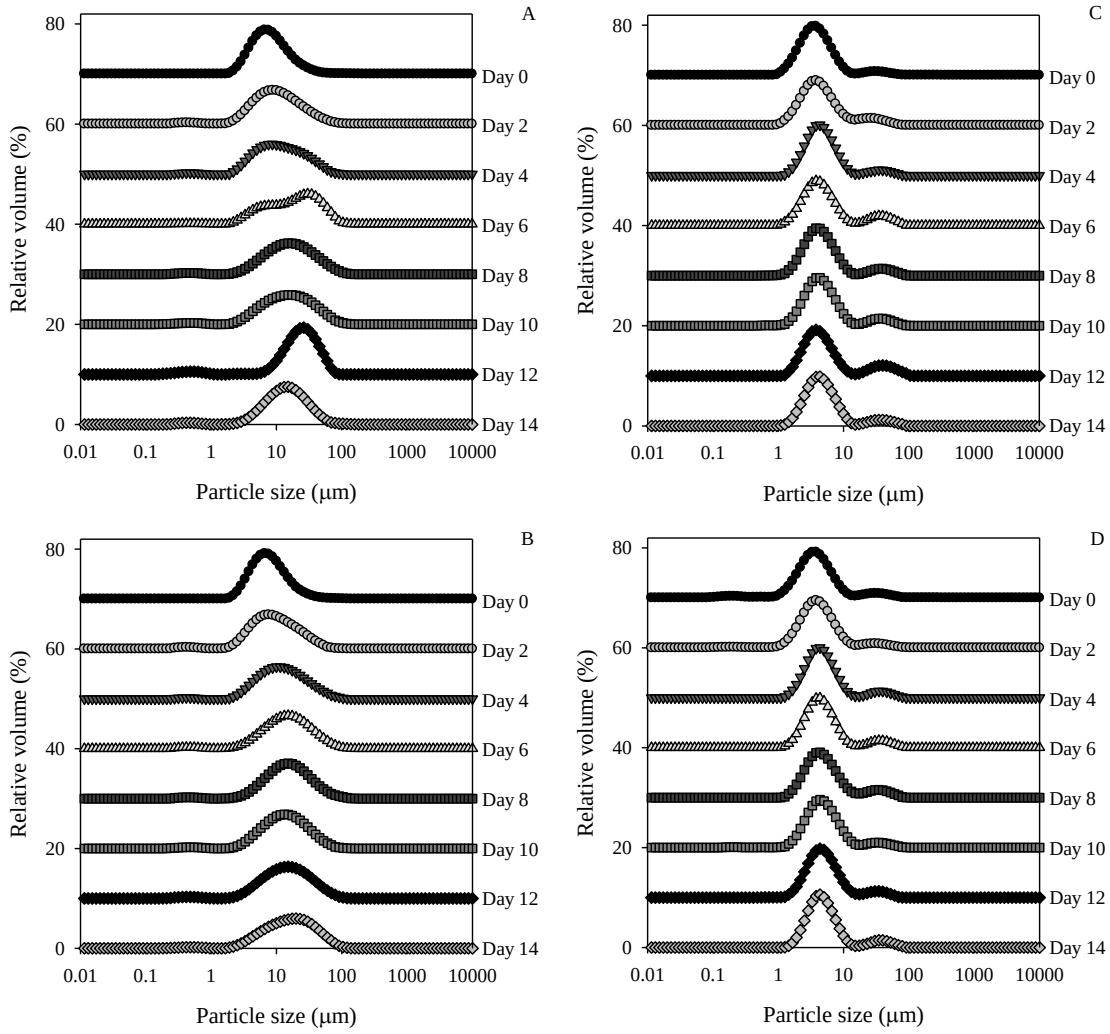

Figure 6.8. Particle size distributions of β-carotene-loaded homogenised oil bodies (H-OB) dispersed in water (A and B) and SDS (C and D) stored under light (A and C) and dark (B and D) conditions at room temperature (~22°C) for 14 days.

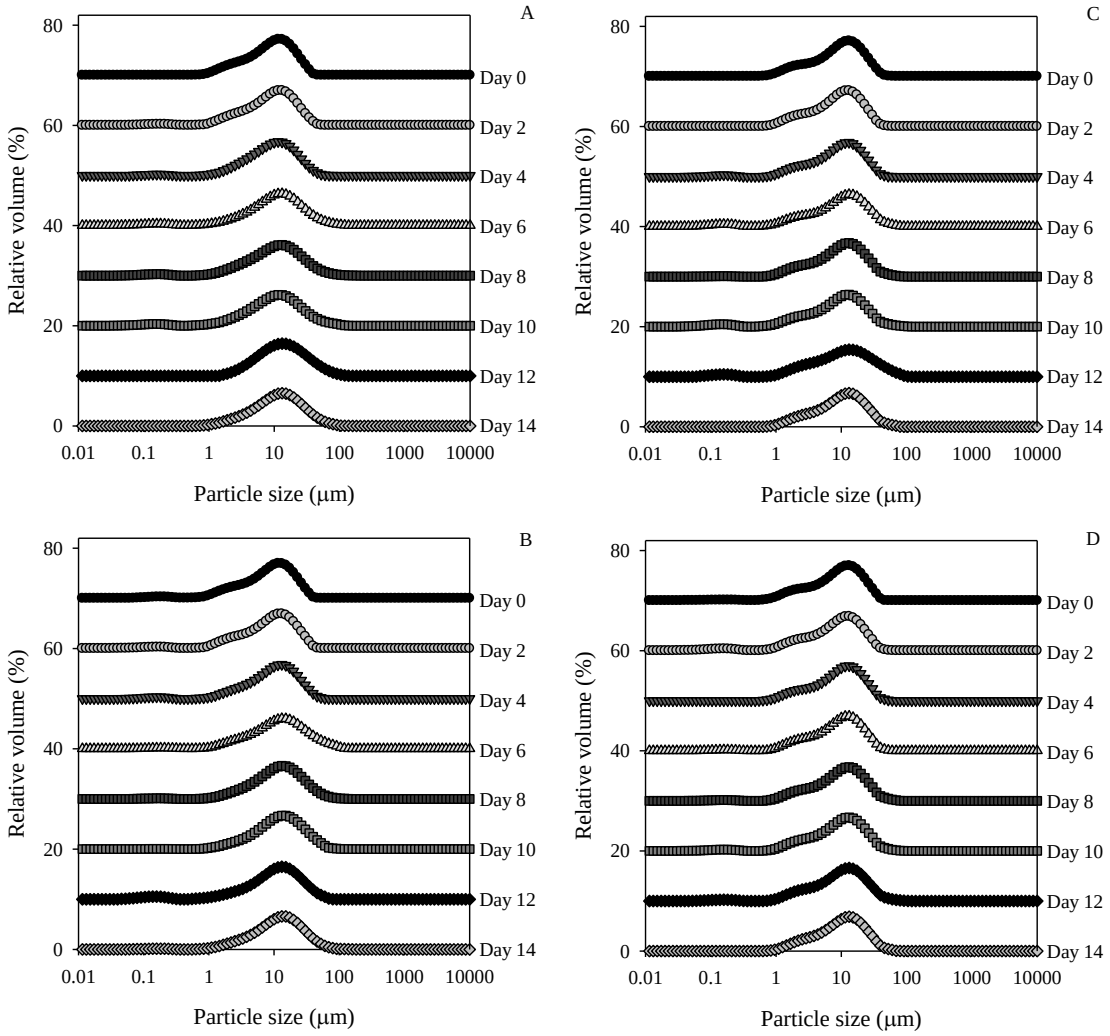

Figure 6.9. Particle size distributions of β-carotene-loaded non-homogenised oil bodies (NH-OB) dispersed in water (A and B) and SDS (C and D) stored under light (A and C) and dark (B and D) conditions at room temperature (~22°C) for 14 days.

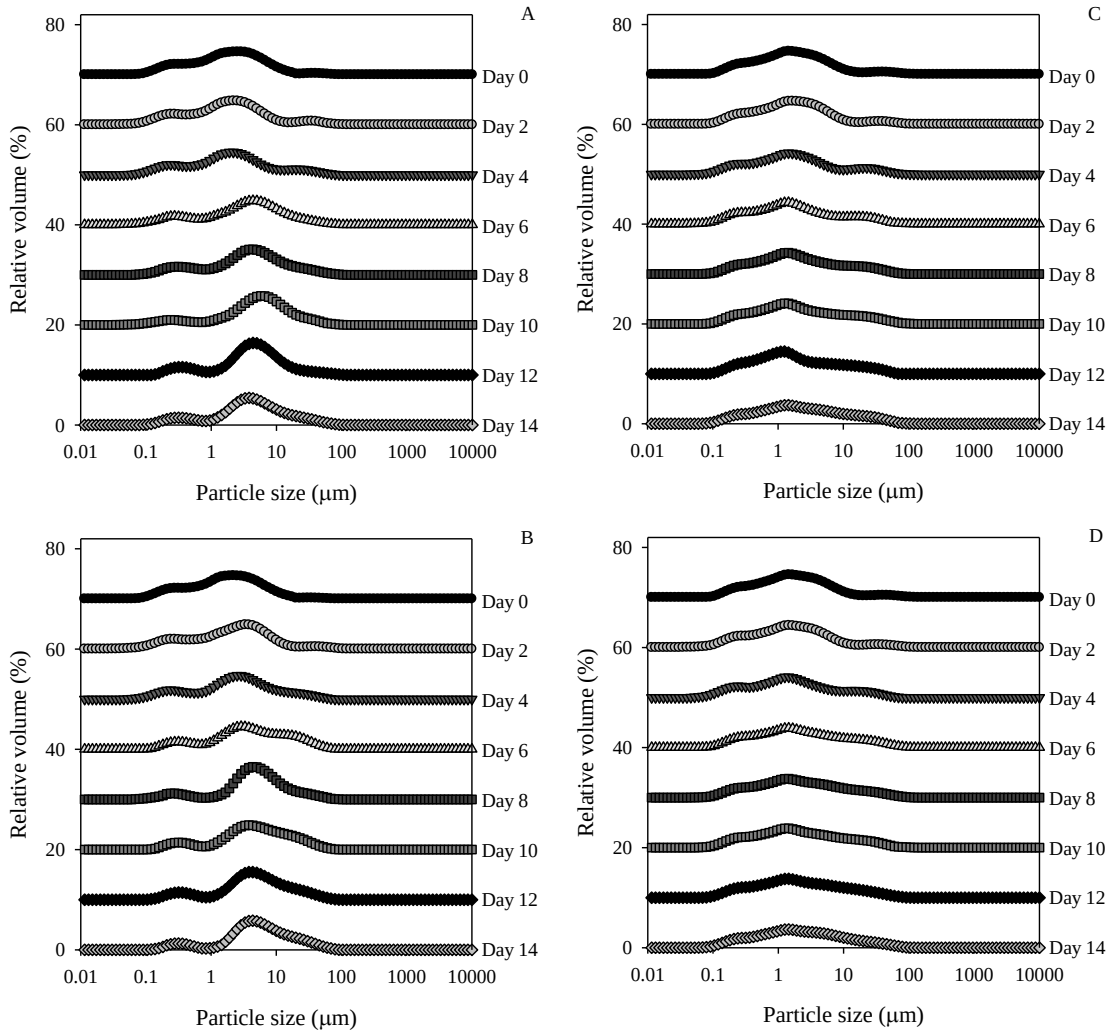

Figure 6.10. Particle size distributions of β-carotene-loaded oil body membrane materials-stabilised emulsion (OBMM-E) dispersed in water (A and B) and SDS (C and D) stored under light (A and C) and dark (B and D) conditions at room temperature (~22°C) for 14 days.

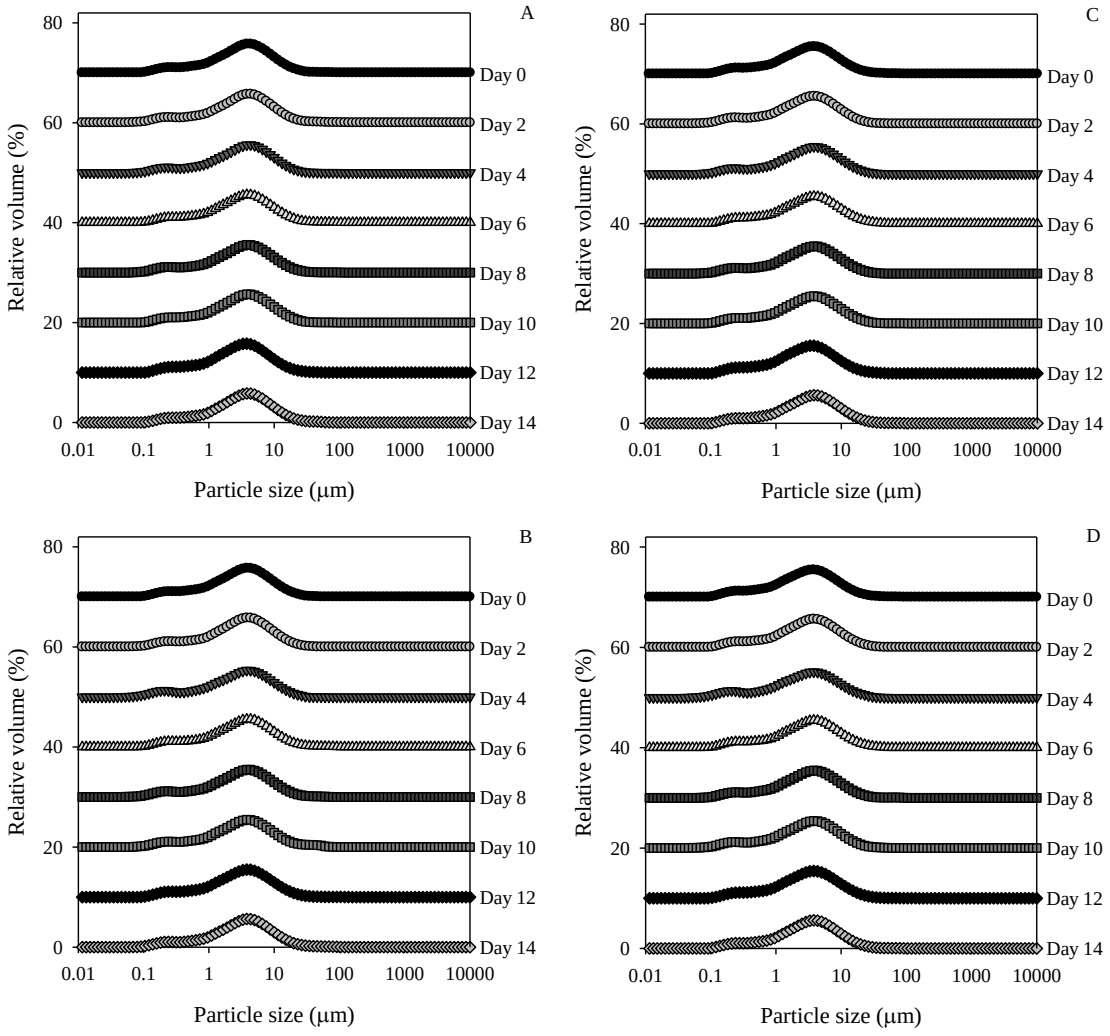

Figure 6.11. Particle size distributions of β-carotene-loaded WPI-stabilised emulsion (WPI-E) dispersed in water (A and B) and SDS (C and D) stored under light (A and C) and dark (B and D) conditions at room temperature (~22°C) for 14 days.

6.2.1.2 ζ-potential

The ζ-potential of the emulsions did not significantly change during the 14-day storage period (Figure 6.12). At different storage temperatures, the ζ-potential values were largely similar with relatively small but significant statistical differences for each sample.

The samples also had significantly different ζ-potential values, with WPI-E having the highest ζ-potential with a mean of around -73 mV. This was followed by NH-OB, H-OB, and OBMM-E with a mean ζ-potential of around -33 mV, -31 mV, and -27 mV, respectively.

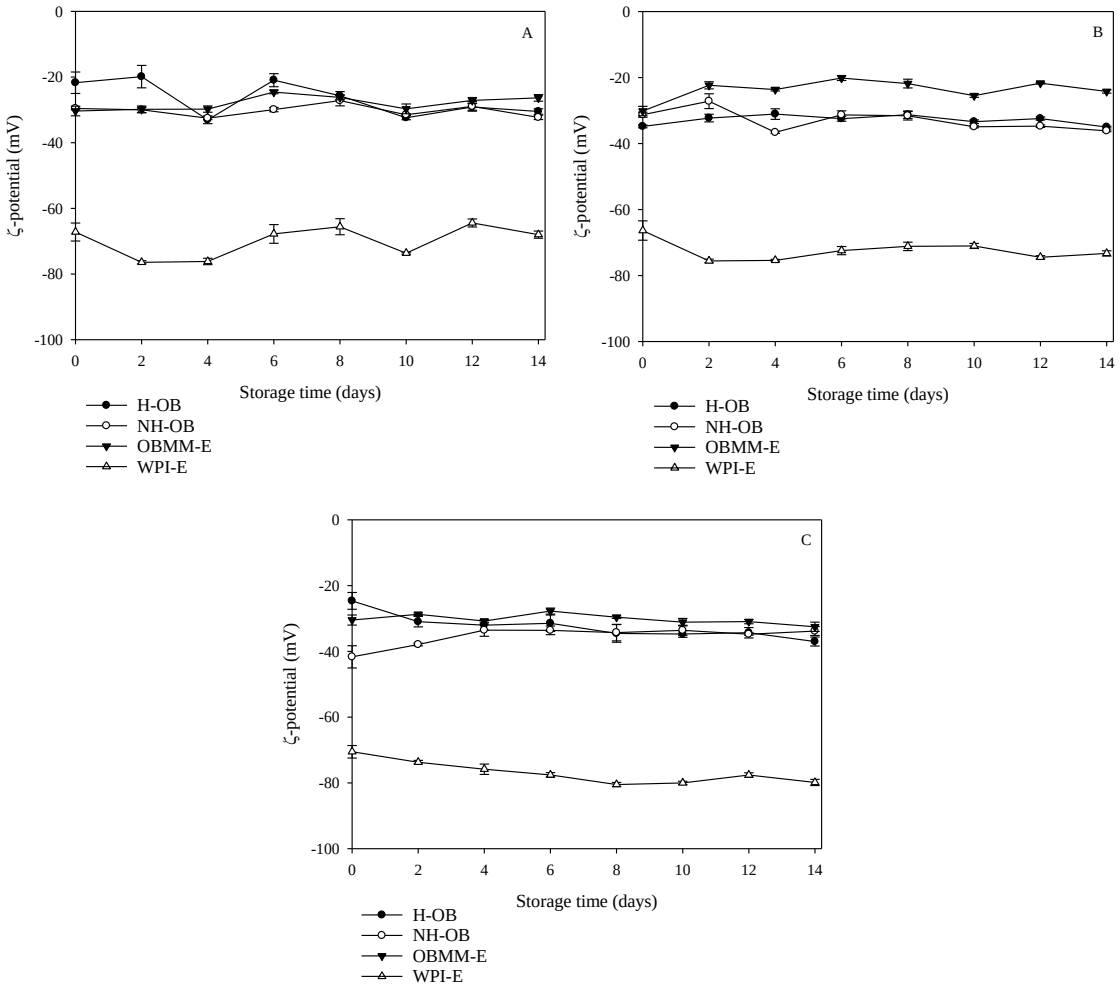

Figure 6.12. ζ-potential (at pH 7) of β-carotene-loaded oil body systems stored at 4°C (A), 22°C (B), and 50°C (C) for 14 days. The oil body systems were as follows: homogenised oil bodies (H-OB), non-homogenised oil bodies (NH-OB), and oil body membrane materials-stabilised emulsion (OBMM-E), with a WPI-stabilised emulsion (WPI-E) as control. Error bars indicate standard error of mean.

The effect of the presence or absence of light on the ζ-potential of the oil body systems is presented in Figure 6.13. Results showed that the presence of light did not significantly affect the ζ-potential during storage. However, a significant difference was observed among the samples, with WPI-E exhibiting the highest magnitude of ζ-potential with a mean of around -73 mV. There was no significant difference between H-OB and NH-OB, having a mean of around -34 mV. The lowest magnitude of ζ-potential was observed for OBMM-E with a mean of around -27 mV.

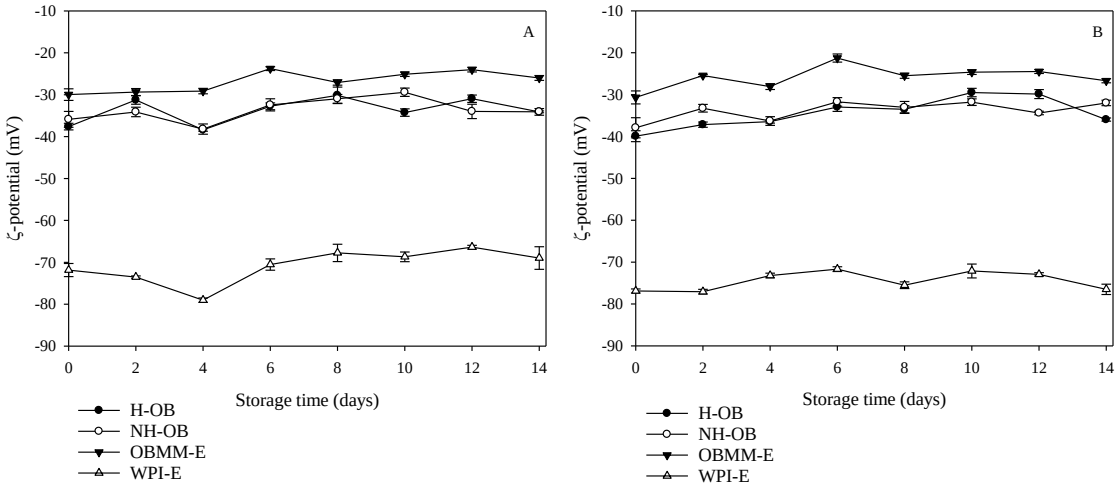

Figure 6.13. ζ-potential (at pH 7) of β-carotene-loaded oil body systems stored under light (A) and dark (B) conditions at room temperature (~22°C) for 14 days. The oil body systems were as follows: homogenised oil bodies (H-OB), non-homogenised oil bodies (NH-OB), and oil body membrane materials-stabilised emulsion (OBMM-E), with a WPI-stabilised emulsion (WPI-E) as control. Error bars indicate standard error of mean.

6.2.2 Effect of storage conditions on β-carotene stability

6.2.2.1 Colour

The influence of storage temperature on the colour (*L**, *a**, and *b** values) of the β-carotene-loaded oil body systems is shown in Figures 6.14, 6.15, and 6.16. In general, a decrease in the lightness (*L**) and colour intensity (*a** for redness and *b** for yellowness) were observed during the storage period, indicating colour fading. There was no significant difference in *L**, *a**, and *b** values at 4°C and 22°C. However, the increase in storage temperature enhanced the degree of colour fading, since a significantly higher reduction in *L**, *a**, and *b** values was observed at 50°C.

The total colour difference (Δ*E**) was calculated from the tristimulus values so that the extent of colour fading of the samples can be compared using a single parameter. Figure 6.17 shows that the storage temperature of 4°C and 22°C did not significantly affect the total colour difference. However, increasing the temperature to 50°C caused a significant increase in colour fading. Among the samples, OBMM-E had a significantly lower degree of colour fading, whereas no significant difference was observed for H-OB, NH-OB, and WPI-E during the storage period.

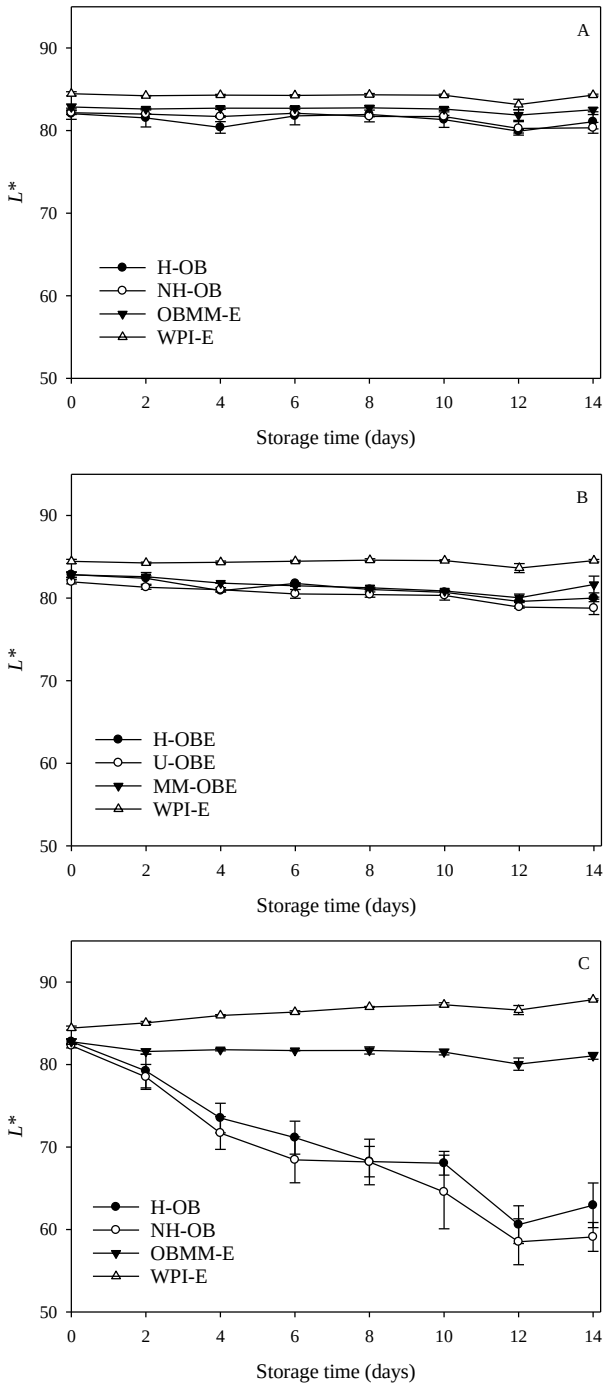

Figure 6.14. *L** values ('lightness') of β-carotene-loaded oil body systems stored at 4°C (A), 22°C (B), and 50°C (C) for 14 days. The oil body systems were as follows: homogenised oil bodies (H-OB), non-homogenised oil bodies (NH-OB), and oil body membrane materials-stabilised emulsion (OBMM-E), with a WPI-stabilised emulsion (WPI-E) as control. Error bars indicate standard error of mean.

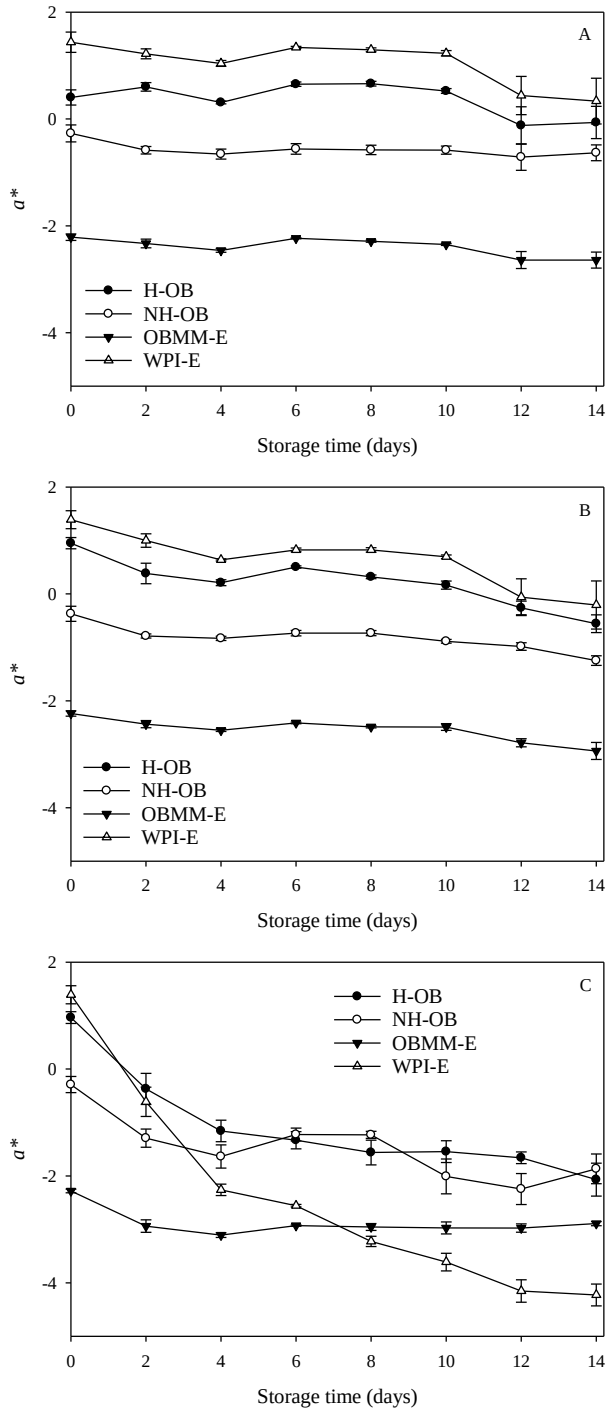

Figure 6.15. *a** values ('redness') of β-carotene-loaded oil body systems stored at 4°C (A), 22°C (B), and 50°C (C) for 14 days. The oil body systems were as follows: homogenised oil bodies (H-OB), non-homogenised oil bodies (NH-OB), and oil body membrane materials-stabilised emulsion (OBMM-E), with a WPI-stabilised emulsion (WPI-E) as control. Error bars indicate standard error of mean.

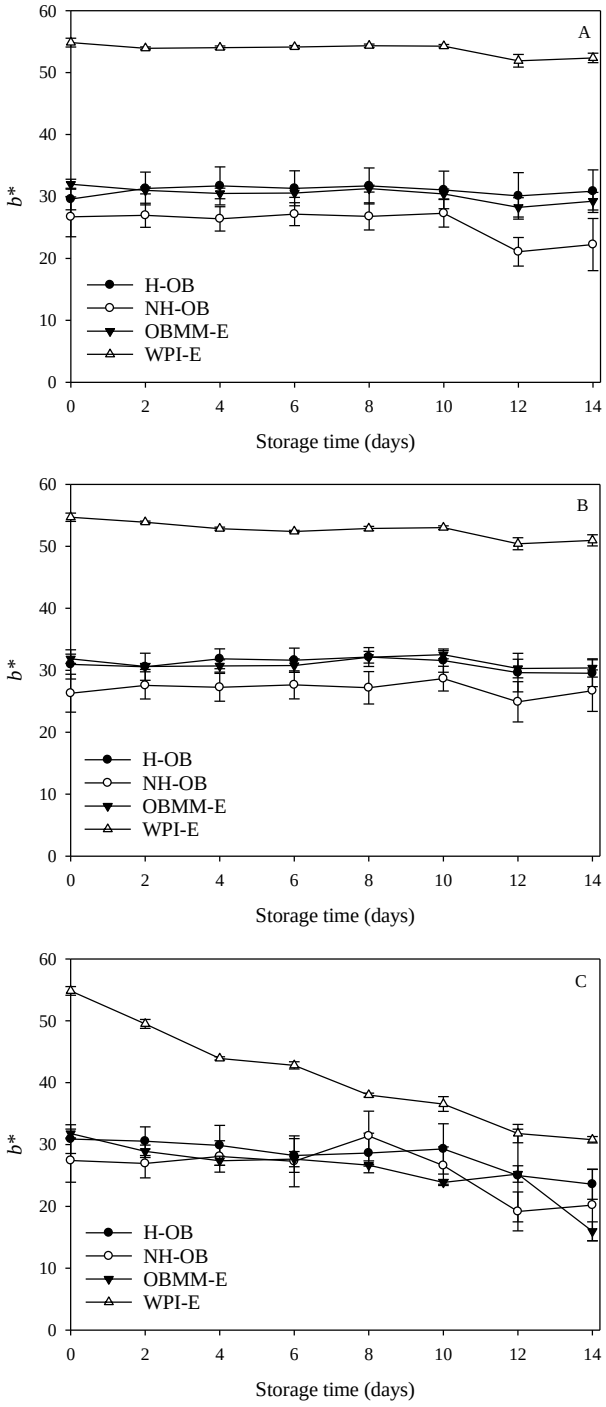

Figure 6.16. *b** values ('yellowness') of β-carotene-loaded oil body systems stored at 4°C (A), 22°C (B), and 50°C (C) for 14 days. The oil body systems were as follows: homogenised oil bodies (H-OB), non-homogenised oil bodies (NH-OB), and oil body membrane materials-stabilised emulsion (OBMM-E), with a WPI-stabilised emulsion (WPI-E) as control. Error bars indicate standard error of mean.

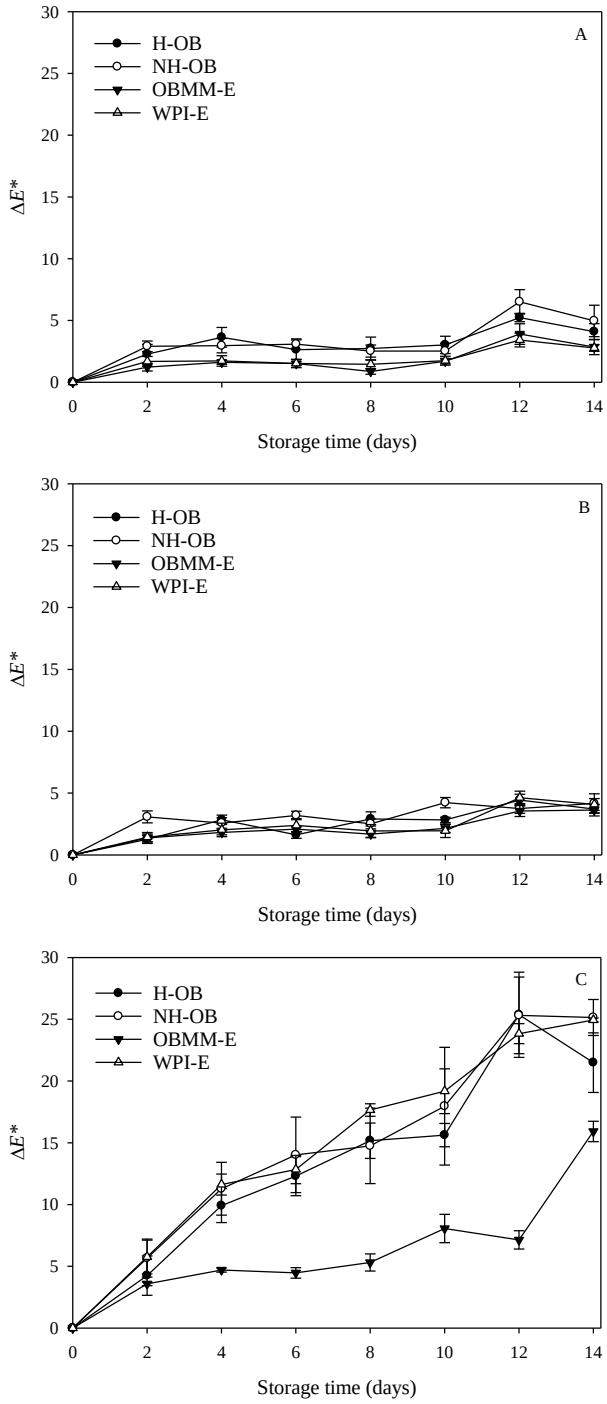

Figure 6.17. Δ*E** values (total colour difference) of β-carotene-loaded oil body systems stored at 4°C (A), 22°C (B), and 50°C (C) for 14 days. The oil body systems were as follows: homogenised oil bodies (H-OB), non-homogenised oil bodies (NH-OB), and oil body membrane materials-stabilised emulsion (OBMM-E), with a WPI-stabilised emulsion (WPI-E) as control. Error bars indicate standard error of mean.

The influence of the presence of light on the colour (L^*, a^*, and b^* values) of the samples during storage at 22°C is shown in Figure 6.18. In general, a decrease in the lightness (L^*) and redness (a^*) of the oil body systems was observed during the storage period, although there was no significant difference in their yellowness (b^*). The presence of light had no significant effect on the L^*, a^*, and b^* values of all the samples during the storage period.

The total colour difference (ΔE^*) of the oil body systems indicated a general increase in colour fading with respect to storage time (Figure 6.19). The presence of light did not have a significant effect on the ΔE^* values of the samples. However, significant differences were observed in their total colour difference during storage. The lowest increase in colour fading was observed for OBMM-E, followed by WPI-E, H-OB, and NH-OB with the highest extent of colour fading. There was no significant difference between H-OB and NH-OB, but they exhibited a significantly larger extent of colour fading compared to OBMM-E.

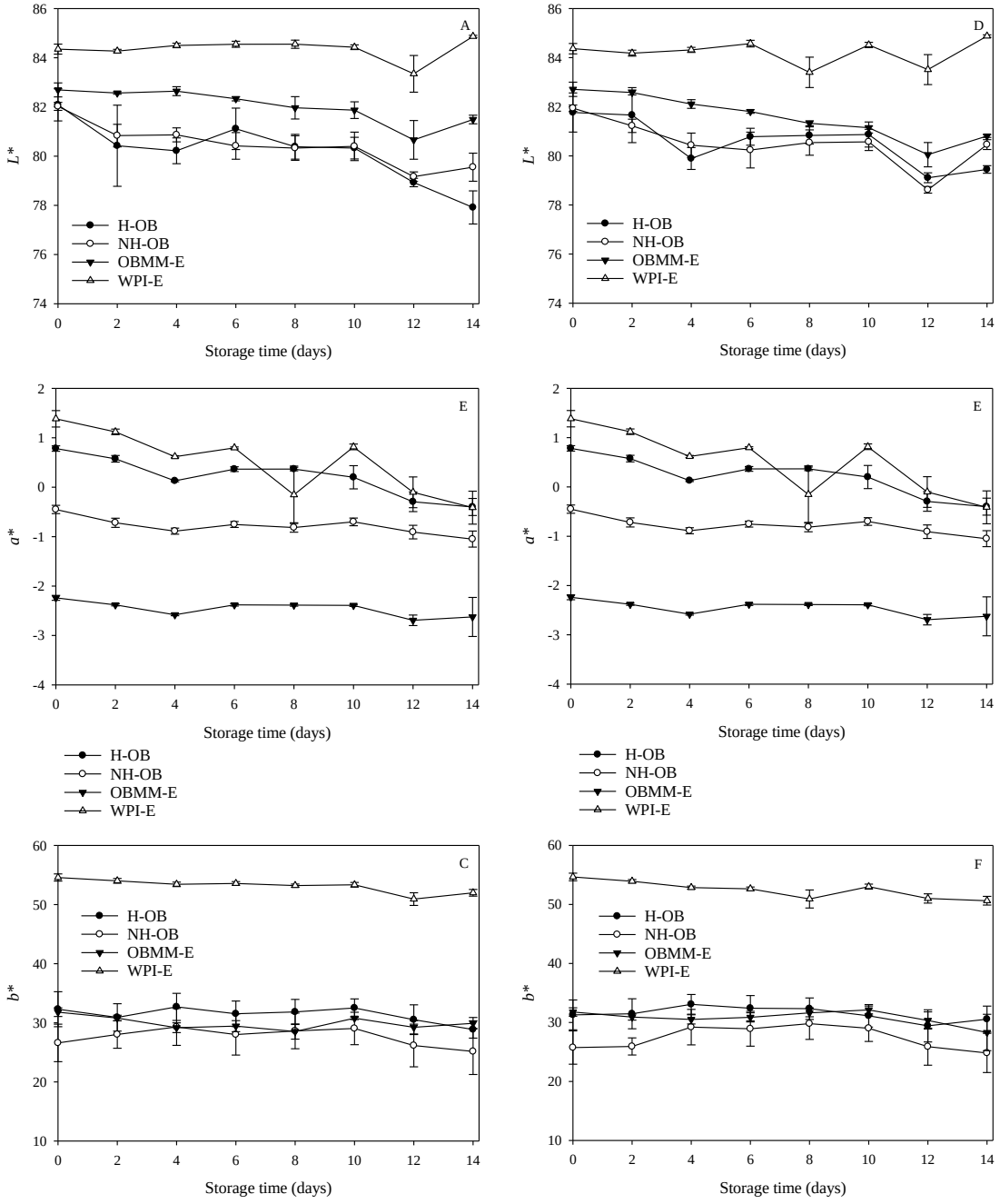

Figure 6.18. *L**, *a**, and *b** values of β-carotene-loaded oil body systems stored exposed to light (A, B, and C) and those stored in dark (D, E, and F) during 14 days of storage. *L** is shown in A and D, *a** is shown in B and E, and *b** values shown in C and F. The oil body systems were as follows: homogenised oil bodies (H-OB), non-homogenised oil bodies (NH-OB), and oil body membrane materials-stabilised emulsion (OBMM-E), with a WPI-stabilised emulsion (WPI-E) as control. Error bars indicate standard error of mean.

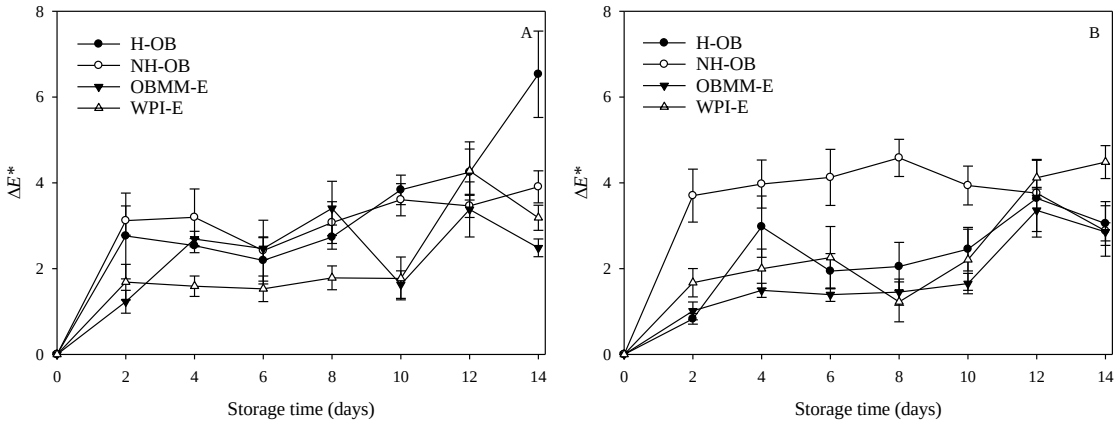

Figure 6.19. Δ*E** values (total colour difference) of β-carotene-loaded oil body systems stored exposed to light (A) and those stored in dark (b) during 14 days of storage. The oil body systems were as follows: homogenised oil bodies (H-OB), non-homogenised oil bodies (NH-OB), and oil body membrane materials-stabilised emulsion (OBMM-E), with a WPI-stabilised emulsion (WPI-E) as control. Error bars indicate standard error of mean.

6.2.2.2 β-carotene quantification

The chemical stability of β-carotene encapsulated in the oil body systems was directly determined through solvent extraction. The influence of storage temperature on the β-carotene concentration is shown in Figure 6.20. Storage at 4°C and 22°C did not have a significant effect on the β-carotene concentration of the samples. However, storage at 50°C resulted in a significant reduction in the β-carotene concentration during the storage period.

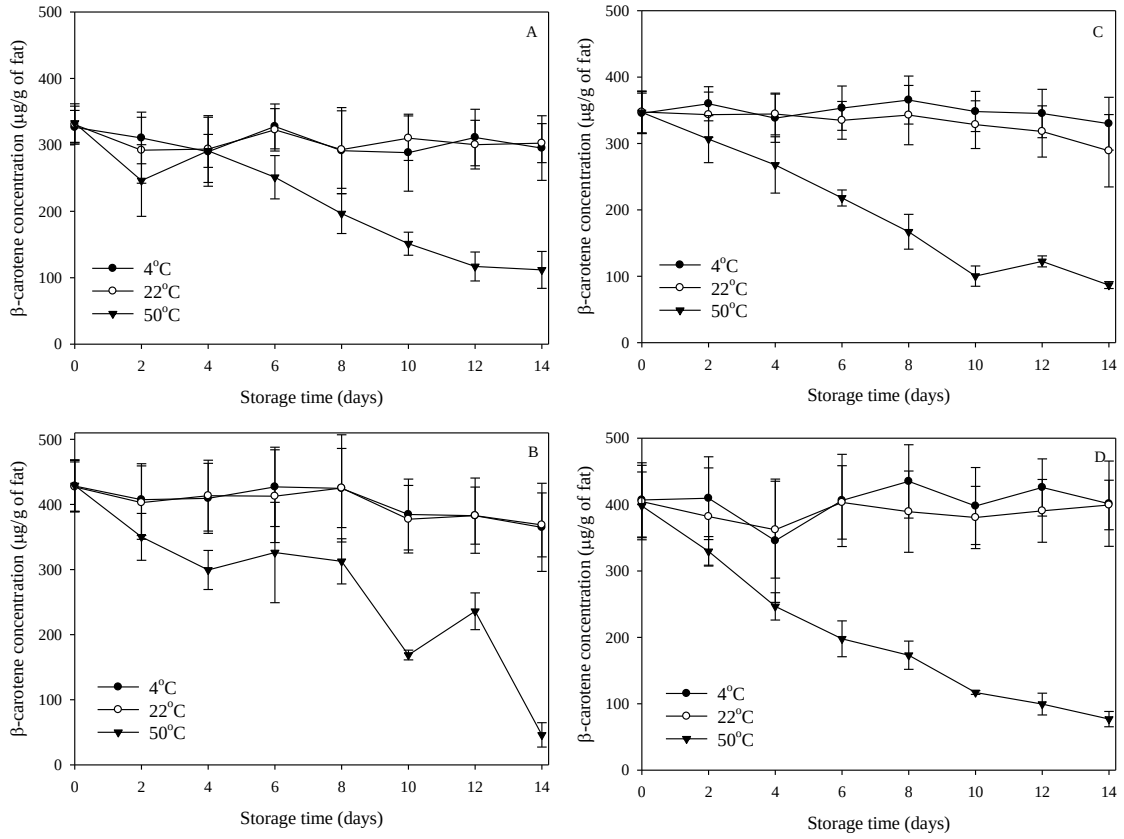

Figure 6.20. β-carotene concentration of β-carotene-loaded oil body systems stored at 4°C, 22°C, and 50°C for 14 days. The oil body systems were as follows: homogenised oil bodies (A), oil body membrane materials (OBMM)-stabilised emulsion (B), and non-homogenised oil bodies (C), with a WPI-stabilised emulsion (D) as control. Error bars indicate standard error of mean.

To compare the degradation of β-carotene in different emulsions during storage, the retention of β-carotene relative to the initial concentration was determined (Figure 6.21). As seen in the figure, no significant difference was observed in the retention of β-carotene when the samples were stored at 4°C and 22°C. However, a significantly lower β-carotene retention was observed at 50°C. Moreover, the samples exhibited a similar degradation rate as no significant difference was observed in their β-carotene retention during the storage period. It can be seen on the graph, however, that OBMM-E had the lowest retention of β-carotene (~10%) at day 14, followed by WPI-E (~20%), NH-OB (~25%), and H-OB with the highest retention of around 32%.

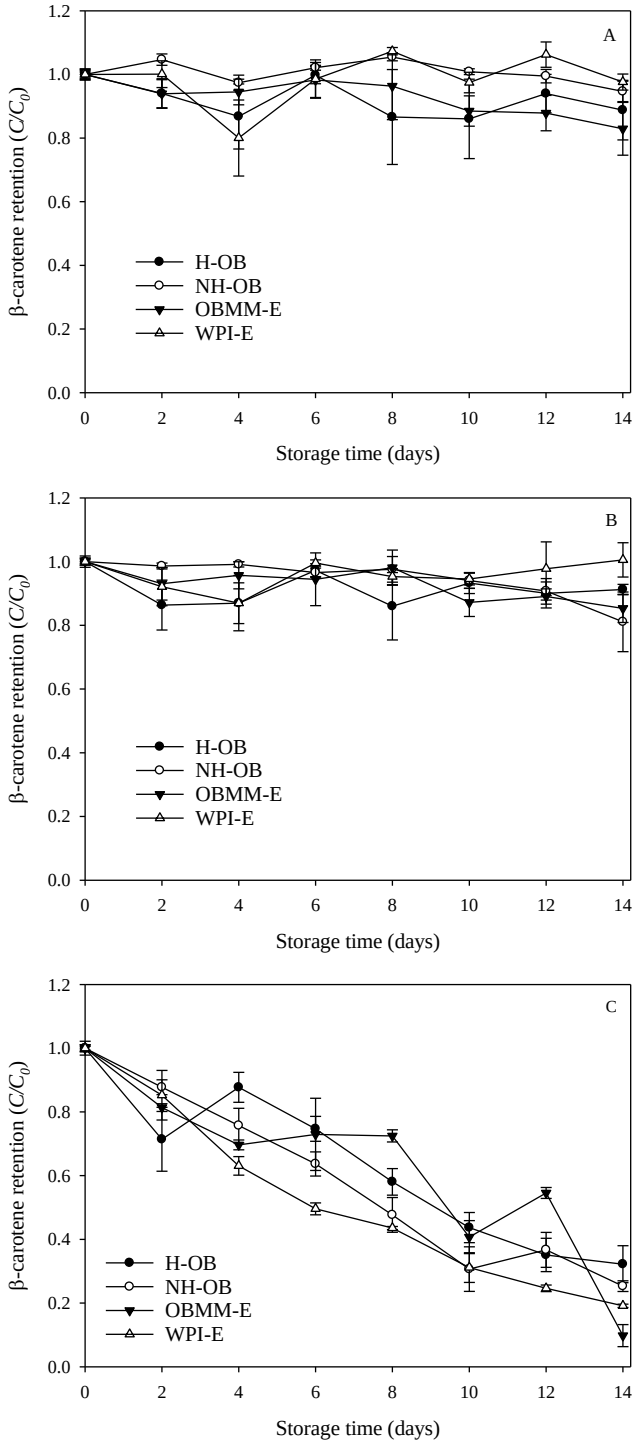

Figure 6.21. β-carotene retention of β-carotene-loaded oil body systems stored at 4°C (A), 22°C (B), and 50°C (C) for 14 days. The oil body systems were as follows: homogenised oil bodies (H-OB), non-homogenised oil bodies (NH-OB), and oil body membrane materials-stabilised emulsion (OBMM-E), with a WPI-stabilised emulsion (WPI-E) as control. Error bars indicate standard error of mean.

On the other hand, the effect of the presence of light on the concentration of β-carotene in the samples stored at room temperature (~22°C) is shown in Figure 6.22. Within the same sample, no significant difference was observed in the β-carotene concentration under storage at light or dark conditions. Also, no significant reduction in the β-carotene concentration was observed in all samples throughout the storage period.

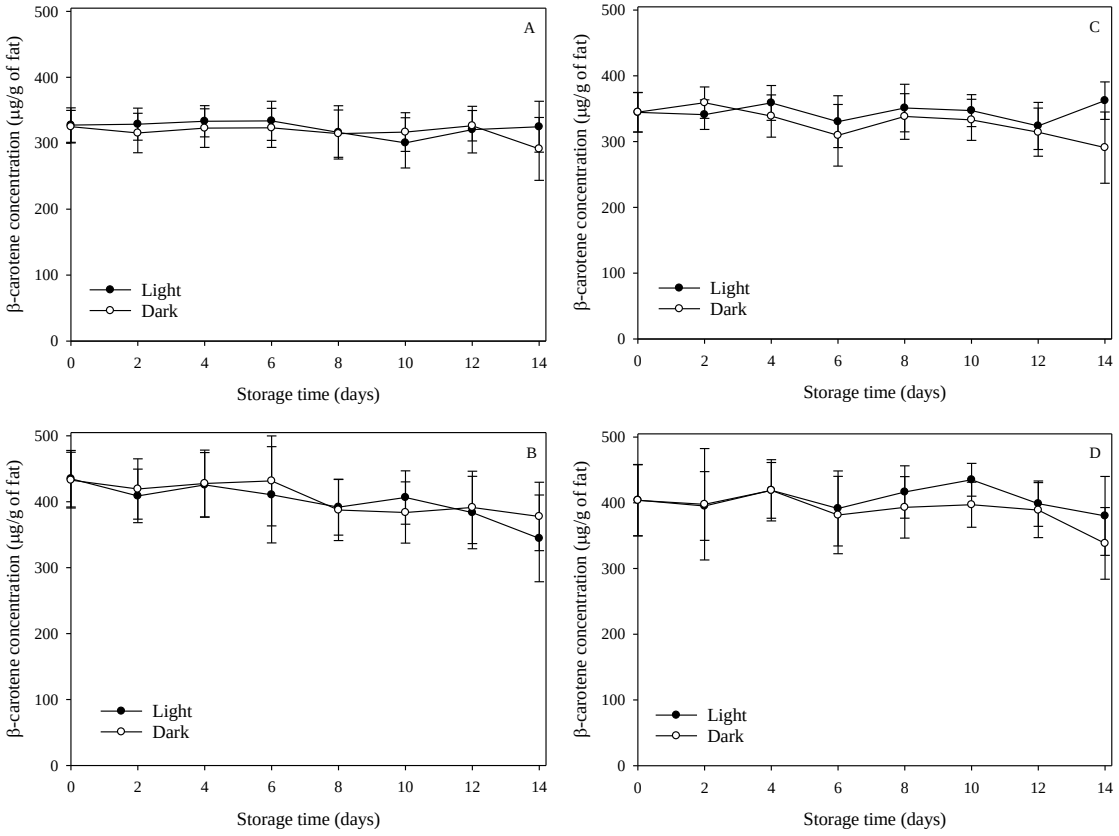

Figure 6.22. β-carotene concentration of β-carotene-loaded oil body systems stored under light and dark conditions for 14 days at room temperature (~22°C). The oil body systems were as follows: homogenised oil bodies (A), oil body membrane materials (OBMM)-stabilised emulsion (B), non-homogenised oil bodies (C), with a WPI-stabilised emulsion (D) as control. Error bars indicate standard error of mean.

The effect of light on the retention of β-carotene in the oil body systems during storage at room temperature (~22°C) is shown in Figure 6.23. At both light and dark conditions, the retention of β-carotene was largely similar with a relatively small but significant statistical difference.

Regarding the different oil body systems, OBMM-E exhibited a significantly lower β-carotene retention compared to the other samples which had no significant difference. Meanwhile, OBMM-E had the lowest retention of β-carotene (~77%) in the presence of light (Figure 6.23 A).

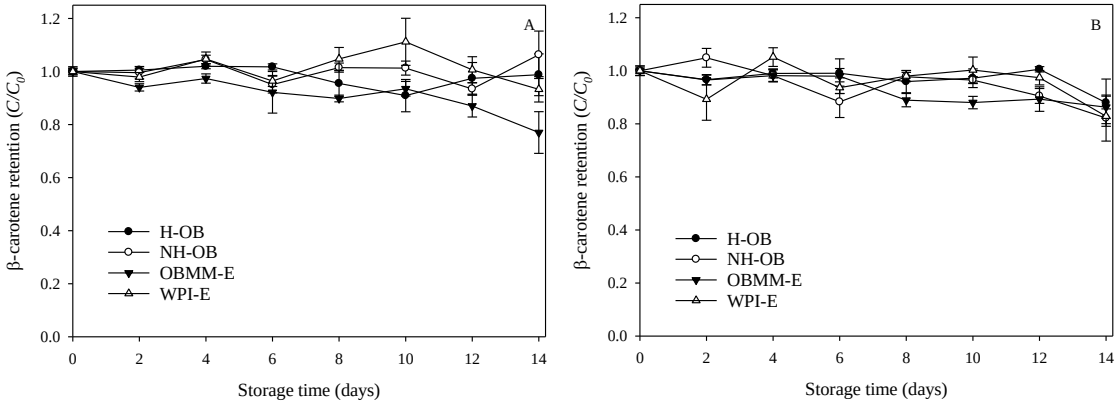

Figure 6.23. β-carotene retention of β-carotene-loaded oil body systems stored under light (A) and dark (B) conditions at room temperature (~22°C) for 14 days. The oil body systems were as follows: homogenised oil bodies (H-OB), non-homogenised oil bodies (NH-OB), and oil body membrane materials-stabilised emulsion (OBMM-E), with a WPI-stabilised emulsion (WPI-E) as control. Error bars indicate standard error of mean.

6.3 Discussion

The stability of delivery systems for bioactive compounds may be affected by changes in their environmental conditions during storage and transport. Moreover, β-carotene degradation is promoted by exposure to heat and light. Thus, the effect of storage temperature and light conditions on the colloidal and chemical stability of β-carotene-loaded oil body systems were investigated in this study to determine the potential of these systems to protect β-carotene from degradation during storage.

6.3.1 Effect of storage conditions on the colloidal stability of oil body systems

In determining the effect of storage temperature on the stability of oil body systems, 4°C, 22°C, and 50°C were chosen to simulate refrigeration, ambient, and elevated storage temperatures, respectively. Commercially, food products are stored or transported at these temperatures, with refrigeration temperatures possibly causing physical changes in the

product such as precipitation and elevated temperatures accelerating the rate of degradation processes, such as oxidation (Borba et al., 2019).

In this study, storage at 4°C and 22°C did not have a significant effect on the droplet size of the oil body systems. However, storage at 50°C caused a significant increase in their size, except for WPI-E (control). An increase in storage temperature has been correlated to the increase in particle size and a decrease in ζ-potential of emulsions (Teng et al., 2020). Generally, increasing the temperature results in the reduction of the viscosity of the continuous phase and enhancement of the thermal energy of the droplets, causing an enhanced collision frequency and promoting coalescence (McClements, 2016; Zhou et al., 2019). Moreover, lipid oxidation could have occurred and caused structural changes in the interfacial components of the oil body systems, resulting in their increased size as observed in nanoemulsions stabilised by soy protein isolate and phosphatidylcholine (Teng et al., 2020). At temperatures above 40°C, phospholipids in MFGM model bilayers undergo phase transitions, which could have affected their morphological characteristics and interactions with proteins at the interface (Murthy et al., 2016). These mechanisms could explain the coalescence and flocculation observed in H-OB, which exhibited an increased particle size even after dispersion in SDS.

WPI-E showed stability against droplet aggregation even at elevated temperatures. This is due to its high surface charge, generating a large electrostatic repulsion between droplets to overcome van der Waals and hydrophobic attraction that causes droplet aggregation (Jo & Kwon, 2014; Kim et al., 2002; McClements, 2016; Zhu et al., 2013). Among the oil body systems, OBMM-E exhibited the most comparable colloidal stability at 50°C to WPI-E despite having a lower surface charge (~27 mV). This can be attributed to having a similar size with WPI-E, and the presence of oleosins and phospholipids at the interface which were able to resist the increase in surface hydrophobicity due to the high temperature (Chen & Ono, 2010; Nikiforidis et al., 2011; Sukhotu et al., 2014). The stability of WPI- and other protein-stabilised emulsions during storage at elevated temperatures has also been observed in other studies. For example, storage at 55°C only resulted in minimal change in droplet size of WPI-stabilised nanoemulsions over a 12-day period, which was attributed to the formation of layers of the emulsifier on the droplet interface (Mao et al., 2010). This interface has imparted steric hindrance and electrostatic repulsion to emulsion droplets to overcome attractive interactions. Similarly, Luo et al.

(2017) did not observe any significant change in the mean particle diameter and ζ-potential of WPI-stabilised nanoemulsions during a 14-day storage at 4°C, 25°C, and 55°C due to the relatively small droplet size of the emulsions. Qian et al. (2012) only observed a slight increase (<15% after 15 days) in mean particle size during storage at 5°C, 20°C, 37°C, and 55°C in β-lactoglobulin nanoemulsions. Meanwhile, Xu et al. (2013) observed a constant droplet size and absence of phase separation during the 7-day storage of WPI-stabilised emulsions at 55°C.

The ζ-potential of the oil body systems remained largely similar during storage at different temperatures, indicating that the storage temperature had minimal effect on the electrical characteristics of the droplet interface. A slight increase in ζ-potential magnitude was however observed at 50°C, suggesting that amphiphilic lipid oxidation products such as free fatty acids and organic acids may have been produced during storage (Wang et al., 2021). In other studies, a reduction in ζ-potential was observed during storage due to changes in protein conformation that resulted in the formation of hydrophobic and hydrogen bonding between adjacent proteins at the interface, promoting droplet aggregation (Teng et al., 2020). This decrease in ζ-potential has been observed in nanoemulsions stabilised by phosphatidylcholine and soy protein isolate when stored at 4°C, 25°C, and 55°C for 30 days (Teng et al., 2020).

Storage of the β-carotene-loaded oil body systems in the presence of light at ambient temperature did not have a significant effect on their mean particle diameter and ζ-potential. As such, changes in these two parameters during storage can be attributed to differences in the structure and composition of the samples. WPI-E (control) exhibited the smallest increase in size and the highest magnitude of ζ-potential during storage. Among the oil body systems, OBMM-E exhibited a comparable size with WPI-E (control), although it had the smallest ζ-potential (although still around -30 mV). This colloidal stability during storage can be attributed to the small droplet size similar to WPI-E. Based on Stokes' law, kinetic stability of oil-in-water emulsions can be achieved with a reduction in the size of the dispersed phase, minimising gravitational separation (Cornacchia & Roos, 2011; McClements, 2016).

Moreover, oil body emulsions stabilised by isolated oil body proteins have been shown to have high physical stability during storage because of their small size and superior

structural integrity, being stable against coalescence and flocculation (Chang et al., 2013; Chen et al., 2004; Chen et al., 2005). These stability features can be explained by the synergistic effect of the oleosins and phospholipids at the interface (Deleu et al., 2010). Oleosins provide steric hindrance and electrostatic repulsion, and the electrostatic interactions between their basic amino acid residues with the negatively-charged phospholipids at the interface form an elastic film that stabilise emulsions with greater efficiency than oleosins or phospholipids alone (Chen et al., 2004; Deleu et al., 2010; Peng et al., 2003). The abovementioned mechanisms also provide great thermostability to oil body proteins-stabilised emulsions at temperatures higher than 60°C, compared with native oil bodies (Chen et al., 2004; Peng et al., 2003). During storage, emulsions stabilised by oil body membrane materials (mixture of phospholipids and isolated oil body proteins) have exhibited colloidal stability. For instance, oil body emulsions stabilised by recombinant caleosin maintained a highly negative surface charge of around -50 mV (Chang et al., 2013) and maintained a similar size profile (Chen et al., 2005) during 7 days of storage at 4°C. A different behaviour was observed by Wijesundera et al. (2013), as oil body emulsions stabilised by an oleosin extract exhibited flocculation but not coalescence during storage for 30 days at 4°C and 40°C. Differences in the physical stability of these emulsions may be attributed to their size, as oil body emulsions stabilised by caleosin were found to be 10 times smaller and have stronger electrostatic repulsion on the surface than those stabilised by oleosin extracts, whose size are comparable to native oil bodies (Chen et al., 2004). Oleosins may also promote the flocculation of droplets during storage due to the attractive forces among oleosins in different droplets, but coalescence is avoided due to steric repulsive forces (Deleu et al., 2010). The ratio between the phospholipids and oil body proteins is also crucial for the stability of emulsions stabilised by oil body membrane materials: a stability similar to native oil bodies can be achieved when oil, phospholipids, and proteins are mixed in the same proportions as that occurring in native oil bodies (Wijesundera et al., 2013).

H-OB had the highest increase in size among the oil body systems and exhibited extensive droplet aggregation despite the strongly negative surface charge (>30 mV). As presented in the previous chapter, homogenised oil bodies exhibited flocculation due to the limited amount of emulsifier to stabilise the higher surface area of the oil formed as a result of homogenisation. As such, extensive particle-particle aggregation could have been

promoted during storage and promoted creaming at the top of the emulsion (Cornacchia & Roos, 2011; McClements, 2016). In other studies, creaming has been observed in homogenised rapeseed oil bodies when stored above 35°C due to the denaturation of oleosins upon exposure to high temperature over prolonged periods, causing a reduction in their emulsifying capacity and particle aggregation (He et al., 2020). In contrast, homogenised soybean oil bodies were found to be stable against aggregation and flocculation even at elevated temperature, with no change in surface charge (Liu et al., 2020). These differences suggest that a better understanding of the properties of different types of oil bodies and their concentration in the emulsion is needed to determine their physical stability at different storage conditions.

On the other hand, NH-OB exhibited a smaller increase in size and change in ζ-potential than H-OB. This can be attributed to the known structural stability of the oil body membrane (Huang, 1994; Tzen & Huang, 1992). In other systems, the stability of oil bodies during storage has also been demonstrated: a low creaming rate was observed for maize germ oil bodies at room temperature (Nikiforidis & Kiosseoglou, 2010); soymilk exhibited good stability against gravitational separation during storage (Zheng et al., 2019); and rapeseed oil bodies exhibited high stability to aggregation and coalescence at room temperature storage (Acevedo et al., 2014).

6.3.2 Effect of storage conditions on the chemical stability of β-carotene in oil body systems

The stability of β-carotene during storage was evaluated by determining the change in its colour (indirect) and concentration (direct) over time. When β-carotene undergoes chemical degradation, the intensity of its orange-red colour decreases: hence, colourimetry methods are used to indirectly measure the degree of colour fading (Luo et al., 2017; Qian et al., 2012). In the tristimulus colour coordinates, L^* represents 'lightness', a^* represents 'redness' ($+a^*$ is red, $-a^*$ is green), and b^* represents 'yellowness' ($+b^*$ is yellow, $-b^*$ is blue) (McClements, 2002). In this study, a significant increase in colour fading was observed in the oil body systems during storage at elevated temperatures, as seen in the reduction in their L^*, a^*, and b^* values at 50°C. Similarly, Luo et al. (2017) and Qian et al. (2012) observed a progressive reduction in the lightness (L^*) and colour intensity (a^* and b^*) of β-carotene nanoemulsions during storage. However, an increase in lightness is associated with the decrease in colour intensity of

emulsions due to the higher fraction of light that is reflected from the surface (McClements, 2002). As such, the observed decrease in lightness during storage could have been due to changes in the intensity of light scattering due to changes in particle size or spatial organisation of the emulsion droplets (Qian et al., 2012).

The relative loss of colour represented by ΔE^* showed the effects of storage temperature on stability. Storage at 55°C caused a significant increase in the total colour difference of the oil body systems. Meanwhile, storage at 4°C and 22°C had no significant effect on the rate of colour fading. Generally, the increase in storage temperature enhances the rate of colour fading due to the chemical degradation of β-carotene at elevated temperatures (Luo et al., 2017; Qian et al., 2012). Similar behaviour was observed in WPI-stabilised β-carotene nanoemulsions wherein a large increase in ΔE^* was observed at 55°C but not at 4°C and 25°C (Luo et al., 2017). Likewise, Qian et al. (2012) reported a rapid acceleration in colour fading when the storage temperature of β-lactoglobulin-stabilised β-carotene emulsions was increased from 20°C to 55°C.

Similar to the degree of colour fading, storage at refrigeration and ambient temperatures did not cause a significant reduction in the β-carotene concentration of the oil body systems. Other studies have also demonstrated this stability of β-carotene at lower temperatures, as protein-stabilised emulsions did not exhibit a reduction in β-carotene concentration at ambient temperatures and below (Cornacchia & Roos, 2011; Jo & Kwon, 2014; Luo et al., 2017). Yuan et al. (2008) also observed a gradual degradation of β-carotene in surfactant-stabilised emulsions stored at 4°C and 25°C for 4 weeks, wherein only 14-25% of β-carotene was lost. Over a 90-day storage period, Borba et al. (2019) reported superior stability of β-carotene nanoemulsions stored at 4°C compared to those stored at 25°C and 37°C as more than 50% of β-carotene was lost after 30 days of storage at 25°C. More differences in the concentrations could be observed at longer durations, as most differences in β-carotene degradation at 4°C occurred in the last 8 weeks of storage in 12 weeks as reported by Tan and Nakajima (2005).

Storage at elevated temperatures caused a significant reduction in the β-carotene concentration of the oil body systems. However, the rate of β-carotene degradation did not significantly differ among the samples. High temperature is known to cause the degradation of β-carotene due to isomerisation and other degradation reactions (Chen et

al., 2017). The double bonds in the β-carotene molecule become oxidized and the breakage of these bonds occurs, resulting in the formation of volatile compounds and larger non-volatile components (Boon et al., 2010). According to Xu et al. (2013), the degradation mechanism is primarily through free radical oxidation as a positive correlation was observed with the formation of protein oxidation products and higher β-carotene degradation rates. Moreover, the fatty acids in the oil phase undergo lipid oxidation at high temperatures; thus, the presence of reactive species could have accelerated the rate of β-carotene oxidation (Borba et al., 2019). The elevated temperature during storage could also have resulted in the evaporation of any dissolved oxygen in the water to the headspace, promoting aggregation and creaming of emulsion droplets and thereby exposing more of the β-carotene to oxidation and losing the protective effect of the emulsifier layer (Mao et al., 2010). A similar effect on β-carotene degradation was observed in other protein-stabilised emulsions, wherein more than 60% of loss was observed after 7 days (Xu et al., 2013) and a total loss was observed after 14 days (Qian et al., 2012) of storage at 55°C.

On the effect of light, storage under the presence of light did not significantly affect the L^*, a^*, b^*, and ΔE^* values of the oil body systems at room temperature (~22°C) storage, although a decrease in the L^* and a^* values and an increase in the ΔE^* was observed. As previously discussed, an increase in the total colour difference of the samples is positively correlated to the degradation of β-carotene. In the degradation of β-carotene in aqueous solutions, an increase in lightness and reduction in redness was observed during a 4-day storage period upon exposure to light from different lamp types (cool white, warm white, and halogen) (Limbo et al., 2007). Moreover, the reduction in a^* was also correlated to the increase in the production of β-ionine, a volatile degradation product of β-carotene (Limbo et al., 2007). As such, the colour values are a good indication of β-carotene degradation during storage.

The presence of light barely influenced the β-carotene retention of the samples, which was contrary to the expected increase in β-carotene degradation as the compound is known to undergo photooxidation (Boon et al., 2010). Upon exposure to light, the excitation of β-carotene molecules occurs and results in the formation of free radicals that promote oxidation (Boon et al., 2010). Limbo et al. (2007) also proposed that the type I pathway of photooxidation could have been favoured in lighted samples of β-carotene in

an aqueous solution in the availability of low oxygen and given the poor water solubility of singlet oxygen. In this mechanism, the absorption of visible and ultraviolet radiation energy resulted in the formation of excited triplet sensitisers that acted as a photochemically activated free radical initiator for a radical compound and formed peroxy radical after reaction with triplet oxygen. An induction time was also observed in the degradation of β-carotene and this induction time was found to be higher in the dark, indicating that light exposure enhanced reaction rates (Limbo et al., 2007). This induction time was attributed to the antioxidant effect of β-carotene through the physical quenching of singlet oxygen and radical trapping and its ability to protect itself from oxidation (Limbo et al., 2007). The photooxidation of β-carotene has been exhibited in other emulsions wherein an increase in light intensity caused an increase in the degradation rate (Calligaris et al., 2019; Limbo et al., 2007). Moreover, nanoemulsions with β-carotene stored without light had higher β-carotene retention of above 50% at 25°C compared to samples stored with light for 90 days (Borba et al., 2019). Furthermore, Borba et al. (2019) used an LED lamp of lower luminous flux in their study; however, the distance between the light source and sample was around 10 times smaller compared to this study. Thus, the absence of the effect of light on β-carotene degradation may be due to the large distance of the samples from the light source, which reduced the amount of light energy they absorbed.

The degradation of β-carotene is autocatalytic and dependent on the induction period in which the accumulation of radicals occurs (Borba et al., 2019). In this study, the lack of significant increase in β-carotene degradation rate in the presence of light could be due to the low temperature and short duration of investigation, which could not have been enough to accelerate radical formation which induces oxidation. For instance, no significant difference was observed in β-carotene retention of nanoemulsions stored at 4°C for 90 days in the presence or absence of light (Borba et al., 2019). Limbo et al. (2007) also did not observe a great effect of storage at lighted conditions on the degradation of β-carotene in an aqueous solution at reduced oxygen conditions. As such, a longer storage duration could potentially give more information on the degradation of β-carotene in emulsions stored in the presence of light.

Among the oil body systems, no differences were observed in the retention of β-carotene upon storage at different temperatures, which agrees with the results on their colour

fading. As such, temperature was the most significant factor that contributed to β-carotene degradation in this study. However, storage in the presence or absence of light at ambient temperature (~22°C) showed significantly lower retention of β-carotene in OBMM-E compared to the other systems, which could be attributed to its lower particle size. An increase in degradation of β-carotene is correlated to the decrease in mean particle diameter due to the larger surface area of the droplets which enhances the interaction of β-carotene with prooxidants in the aqueous phase (Cornacchia & Roos, 2011; Hu et al., 2003; Jo & Kwon, 2014; Tan & Nakajima, 2005). Moreover, free radicals could be generated during homogenisation, promoting oxidation during storage (Tan & Nakajima, 2005).

The other oil body systems (H-OB and NH-OB) exhibited comparable β-carotene retention to WPI-E during storage despite their higher particle size. Protein-stabilised emulsions are known to enhance the stability of β-carotene in emulsions due to the behaviour and antioxidant capacity of the proteins at the interface (Cornacchia & Roos, 2011; Jo & Kwon, 2014; Mao et al., 2010; McClements & Decker, 2000; Qian et al., 2012). For instance, WPI contains β-lactoglobulin and α-lactalbumin which contain cysteyl residues, disulphide bonds, and thiol functional groups that can inhibit lipid oxidation through the scavenging of free radicals (Hu et al., 2003; Mao et al., 2010; Qian et al., 2012; Sun et al., 2007). Moreover, WPI imparts a steric hindrance at the droplet interface and a larger charge density that hinders the interaction of β-carotene with the ions in the aqueous phase (Cornacchia & Roos, 2011). The stability of the oil body systems can be attributed to similar reasons, with oleosins at the interface providing steric hindrance and electrostatic repulsion on the droplets (Huang, 1994; Tzen & Huang, 1992). Aside from the oil body proteins, the phospholipids also play a role in the prevention of β-carotene degradation. The orientation of the phospholipids at the interface and their electrostatic interaction with the oleosins provide a firm anchorage of oleosins, which strengthens the interfacial network (Nikiforidis, 2019; Payne et al., 2014). This structural arrangement of phospholipids and oleosins at the interface may also impart an antioxidant effect, as the oleosins at the surface may act as a barrier to oxygen and reactive hydroperoxides and protect the TAG core from oxidative reactions (Fisk et al., 2008; Gray et al., 2010; Wijesundera et al., 2013). Phospholipids have also been shown to

possess antioxidant activity through free radical scavenging at the oil/water interface, thereby protecting β-carotene from degradation (Chen & Zhong, 2015; Guan et al., 2016).

Oil bodies have also shown protective effects on encapsulated hydrophobic compounds in their matrix because of their unique structure and stability imparted by their membrane components (Bettini et al., 2013; Chang et al., 2013; Chen et al., 2005). For example, curcumin has been protected from degradation in emulsions stabilised by soybean and rapeseed oil bodies especially during digestion (He et al., 2020; Liu et al., 2020). The bioavailability of curcumin and cyclosporine A have also been improved by encapsulating in artificial oil bodies stabilised by recombinant caleosin (Chang et al., 2013; Chen et al., 2005). The presence of tocopherol in hempseed oil could also have enhanced the protection of β-carotene against oxidative reactions (Callaway, 2004; Teh & Birch, 2013). The antioxidant content of the oil bodies has also been attributed to the stability of astaxanthin encapsulated in oil bodies from *Brassica napus* as observed in their low degradation rate at room temperature (Acevedo et al., 2014).

6.4 Conclusion

The physical and chemical stability of β-carotene-loaded oil body systems were investigated during storage at various temperature and light conditions and compared against a WPI-stabilised emulsion. The oil body systems exhibited colloidal and chemical stability at refrigerated and ambient conditions. On the other hand, they were unstable at elevated temperatures as seen in the aggregation of emulsion droplets and degradation of β-carotene over the storage period. On the effect of light, storage under the presence of light did not have a significant effect on the physical stability of the oil body systems at ambient temperature and the degradation of β-carotene was dependent on the droplet size and interfacial composition of the systems.

Among the oil body systems, OBMM-E exhibited comparable colloidal stability with WPI-E during storage at elevated temperatures. This was attributed to its smaller particle size compared to the other oil body systems. A drawback of the small size, however, is the enhanced rate of β-carotene degradation during storage as it exhibited the lowest retention of β-carotene after 14 days. On the other hand, H-OB and NH-OB had the highest increase in size during storage, as evidenced by the presence of flocculation for both and even coalescence for H-OB. Despite this physical instability, both systems

showed a comparable protective effect on β-carotene as WPI-E during storage which was attributed to the antioxidant properties of the oleosins and phospholipids at their interface.

Overall, the oil body systems have shown their potential as encapsulation systems for β-carotene. However, a balance between the colloidal and chemical stability of these systems must be achieved to improve their functionality, especially in commercial applications. NH-OB showed the greatest potential as a delivery system for β-carotene among the oil body systems studied due to the ease of its preparation and protective effect on β-carotene. However, its colloidal stability must be further improved such that flocculation may be avoided during long-term storage. Additional studies on the improvement of the stability of the oil body systems at elevated temperatures are necessary, as well as determining the effect of light in a more controlled manner and at longer storage periods. Further improvement of the stability of these systems and their interaction with other food components, when applied in food products, will also be useful since the degradation of β-carotene poses a serious problem in their commercial application.

Chapter 7 Conclusions, limitations of current work, and avenues for future work

7.1 Conclusions

This study compared the characteristics of oil bodies from hemp and mustard seeds. The extraction method used was successful in isolating hemp oil bodies, which were further used to create oil body-based delivery systems for β-carotene. The colloidal and chemical stability of these systems were determined over 14 days at different storage temperatures and light conditions. This work provides insights on the use of plant-based materials in emulsion systems for the delivery of bioactive compounds to foods.

The recovery of oil bodies as an oil-in-water emulsion from plant-based sources presents the potential of being utilised in a variety of food applications. Compared to the conventional process of oil recovery from oil-bearing plants, the extraction of oil bodies has a lesser environmental impact since the use of organic solvents and the subsequent process of oil refining is avoided. Moreover, there is no need for an additional emulsification step that uses high-energy methods and synthetic emulsifiers because a stable emulsion can be obtained depending on the extraction conditions used. Oil bodies have been isolated from a variety of oleaginous seeds and tissues, and differences in their properties are species-specific. As such, consideration must be taken in choosing oil bodies for certain types of applications. For instance, the cost of raw material and its availability may impact its potential application as a large amount of raw material is needed to obtain a substantial amount of oil bodies. Hence, the side streams of the food industry could be considered as a feasible option to explore other sources of oil bodies. Moreover, the ease of their extractability without the need for extensive washing procedure is vital in the upscale of their isolation and reduction of other processing-related costs. The size of the oil bodies is also important as it could impact their physical stability during storage, while the composition of the oil (e.g., presence of antioxidants) inside the oil bodies can increase their potential for the encapsulation of hydrophobic compounds that are sensitive to oxidation.

Results of the study showed that aqueous extraction can be used to extract oil bodies from hemp and mustard seeds in the form of an oil-in-water emulsion. However, using the extraction protocol used in this study, the mustard oil bodies were entrapped in protein

flocs and difficulties were encountered in their release from these flocs of co-extracted storage proteins even with the use of an alkaline (pH 9.0) grinding medium. Difficulties in the extraction of oil bodies from other *Brassica* species have been acknowledged by other researchers (De Chirico et al., 2018; Romero-Guzmán, Jung, et al., 2020). De Chirico et al. (2020) determined that exogenous proteins may be removed from rapeseed oil bodies through the effect of pH and salt (grinding media of pH 9.5, 0.1 M sodium bicarbonate solution,) and low solid-to-media load (1:7 w/w). On the other hand, Romero-Guzmán, Jung, et al. (2020) proposed a new protocol that used a twin-screw press for the large scale extraction of rapeseed oil bodies.

In contrast, hemp oil bodies were successfully isolated with minimal flocculation even without the use of an extensive washing procedure in their extraction. They also exhibited a high surface charge and behaved similarly to protein-stabilised emulsions at different pH and ionic strength conditions. These indicate that crude hemp oil bodies can provide a naturally stable oil-in-water emulsion and further purification to improve their stability in aqueous systems may not be necessary. Moreover, the oleosins and phospholipids that stabilise their interface provide steric hindrance and electrostatic repulsion and give information on their possible behaviour when utilised in food matrices. Due to their ease of extractability and stability upon extraction, hemp oil bodies were used in the further investigation of the potential of oil bodies as a delivery system for bioactive compounds.

Using an unwashed oil body fraction presents a higher efficiency for oil body applications compared to washed or purified extracts. It does not entail the use of non-food-grade chemicals for extraction nor the use of other equipment for oil body purification. Moreover, the presence of co-extracted extrinsic proteins has been found to aid in the stabilisation of oil bodies. Different approaches were explored to encapsulate β-carotene in hemp oil body systems. When solvents were used, β-carotene did not partition into the oil body significantly resulting in poor encapsulation efficiency. This was attributed to the higher affinity of β-carotene in the solvents compared to hemp oil. Interactions between the solvents and the membrane components of oil bodies must be elucidated to determine the mechanisms of their partitioning and how it can be further improved. It may also be worthwhile to explore using a combination of solvents or application of treatments such as heat to aid in the partitioning of bioactive substances into intact oil

bodies. Moreover, the use of other bioactive substances with a higher affinity towards oil than the solvent may be investigated.

Heating and sonication were able to directly incorporate crystalline β-carotene into hemp oil bodies without disrupting their structure. This was attributed to the enhanced molecular movement and possible release of extrinsic proteins from the interface brought about by heating and the ability of ultrasound to improve the diffusion of solutes due to the cavitation phenomena. This method is promising because the dissolution of β-carotene in another medium was not necessary, and the treatment was short and not intensive.

Through homogenisation, the oil body membrane broke down into fragments, not separately as oleosins and phospholipids, and adsorbed at the interface, stabilising the newly formed droplets. This indicates that crude oil body fractions may be utilised to provide emulsifying material in an emulsion. Further purification may not be necessary as the additional non-oil body proteins may aid in emulsification and adsorb on the droplet interface. However, bridging flocculation was observed as the concentration of the membrane materials in the oil bodies was not sufficient to cover the increased surface area of the lipid phase after homogenisation. Thus, the amount of oil bodies in the system must be optimised to ensure that the droplets are sufficiently covered with the membrane fragments of oil bodies to avoid flocculation.

The last approach involved the extraction of oil body membrane materials (OBMM) which was achieved through the application of heat and shear. Heat treatment at 70°C resulted in the (1) destabilisation of oil bodies and (2) detachment of extrinsic proteins, which precipitated in solution, from the oil body surface. As such, the heat-extracted OBMM could be a mixture of intact oil bodies, destabilised oil bodies, oil body interfacial components (oleosins and phospholipids), and partially denatured extrinsic proteins. Using this material, a β-carotene-loaded hemp oil emulsion was stabilised through the embedment of oleosins, phospholipids, and possibly some extrinsic proteins on the dispersed phase. No sedimentation was observed in the emulsion formed, suggesting that the complexes formed between the unfolded protein aggregates and oleosins that stabilise the interface may be stable in the time scales used in this study. Although heating was able to extract membrane materials, optimisation of the extraction procedure must be conducted to improve the yield (as a substantial amount of oil bodies remained intact in the process) without losing the surface activity of these membrane components.

In terms of encapsulation efficiency, a higher amount of β-carotene was encapsulated in the OBMM-stabilised emulsion since β-carotene was directly incorporated into hemp oil before emulsification with OBMM. In the case of non-homogenised and homogenised oil bodies, β-carotene was incorporated in the crude oil body fraction; as such, the interfacial components and possibly other bound proteins may have hindered the incorporation of β-carotene in the TAG core. A longer heating and sonication process may be explored to improve this, although it must be optimised such that the destabilisation of the oil bodies does not occur. Lower encapsulation efficiency was observed for homogenised compared to non-homogenised ones, and further study is needed on the effect of the homogenisation process on β-carotene degradation.

The colloidal stability of oil body systems was affected by the storage temperature but not by the presence of light. At refrigeration and ambient temperatures, they exhibited physical stability; however, storage at elevated temperatures resulted in their poor colloidal stability which could be attributed to flocculation. Among the oil body systems, the OBMM-stabilised emulsion exhibited the highest physical stability during storage that was comparable to the WPI-stabilised emulsion. This could be attributed to its smaller size compared to the homogenised and non-homogenised oil bodies. Its performance can be further improved by having the membrane material in powdered form for ease in incorporation in emulsions.

Similarly, the stability of β-carotene during storage was affected by temperature but not by the presence of light as exhibited by the high increase in colour loss and decrease in β-carotene concentration over time. This was attributed to the isomerisation and oxidation of β-carotene at elevated temperatures. In agreement with the size of the oil body systems, the OBMM-stabilised emulsion showed the highest degradation of β-carotene as the droplet size was lower compared to the other oil body systems. On the other hand, the non-homogenised and homogenised oil bodies exhibited comparable chemical stability to the WPI-stabilised emulsion. This could be due to the protective effects of the membrane components of oil bodies that prevented the contact of β-carotene with prooxidants in the environment. Thus, it is important to achieve a balance between colloidal and chemical stability of the delivery systems during storage to be able to fully utilise their functionality.

Since the presence of light did not have a significant effect on the colloidal nor chemical stability of the systems, a different approach utilising different types of light sources (e.g., UV light) at different intensities may be considered to fully understand the photodegradation of β-carotene in oil body systems. Moreover, it is worthwhile to determine the presence of antioxidants inside the oil bodies to better explain the protective mechanism of encapsulation of β-carotene in oil body systems.

Overall, the utilisation of oil bodies in the food industry is promising because of their unique structure and stability. Their membrane materials have also exhibited high surface activity, which shows their potential as food-grade emulsifiers. With the increasing attention in the food industry on the use of green and sustainable materials and processes, oil bodies can be used in different novel applications especially in emulsion-based systems.

7.2 Limitations of current work

This study was limited to an initial characterisation of oil bodies and exploration of methods that could potentially encapsulate β-carotene into hemp oil body-based emulsified systems for future applications into food matrices. Due to time constraints, some limitations in this study were as follows:

1. The optimisation of the extraction of mustard oil bodies and their characterisation was not conducted due to the unavailability of time (Covid-19 lockdown). Because of their small size, challenges were encountered to isolate mustard oil bodies from extraneous proteins, and only changing the pH of the grinding medium was tested to improve their extractability. Further experiments are needed for the oil bodies to be isolated with minimal amounts of extraneous proteins.

   The analysis of the protein profile of the mustard oil body fraction may be done to get a better understanding of the types of proteins that entrap the oil bodies after aqueous extraction. Methods to improve their isolation could be the use of a higher solid-to-solvent ratio for their extraction, extraction at higher pH values, or a prior dehulling of the seeds before soaking to improve extractability. Once a more purified extract has been obtained, a more thorough investigation of their physicochemical properties and behaviour at different environmental conditions can be conducted to examine their functionality for potential applications.

2. The oil body membrane materials were not characterised. Knowing more information on the membrane components of oil bodies and extracted membrane materials can provide a better understanding of their ability to stabilise the lipid droplets and incorporate the bioactive compound. Once their membrane has been characterised, the stability of emulsions can be improved and their potential application in food systems can be enhanced.

3. The use of other solvents or techniques to improve the passive partitioning of β-carotene into intact oil bodies was not explored. Further exploration of the use of passive partitioning of β-carotene into intact oil bodies is recommended to utilise the natural structure and stability of native oil bodies. This can be achieved by using other solvents to dissolve β-carotene, using a combination of solvents, or combining the use of solvents with other treatments such as heat to enhance the partitioning of β-carotene to the TAG core of oil bodies.

4. Differences in the interfacial structure and composition of emulsions were not characterised. The differences in the structure and composition of interfacial biomaterial may provide insights into their colloidal stability.

5. The effect of lights of different wavelengths was not conducted due to the short duration of the project. In this study, storage of the oil body systems in the presence of light did not show a significant effect on the degradation of encapsulated β-carotene. The use of other types of light sources with different wavelengths and a set-up that can ensure the uniform exposure of the samples to the light can be tested. This can give insights into the types of packaging materials that will be suitable once the emulsified systems are used commercially.

7.3 Avenues for future work

Based on the limitations and findings of this research, avenues for future work are listed as follows:

1. **Detailed characterisation of hemp and mustard oil body interfacial components and the membrane material extracted therefrom**

   In this study, the interfacial components and extracted membrane materials from oil bodies were only qualitatively characterised using CLSM. Using a quantitative approach for the analysis and profiling of these interfacial materials (e.g.,

quantification and profiling of phospholipid and protein composition) in the oil body fraction and after extraction from destabilised oil bodies can provide more information on their surface activity and mechanism for stabilising oil body systems.

2. **Comparison of the structural properties of native oil bodies and oil body systems**

   Following the recommendation above, a comparison of the structural properties of native oil bodies and oil body systems could give further insights if the methodologies used to incorporate β-carotene, such as the use of solvents, heat treatment, and sonication, cause alterations on the interface of the oil bodies. Moreover, further study on the interfacial components of homogenised oil bodies could provide a better understanding of how membrane fragments reassociate and stabilise the interface of new droplets, and if the membrane components rearrange in a manner similar to that of native oil bodies. Likewise, this could elucidate if membrane materials obtained after the heat-destabilisation of oil bodies behave similarly with the membrane fragments of homogenised oil bodies.

3. **Determination of the antioxidant content and composition of oil bodies**

   In the application of oil bodies as encapsulation systems of bioactive compounds, especially those susceptible to oxidation like β-carotene, gaining information on the types and composition of antioxidants contained in the oil inside the oil bodies can be vital in understanding if certain types of oil bodies would be more suitable for this application. Oil bodies that contain high amounts of antioxidants may reduce the degradation of the bioactive substance and aid in the retention of their bioactivity.

4. **Analysis of the oxidative stability of the oil bodies with and without the encapsulated bioactive compound**

   After determining the antioxidant content of the oil in hemp oil bodies, the oxidative stability of the oil bodies and the oil body systems may be determined to gain a better understanding if they confer a protective effect on β-carotene against degradation during storage.

5. **Analysis of the kinetics of migration of hydrophobic compounds into the oil bodies**

   A deeper understanding of the kinetics of mass transfer from the aqueous phase to the oil phase inside the intact oil bodies can give insights on how to further improve the incorporation of hydrophobic compounds into oil bodies, as well as factors affecting their partitioning to the TAG core.

6. **Spray- or freeze-drying of the β-carotene-loaded oil body systems**

   Spray- or freeze-drying may improve the storage stability of β-carotene-loaded oil body systems because of the low moisture content. Hence, the properties of liquid emulsions and oil body systems in powder form may be examined to see if drying would affect the stability of β-carotene during storage.

7. **Determination of the bioavailability of β-carotene-loaded oil body systems**

   The conduct of *in vitro* digestion studies can give information on the physical stability of the emulsions and the chemical stability of β-carotene as it passes through the gastrointestinal tract, and whether encapsulation in the delivery systems can improve the bioavailability of β-carotene.

8. **Improvement of the colloidal stability of β-carotene-loaded oil body systems**

   The addition of biopolymers in the continuous phase has been shown to improve the physical stability of emulsions. Thus, it may be worthwhile to investigate their interaction with oil bodies and whether they can enhance the physical stability of the oil body systems.

9. **Improvement of the heat stability of β-carotene-loaded oil body systems**

   Although the oil body systems exhibited stability at refrigeration and ambient temperatures, more work is needed to improve their colloidal and chemical stability at high temperatures. This is because food products are often subjected to high temperatures during processing, transport, and storage, and improving their stability can enhance their future utilisation in the food industry.

10. **Investigation of other methods to extract the membrane materials of oil bodies**

    Heating was able to extract membrane materials from hemp oil bodies; however, it involved the use of a large amount of oil body fraction and resulted in minimal quantities of the membrane material. Hence, other techniques to isolate membrane

materials from oil bodies may be investigated to obtain a higher percentage of membrane materials with minimal processing.

11. **Encapsulation of other types of bioactive compounds**

    The encapsulation of other types of hydrophobic bioactive compounds with different structures and solubilities in hemp oil may be examined to determine if the differences in the structures of the bioactive compound can affect their encapsulation into oil bodies using the methodologies investigated in this study.

12. **Applications of β-carotene-loaded oil body systems for different uses**

    Oil body systems that contain β-carotene may be applied for commercial application in oil-in-water emulsion type foods or beverages to improve their nutritional quality. Encapsulation in oil bodies may enhance the stability of β-carotene in these products, examples of which include plant-based beverages, plant-based dairy analogues like yoghurt, beverages with probiotic properties, mayonnaise, and salad dressings. Another application of oil bodies is their incorporation into edible films and coatings to improve their flexibility and surface hydrophobicity or as carriers of functional compounds to the food surface. Moreover, oil bodies or their isolated membrane materials can be used as substitutes for synthetic emulsifiers in stabilising oil emulsions. The use of intact oil bodies as Pickering stabilisers may be examined and their membrane materials may be used to create artificial oil body emulsions with comparable or improved stability to native ones.

References

Abdullah, Weiss, J., & Zhang, H. (2020). Recent advances in the composition, extraction and food applications of plant-derived oleosomes. *Trends in Food Science & Technology, 106*, 322-332. https://doi.org/10.1016/j.tifs.2020.10.029

Acevedo-Fani, A., Dave, A., & Singh, H. (2020). Nature-assembled structures for delivery of bioactive compounds and their potential in functional foods. *Frontiers in Chemistry, 8*, 22, Article 564021. https://doi.org/10.3389/fchem.2020.564021

Acevedo, F., Rubilar, M., Jofre, I., Villarroel, M., Navarrete, P., Esparza, M., Romero, F., Vilches, E. A., Acevedo, V., & Shene, C. (2014). Oil bodies as a potential microencapsulation carrier for astaxanthin stabilisation and safe delivery. *Journal of Microencapsulation, 31*(5), 488-500. https://doi.org/10.3109/02652048.2013.879931

Alshehab, M., & Nitin, N. (2019). Encapsulation and release of curcumin using an intact milk fat globule delivery system. *Food & Function, 10*(11), 7121-7130. https://doi.org/10.1039/C9FO00489K

Alshehab, M., Reis, M. G., Day, L., & Nitin, N. (2019). Milk fat globules, a novel carrier for delivery of exogenous cholecalciferol. *Food Research International, 126*. https://doi.org/10.1016/j.foodres.2019.108579

Amorim-Carrilho, K. T., Cepeda, A., Fente, C., & Regal, P. (2014). Review of methods for analysis of carotenoids. *Trends in Analytical Chemistry, 56*, 49-73. https://doi.org/10.1016/j.trac.2013.12.011

Beisson, F., Ferté, N., Voultoury, R., & Arondel, V. (2001). Large scale purification of an almond oleosin using an organic solvent procedure. *Plant Physiology and Biochemistry, 39*(7), 623-630. https://doi.org/10.1016/S0981-9428(01)01275-X

Bettini, S., Vergara, D., Bonsegna, S., Giotta, L., Toto, C., Chieppa, M., Maffia, M., Giovinazzo, G., Valli, L., & Santino, A. (2013). Efficient stabilization of natural curcuminoids mediated by oil body encapsulation. *RSC Advances, 3*(16), 5422-5429. https://doi.org/10.1039/c3ra40552d

Bligh, E. G., & Dyer, W. J. (1959). A rapid method of total lipid extraction and purification. *Canadian Journal of Biochemistry and Physiology, 37*(8), 911-917.

Bonsegna, S., Bettini, S., Pagano, R., Zacheo, A., Vergaro, V., Giovinazzo, G., Caminati, G., Leporatti, S., Valli, L., & Santino, A. (2011). Plant oil bodies: Novel carriers to deliver lipophilic molecules. *Applied Biochemistry and Biotechnology, 163*(6), 792-802. https://doi.org/10.1007/s12010-010-9083-0

Boon, C. S., McClements, D. J., Weiss, J., & Decker, E. A. (2010). Factors influencing the chemical stability of carotenoids in foods. *Critical Reviews in Food Science and Nutrition, 50*(6), 515-532. https://doi.org/10.1080/10408390802565889

Borba, C. M., Tavares, M. N., Macedo, L. P., Araújo, G. S., Furlong, E. B., Dora, C. L., & Burkert, J. F. M. (2019). Physical and chemical stability of β-carotene nanoemulsions during storage and thermal process. *Food Research International, 121*, 229-237. https://doi.org/10.1016/j.foodres.2019.03.045

Boucher, J., Cengelli, F., Trumbic, D., & Marison, I. W. (2008). Sorption of hydrophobic organic compounds (HOC) in rapeseed oil bodies. *Chemosphere, 70*(8), 1452-1458. https://doi.org/10.1016/j.chemosphere.2007.08.065

Callaway, J. C. (2004). Hempseed as a nutritional resource: An overview. *Euphytica, 140*(1), 65-72. https://doi.org/10.1007/s10681-004-4811-6

Calligaris, S., Manzocco, L., Valoppi, F., Comuzzo, P., & Nicoli, M. C. (2019). Microemulsions as delivery systems of lemon oil and β-carotene into beverages: stability test under different light conditions. *Journal of the Science of Food and Agriculture, 99*(15), 7016-7020.

Capuano, E., Pellegrini, N., Ntone, E., & Nikiforidis, C. V. (2018). In vitro lipid digestion in raw and roasted hazelnut particles and oil bodies. *Food & Function, 9*(4), 2508-2516. https://doi.org/10.1039/C8FO00389K

Carvalho, L. M. J., Ortiz, D.-G., Ribeiro, E. M. G., Smiderle, L., Pereira, E. J., & Carvalho, J. L. V. (2013). Beta-carotene: Functions, health benefits, adverse effects and applications. In M. Lefevre (Ed.), *Beta-carotene: Functions, Health Benefits and Adverse Effects* (pp. 59-80). Nova Science Publishers, Inc.

Chang, M. T., Tsai, T. R., Lee, C. Y., Wei, Y. S., Chen, Y. J., Chen, C. R., & Tzen, J. T. C. (2013). Elevating bioavailability of curcumin via encapsulation with a novel formulation of artificial oil bodies. *Journal of Agricultural Food Chemistry, 61*(40), 9666-9671. https://doi.org/10.1021/jf4019195

Chemat, F., Zill e, H., & Khan, M. K. (2011). Applications of ultrasound in food technology: Processing, preservation and extraction. *Ultrasonics Sonochemistry, 18*(4), 813-835. https://doi.org/10.1016/j.ultsonch.2010.11.023

Chen, B., McClements, D. J., Gray, D. A., & Decker, E. A. (2012). Physical and oxidative stability of pre-emulsified oil bodies extracted from soybeans. *Food Chemistry, 132*(3), 1514-1520. https://doi.org/10.1016/j.foodchem.2011.11.144

Chen, H., & Zhong, Q. (2015). Thermal and UV stability of β-carotene dissolved in peppermint oil microemulsified by sunflower lecithin and Tween 20 blend. *Food Chemistry, 174*, 630-636. https://doi.org/10.1016/j.foodchem.2014.11.116

Chen, J., Li, F., Li, Z., McClements, D. J., & Xiao, H. (2017). Encapsulation of carotenoids in emulsion-based delivery systems: Enhancement of β-carotene water-dispersibility and chemical stability. *Food Hydrocolloids, 69*, 49-55. https://doi.org/10.1016/j.foodhyd.2017.01.024

Chen, M. C. M., Chyan, C. L., Lee, T. T. T., Huang, S. H., & Tzen, J. T. C. (2004). Constitution of stable artificial oil bodies with triacylglycerol, phospholipid, and caleosin. *Journal of Agricultural and Food Chemistry, 52*(12), 3982-3987. https://doi.org/10.1021/jf035533g

Chen, M. C. M., Wang, J. L., & Tzen, J. T. C. (2005). Elevating bioavailability of cyclosporine A via encapsulation in artificial oil bodies stabilized by caleosin. *Biotechnology Progress, 21*(4), 1297-1301. https://doi.org/10.1021/bp050030b

Chen, Y., & Ono, T. (2010). Simple extraction method of non-allergenic intact soybean oil bodies that are thermally stable in an aqueous medium. *Journal of Agricultural and Food Chemistry, 58*(12), 7402-7407. https://doi.org/10.1021/jf1006159

Chen, Y. M., Zhao, L. P., Kong, X. Z., Zhang, C. M., & Hua, Y. F. (2014). The properties and the related protein behaviors of oil bodies in soymilk preparation. *European Food Research and Technology, 239*(3), 463-471. https://doi.org/10.1007/s00217-014-2239-3

Chiang, C.-J., Lin, C.-C., Lu, T.-L., & Wang, H.-F. (2011). Functionalized nanoscale oil bodies for targeted delivery of a hydrophobic drug. *Nanotechnology, 22*(41), 415102.

Cobb, C. E., Juliao, S. F., Balasubramanian, K., Staros, J. V., & Beth, A. H. (1990). Effects of diethyl ether on membrane lipid ordering and on rotational dynamics

of the anion exchange protein in intact human erythrocytes: Correlations with anion exchange function. *Biochemistry, 29*(48), 10799-10806.

Cornacchia, L., & Roos, Y. H. (2011). Stability of β-carotene in protein-stabilized oil-in-water delivery systems. *Journal of Agricultural and Food Chemistry, 59*(13), 7013-7020. https://doi.org/10.1021/jf200841k

Craft, N. E., & Soares, J. H. (1992). Relative solubility, stability, and absorptivity of lutein and beta-carotene in organic solvents. *Journal of Agricultural and Food Chemistry, 40*(3), 431-434. https://doi.org/10.1021/jf00015a013

Cui, X.-H., Chen, S.-J., Wang, Y., & Han, J.-R. (2013). Fermentation conditions of walnut milk beverage inoculated with kefir grains. *LWT - Food Science and Technology, 50*(1), 349-352. https://doi.org/10.1016/j.lwt.2012.07.043

Da Porto, C., Natolino, A., & Decorti, D. (2015). Effect of ultrasound pre-treatment of hemp (*Cannabis sativa* L.) seed on supercritical CO_2 extraction of oil. *Journal of Food Science and Technology, 52*(3), 1748-1753. https://doi.org/10.1007/s13197-013-1143-3

Dave, A. C., Ye, A. Q., & Singh, H. (2019). Structural and interfacial characteristics of oil bodies in coconuts (*Cocos nucifera* L.). *Food Chemistry, 276*, 129-139. https://doi.org/10.1016/j.foodchem.2018.09.125

De Chirico, S., di Bari, V., Foster, T., & Gray, D. (2018). Enhancing the recovery of oilseed rape seed oil bodies (oleosomes) using bicarbonate-based soaking and grinding media. *Food Chemistry, 241*, 419-426. https://doi.org/10.1016/j.foodchem.2017.09.008

De Chirico, S., di Bari, V., Romero Guzmán, M. J., Nikiforidis, C. V., Foster, T., & Gray, D. (2020). Assessment of rapeseed oil body (oleosome) lipolytic activity as an effective predictor of emulsion purity and stability. *Food Chemistry, 316*, 126355. https://doi.org/10.1016/j.foodchem.2020.126355

De Young, L. R., & Dill, K. A. (1988). Solute partitioning into lipid bilayer-membranes. *Biochemistry, 27*(14), 5281-5289. https://doi.org/10.1021/bi00414a050

Deleu, M., Vaca-Medina, G., Fabre, J.-F., Roïz, J., Valentin, R., & Mouloungui, Z. (2010). Interfacial properties of oleosins and phospholipids from rapeseed for the stability of oil bodies in aqueous medium. *Colloids and Surfaces B: Biointerfaces, 80*(2), 125-132. https://doi.org/10.1016/j.colsurfb.2010.05.036

Demetriades, K., Coupland, J. N., & McClements, D. J. (1997). Physical properties of whey protein stabilized emulsions as related to pH and NaCl. *Journal of Food Science, 62*(2), 342-347. https://doi.org/10.1111/j.1365-2621.1997.tb03997.x

Dimitrov, S. D., Dimitrova, N. C., Walker, J. D., Veith, G. D., & Mekenyan, O. G. (2002). Predicting bioconcentration factors of highly hydrophobic chemicals: Effects of molecular size. *Pure and Applied Chemistry, 74*(10), 1823-1830. https://doi.org/10.1351/pac200274101823

Ding, J., Xu, Z. J., Qi, B. K., Liu, Z. Z., Yu, L. L., Yan, Z., Jiang, L. Z., & Sui, X. N. (2020). Thermally treated soya bean oleosomes: the changes in their stability and associated proteins. *International Journal of Food Science and Technology, 55*(1), 229-238. https://doi.org/10.1111/ijfs.14266

Edwards, D., Salisbury, P. A., Burton, W. A., Hopkins, C. J., & Batley, J. (2007). Indian mustard. In C. Kole (Ed.), *Oilseeds* (pp. 179-210). Springer Berlin Heidelberg. https://doi.org/10.1007/978-3-540-34388-2_5

Efthymiou, C., Williams, M. A. K., & McGrath, K. M. (2017). Revealing the structure of high-water content biopolymer networks: Diminishing freezing artefacts in cryo-SEM images. *Food Hydrocolloids, 73*, 203-212. https://doi.org/10.1016/j.foodhyd.2017.06.040

Eskin, M. N., Aladedunye, F., Unger, E. H., Shah, S., Chen, G., & Jones, P. J. (2020). Canola oil. In F. Shahidi (Ed.), *Bailey's Industrial Oil and Fat Products* (pp. 1-63). https://doi.org/10.1002/047167849X.bio004.pub2

Everett, D. W. (2007). Cream Products. In Y. H. Hui (Ed.), *Handbook of Food Products Manufacturing* (pp. 725-749). John Wiley & Sons, Inc. https://doi.org/10.1002/9780470113554.ch32

Fikselova, M., Silhar, S., Marecek, J., & Francakova, H. (2008). Extraction of carrot (*Daucus carota* L.) carotenes under different conditions. *Czech Journal of Food Sciences, 26*(4), 268-274. https://doi.org/10.17221/9/2008-cjfs

Fisk, I. D., White, D. A., Carvalho, A., & Gray, D. A. (2006). Tocopherol - An intrinsic component of sunflower seed oil bodies. *Journal of the American Oil Chemists Society, 83*(4), 341-344. https://doi.org/10.1007/s11746-006-1210-2

Fisk, I. D., White, D. A., Lad, M., & Gray, D. A. (2008). Oxidative stability of sunflower oil bodies. *European Journal of Lipid Science and Technology, 110*(10), 962-968. https://doi.org/10.1002/ejlt.200800051

Frandsen, G. I., Mundy, J., & Tzen, J. T. C. (2001). Oil bodies and their associated proteins, oleosin and caleosin. *Physiologia Plantarum, 112*(3), 301-307. https://doi.org/10.1034/j.1399-3054.2001.1120301.x

Fu, L., He, Z., Zeng, M., Qin, F., & Chen, J. (2020). Effects of preheat treatments on the composition, rheological properties, and physical stability of soybean oil bodies. *Journal of Food Science, 85*(10), 3150-3159. https://doi.org/10.1111/1750-3841.15411

Fukushima, D. (1969). Denaturation of soybean proteins by organic solvents. *Cereal Chemistry, 46*(2), 156-163.

Gallier, S., Gordon, K. C., & Singh, H. (2012). Chemical and structural characterisation of almond oil bodies and bovine milk fat globules. *Food Chemistry, 132*(4), 1996-2006. https://doi.org/10.1016/j.foodchem.2011.12.038

Gray, D. A., Payne, G., McClements, D. J., Decker, E. A., & Lad, M. (2010). Oxidative stability of *Echium plantagineum* seed oil bodies. *European Journal of Lipid Science and Technology, 112*(7), 741-749. https://doi.org/10.1002/ejlt.200900280

Guan, Y., Wu, J., & Zhong, Q. (2016). Eugenol improves physical and chemical stabilities of nanoemulsions loaded with β-carotene. *Food Chemistry, 194*, 787-796. https://doi.org/10.1016/j.foodchem.2015.08.097

Gul, K., Tak, A., Singh, A. K., Singh, P., Yousuf, B., & Wani, A. A. (2015). Chemistry, encapsulation, and health benefits of β-carotene - A review. *Cogent Food & Agriculture, 1*(1), 1018696. https://doi.org/10.1080/23311932.2015.1018696

He, S., & Ye, A. (2019). Formation and gastrointestinal digestion of β-carotene emulsion stabilized by milk fat globule membrane. *Journal of Food Process Engineering, 42*(8), e13301. https://doi.org/10.1111/jfpe.13301

He, S., Zhou, S., Guo, W., Wang, Y., Liu, C., Wang, R., & Xiao, F. (2020). Investigation of curcumin emulsion stability and gastrointestinal digestion prepared with rapeseed oil body. *Journal of Food Process Engineering, 43*(12), e13556. https://doi.org/10.1111/jfpe.13556

Hou, Z., Liu, Y., Lei, F., & Gao, Y. (2014). Investigation into the in vitro release properties of β-carotene in emulsions stabilized by different emulsifiers. *LWT - Food Science and Technology, 59*(2, Part 1), 867-873. https://doi.org/10.1016/j.lwt.2014.07.045

Hu, M., McClements, D. J., & Decker, E. A. (2003). Lipid oxidation in corn oil-in-water emulsions stabilized by casein, whey protein isolate, and soy protein isolate. *Journal of Agricultural and Food Chemistry, 51*(6), 1696-1700. https://doi.org/10.1021/jf020952j

Huang, A. H. C. (1992). Oil bodies and oleosins in seeds. *Annual Review of Plant Physiology and Plant Molecular Biology, 43*(1), 177-200. https://doi.org/10.1146/annurev.pp.43.060192.001141

Huang, A. H. C. (1994). Structure of plant seed oil bodies. *Current Opinion in Structural Biology, 4*(4), 493-498. https://doi.org/10.1016/S0959-440X(94)90210-0

Huang, A. H. C. (1996). Oleosins and oil bodies in seeds and other organs. *Plant Physiology, 110*(4), 1055-1061. https://doi.org/10.1104/pp.110.4.1055

Ingram, L. O. (1989). Ethanol tolerance in bacteria. *Critical Reviews in Biotechnology, 9*(4), 305-319.

Ishii, T., Matsumiya, K., Nambu, Y., Samoto, M., Yanagisawa, M., & Matsumura, Y. (2017). Interfacial and emulsifying properties of crude and purified soybean oil bodies. *Food Structure, 12*, 64-72. https://doi.org/10.1016/j.foostr.2016.12.005

Iwanaga, D., Gray, D. A., Fisk, I. D., Decker, E. A., Weiss, J., & McClements, D. J. (2007). Extraction and characterization of oil bodies from soy beans: A natural source of pre-emulsified soybean oil. *Journal of Agricultural and Food Chemistry*, *55*(21), 8711-8716. https://doi.org/10.1021/jf071008w

Jo, Y.-J., & Kwon, Y.-J. (2014). Characterization of β-carotene nanoemulsions prepared by microfluidization technique. *Food Science and Biotechnology, 23*(1), 107-113.

Jung, S., de Moura, J. M. L. N., Campbell, K. A., & Johnson, L. A. (2012). Enzyme-assisted aqueous extraction of oilseeds. In N. Lebovka, E. Vorobiev, & F. Chemat (Eds.), *Enhancing Extraction Processes in the Food Industry* (pp. 477-518). CRC Press.

Karefyllakis, D., Octaviana, H., van der Goot, A. J., & Nikiforidis, C. V. (2019). The emulsifying performance of mildly derived mixtures from sunflower seeds. *Food Hydrocolloids, 88*, 75-85. https://doi.org/10.1016/j.foodhyd.2018.09.037

Karefyllakis, D., van der Goot, A. J., & Nikiforidis, C. V. (2019a). The behaviour of sunflower oleosomes at the interfaces. *Soft Matter, 15*(23), 4639-4646. https://doi.org/10.1039/c9sm00352e

Karefyllakis, D., van der Goot, A. J., & Nikiforidis, C. V. (2019b). Multicomponent emulsifiers from sunflower seeds. *Current Opinion in Food Science, 29*, 35-41. https://doi.org/10.1016/j.cofs.2019.07.005

Kawa, R., Ansmann, A., Prinz, D., & Both, S. (2009). *Oil bodies for cosmetic compositions containing cyclohexyl cyclohexane* (United States Patent No. US 7,572.435 B2). United States Patent.

Keogh, M. K., & O'Kennedy, B. T. (1999). Milk fat microencapsulation using whey proteins. *International Dairy Journal, 9*(9), 657-663. https://doi.org/10.1016/S0958-6946(99)00137-5

Kim, H.-J., Decker, E., & McClements, D. (2002). Role of postadsorption conformation changes of β-lactoglobulin on its ability to stabilize oil droplets against flocculation during heating at neutral pH. *Langmuir, 18*(20), 7577-7583.

Komatsu, H., & Okada, S. (1997). Effects of ethanol on permeability of phosphatidylcholine/cholesterol mixed liposomal membranes. *Chemistry and Physics of Lipids, 85*(1), 67-74.

Lan, X., Qiang, W., Yang, Y., Gao, T., Guo, J., Du, L., Noman, M., Li, Y., Li, J., Li, H., Li, X., & Yang, J. (2020). Physicochemical stability of safflower oil body emulsions during food processing. *LWT, 132*, 109838. https://doi.org/10.1016/j.lwt.2020.109838

Limbo, S., Torri, L., & Piergiovanni, L. (2007). Light-induced changes in an aqueous β-carotene system stored under halogen and fluorescent lamps, affected by two oxygen partial pressures. *Journal of Agricultural and Food Chemistry, 55*(13), 5238-5245.

Lin, Q., Liang, R., Zhong, F., Ye, A., & Singh, H. (2018). Physical properties and biological fate of OSA-modified-starch-stabilized emulsions containing β-carotene: Effect of calcium and pH. *Food Hydrocolloids, 77*, 549-556. https://doi.org/10.1016/j.foodhyd.2017.10.033

Liu, C. H., Wang, R. C., He, S. H., Cheng, C. L., & Ma, Y. (2020). The stability and gastro-intestinal digestion of curcumin emulsion stabilized with soybean oil

bodies. *LWT - Food Science and Technology, 131*, 7. https://doi.org/10.1016/j.lwt.2020.109663

Loman, A. A., Callow, N. V., Islam, S. M. M., & Ju, L.-K. (2018). Single-step enzyme processing of soybeans into intact oil bodies, protein bodies and hydrolyzed carbohydrates. *Process Biochemistry, 68*, 153-164. https://doi.org/10.1016/j.procbio.2018.02.015

Luo, X., Zhou, Y., Bai, L., Liu, F., Deng, Y., & McClements, D. J. (2017). Fabrication of β-carotene nanoemulsion-based delivery systems using dual-channel microfluidization: Physical and chemical stability. *Journal of Colloid and Interface Science, 490*, 328-335. https://doi.org/10.1016/j.jcis.2016.11.057

Ma, P., Zeng, Q., Tai, K., He, X., Yao, Y., Hong, X., & Yuan, F. (2017). Preparation of curcumin-loaded emulsion using high pressure homogenization: Impact of oil phase and concentration on physicochemical stability. *LWT - Food Science and Technology, 84*, 34-46. https://doi.org/10.1016/j.lwt.2017.04.074

MacCallum, J. L., & Tieleman, D. P. (2006). Computer simulation of the distribution of hexane in a lipid bilayer: Spatially resolved free energy, entropy, and enthalpy profiles. *Journal of the American Chemical Society, 128*(1), 125-130. https://doi.org/10.1021/ja0535099

Mantzouridou, F. T., Naziri, E., Kyriakidou, A., Paraskevopoulou, A., Tsimidou, M. Z., & Kiosseoglou, V. (2019). Oil bodies from dry maize germ as an effective replacer of cow milk fat globules in yogurt-like product formulation. *LWT, 105*, 48-56. https://doi.org/10.1016/j.lwt.2019.01.068

Mao, L., Wang, D., Liu, F., & Gao, Y. (2018). Emulsion design for the delivery of β-carotene in complex food systems. *Critical Reviews in Food Science and Nutrition, 58*(5), 770-784. https://doi.org/10.1080/10408398.2016.1223599

Mao, L., Yang, J., Xu, D., Yuan, F., & Gao, Y. (2010). Effects of homogenization models and emulsifiers on the physicochemical properties of β-carotene nanoemulsions. *Journal of Dispersion Science and Technology, 31*(7), 986-993. https://doi.org/10.1080/01932690903224482

Matsakidou, A., Biliaderis, C. G., & Kiosseoglou, V. (2013). Preparation and characterization of composite sodium caseinate edible films incorporating naturally emulsified oil bodies. *Food Hydrocolloids, 30*(1), 232-240. https://doi.org/10.1016/j.foodhyd.2012.05.025

Matsakidou, A., Tsimidou, M. Z., & Kiosseoglou, V. (2019). Storage behavior of caseinate-based films incorporating maize germ oil bodies. *Food Research International, 116,* 1031-1040. https://doi.org/10.1016/j.foodres.2018.09.042

Matthaus, B., & Bruhl, L. (2008). Virgin hemp seed oil: An interesting niche product. *European Journal of Lipid Science and Technology, 110*(7), 655-661. https://doi.org/10.1002/ejlt.200700311

Maurer, S., Waschatko, G., Schach, D., Zielbauer, B. I., Dahl, J., Weidner, T., Bonn, M., & Vilgis, T. A. (2013). The role of intact oleosin for stabilization and function of oleosomes. *The Journal of Physical Chemistry B, 117*(44), 13872-13883. https://doi.org/10.1021/jp403893n

McClements, D. J. (2002). Theoretical prediction of emulsion color. *Advances in Colloid and Interface Science, 97*(1), 63-89. https://doi.org/10.1016/S0001-8686(01)00047-1

McClements, D. J. (2007). Critical review of techniques and methodologies for characterization of emulsion stability. *Critical Reviews in Food Science and Nutrition, 47*(7), 611-649. https://doi.org/10.1080/10408390701289292

McClements, D. J. (2010). Emulsion design to improve the delivery of functional lipophilic components. *1*(1), 241-269. https://doi.org/10.1146/annurev.food.080708.100722

McClements, D. J. (2012). Crystals and crystallization in oil-in-water emulsions: Implications for emulsion-based delivery systems. *Advances in Colloid and Interface Science, 174*, 1-30. https://doi.org/10.1016/j.cis.2012.03.002

McClements, D. J. (2016). *Food emulsions: Principles, practices, and techniques* (3rd ed.). CRC Press, Taylor & Francis Group.

McClements, D. J., & Decker, E. A. (2000). Lipid oxidation in oil-in-water emulsions: Impact of molecular environment on chemical reactions in heterogeneous food systems. *Journal of Food Science, 65*(8), 1270-1282. https://doi.org/10.1111/j.1365-2621.2000.tb10596.x

McClements, D. J., Decker, E. A., & Weiss, J. (2007). Emulsion-based delivery systems for lipophilic bioactive components. *Journal of Food Science, 72*(8), R109-R124. https://doi.org/10.1111/j.1750-3841.2007.00507.x

Mikulcová, V., Kašpárková, V., Humpolíček, P., & Buňková, L. (2017). Formulation, characterization and properties of hemp seed oil and its emulsions. *Molecules (Basel, Switzerland)*, *22*(5), 700. https://doi.org/10.3390/molecules22050700

Miller, D. L., Pislaru, S. V., & Greenleaf, J. F. (2002). Sonoporation: Mechanical DNA delivery by ultrasonic cavitation. *Somatic Cell and Molecular Genetics*, *27*(1), 115-134.

Ministry for Primary Industries. (2020). A guide to hemp seeds as food. https://www.mpi.govt.nz/dmsdocument/31623-A-Guide-to-Hemp-Seeds-as-Food

Mishra, S., & Mishra, H. N. (2013). Effect of synbiotic interaction of fructooligosaccharide and probiotics on the acidification profile, textural and rheological characteristics of fermented soy milk. *Food and Bioprocess Technology*, *6*(11), 3166-3176. https://doi.org/10.1007/s11947-012-1021-4

Murray, E. W., Boothe, J., & Markley, N.-A. (2007). *Methods for preparing oil bodies comprising active ingredients* (United States Patent Application Publication No. US 2007/0196914 A1).

Murthy, A. V. R., Guyomarc'h, F., & Lopez, C. (2016). The temperature-dependent physical state of polar lipids and their miscibility impact the topography and mechanical properties of bilayer models of the milk fat globule membrane. *Biochimica et Biophysica Acta (BBA) - Biomembranes*, *1858*(9), 2181-2190. https://doi.org/10.1016/j.bbamem.2016.06.020

Napier, J. A., Beaudoin, F., Tatham, A. S., Alexander, L. G., & Shewry, P. R. (2001). The seed oleosins: Structure, properties and biological role. In J. A. Callow (Ed.), *Advances in Botanical Research* (Vol. 35, pp. 111-138). Academic Press. https://doi.org/10.1016/S0065-2296(01)35005-X

Nikiforidis, C. V. (2019). Structure and functions of oleosomes (oil bodies). *Advances in Colloid and Interface Science*, *274*, 102039. https://doi.org/10.1016/j.cis.2019.102039

Nikiforidis, C. V., Biliaderis, C. G., & Kiosseoglou, V. (2012). Rheological characteristics and physicochemical stability of dressing-type emulsions made of oil bodies–egg yolk blends. *Food Chemistry*, *134*(1), 64-73. https://doi.org/10.1016/j.foodchem.2012.02.058

Nikiforidis, C. V., Donsouzi, S., & Kiosseoglou, V. (2016). The interplay between diverse oil body extracts and exogenous biopolymers or surfactants. *Food Research International*, *83*, 14-24. https://doi.org/10.1016/j.foodres.2016.02.007

Nikiforidis, C. V., Karkani, O. A., & Kiosseoglou, V. (2011). Exploitation of maize germ for the preparation of a stable oil-body nanoemulsion using a combined aqueous extraction–ultrafiltration method. *Food Hydrocolloids*, *25*(5), 1122-1127. https://doi.org/10.1016/j.foodhyd.2010.10.009

Nikiforidis, C. V., & Kiosseoglou, V. (2009). Aqueous extraction of oil bodies from maize germ (*Zea mays*) and characterization of the resulting natural oil-in-water emulsion. *Journal of Agricultural and Food Chemistry*, *57*(12), 5591-5596. https://doi.org/10.1021/jf900771v

Nikiforidis, C. V., & Kiosseoglou, V. (2010). Physicochemical stability of maize germ oil body emulsions as influenced by oil body surface−xanthan gum interactions. *Journal of Agricultural and Food Chemistry*, *58*(1), 527-532. https://doi.org/10.1021/jf902544j

Nikiforidis, C. V., Kiosseoglou, V., & Scholten, E. (2013). Oil bodies: An insight on their microstructure — maize germ vs sunflower seed. *Food Research International*, *52*(1), 136-141. https://doi.org/10.1016/j.foodres.2013.02.052

Nikiforidis, C. V., Matsakidou, A., & Kiosseoglou, V. (2014). Composition, properties and potential food applications of natural emulsions and cream materials based on oil bodies. *RSC Advances*, *4*(48), 25067-25078. https://doi.org/10.1039/c4ra00903g

Ntone, E., Bitter, J. H., & Nikiforidis, C. V. (2020). Not sequentially but simultaneously: Facile extraction of proteins and oleosomes from oilseeds. *Food Hydrocolloids*, *102*, 105598. https://doi.org/10.1016/j.foodhyd.2019.105598

Nykiforuk, C. L. (2016). Liquid-liquid phase separation of oil bodies from seeds. In J. MacDonald, I. Kolotilin, & R. Menassa (Eds.), *Recombinant proteins from plants: Methods and protocols* (2nd ed., pp. 173-188). Humana Press.

Onsaard, E., Vittayanont, M., Srigam, S., & McClements, D. J. (2006). Comparison of properties of oil-in-water emulsions stabilized by coconut cream proteins with those stabilized by whey protein isolate. *Food Research International*, *39*(1), 78-86. https://doi.org/10.1016/j.foodres.2005.06.003

Oomah, B. D., Busson, M., Godfrey, D. V., & Drover, J. C. G. (2002). Characteristics of hemp (*Cannabis sativa* L.) seed oil. *Food Chemistry, 76*(1), 33-43. https://doi.org/10.1016/S0308-8146(01)00245-X

Parenti-Castelli, G., Bertoli, E., Sechi, A. M., Silvestrini, M. G., & Lenaz, G. (1974). Effect of soluble and membrane proteins upon diethyl ether extraction of aqueous phospholipid dispersions. *Lipids, 9*(4), 221-228. https://doi.org/10.1007/BF02532197

Payne, G., Lad, M., Foster, T., Khosla, A., & Gray, D. (2014). Composition and properties of the surface of oil bodies recovered from *Echium plantagineum*. *Colloids and Surfaces B: Biointerfaces, 116*, 88-92. https://doi.org/10.1016/j.colsurfb.2013.11.043

Peng, C., Svirskis, D., Lee, S. J., Oey, I., Kwak, H. S., Chen, G. Y., Bunt, C., & Wen, J. Y. (2018). Design of microemulsion system suitable for the oral delivery of poorly aqueous soluble beta-carotene. *Pharmaceutical Development and Technology, 23*(7), 682-688. https://doi.org/10.1080/10837450.2017.1287729

Peng, C. C., Lin, I. P., Lin, C. K., & Tzen, J. T. C. (2003). Size and stability of reconstituted sesame oil bodies. *Biotechnology Progress, 19*(5), 1623-1626. https://doi.org/10.1021/bp034129z

Peng, X., Ren, C., & Guo, S. (2016). Particle formation and gelation of soymilk: Effect of heat. *Trends in Food Science & Technology, 54*, 138-147. https://doi.org/10.1016/j.tifs.2016.06.005

Qian, C., Decker, E. A., Xiao, H., & McClements, D. J. (2012). Physical and chemical stability of β-carotene-enriched nanoemulsions: Influence of pH, ionic strength, temperature, and emulsifier type. *Food Chemistry, 132*(3), 1221-1229. https://doi.org/10.1016/j.foodchem.2011.11.091

Raikos, V., Konstantinidi, V., & Duthie, G. (2015). Processing and storage effects on the oxidative stability of hemp (*Cannabis sativa* L.) oil-in-water emulsions. *International Journal of Food Science & Technology, 50*(10), 2316-2322. https://doi.org/10.1111/ijfs.12896

Raikos, V., & Ranawana, V. (2017). Designing emulsion droplets of foods and beverages to enhance delivery of lipophilic bioactive components – a review of recent advances. *International Journal of Food Science & Technology, 52*(1), 68-80. https://doi.org/10.1111/ijfs.13272

Richards, A., Wijesundera, C., & Salisbury, P. (2008). Genotype and growing environment effects on the tocopherols and fatty acids of *Brassica napus* and *B. juncea*. *Journal of the American Oil Chemists Society, 85*(2), 159-168. https://doi.org/10.1007/s11746-007-1181-y

Romero-Guzmán, M. J., Jung, L., Kyriakopoulou, K., Boom, R. M., & Nikiforidis, C. V. (2020). Efficient single-step rapeseed oleosome extraction using twin-screw press. *Journal of Food Engineering, 276*, 109890. https://doi.org/10.1016/j.jfoodeng.2019.109890

Romero-Guzmán, M. J., Köllmann, N., Zhang, L., Boom, R. M., & Nikiforidis, C. V. (2020). Controlled oleosome extraction to produce a plant-based mayonnaise-like emulsion using solely rapeseed seeds. *LWT, 123*, 109120. https://doi.org/10.1016/j.lwt.2020.109120

Salvia-Trujillo, L., Qian, C., Martín-Belloso, O., & McClements, D. J. (2013). Influence of particle size on lipid digestion and β-carotene bioaccessibility in emulsions and nanoemulsions. *Food Chemistry, 141*(2), 1472-1480. https://doi.org/10.1016/j.foodchem.2013.03.050

Seow, C. C., & Gwee, C. N. (1997). Coconut milk: chemistry and technology. *International Journal of Food Science & Technology, 32*(3), 189-201.

Shakerardekani, A., Karim, R., & Vaseli, N. (2013). The effect of processing variables on the quality and acceptability of pistachio milk. *Journal of Food Processing and Preservation, 37*(5), 541-545.

Shrestha, K., Gemechu, F. G., & De Meulenaer, B. (2013). A novel insight on the high oxidative stability of roasted mustard seed oil in relation to phospholipid, Maillard type reaction products, tocopherol and canolol contents. *Food Research International, 54*(1), 587-594. https://doi.org/10.1016/j.foodres.2013.07.043

Shrestha, K., Stevens, C. V., & De Meulenaer, B. (2012). Isolation and identification of a potent radical scavenger (canolol) from roasted high erucic mustard seed oil from Nepal and its formation during roasting. *Journal of Agricultural and Food Chemistry, 60*(30), 7506-7512. https://doi.org/10.1021/jf301738y

Sikkema, J., de Bont, J. A., & Poolman, B. (1995). Mechanisms of membrane toxicity of hydrocarbons. *Microbiological Reviews, 59*(2), 201-222.

Small, E. (2017). *Cannabis: A complete guide*. CRC Press, Taylor & Francis Group.

Sukhija, P. S., & Palmquist, D. L. (1988). Rapid method for determination of total fatty-acid content and composition of feedstuffs and feces. *Journal of Agricultural and Food Chemistry*, *36*(6), 1202-1206. https://doi.org/10.1021/jf00084a019

Sukhotu, R., Shi, X., Hu, Q., Nishinari, K., Fang, Y., & Guo, S. (2014). Aggregation behaviour and stability of maize germ oil body suspension. *Food Chemistry*, *164*, 1-6. https://doi.org/10.1016/j.foodchem.2014.05.003

Sun, C., Gunasekaran, S., & Richards, M. P. (2007). Effect of xanthan gum on physicochemical properties of whey protein isolate stabilized oil-in-water emulsions. *Food Hydrocolloids*, *21*(4), 555-564. https://doi.org/10.1016/j.foodhyd.2006.06.003

Tan, C. P., & Nakajima, M. (2005). β-carotene nanodispersions: preparation, characterization and stability evaluation. *Food Chemistry*, *92*(4), 661-671. https://doi.org/10.1016/j.foodchem.2004.08.044

Teh, S.-S., & Birch, J. (2013). Physicochemical and quality characteristics of cold-pressed hemp, flax and canola seed oils. *Journal of Food Composition and Analysis*, *30*(1), 26-31. https://doi.org/10.1016/j.jfca.2013.01.004

Teng, F., He, M., Xu, J., Chen, F., Wu, C., Wang, Z., & Li, Y. (2020). Effect of ultrasonication on the stability and storage of a soy protein isolate-phosphatidylcholine nanoemulsions. *Scientific Reports*, *10*(1), 14010. https://doi.org/10.1038/s41598-020-70462-8

Thomas, J., Kuruvilla, K. M., & Hrideek, T. K. (2012). Mustard. In K. V. Peter (Ed.), *Handbook of Herbs and Spices* (2nd ed., pp. 388-398). Woodhead Publishing. https://doi.org/10.1533/9780857095671.388

Ting, J. T. L., Lee, K., Ratnayake, C., Platt, K. A., Balsamo, R. A., & Huang, A. H. C. (1996). Oleosin genes in maize kernels having diverse oil contents are constitutively expressed independent of oil contents. *Planta*, *199*(1), 158-165. https://doi.org/10.1007/BF00196892

Trentin, A., De Lamo, S., Güell, C., López, F., & Ferrando, M. (2011). Protein-stabilized emulsions containing beta-carotene produced by premix membrane emulsification. *Journal of Food Engineering*, *106*(4), 267-274. https://doi.org/10.1016/j.jfoodeng.2011.03.013

Tzen, J. T. C., Cao, Y. Z., Laurent, P., Ratnayake, C., & Huang, A. H. C. (1993). Lipids, proteins, and structure of seed oil bodies from diverse species. *Plant Physiology, 101*(1), 267-276. https://doi.org/10.1104/pp.101.1.267

Tzen, J. T. C., & Huang, A. H. C. (1992). Surface-structure and properties of plant seed oil bodies. *Journal of Cell Biology, 117*(2), 327-335. https://doi.org/10.1083/jcb.117.2.327

Tzen, J. T. C., Peng, C.-C., Cheng, D.-J., Chen, E. C. F., & Chiu, J. M. H. (1997). A new method for seed oil body purification and examination of oil body integrity following germination. *The Journal of Biochemistry, 121*(4), 762-768. https://doi.org/10.1093/oxfordjournals.jbchem.a021651

Vaidya, B., & Choe, E. (2011a). Effects of seed roasting on tocopherols, carotenoids, and oxidation in mustard seed oil during heating. *Journal of the American Oil Chemists' Society, 88*(1), 83-90. https://doi.org/10.1007/s11746-010-1656-0

Vaidya, B., & Choe, E. (2011b). Stability of tocopherols and lutein in oil extracted from roasted or unroasted mustard seeds during the oil oxidation in the dark. *Food Science and Biotechnology, 20*(1), 193-199. https://doi.org/10.1007/s10068-011-0026-5

Verrijssen, T. A. J., Smeets, K. H. G., Christiaens, S., Palmers, S., Van Loey, A. M., & Hendrickx, M. E. (2015). Relation between in vitro lipid digestion and β-carotene bioaccessibility in β-carotene-enriched emulsions with different concentrations of l-α-phosphatidylcholine. *Food Research International, 67*, 60-66. https://doi.org/10.1016/j.foodres.2014.10.024

Vilkhu, K., Mawson, R., Simons, L., & Bates, D. (2008). Applications and opportunities for ultrasound assisted extraction in the food industry — A review. *Innovative Food Science & Emerging Technologies, 9*(2), 161-169. https://doi.org/10.1016/j.ifset.2007.04.014

Vinatoru, M. (2001). An overview of the ultrasonically assisted extraction of bioactive principles from herbs. *Ultrasonics Sonochemistry, 8*(3), 303-313. https://doi.org/10.1016/S1350-4177(01)00071-2

Wang, X., Yu, K., Cheng, C., Peng, D., Yu, X., Chen, H., Chen, Y., McClements, D. J., & Deng, Q. (2021). Effect of sesamol on the physical and chemical stability of plant-based flaxseed oil-in-water emulsions stabilized by proteins or phospholipids. *Food & Function, 12*(5), 2090-2101.

Waschatko, G., Junghans, A., & Vilgis, T. A. (2012). Soy milk oleosome behaviour at the air–water interface. *Faraday Discussions, 158*, 157-169.

White, S. H., King, G. I., & Cain, J. E. (1981). Location of hexane in lipid bilayers determined by neutron diffraction. *Nature, 290*(5802), 161-163.

Wijesundera, C., Boiteau, T., Xu, X., Shen, Z., Watkins, P., & Logan, A. (2013). Stabilization of fish oil-in-water emulsions with oleosin extracted from canola meal. *Journal of Food Science, 78*(9), C1340-C1347.

WHO Expert Committee on Drug Dependence. (2018). *Extracts and tinctures of cannabis*. World Health Organization. https://www.who.int/medicines/access/controlled-substances/Extracts-and-tinctures.pdf

Xu, D., Wang, X., Jiang, J., Yuan, F., Decker, E. A., & Gao, Y. (2013). Influence of pH, EDTA, α-tocopherol, and WPI oxidation on the degradation of β-carotene in WPI-stabilized oil-in-water emulsions. *LWT - Food Science and Technology, 54*(1), 236-241. https://doi.org/10.1016/j.lwt.2013.05.029

Yan, Z., Zhao, L., Kong, X., Hua, Y., & Chen, Y. (2016). Behaviors of particle size and bound proteins of oil bodies in soymilk processing. *Food Chemistry, 194*, 881-890. https://doi.org/10.1016/j.foodchem.2015.08.100

Yang, N., Su, C., Zhang, Y., Jia, J., Leheny, R. L., Nishinari, K., Fang, Y., & Phillips, G. O. (2020). In situ nanomechanical properties of natural oil bodies studied using atomic force microscopy. *Journal of Colloid and Interface Science, 570*, 362-374. https://doi.org/10.1016/j.jcis.2020.03.011

Yi, J., Li, Y., Zhong, F., & Yokoyama, W. (2014). The physicochemical stability and in vitro bioaccessibility of beta-carotene in oil-in-water sodium caseinate emulsions. *Food Hydrocolloids, 35*, 19-27. https://doi.org/10.1016/j.foodhyd.2013.07.025

Yin, J. T., Xiang, C. Y., Wang, P. Q., Yin, Y. Y., & Hou, Y. T. (2017). Biocompatible nanoemulsions based on hemp oil and less surfactants for oral delivery of baicalein with enhanced bioavailability. *International Journal of Nanomedicine, 12*, 2923-2931. https://doi.org/10.2147/ijn.S131167

Yu, L. L., Zhou, K. K., & Parry, J. (2005). Antioxidant properties of cold-pressed black caraway, carrot, cranberry, and hemp seed oils. *Food Chemistry, 91*(4), 723-729. https://doi.org/10.1016/j.foodchem.2004.06.044

Yuan, Y., Gao, Y., Zhao, J., & Mao, L. (2008). Characterization and stability evaluation of β-carotene nanoemulsions prepared by high pressure homogenization under various emulsifying conditions. *Food Research International, 41*(1), 61-68. https://doi.org/10.1016/j.foodres.2007.09.006

Zderic, A., Almeida-Rivera, C., Bongers, P., & Zondervan, E. (2016). Product-driven process synthesis for the extraction of oil bodies from soybeans. *Journal of Food Engineering, 185*, 26-34. https://doi.org/10.1016/j.jfoodeng.2016.03.030

Zhao, L., Chen, Y., Chen, Y., Kong, X., & Hua, Y. (2016). Effects of pH on protein components of extracted oil bodies from diverse plant seeds and endogenous protease-induced oleosin hydrolysis. *Food Chemistry, 200*, 125-133. https://doi.org/10.1016/j.foodchem.2016.01.034

Zheng, B., & McClements, D. J. (2020). Formulation of more efficacious curcumin delivery systems using colloid science: Enhanced solubility, stability, and bioavailability. *Molecules (Basel, Switzerland), 25*(12), 2791. https://www.mdpi.com/1420-3049/25/12/2791

Zheng, B., Zhang, X., Peng, S., & Julian McClements, D. (2019). Impact of curcumin delivery system format on bioaccessibility: nanocrystals, nanoemulsion droplets, and natural oil bodies. *Food & Function, 10*(7), 4339-4349. https://doi.org/10.1039/C8FO02510J

Zhou, L.-Z., Chen, F.-S., Hao, L.-H., Du, Y., & Liu, C. (2019). Peanut oil body composition and stability. *Journal of Food Science, 84*(10), 2812-2819. https://doi.org/10.1111/1750-3841.14801

Zhu, K. X., Li, J., Li, M., Guo, X. N., Peng, W., & Zhou, H. M. (2013). Functional properties of chitosan-xylose Maillard reaction products and their application to semi-dried noodle. *Carbohydrate Polymers, 92*(2), 1972-1977. https://doi.org/10.1016/j.carbpol.2012.11.078

Zielbauer, B. I., Jackson, A. J., Maurer, S., Waschatko, G., Ghebremedhin, M., Rogers, S. E., Heenan, R. K., Porcar, L., & Vilgis, T. A. (2018). Soybean oleosomes studied by small angle neutron scattering (SANS). *Journal of Colloid and Interface Science, 529*, 197-204. https://doi.org/10.1016/j.jcis.2018.05.080

Appendix

Permission from Huang for reprinting Figure 2.1. Copyright (1992) Annual Reviews, Inc.

Annual Reviews, Inc. - License Terms and Conditions

This is a License Agreement between Francesca Louise Garcia / Massey University ("You") and Annual Reviews, Inc. ("Publisher") provided by Copyright Clearance Center ("CCC"). The license consists of your order details, the terms and conditions provided by Annual Reviews, Inc., and the CCC terms and conditions.

All payments must be made in full to CCC.

Order Date	12-Mar-2021	**Type of Use**	Republish in a thesis/dissertation
Order license ID	1103667-1	**Publisher**	ANNUAL REVIEWS
ISSN	1545-2123	**Portion**	Chart/graph/table/figure

LICENSED CONTENT

Publication Title	Annual review of plant biology	**Country**	United States of America
Author/Editor	Annual Reviews, Inc.	**Rightsholder**	Annual Reviews, Inc.
Date	01/01/2002	**Publication Type**	e-Journal
Language	English	**URL**	http://arjournals.annualreviews.org/loi/ar...

REQUEST DETAILS

Portion Type	Chart/graph/table/figure	**Distribution**	Worldwide
Number of charts / graphs / tables / figures requested	1	**Translation**	Original language of publication
		Copies for the disabled?	No
Format (select all that apply)	Print, Electronic	**Minor editing privileges?**	Yes
Who will republish the content?	Academic institution	**Incidental promotional use?**	No
Duration of Use	Life of current edition	**Currency**	USD
Lifetime Unit Quantity	Up to 499		
Rights Requested	Main product		

NEW WORK DETAILS

Title	Masters thesis	**Institution name**	Massey University
Instructor name	n/a	**Expected presentation date**	2021-04-01

ADDITIONAL DETAILS

Order reference number	N/A	**The requesting person / organization to appear on the license**	Francesca Louise Garcia / Massey University

REUSE CONTENT DETAILS

Title, description or numeric reference of the portion(s)	Figure 3 A model of a maize oil body	**Title of the article/chapter the portion is from**	Oil bodies and oleosins in seeds
Editor of portion(s)	N/A	**Author of portion(s)**	N/A
Volume of serial or monograph	43	**Issue, if republishing an article from a serial**	N/A
Page or page range of portion	191	**Publication date of portion**	1992-06-01

Permission from Gray et al. for reprinting Figure 2.3. Copyright (2010) John Wiley and Sons.

JOHN WILEY AND SONS LICENSE TERMS AND CONDITIONS

Mar 15, 2021

This Agreement between Ms. Francesca Louise Garcia ("You") and John Wiley and Sons ("John Wiley and Sons' consists of your license details and the terms and conditions provided by John Wiley and Sons and Copyright Clearance Center.

License Number	5030070311323
License date	Mar 15, 2021
Licensed Content Publisher	John Wiley and Sons
Licensed Content Publication	European Journal of Lipid Science and Technology
Licensed Content Title	Oxidative stability of Echium plantagineum seed oil bodies
Licensed Content Author	Mita Lad, Eric A. Decker, David Julian McClements, et al
Licensed Content Date	Jul 14, 2010
Licensed Content Volume	112
Licensed Content Issue	7
Licensed Content Pages	9
Type of Use	Dissertation/Thesis
Requestor type	University/Academic
Format	Print and electronic
Portion	Figure/table
Number of figures/tables	1
Will you be translating?	No
Title	Masters thesis
Institution name	Massey University
Expected presentation date	Apr 2021
Portions	Figure 1
Requestor Location	Ms. Francesca Louise Garcia 383 Jose Street Aurea Village Subic Baliuag, Bulacan 3006 Philippines Attn: Ms. Francesca Louise Garcia
Publisher Tax ID	EU826007151

Permission from Dave et al. for reprinting Figure 2.4. Copyright (2019) Elsevier.

ELSEVIER LICENSE
TERMS AND CONDITIONS

Mar 15, 2021

This Agreement between Ms. Francesca Louise Garcia ("You") and Elsevier ("Elsevier") consists of your license details and the terms and conditions provided by Elsevier and Copyright Clearance Center.

License Number	5030070545507
License date	Mar 15, 2021
Licensed Content Publisher	Elsevier
Licensed Content Publication	Food Chemistry
Licensed Content Title	Structural and interfacial characteristics of oil bodies in coconuts (Cocos nucifera L.)
Licensed Content Author	Anant C. Dave,Aiqian Ye,Harjinder Singh
Licensed Content Date	Mar 15, 2019
Licensed Content Volume	276
Licensed Content Issue	n/a
Licensed Content Pages	11
Start Page	129
End Page	139
Type of Use	reuse in a thesis/dissertation
Portion	figures/tables/illustrations
Number of figures/tables/illustrations	1
Format	both print and electronic
Are you the author of this Elsevier article?	No
Will you be translating?	No
Title	Masters thesis
Institution name	Massey University
Expected presentation date	Apr 2021
Portions	Figure 1
Requestor Location	Ms. Francesca Louise Garcia 383 Jose Street Aurea Village Subic Baliuag, Bulacan 3006 Philippines Attn: Ms. Francesca Louise Garcia
Publisher Tax ID	GB 494 6272 12

Permission from Small for reprinting Figure 2.5. Copyright (2017) Taylor and Francis Group LLC (Books) US.

Free Of Charge Licence Terms

Licence Date:	25/03/2021
PLSclear Ref No:	48898

The Licensor

Company name:	Taylor and Francis Group LLC (Books) US
Address:	711 3rd Avenue New York 10017 United States US

The Licensee

Licensee Contact Name:	Francesca Louise Garcia
Licensee Address:	383 Jose Street Aurea Village, Subic Baliuag 3006 Philippines

Licensed Material

title:	Cannabis A Complete Guide
ISBN:	9781498761635
publisher:	Taylor and Francis Group LLC (Books) US
Are you requesting permission to reuse the cover of the publication?	No
Figure number & title	Figure 8.3 Diagrams of sectioned achenes of C. sativa
Page numbers	145
Name of illustrator	B. Flahey
Are you requesting permission to reuse your own work?	Yes
Additional Information	for reprinting in masters thesis
Will it be cropped	Yes
Full details of how it will be altered	figure label removed

For Use In Licensee's Publication(s)

usage type	Book, Journal, Magazine or Academic Paper-Thesis / Dissertation
Will your dissertation be placed in an online repository?	Yes
Author	Francesca Louise P. Garcia
Estimated publication date	April 2021
Language	English
Title of dissertation/thesis	Characterisation of plant oil bodies and their application as delivery systems of bioactive compounds
University or institution	Massey University
Unlimited circulation?	Yes

Rights Granted

Exclusivity:	Non-Exclusive
Format:	Thesis / Dissertation
Language:	English
Territory:	World
Duration:	Lifetime of Licensee's Edition
Maximum Circulation:	0

Permission from Callaway for reprinting Table 2.1 and Table 2.2. Copyright (2004) Springer Nature.

SPRINGER NATURE LICENSE TERMS AND CONDITIONS

Mar 15, 2021

This Agreement between Ms. Francesca Louise Garcia ("You") and Springer Nature ("Springer Nature") consists your license details and the terms and conditions provided by Springer Nature and Copyright Clearance Center.

License Number	5030071253211
License date	Mar 15, 2021
Licensed Content Publisher	Springer Nature
Licensed Content Publication	Euphytica
Licensed Content Title	Hempseed as a nutritional resource: An overview
Licensed Content Author	J. C. Callaway
Licensed Content Date	Jan 1, 2004
Type of Use	Thesis/Dissertation
Requestor type	academic/university or research institute
Format	print and electronic
Portion	figures/tables/illustrations
Number of figures/tables/illustrations	2
Will you be translating?	no
Circulation/distribution	1 - 29
Author of this Springer Nature content	no
Title	Masters thesis
Institution name	Massey University
Expected presentation date	Apr 2021
Portions	Table 1, Table 4
Requestor Location	Ms. Francesca Louise Garcia 383 Jose Street Aurea Village Subic Baliuag, Bulacan 3006 Philippines Attn: Ms. Francesca Louise Garcia

Permission from Thomas et al. for reprinting Table 2.4. Copyright (2012) Elsevier.

ELSEVIER LICENSE
TERMS AND CONDITIONS

Mar 15, 2021

This Agreement between Ms. Francesca Louise Garcia ("You") and Elsevier ("Elsevier") consists of your license details and the terms and conditions provided by Elsevier and Copyright Clearance Center.

License Number	5030080219849
License date	Mar 15, 2021
Licensed Content Publisher	Elsevier
Licensed Content Publication	Elsevier Books
Licensed Content Title	Handbook of Herbs and Spices
Licensed Content Author	J. Thomas,K.M. Kuruvilla,T.K. Hrideek
Licensed Content Date	Jan 1, 2012
Licensed Content Pages	11
Start Page	388
End Page	398
Type of Use	reuse in a thesis/dissertation
Portion	figures/tables/illustrations
Number of figures/tables/illustrations	1
Format	both print and electronic
Are you the author of this Elsevier chapter?	No
Will you be translating?	No
Title	Masters thesis
Institution name	Massey University
Expected presentation date	Apr 2021
Portions	Table 21.1
Requestor Location	Ms. Francesca Louise Garcia 383 Jose Street Aurea Village Subic Baliuag, Bulacan 3006 Philippines Attn: Ms. Francesca Louise Garcia
Publisher Tax ID	GB 494 6272 12

Permission from Vaidya & Choe for reprinting Table 2.5. Copyright (2011) Springer Nature.

SPRINGER NATURE LICENSE TERMS AND CONDITIONS

Mar 15, 2021

This Agreement between Ms. Francesca Louise Garcia ("You") and Springer Nature ("Springer Nature") consists your license details and the terms and conditions provided by Springer Nature and Copyright Clearance Center.

License Number	5030080388022
License date	Mar 15, 2021
Licensed Content Publisher	Springer Nature
Licensed Content Publication	Food Science and Biotechnology
Licensed Content Title	Stability of tocopherols and lutein in oil extracted from roasted or unroasted mustard seeds during the oil oxidation in the dark
Licensed Content Author	Bipin Vaidya et al
Licensed Content Date	Feb 28, 2011
Type of Use	Thesis/Dissertation
Requestor type	academic/university or research institute
Format	print and electronic
Portion	figures/tables/illustrations
Number of figures/tables/illustrations	1
Will you be translating?	no
Circulation/distribution	1 - 29
Author of this Springer Nature content	no
Title	Masters thesis
Institution name	Massey University
Expected presentation date	Apr 2021
Portions	Table 1
Requestor Location	Ms. Francesca Louise Garcia 383 Jose Street Aurea Village Subic Baliuag, Bulacan 3006 Philippines Attn: Ms. Francesca Louise Garcia

Permission from Tzen et al. for reprinting Table 2.7. Copyright (1993) Oxford University Press.

OXFORD UNIVERSITY PRESS LICENSE TERMS AND CONDITIONS

Mar 15, 2021

This Agreement between Ms. Francesca Louise Garcia ("You") and Oxford University Press ("Oxford University Press") consists of your license details and the terms and conditions provided by Oxford University Press and Copyright Clearance Center.

License Number	5030080494592
License date	Mar 15, 2021
Licensed Content Publisher	Oxford University Press
Licensed Content Publication	CONFIDENTIAL - Plant Physiology
Licensed Content Title	Lipids, Proteins, and Structure of Seed Oil Bodies from Diverse Species
Licensed Content Author	Tzen, JTC.; Cao, Yz.
Licensed Content Date	Jan 1, 1993
Type of Use	Thesis/Dissertation
Institution name	
Title of your work	Masters thesis
Publisher of your work	Massey University
Expected publication date	Apr 2021
Permissions cost	0.00 USD
Value added tax	0.00 USD
Total	**0.00 USD**
Title	Masters thesis
Institution name	Massey University
Expected presentation date	Apr 2021
Portions	Table 1
Requestor Location	Ms. Francesca Louise Garcia 383 Jose Street Aurea Village Subic Baliuag, Bulacan 3006 Philippines Attn: Ms. Francesca Louise Garcia
Publisher Tax ID	GB125506730